EFFECT OF GAS BUBBLES ON THE SEA BED BEHAVIOUR

by

S.Nageswaran

St.Catherine's College Oxford

A thesis submitted to the University of Oxford

for the degree of

Doctor of Philosophy

Trinity 1983

ACKNOWLEDGEMENT

Dr.G.C.Sills suggested this subject to me in 1980 and subsequently supervised me throughout the study. It is the effort, time, and above all, the patience and willingness she devoted to our frequent discussion which made this research a truly educational experience. For this I shall always be grateful.

The staff and technicians in the soil mechanics group at Oxford University have provided invaluable help in this study and I owe special thanks to all of them.

The financial support of the Science and Engineering Research Council is gratefully acknowledged.

Finally, to Dharshini for her patience and understanding during the course of this work.

TABLE OF CONTENTS

ABSTRACT

Effect of gas bubbles on the sea bed behaviour

by

S.Nageswaran

St.Catherine's College, Oxford.

A thesis submitted to the University of Oxford

for the degree of Doctor of Philosophy.

Trinity 1983.

This thesis examines the effect of undissolved gas bubbles on the geotechnical properties of marine clayey soils. A large portion of the work is devoted to study the effect of gas bubbles on the volume change behaviour of clayey soils under K_o conditions.

Chapter two describes the technique used to introduce controllable amount of gas bubbles into reconstituted clayey soils. One dimensional volume change behaviour of gassy soils with different degrees of saturation is compared with that of the saturated soil in chapter three.

A theoretical model is developed in chapter four to describe the consolidation behaviour of soils containing a compressible pore fluid and is compared with the experimental results. The pore water pressure response in gassy soil for undrained total stress changes under K_o conditions is also analysed in this chapter.

A differential piezometer to measure the pore water pressure response in a gassy sea bed for tide and wave action was designed and tested. Chapter five describes the features of this instrument and the results obtained in two field trials.

Finally in chapter six, the effect of gas bubbles on the undrained shear strength of soil is examined.

CHAPTER 1 INTRODUCTION

CHAPTER 1

INTRODUCTION TO GASSY SOIL

1.1 INTRODUCTION:

Recent offshore activities in connection with petroleum and mineral exploration, platform and pipe line installation, nuclear waste disposal etc, have resulted in numerous challenges for marine engineers. Marine geotechnics must be defined in relationship to the state of art on land because geotechnical engineers are familiar with onshore soil behaviour and design procedures. Certainly there are special problems and physical or economic constraints that make offshore engineering different, but it is reasonable to expect the same general principles, such as the principle of effective stress, to apply offshore as onshore. Thus the total stresses and the pore water pressures may be high in the sea bed due to high water depths, but the magnitude of the shear strength, which is still governed by the effective stress, the difference between total stress and pore fluid pressure, is the same as onshore for a given depth of soil.

The problems encountered in the marine environment divide into different categories:

(1) Natural forces and conditions which do not arise on land cause problems when the engineer tries to interact with sea bed construction.

Some of these problems are:

Erosion of sea bed: Scour protection is necessary to prevent erosion of the sea bed near off shore structures since most of the foundation designs assume that the underlying soil remains in position. Erosion causes damage to pipe lines and they should ideally be laid on a stable sea bed, avoiding likely erodable sea bed formation such as sand ripples, sand waves, dunes or unstable slopes.

Dynamic loading: The magnitudes of the stresses induced by the repeated action of wave or storm loading and the effect of these loadings on the behaviour of soil (eg- the pore water pressure generation caused by repeated shearing of soil) are very difficult to estimate.

Rapid deposition of sediment: Rapid sedimentation causes navigation problems (frequent dredging is necessary) and if the sedimentation rate is high and continuous, the soil remains under consolidated. Under consolidated soil is a soil in which the pore water pressure is greater than the hydrostatic pressure, so that full consolidation has not been achieved for a given overburden pressure.

Gas in seabed: The presence of undissolved gas in soil makes the fundamental behaviour of the soil different from that of the fully saturated soil. It has the effect of making the pore fluid compressible, causing volume change for undrained loading conditions. Most of the gassy sediments are known to be under consolidated and have very low shear strengths (Bea and Arnold 1973).

(2) Difficulties in tackling problems due to inconvenience of environment:

Sampling: High quality undisturbed soil samples are difficult to obtain and expensive. The reduction in pore water pressures involved during sampling offshore is much greater than that onshore due to the high water depth and as a result the dissolved gas reappears, expands and disturbs the samples. Even if the sample is saturated in-situ, gas may appear in the sample when brought back to the surface. The reduction in effective stress due to the removal of the overburden adds to the effect.

In-situ measurement and data collection: Existing in-situ probes for onshore testing have to be modified to cope with the high water depths and the environmental conditions. Weather is a crucial factor for offshore soil investigation and causes problems in

positioning drill ships. Remotely controlled wire line probes (remote vane, cone penetrometer) are often used and comparatively little high quality data are available for designers due to the high cost involved in hiring ships and equipment.

In category(1) a better understanding of the natural process, with changes to the soil model or in the specified boundary conditions will be needed and in category(2) the main hopes of tackling the problems will lie in mechanical developments.

The author is focussing his interest on the effect of gas bubbles on the behaviour of sea bed because it is not well understood and has important consequences in some specific areas.

1.2 BACKGROUND

1.2.1 THE PRESENCE OF GAS IN MARINE SOIL

The presence of gas in marine soil and the special features associated with it have been identified in many parts of the world. Gas is very easily detectable in bogs, swamps and marshes as the bubbles apppear on the surfaces. Marine geological surveys carried out in the Gulf of Mexico, utilizing side scan sonar, have identified a variety of subaqueous land slides which appeared to be caused by very low angle (0.2-3.0deg) slope instability. Geochemical analysis of cores taken from these very soft sediments showed the presence of gas, mainly methane, in the sediment (Whelan et al 1976). The mechanism for the slope instability and the large sea floor movement is not well established but is believed to be caused by the combined effects of the presence of undissolved gas bubbles, the rapid sedimentation and storm action.

The presence of gas has been detected also in the North Sea by the Institute of Geological Science (I.G.S) during the course of regional geological mapping surveys. Their investigations detected special features known as "pockmarks". Pockmarks are cone shaped depressions which occur in fine sediments on the sea floor. Pockmarks can vary in size and shape, but in the North Sea (in the I.G.S study area) they are typically oval in form with length to breadth ratios of 1.4:1. These features have a depth range of 2-8m with an approximate density of 35 per square

kilometre (Fannin 1974). Such features are also observed off the east cost of Canada, Barents Sea, Malaysia, Thailand and Borneo. It is now generally accepted that pockmarks are an escape phenomenon and model experiments have shown that gas bubbled through soft clays will produce a shallow depression. In addition to pockmarks, gas bubbles filling voids in the sediment are common in many parts of the North Sea (Fannin 1974) and Gulf of Mexico.

Fig (1.1) shows a flow chart demonstrating a wide range of mechanisms capable of producing pockmarks or other sea bed slope failures (Prior and Coleman 1977).

1.2.2 THE ORIGIN OF GAS

Gas in marine soil arises mainly from three sources.
(a) Gas produced from biogenic degradation of organic matter - referred to as biogenic gas
(b) Gas diffusing upward from depth where it has been produced by thermal cracking of the complex organic and inorganic compounds - referred to as thermogenic gas.
(c) The gas produced by submarine volcanic or geothermal processes - referred to as vulcanogenic gas

Biogenic gas is the most widespread of these gases. It is derived mainly from organic matter in the sediment and mostly found in delta areas and on continental shelves. Methane is the important biogenic gas produced

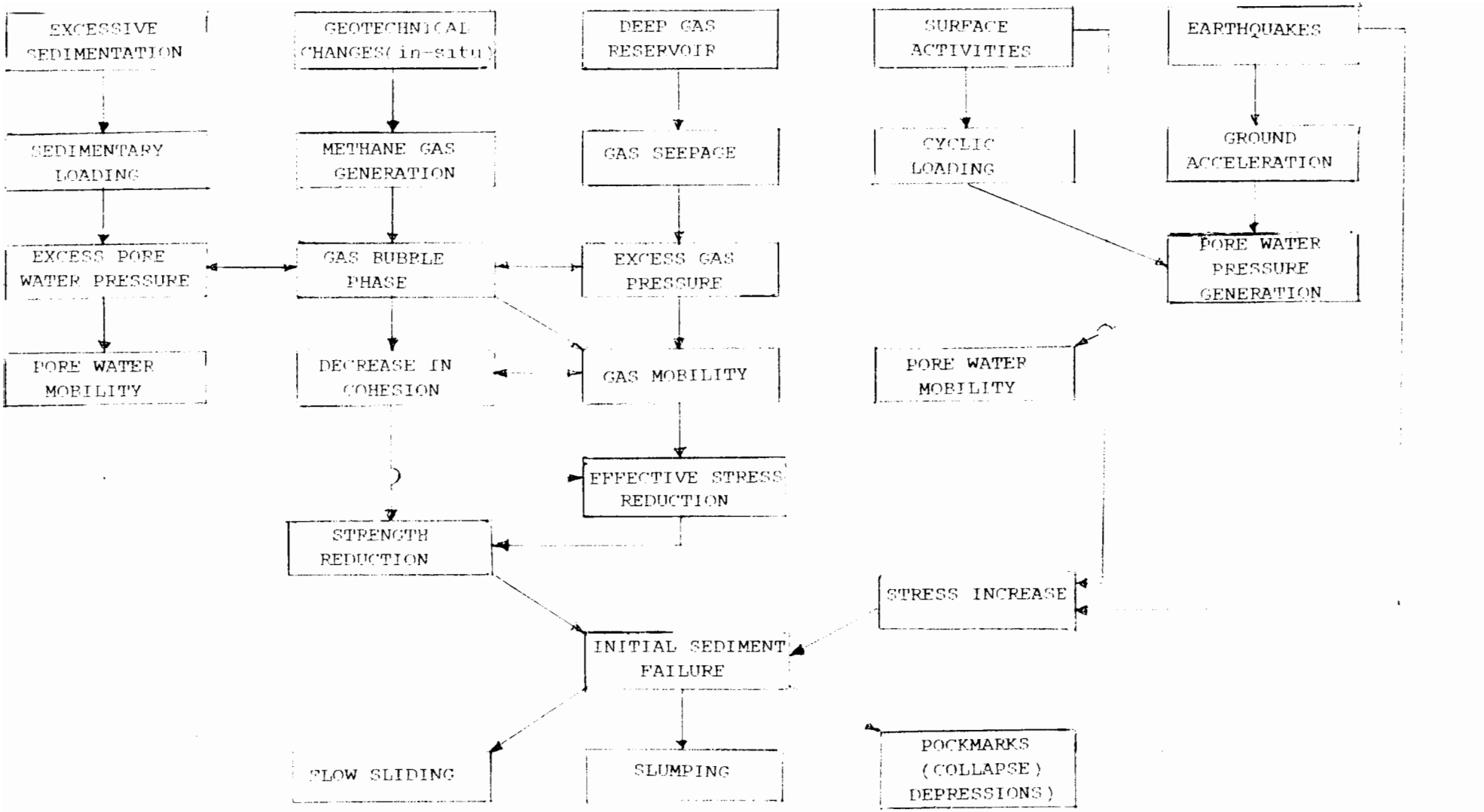

FIG 1.1 SUMMARY OF FACTORS LEADING TO POCKMARKS AND SLUMPING

FROM: PRIOR AND COLEMAN

and it is achieved by the action of bacteria on organic matter under anaerobic conditions.

Fig (1.2) shows the biological processes and the dissolved species in a typical sedimentary column. The first metre or two of the sediment contains dissolved oxygen in the pore water and only aerobic reductions take place. In the zone below, the dissolved oxygen is completely reduced (anaerobic), sulphate reduction starts and the organic matter is transformed into biocarbonates and sulfides.

$$2[CH_2O] + SO_4^{--} = 2HCO_3 + HS^- + H^-$$

Methane first appears in the sediments below the sulphate reducing zone. The presence of dissolved sulphate is less favourable to methane production. There are various pathways capable of producing methane, and the only one capable of producing methane in sufficient quantities to correlate with the observed data is biological reduction of carbon dioxide by biologically produced hydrogen.

$$CO_2 + 4H_2 = CH_4 + 2H_2O$$

As the depth increases the amount of methane production is limited by the availability of organic matter. Methane production can be expected only in a sedimentary environment in which organic matter has been deposited at a rate exceeding the supply of dissolved

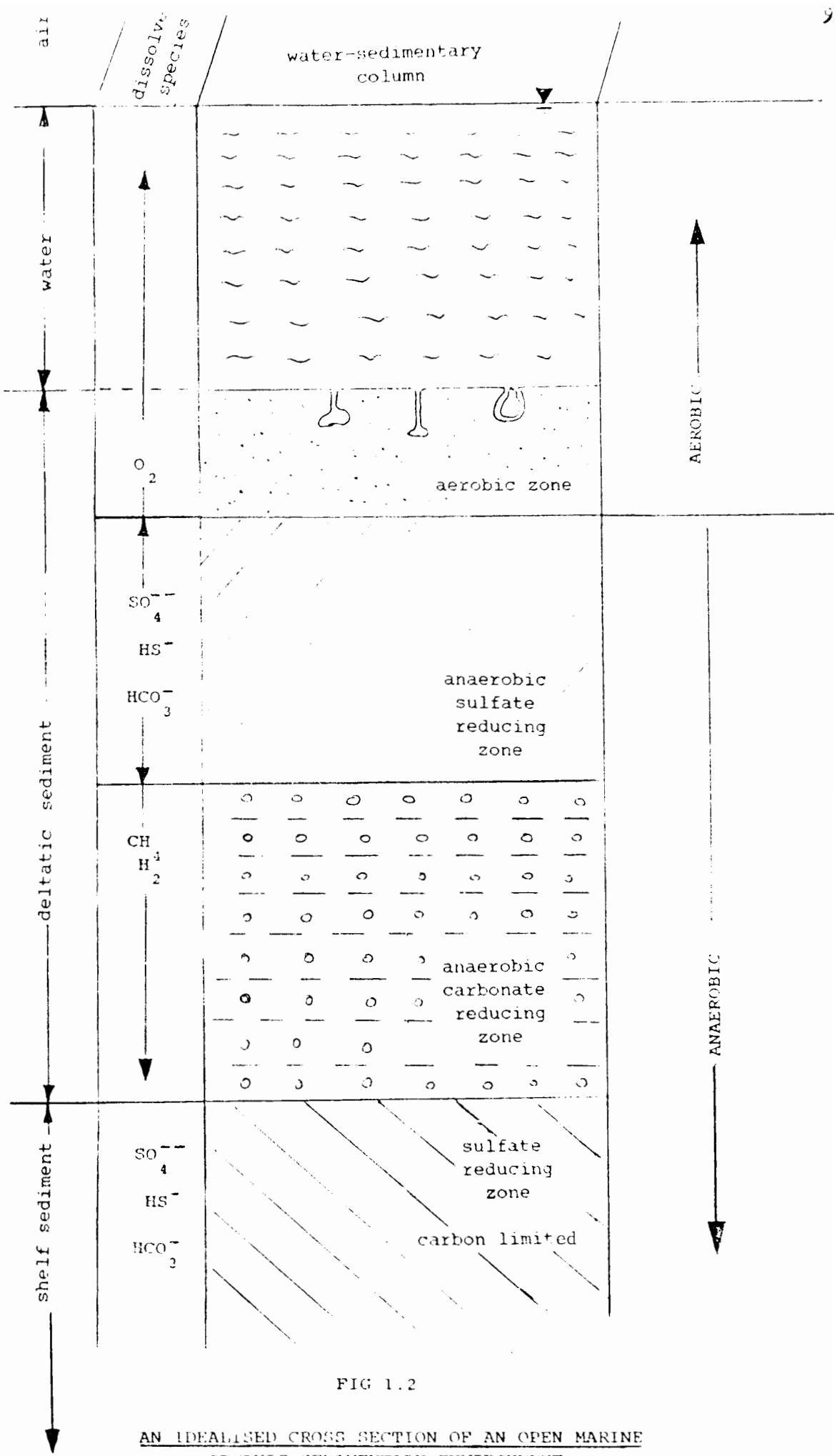

FIG 1.2

AN IDEALISED CROSS SECTION OF AN OPEN MARINE ORGANIC SEDIMENTARY ENVIRONMENT

FROM: CLAYPOOL AND KAPLAN

oxygen and where dissolved sulphate is not present. In most circumstances sulphate is reduced before methane is produced. Oxygen, hydrogen, hydrogen sulfide and carbon monoxide are also found in marine sediments in small quantities.

1.2.3 IDENTIFICATION AND MEASUREMENT OF THE AMOUNT OF GAS IN MARINE SEDIMENTS:

The presence of gas in marine sediments is often indicated by geophysical methods due to the distinctive acoustic properties. Seismic profiling is part of a geophysical survey and is carried out using acoustic devices (sparker, boomer, pinger or side scan sonar) in order to study the sea bed strata variations. An acoustic signal is transmitted from a source above the sea bed and the signal is reflected from various interfaces within the sea bed and monitored. The reflected waves are associated with a change in the acoustic impedance, defined as the product of density and sound speed. However if gas bubbles exist, then they will have three effects: (a) if the acoustic signal has a frequency below the resonant frequency of the bubbles, then the sound speed is substantially reduced and an acoustic interface is recorded, (b) the attenuation of the signal is increased, limiting the penetration, and (c) due to the changed compressibility, the return signal is out of phase with the transmitted signal. If the sediment is saturated the

return signal is in phase with the transmitted signal. The effects of gas in the sediments appear as dark patches (known as acoustic blanking or acoustic turbidity) in the seismic records because the gas bubbles absorb most of the energy and reduce further transmission of the signal. The presence of gas is confirmed by the phase shift uniquely associated with it. Even though the presence of gas in marine soil can be detected using acoustic geophysical instruments such as boomers or sparkers, the amount of gas present in the sediments has not been predicted successfully.

The technique which is used to quantify the amount of gas in the sea bed is by direct sampling (coring). The cores are normally brought to the surface from the sea bed for analysis and as a result the sample undergoes very large reductions in total stress and pore water pressure. Any gas bubbles that existed in-situ expand while the dissolved gas present in the pore water reappears and adds to the total gas volume. Sample growth and escape of gas bubbles along the core liners have been noted in many instances. These samples are then analysed for gas content at atmospheric pressure and the in-situ gas concentration is calculated, based on the following assumptions:

(a) No gas escapes during the sampling and recovery stages

(b) The amount of gas is experimentally determined at

atmospheric pressure, and the in-situ gas content is calculated using Boyle's and Henry's laws.

The gas analysis carried out using standard core samples indicates that in-situ degrees of saturation of Mississippi Delta sediments vary between 90% and 100% (Esrig and Kirby 1977). The above figures matched reasonably the values obtained from independent measurements of the sulphate deficit, the reduction in the amount of sulphate in the sediment by comparison with the sulphate in normal sea water, since the amount of methane produced is proportional to the sulphate deficit (Whelan III 1976).

The above method of finding the in-situ degree of saturation is not very accurate because of the loss of gas during recovery and the assumptions involved in the calculations. Various attempts have been made to avoid gas escape during sampling using pressurised core samplers where the samples are sealed at in-situ pressures and brought to the surface. However these techniques are very expensive and not used very often. Instruments for direct in-situ measurement of gas content are not available.

Fig 1.3 shows some of the different forms in which gas may exist in the soil. Depending on the amount and the distribution, gas exists as (a) inter-connected voids, (b) discrete large bubbles of irregular shape making solid-gas and water-gas interfaces, (c) small spherical

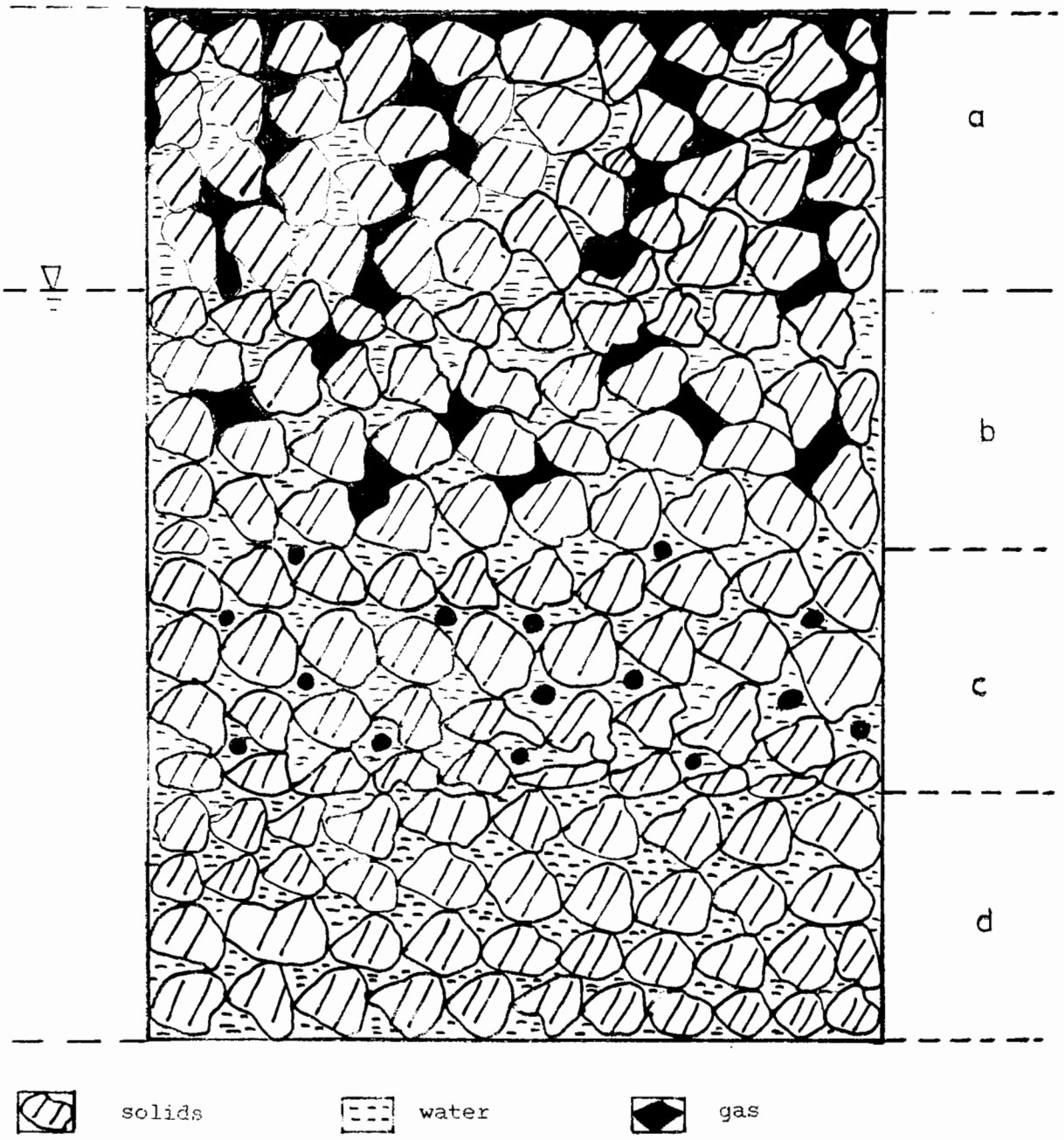

(a) Interconnected gas voids (c) Small spherical bubbles in water

(b) Discrete large bubbles (d) Dissolved bubbles

Fig 1.3 DIFFERENT FORMS OF GAS PHASE IN SOIL

bubbles completely surrounded by pore water in the voids, and (d) dissolved in the pore water. The higher degrees of saturation (>90%) in marine soils suggest that gas exists as discrete bubble form in-situ (ie. (b) and (c) in fig1.3) which is confirmed by the acoustic attenuation in these sediments.

1.2.4 PARTIALLY SATURATED SOIL AND GASSY SOIL:

The term "partially saturated" is often used in geotechnical engineering. Partially saturated soil consists of solid soil particles, pore water and pore gas (often air). The top few metres of land soil is often partially saturated due to the evaporation of water or due to a lowered water table. The soil above the water table holds water by capillary action and the pore water pressure can be below atmospheric pressure, causing pore suction due to the curvature of the air water menisci. The pore gas pressure is the same as atmospheric pressure when air voids are interconnected and exposed to atmosphere. Some type of partially saturated soils swell (eg.cotton clays) or collapse (mostly in silty soils) when the water table rises, wetting the soil and damaging the soil structures. A large amount of research work has been carried out to study the behaviour of partially saturated soils which contain high proportions of air voids to water voids (Bishop et al 1960, Jennings and Burland 1962, Matyas and Radhakrishna 1968, Fredlund 1978).

The soil beneath the water table (eg. marine soil) can also contain gas voids, typically with high water to gas volume ratio. As the water depth increases, the gas volume decreases and interconnected gas voids become discrete gas voids. The degree of saturation is generally comparatively high (90%-100%) and the pore water pressure is above atmospheric pressure (positive pore water pressure). Marine soils containing gas bubbles fall into this special category of partially saturated soil and the term "**Gassy Soil**" is used by the author.

" A GASSY SOIL IS A PARTIALLY SATURATED SOIL WITH SUFFICIENTLY HIGH DEGREES OF SATURATION FOR THE GAS TO EXIST IN BUBBLE FORM. The bubbles may be spherical or irregular in shape."

1.2.5 EFFECT OF GAS ON THE GEOTECHNICAL PROPERTIES OF SEDIMENT

The pore fluid of the sediments containing undissolved gas bubbles is compressible and the soil undergoes volume changes during undrained loading, unlike saturated soil. The pore water pressure increment (Δu_w) in a soil due to the principal total stress increment ($\Delta\sigma_1$, $\Delta\sigma_2$, $\Delta\sigma_3$) is given by

$$\Delta u_w = b\,[\Delta p + a\,(\Delta\tau_{oct})\,]$$

where $p=(\sigma_1+\sigma_2+\sigma_3)/3$

and $\tau_{oct}=[\sum(\sigma_i-\sigma_j)^2]^{1/2}$ for $i,j=1$ to 3

a,b are constants

$b=1$ for saturated soil

and $b<1$ for gassy soil

For one dimensional (K_o) undrained loading conditions (such as water depth changes in the sea bed)

$$\Delta u_w = B\,[\Delta\sigma_v]$$

the pore pressure increment will be less than the vertical stress increment in a gassy soil, leading to an effective stress change. The undrained behaviour of gassy soil is different from that of saturated soil due to the compressibility of the pore fluid.

Esrig and Kirby (1977) suggested that the pore pressure generation in gassy soil would be small during the application of shear stress ($B<1$), so that the failure undrained shear strength would be high when compared with saturated soil at the same state (stress and history).

But the measurements on gassy soils show that the shear strength is very low for a given over burden pressure [Bea and Arnold 1973]. Gassy sediments in the Mississippi Delta area have been observed to be very unstable and this results in large sea bed movement. In-situ vane shear tests carried out in this location show a typical profile fig (1.4), indicating low shear strength and this profile seems to match the insitu gas content profile. It is also observed that these sediments were underconsolidated since the preconsolidation pressure measured in the oedometer test is less than that of the in-situ vertical stress. The mechanism for low shear strengths may be due to the underconsolidation of the gassy sediments.

The in-situ pore pressures in a gassy sea bed in the Mississippi Delta area were measured [Project SEASWAB-1977] in order to understand the behaviour (low shear strength and underconsolidation) of the gassy sediments. Pore pressure measurements were obtained from piezometers. The initial driving pressures and the subsequent dissipation behaviour of the of these pressures were monitored. Fig (1.5) shows the measurements obtained in two field tests. The driving pressures dissipated and reached equilibrium at higher pressures than the hydrostatic pressures, indicating the existence of the high equilibrium excess pore pressures. Sudden increases in pore pressures were also observed instead of smooth dissipation curves. This behaviour may be caused by the

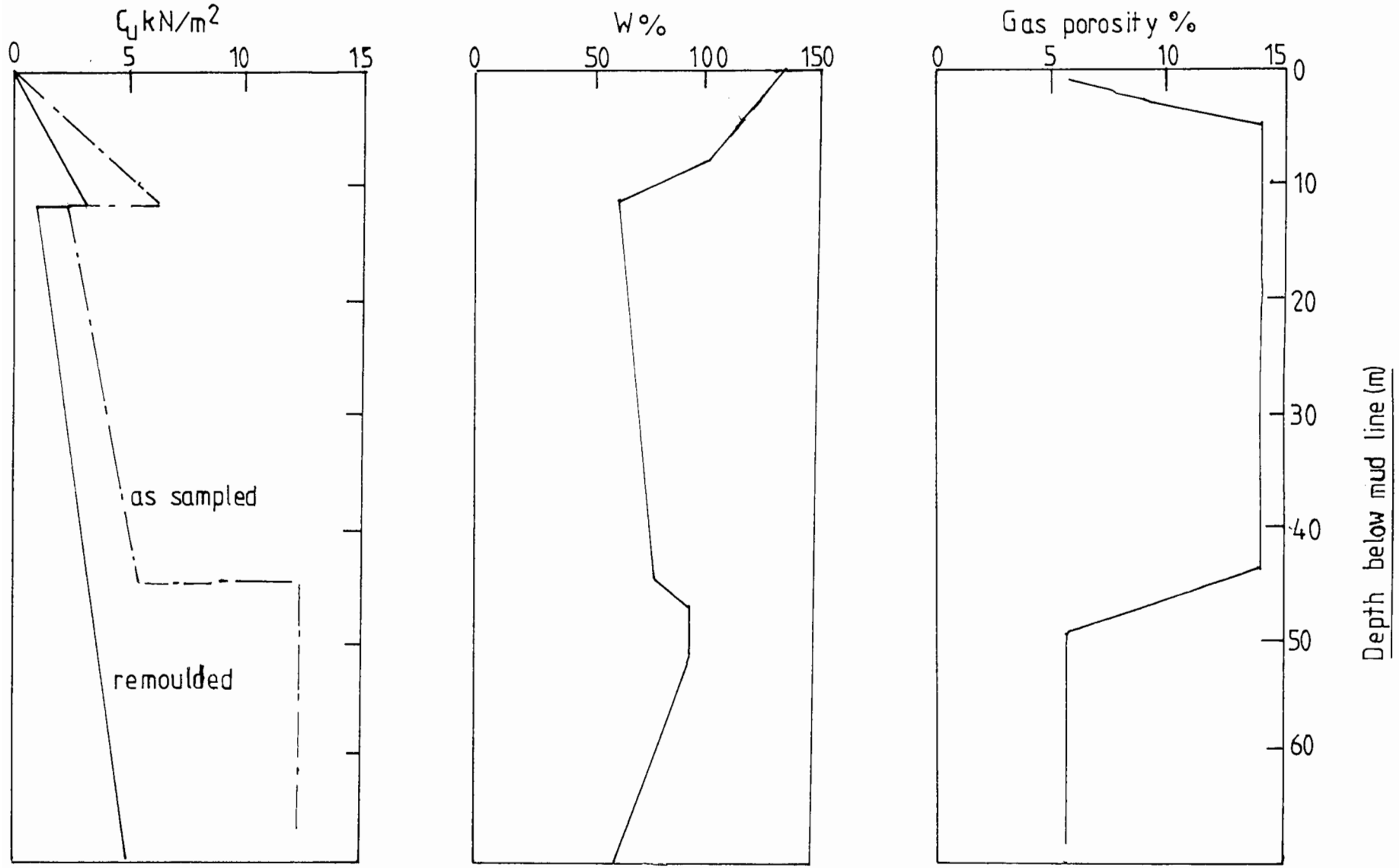

FIG 1.4 SOIL PROPERTIES MEASURED IN BORE HOLE

BEA AND AUDIBERT (1980)

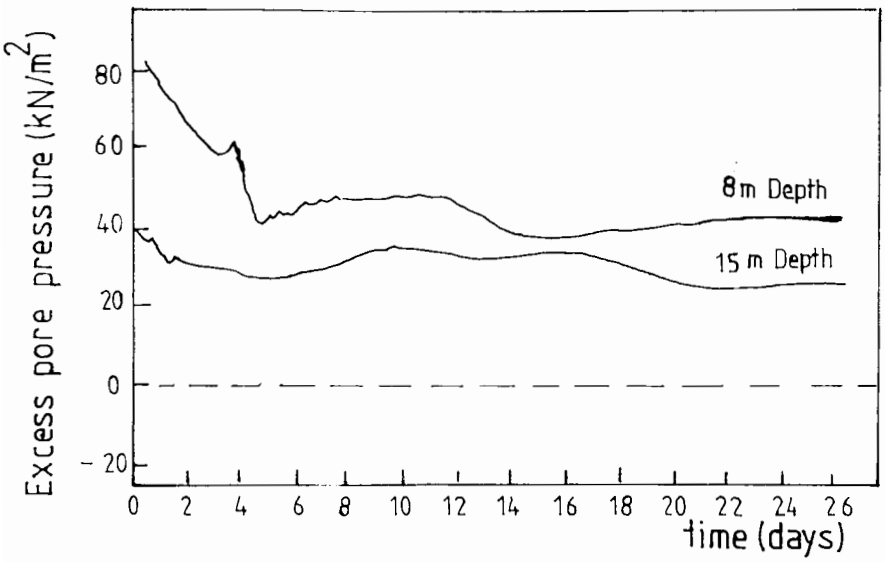

SEASWAB I

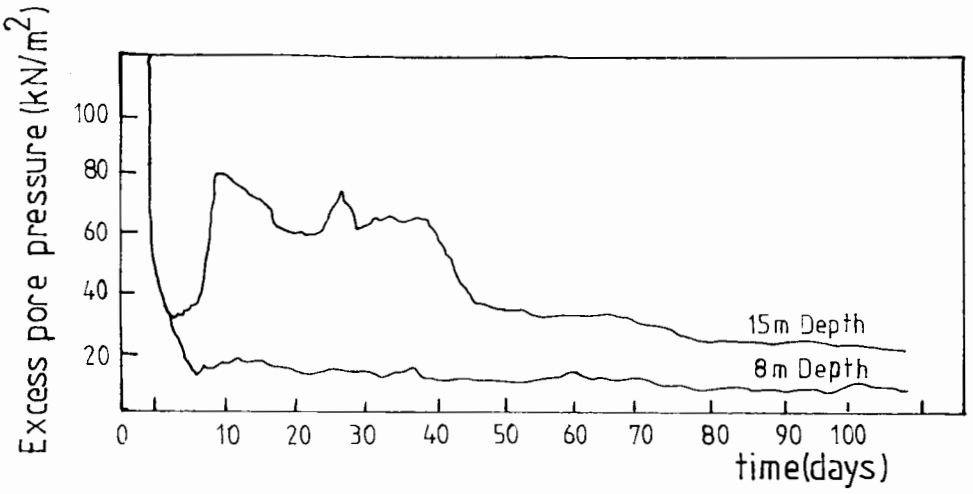

SEASWAB II

FIG 1.5 EXCESS PORE WATER PRESSURES FROM NOAA PIEZOMETER

BENNETT (1977)

presence of gas, continuous production of gas or a rapid rate of sedimentation.

Shear strength tests carried out on core samples taken from the acoustically impenetrable zones using a miniature vane, showed low values of shear strength and very small increments in strength with increasing overburden pressure (Whelan III 1976). In normally consolidated sediments, the shear strength typically increases with depth of burial. Even though the shear strength tests were performed as soon as the samples were on board ship, sample growths due to gas expansion were observed. As a result it was difficult to come to a conclusion as to whether the low shear strength was due to the presence of undissolved gas bubbles in the soil or due to the sample distubance caused by gas expansion.

In summary, measurements on gassy marine clays or silty clays indicate:

(a) Very low shear strength for a given over burden pressure.

(b) Underconsolidated, unstable sea bed slopes.

and (c) Positive equilibrium excess pore pressures.

1.2.6 EFFECTIVE STRESS LAW FOR PARTIALLY SATURATED SOIL.

Terazaghi (1923) showed experimentally that the stress controlling the changes in volume and the strength of a soil containing a single pore fluid is defined by the difference between total stress and pore fluid pressure,

Thus $\sigma' = \sigma - u$ (1)

where σ= total stress

u = pore fluid pressure

σ' = effective stress

If the soil is saturated with water $\sigma' = \sigma - u_w$, where u_w is the pore water pressure and the degree of saturation(S) is 100%

If the soil is perfectly dry $\sigma' = \sigma - u_a$, where u_a is the pore gas pressure and the degree of saturation is 0%

For partially saturated soil which contains both gas and water as pore fluids, Bishop (1959) proposed a modification of Terzaghi's classical expression for effective stress to the following form

$$\sigma' = (\sigma - u_a) + \chi(u_a - u_w) \quad (2)$$

The degree of saturation (volume of water/volume of voids) is between 100% and 0% where χ is a parameter ($0<\chi<1$) which depends only on the degree of saturation for a given soil.

$\chi=1$ S=100%

$\chi=0$ S=0%

Bishop (1960) carried out triaxial drained tests on Braehead silt to examine the validity of equation (2) by observing the effect of change in the values of σ, u_w and u_a on the shear stress-strain curve. He varied σ_3, u_a and u_w independently, keeping σ_3-u_a and u_a-u_w constant throughout the test and observed no changes in the shape of the shear stress-strain curve. When σ_3-u_a or u_a-u_w was changed in the test, he noticed sudden discontinuities in the stress-strain curve. Fig (1.6) shows the shear stess-strain curve for a partly saturated silty soil in a drained test. The discontinuity occurred when $(\sigma_3-u_a)$is changed from a constant value 30 p.s.i to 45 p.s.i. Therefore he concluded that the form of equation (2) was correct since the shear strength was controlled by $\sigma-u_a$ and u_a-u_w. Using the equation (2), Bishop calculated values for the parameter χ for different degrees of saturation ($20\%<S<100\%$) assuming the failure shear stress of the saturated soil and the partially saturated soil are the same at the same failure voids ratio. He measured pore water pressures and pore gas pressures separately in the unsaturated sample during testing. Pore water pressure was measured using high air entry value porous stones at the base of the sample and a null indicator which ensured no flow of water from the sample to the mercury manometer. Pore gas pressure was measured using a similar system but with low air entry stones (glass fibre discs) and air in the measuring system instead of water. This has been accepted as a standard technique to measure

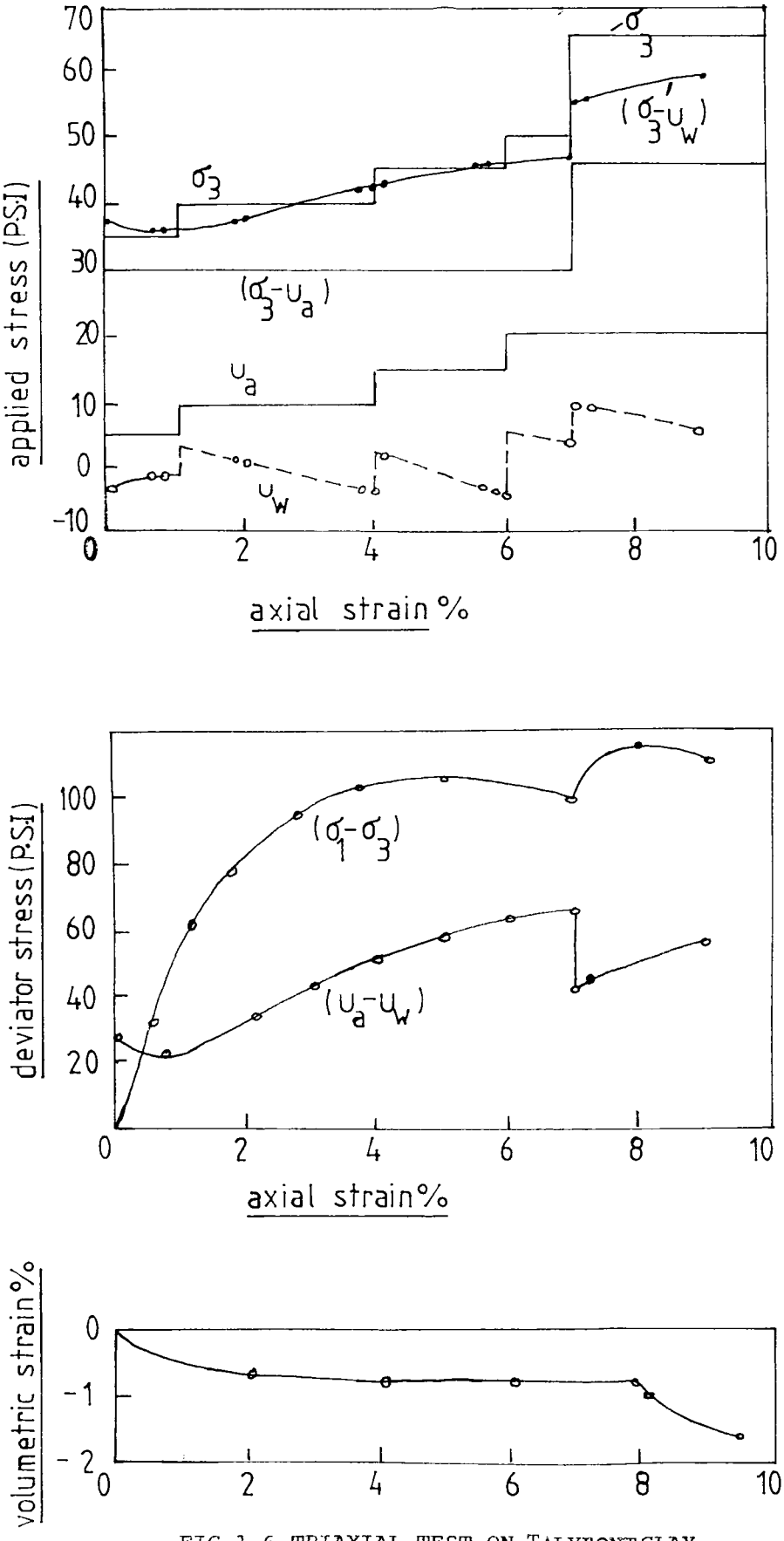

FIG 1.6 TRIAXIAL TEST ON TALYBONTCLAY
(This illustrates the dependency of shear strength and the volumetric strain on the pressure difference (σ-U_a) when the water content is kept constant)

BISHOP AND DONALD (1961)

pore gas and pore water pressures. The measured gas pressure was assumed to be the same as the pore gas pressures in the voids. This may be true when the gas voids are largely continuous, but when the degree of saturation is high the gas may form occluded bubbles and the gas pressure measured may not represent the mean pore gas pressure. Therefore measurements of pore gas pressure in partly saturated soils can be difficult to interpret.

Bishop stated that the parameter χ obtained from the drained shear test depended only on the degree of saturation and suggested that equation (2) was a valid expression for the effective stress.

However, Jennings and Burland (1962) pointed out that in order to describe the behaviour of partially saturated soil by a single stress parameter σ' given by the equation(2), it was necessary to prove that the soil behaviour was not affected by changes in $(\sigma-u_a)$ and $\chi(u_a-u_w)$ such that their sum (equal to σ') is constant. Bishop had shown only that soil behaviour was unaffected by changes in σ, u_a and u_w where $(\sigma-u_a)$ and (u_a-u_w) were separately constant in the shear test. They carried out oedometer tests on compacted silts to examine the validity of equation (2) qualitatively for volume change behaviour.

When the gas voids are exposed to atmospheric pressure the pore gas pressure becomes zero. Therefore the equation (2) becomes

$$\sigma' = \sigma - Xu_w \qquad (2)^*$$

where u_w is the pore suction (u_w is negative due to the surface tension effect ($u_w = u_a - 2T/r$) and σ' is greater than σ. When the dry silt was saturated using back pressure under constant load, a large reduction in voids was observed (Fig 1.7). During saturation the value (χu_w) increases from a negative value to a positive value. This implied from equation (2)* a reduction in effective stress (σ') so that the voids ratio would be expected to increase. However this contradicted the experimental observations so that equation (2) is not a valid expression for effective stress. They stated that the stress given by the equation should not be termed as an effective stress. Effective stress is the stress which controls the behaviour of the soil (both shear and the volume change).

Bishop and Blight (1963) re-examined equation (2) by triaxial drained tests on clays (using the same techniques used by Bishop 1960). They carried out drained triaxial shear tests on different compacted clays, with different stress paths,

(1) keeping the water content constant and varying $(\sigma_3 - u_a)$

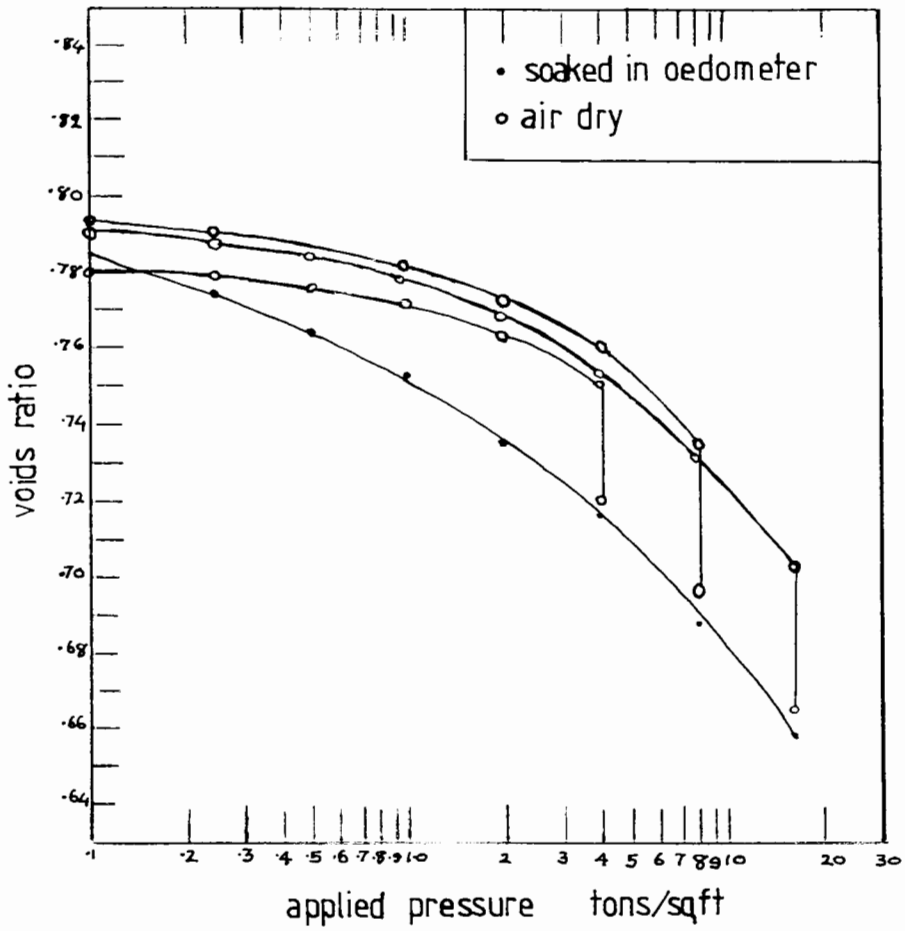

FIG 1.7 OEDOMETER CURVES FOR AIR-DRY SAMPLES SOAKED AT CONSTANT APPLIED PRESSURES

JENNINGS AND BURLAND (1962)

(2) keeping (σ_3-u_a) constant and varying the initial compaction water content and (u_a-u_w).

Fig (1.8) shows the correlation between χ and the degree of saturation for different type of soils. Although the relationship between χ and the degree of saturation is different for each soil, all the curves follow a similar trend.

They calculated values for the parameter χ for different stress paths (using Bishop's method) and found that the parameter χ was path dependent. The changes in (u_a-u_w) were almost invariably accompanied by significant changes in χ values. This implied the parameter χ was not a unique function of the degree of saturation. They concluded that equation(2) could be succesfully used to predict the failure shear strength since it is controlled by the inter granular stress at the time of failure, but not the volume change behaviour where the stress path is primarily important.

Matyas and Radhakrishna (1968) suggested that volume change behaviour can be expressed as a function of two independent stress components $(\sigma-u_a)$ and (u_a-u_w), forming a three dimensional constitutive surface rather than by a single effective stress equation (2).

$$e=F[(\sigma-u_a),(u_a-u_w)]$$

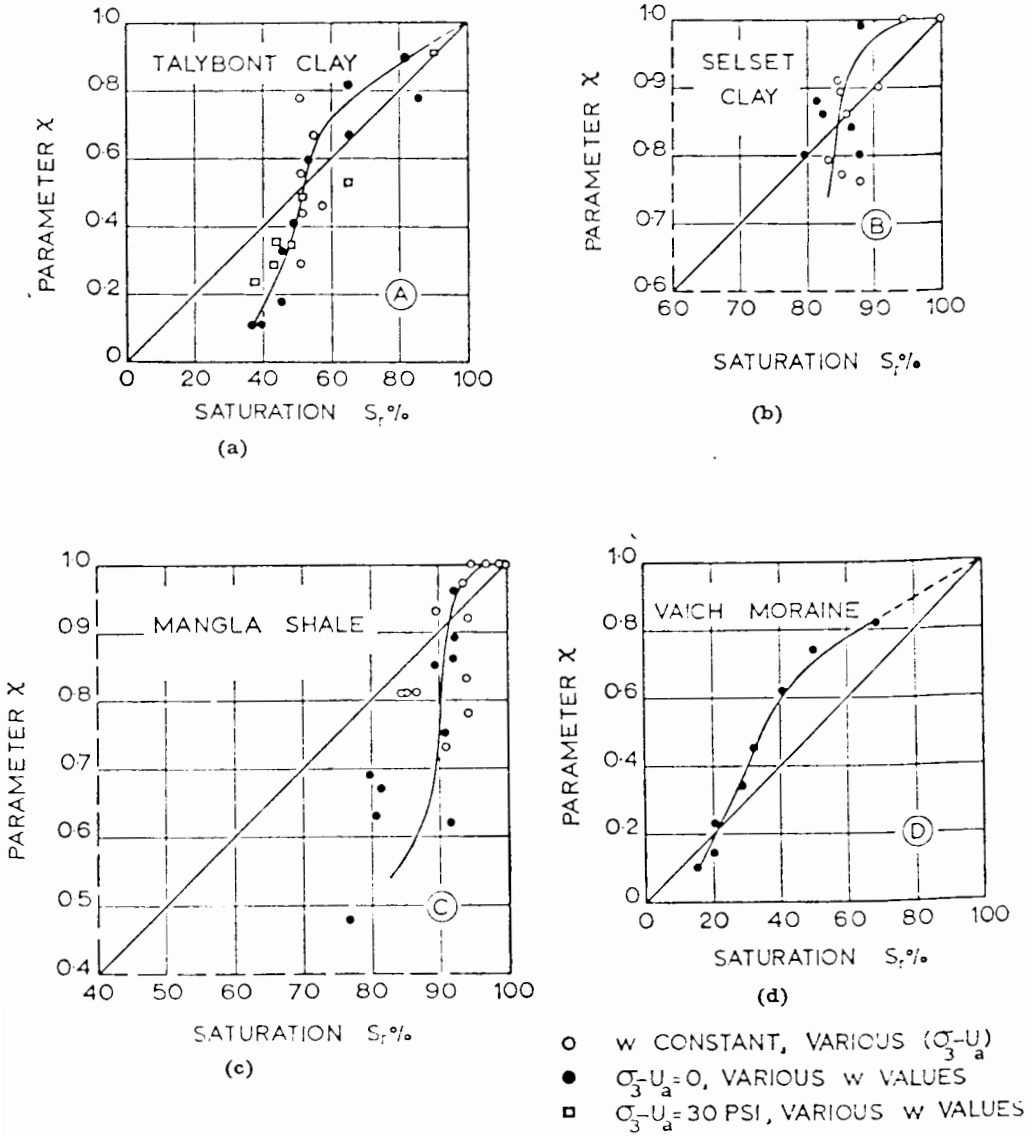

FIG 1.8 VARIATION OF THE PARAMETER X WITH DEGREE OF SATURATION S_r FOR FOUR COMPACTED PARTLY SATURATED SOILS VALUES WERE DETERMINED FROM TRIAXIAL COMPRESSION TESTS

BISHOP AND BLIGHT (1963)

and

$$S=\Phi[(\sigma-u_a),(u_a-u_w)]$$

They confirmed this by isotropic compression tests on unsaturated clays. They followed different stress paths (including the stress paths Jennings and Burland (1962) had followed) and interpreted their results in terms of a unique three dimensional constitutive surface in e, $(\sigma-u_a)$, and (u_a-u_w) space.

Fredlund (1978) showed that the above stress parameters $(\sigma-u_a)$, (u_a-u_w) could be used to describe the shear behaviour as well as the volume change behaviour of the soil. He expressed the behaviour of the soil mathematically as follows:

Volume change behaviour of soil:

$$e=e_1+ A \ln(\sigma-u_a) +B \ln(u_a-u_w)$$

where A,B are constants and e_1 is voids ratio of the soil at unit stress.

Shear behaviour of the soil:

$$\tau=(\sigma-u_a)\tan\Phi' +(u_a-u_w)\tan\Phi_b+C$$

where Φ' is the angle of friction from drained triaxial test on saturated soil.

Φ_b is the friction angle with respect to changes in (u_a-u_w) obtained from triaxial tests on unsaturated soil for known (u_a-u_w).

The gassy soils encountered in the marine environment appear to exist at degrees of saturation from about 80% upwards. The pore fluid pressures are high and gas may exist in isolated bubble form. The pore pressure measuring systems are expected to register only the pore water pressure in these gassy soils since the pore gas continuity is poor (Fredlund 1978). In order to apply the existing theories for unsaturated soil to the soils of high degrees of saturation, it is necessary to measure the pore gas pressure which is difficult to achieve. Therefore some assumptions have to be made in order to predict the behaviour of the gassy soil in terms of effective stresses. ie. an alternative approach, with assumptions that obviate the need for measurement of the pore gas pressure. Total stress σ and pore water pressure u_w are measurable while pore gas pressure u_a is difficult to obtain.

The development of the effective stress laws over the past years can be summarised as follows:

(1) Terzaghi:- $\sigma' = \sigma - u_w$ for saturated soils

$\tau = \sigma' \tan\Phi' + C$

$e = e_o + A\ln(\sigma')$

(2) Bishop:- $\sigma' = (\sigma - u_a) + \chi(u_a - u_w)$

only for shear strength of partly saturated soils

(3) Matyas:- volume change behaviour of partly saturated soil could be described

in terms of two independent stresses $(\sigma-u_a)$ and (u_a-u_w) rather than by a single effective stress.

(4) Fredlund:- $e=e_o+A\ln(\sigma-u_a)+B\ln(u_a-u_w)$

$\tau=(\sigma-u_a)\tan\Phi'+(u_a-u_w)\tan\Phi_b+C$

Φ'-angle of friction from drained triaxial tests on saturated soil.

Φ_b-friction angle with respect to changes in (u_a-u_w) obtained from triaxial tests on unsturated soil for known (u_a-u_w).

1.3 PURPOSE AND OUTLINE OF THIS THESIS:

Field tests on gassy marine soil indicate that these gassy soils are very soft, frequently under consolidated, unstable, compressible and possess low shear strength and positive excess equilibrium pore water pressures. It is not known whether these characteristics arise only from the presence of gas or are due to other events such as wave or storm loading, rapid rates of sedimentation or a combination of all these factors. A study of the effect of these factors individually on the marine sediments is valuable in order to understand these phenomena associated with gassy marine soils.

This thesis is devoted to an examination of the effect of gas on the behaviour of a estuarine soil. Most of the testing is performed on reconstituted soil (clayey silt) which contains artificially produced gas bubbles, rather than on core samples from a gassy sea bed due to the difficulties involved in obtaining undisturbed samples. The reconstituted soil is consolidated from a suspension under its own weight or by external loads to examine the following properties of gassy soil:

(a) Do these gassy samples attain full consolidation for a given stress as does the saturated soil?

(b) Do gassy samples possess equilibrium undissipated excess pore water pressures? How does the gas affect the dissipation of pore pressures and settlement rates and magnitudes?

(c) What form of effective stress law is appropriate for gassy soil?

(d) Do gassy soils possess very low shear strength?

In addition to answering the above questions which arose primarily from the field measurements in gassy soil, a field instrument has been developed to study the pore water pressure behaviour of gassy sediments for tide and wave action. This instrument can also be used, in certain conditions and with the measurement of the stress-strain properties of the soil, to assess the in-situ degree of saturation of the marine soil.

CHAPTER 2

PREPARATION OF RECONSTITUTED GASSY SAMPLES

2.1 Introduction

2.2 Method of preparation of partially saturated samples

2.3 Technique used to prepare gassy soil

2.4 Properties of zeolite

2.5 Gassy soil preparation

2.6 Calibration of gassy soil for degree of saturation

2.7 The appearance of gassy soil

2.8 Effect of zeolite on the properties of soil

CHAPTER 2

PREPARATION OF RECONSTITUTED GASSY SAMPLES

2.1 INTRODUCTION:

In order to understand the fundamental behaviour of gassy soil, both laboratory and field measurements are required. However the difficulties associated with testing natural, undisturbed gassy soil samples in the laboratory are formidable as, in addition to the normal problem of sample disturbance, the gas in the soil will expand as the confining pressure is reduced, causing irreversible damage. However, if reconstituted soil samples can be made in the laboratory containing a uniform, repeatable distribution of gas bubbles, then a test programme can be undertaken to discover the effect of different gas contents in otherwise identical samples on characteristics such as compressibility and shear strength. From this comparison, it should then be possible to develop theoretical models for gassy soil behaviour, and to determine when these models must be used in design calculation. This chapter describes a successful method of laboratory preparation of reconstituted gassy soil.

2.2 THE METHODS USED FOR THE PREPARATION OF PARTIALLY SATURATED SOIL:

Some of the techniques that have been used to prepare three phase soil samples consisting of solids, water and gas in order to study the behaviour of onshore partially saturated soils are:

(a) Compaction: Bishop(1960), Matyas and Radhakrishna (1968)

The specimens for triaxial tests were prepared by mixing dry soil (silty clay) with a known percentage of water and statically compacting the mixture to an arbitrary density. This was achieved by compressing a predetermined weight of soil into one inch thick layers in a compression machine at a steady rate of 2.0mm/min. This method provided a close control of dry density. The specimen is sealed after mounting on the triaxial base and left for 10 hours for the pore water pressures to reach equilibrium values.

(b) Drying saturated soil: Jennings and Burland (1962)

The soil at its liquid limit was placed in moulds and left in the atmosphere to dry. At various stages in the drying process the samples were remoulded and placed under sealed jars for 7 days to allow time for moisture equilibrium in the samples.

(c) Application of suction pressure: Bishop(1960)

The initial degree of saturation of the triaxial samples (prepared by the compaction method) was varied by adjusting the pore water and pore air pressures. The degree of saturation is calculated from the measurements of the air and the water volume changes during the application of initial suction.

The above methods yield largely interconnected air voids and pore suctions (u_w is less than atmospheric pressure) in the soil. Therefore a different technique is used to prepare gassy soil with bubbles.

2.3 TECHNIQUE USED TO PREPARE GASSY SOIL:

Methane was selected as the gas medium in the soil to duplicate the field condition by matching the solubility and surface tension effect. Blowing pressurised methane gas into saturated soil through a fine porous stone or chemically producing methane by mixing aluminium carbide with saturated soil were tried initially to produce gassy soil, with little success because these methods create large bubbles rapidly in the soil which escape from the soil while mixing it to obtain uniform distribution of bubbles. However an alternative approach using an inert synthetic substance called Zeolite which is used as a molecular sieve in the chemical industry to absorb gas

selectively and recycle it, was successfully used to introduce methane bubbles into saturated soil.

The zeolite has the ability to take up gas molecules with smaller diameters than its pore size into its crystal structure, and then let them out in favour of polarised compounds such as water. When zeolite containing methane is mixed with saturated soil, methane gas bubbles are formed as the water molecules replace the methane. The release of methane from zeolite takes place over a period of some hours, hence allowing time for a thorough mixing of the zeolite with soil and remoulding into sample preparation moulds. Fine zeolite powder ensures good distribution of small methane bubbles in the soil.

2.4 PROPERTIES OF ZEOLITE:

Zeolites have a three dimensional framework with channels and inter-connecting cavities forming pores which normally contain water of hydration. A property unique to zeolite crystal is that the water of hydration can be driven off by heating without causing collapse of the crystal, which remains unchanged and robust with empty cavities or pores. The zeolite is then able to take into its crystal molecules of a suitable small size, and hold them until the opportunity arises to replace them. Synthetic zeolites developed by Union Carbide Linde Division (1954), have a regular crystal structure and

uniform pore size, and absorb only a narrow range in size of molecules smaller than its pore size. In this application, the dehydrated zeolite is impregnated with methane under pressure.

The choice of zeolite is made by comparing the molecular diameter of methane, which is 4.0 Angstrom, with the pore sizes available in different zeolite crystals. Calcium alumino silicate, $Ca_4Na_3(AlO_2)_7.SiO_2.30H_2O$ has a pore diameter of 5.0 Angstrom and can be obtained in powder of particle size not greater than 6μm so that it mixes easily with clay size particles in a natural soil. Its mineral composition is not dissimilar to natural sediments, and its specific gravity of 2.41 is acceptably close to typical soil values between 2.60 and 2.70, so that adding a comparatively small proportion to a soil should not greatly affect the soil behaviour.

Zeolites have a very strong affinity for polar molecules such as water. When the methane impregnated zeolite is mixed with a soil slurry, it takes up water, which replaces the methane. The quantity of methane taken up by a given amount of zeolite, and subsequently expelled will depend on a number of factors, including the temperature, pressure at which the methane is absorbed, the time for methane absorption, the length of time elapsed since the zeolite encountered water and the ambient pressure during this time. It will also depend on the soil itself, since the solubility of methane in clay

soil is probably lower than its solubility in water. In particular, the relative importance of absorption pressure and time on the production of methane was examined, using the experimental procedure as follows:

The zeolite was dried at a temperature of 105^{O}C for 24 hours, and then held in a vacuum of -100 kN/m^2 for 8 hours in a sealed cylinder. This procedure makes the largest possible pore volume of the zeolite available for occupation by methane. The zeolite is then pressurised by methane at different pressures and for different periods in the same cylinder without exposing it to the atmosphere to avoid air absorption by the zeolite. Subsequently 25g of zeolite is mixed in water and placed in a 250ml beaker (fig 2.1) which is then filled with water. The beaker is fitted with a rubber stopper and a drain tube. Water from the beaker is displaced through the tube as the gas is generated and its volume is monitored using a measuring cylinder. The volume of water displaced is a measure of the volume of gas released from the zeolite. The effect of water pressure on the release of gas is also studied. The water pressure (back pressure) is varied by placing the beaker and the measuring cylinder in a separate container which can be sealed and pressurised.

Fig 2.2 shows the effects of varying the time allowed for absorption of methane at an absorption pressure of 200kN/m^2. The longer the time allowed for absorption, the larger the ultimate volume of methane produced. Twenty

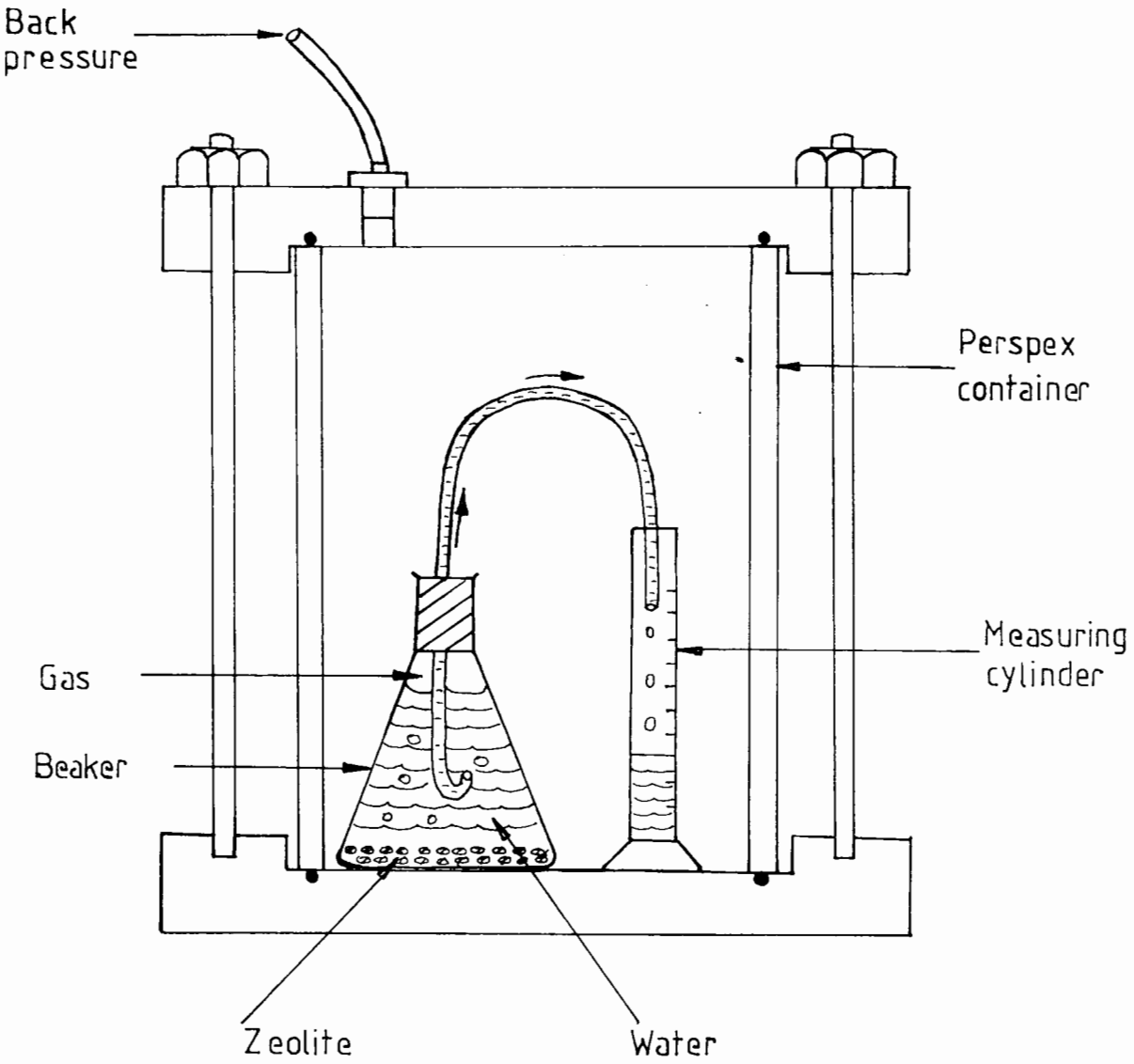

Fig 2.1 Schematic diagram of the apparatus used to measure the properties of the zeolite

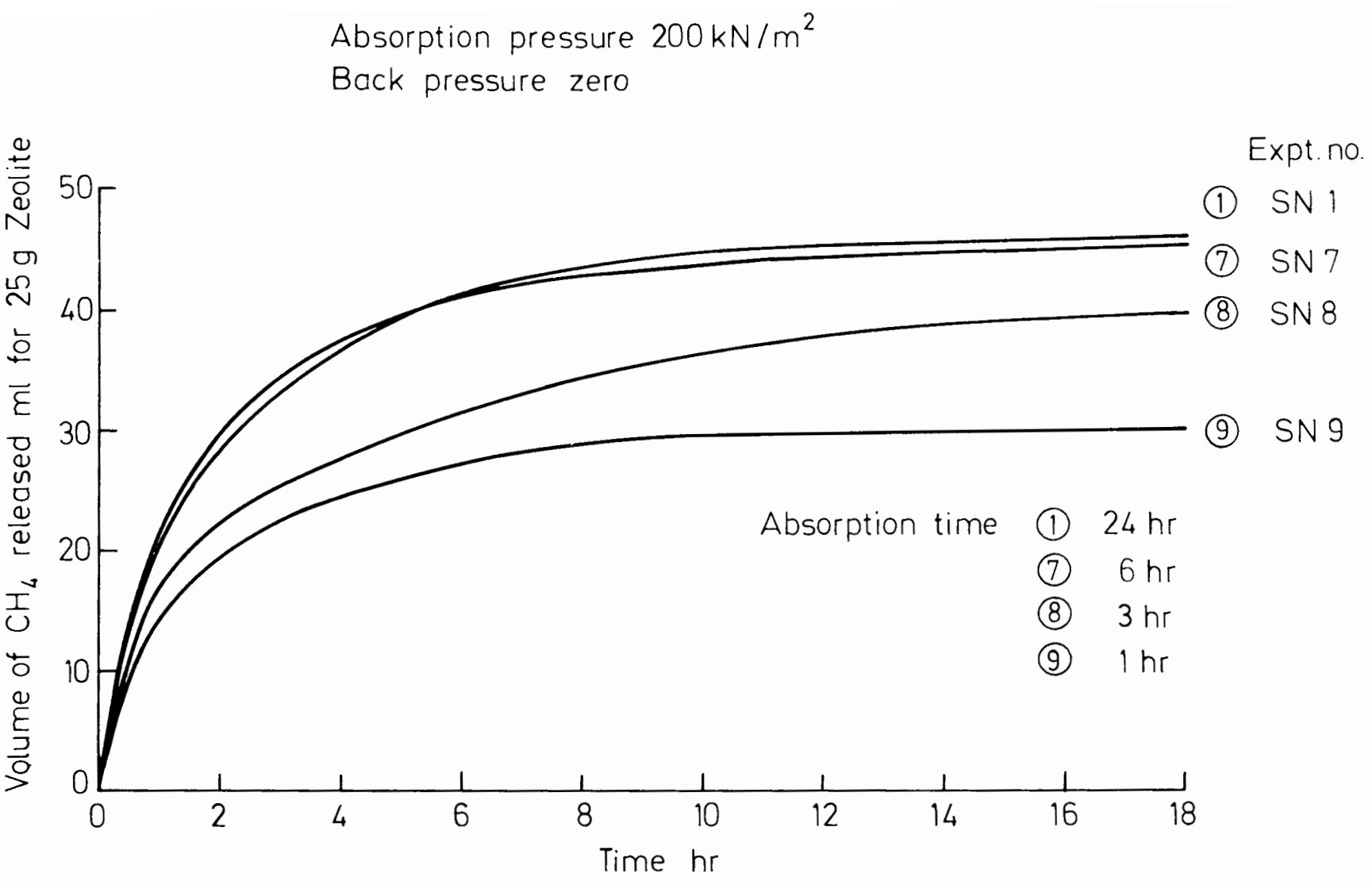

Fig 2.2 Effect of absorption time on subsequent methane production at atmospheric pressure

four hours of absorption is considered a suitable time of absorption for the subsequent work. Similarly, fig 2.3 shows that, for a constant absorption time of 24 hours, the higher the absorption pressure, up to 100 kN/m^2, the larger the ultimate volume of methane produced. The actual gas volume produced in soil may be some what higher due to differences in methane solubility. Both figures show that the time taken to release practically all the captured methane lies between 7 and 12 hours. This will normally allow time to prepare the reconstituted soil containing the zeolite for testing without too much loss of gas. The effect of back pressure on the production of methane is also examined. Fig 2.4 shows the evolution of gas from 25g of zeolite (saturated in methane at a pressure of $200kN/m^2$ for 24 hours) in water under pressure. At the highest back pressure of $300kN/m^2$, the volume of gas is about 11 ml: on reducing the pressure, this volume increases immediately to about 43 ml at atmosperic pressure. This value is close to the maximum value obtained in the experiment where no back pressure is applied , indicating the replacement process of methane by water is not affected by the water pressure.

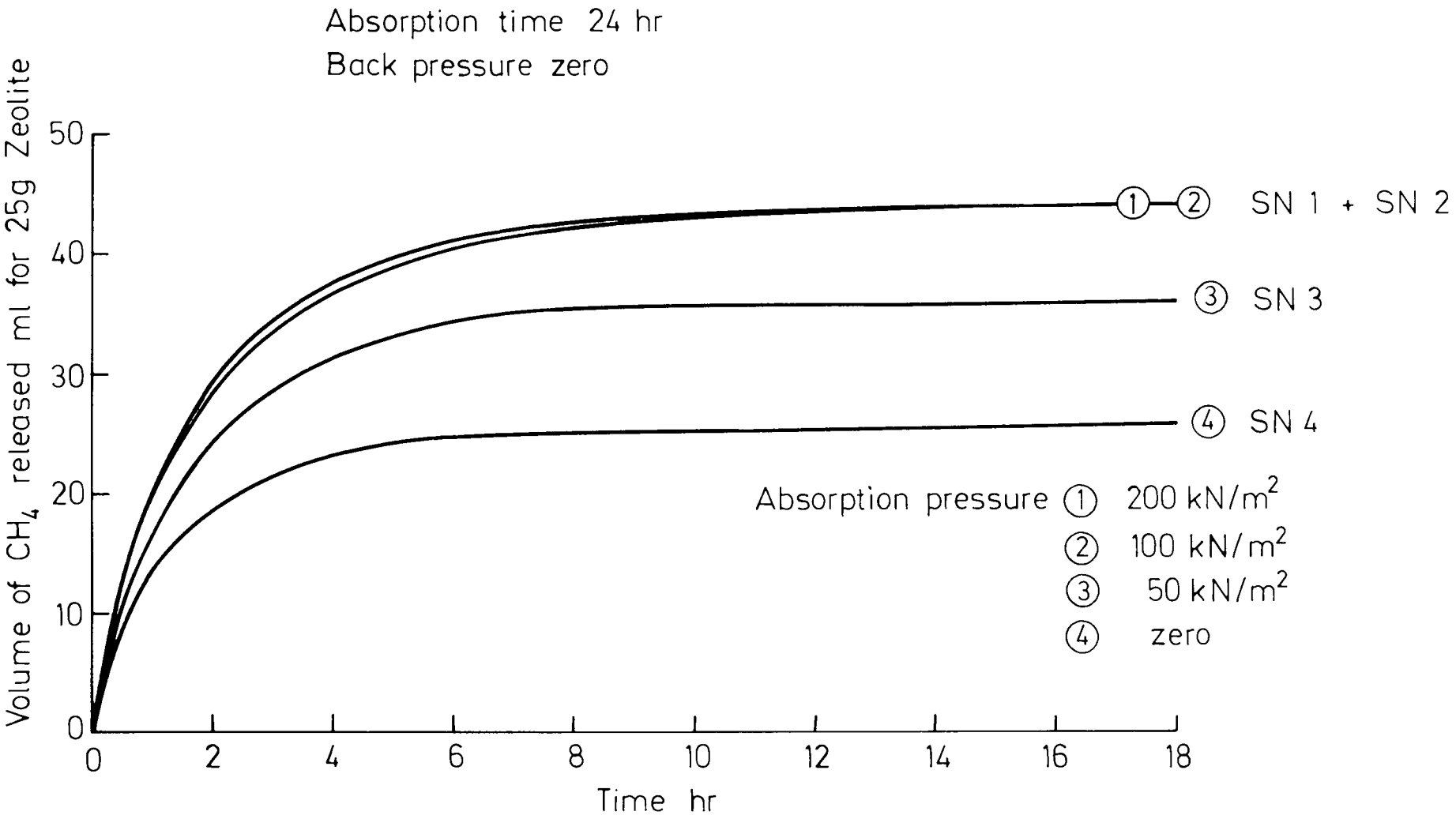

Fig 2.3 Effect of absorption pressure on subsequent methane production at atmospheric pressure

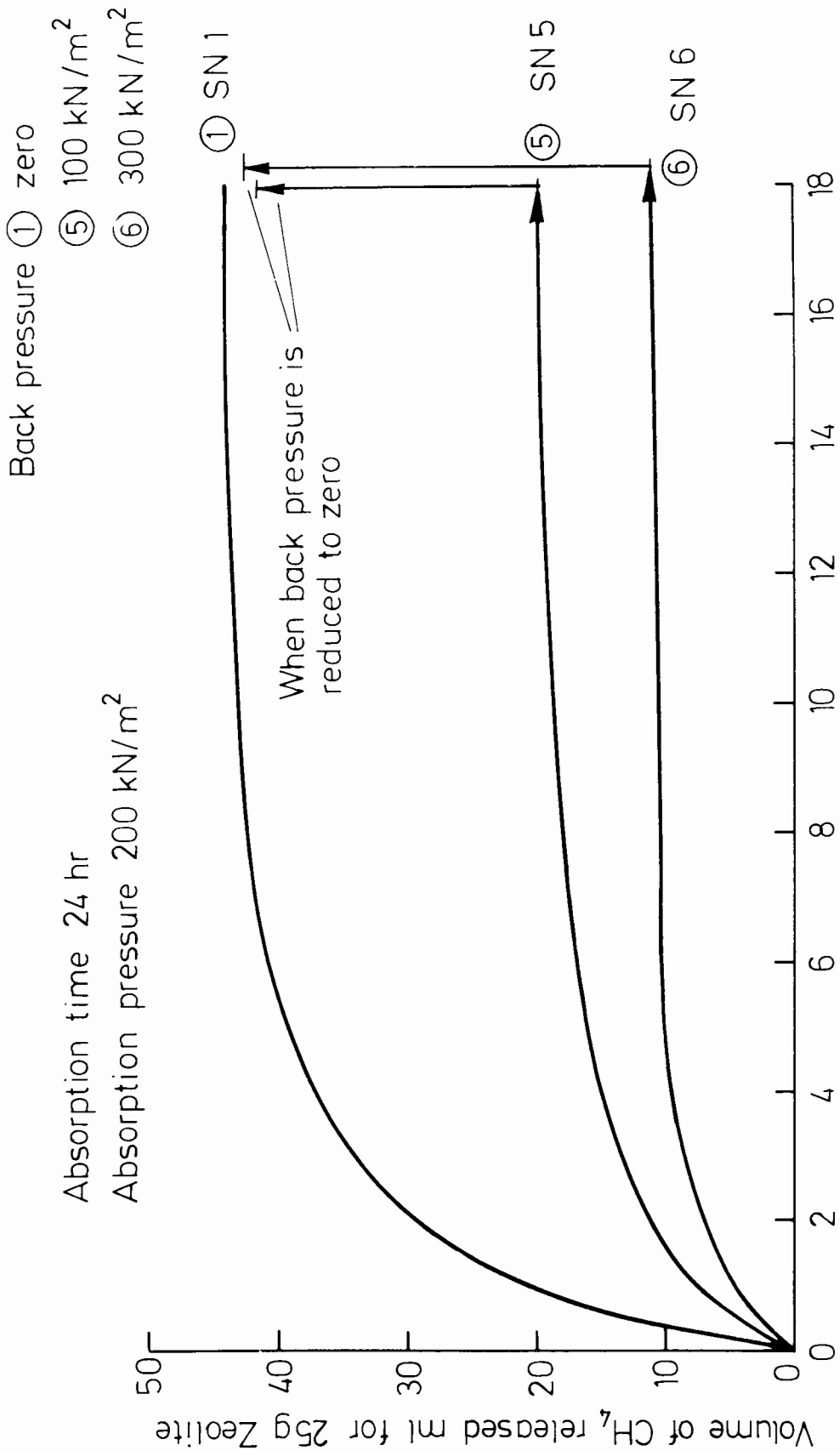

Fig 2.4 Methane production under increased pressures

2.5 GASSY SOIL SAMPLE PREPARATION

An estuarine clayey silt taken from the river Parrett at Combwich in Somerset, England is used to prepare the gassy soil samples. A typical particle size distribution is shown in fig 2.5. The liquid and the plastic limits of the soil are 62% and 31% respectively. The soil is mixed with water to obtain a slurry at a moisture content of 150% (corresponding to a unit weight of 12-13kN/m^2, at a density 1.2-1.3g/cc) and treated zeolite is added and mixed thoroughly for a few minutes before being placed in a specially designed consolidation cell or in a sample preparation mould. The suitable water content for the slurry will depend on the specific soil, but the aim is for the lowest value consistent with uniform mixing of the zeolite (very wet mixture will result in loss of gas bubbles while mixing).

The degree of saturation achieved in the soil sample will depend on the sample preparation process, the treatment of the zeolite and the soil type. In order to obtain a repeatable degree of saturation for a given amount of zeolite, the following processes are strictly observed.

(a) The zeolite is dried for 24 hours at 105^{0}C.

(b) The zeolite is evacuated for 8 hours at -100kN/m^2.

(c) The zeolite is pressurised by methane gas for 18 hours at 200kN/m^2.

(d) The zeolite is mixed with soil slurry (at a

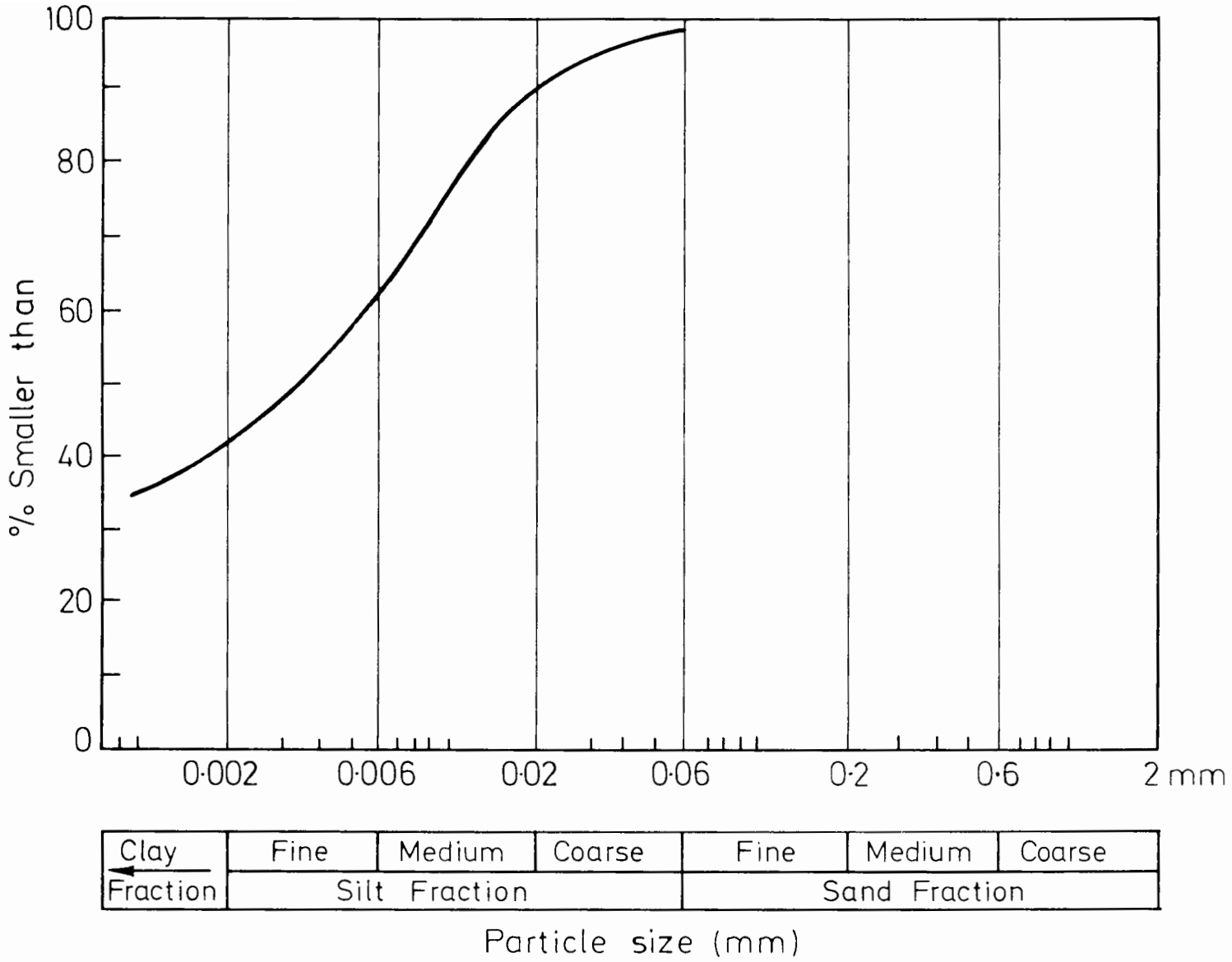

Fig 2.5 Particle size distribution of combwich 4 mud

moisture content of 150%) for one minute.

(e) The resulting slurry is transferred into sample moulds without further delay.

(f) The slurry is allowed to stand for 24 hours for all the gas bubbles to develop before any testing is carried out.

2.6 CALIBRATION OF GASSY SOIL FOR DEGREE OF SATURATION.

Gassy soil prepared by the method described is calibrated for degree of saturation against the amount of zeolite used to prepare it. This will allow the preparation of a gassy soil sample of the required degree of saturation by adding the required amount of zeolite obtained from the calibration curve.

The measurement of degree of saturation is performed on consolidated soil samples rather than on the slurry due to the difficulties involved in handling the slurry without loss of gas during measurement. Consolidation is carried out in a 38 mm diameter and 100 mm high perspex mould using porous pistons on both ends and dead weights. Both water and gas flow out of the sample during consolidation, changing the degree of saturation and all the calibration samples are consolidated to 35 kN/m^2 vertical stress. The degree of saturation measured from these samples will correspond only to that particular stress level at atmospheric pressure.

The degree of saturation is measured gravimetrically. The wet weight of the sample, the total volume of wet sample, the dry weight of the sample and the specific gravity of the soil/zeolite mixture are necessary for the calculation of the degree of saturation. The total wet volume of the sample is measured by measuring the weight of the displaced water by the sample and this causes most of the uncertainties in the calculation. Fig 2.6 shows the relationship between the measured degree of saturation of samples consolidated to 35 kN/m^2 and the amount of zeolite used. The repeatability of the measured degree of saturation for a given amount of zeolite is ±2%.

2.7 THE APPEARANCE OF GASSY SOIL.

The effect of gas bubbles on the appearance and the texture of the soil sample can be seen clearly in Fig 2.7, 2.8 and 2.9. All these photographs show soil samples that have been consolidated in an oedometer from a soil/zeolite slurry and dried. In fig 2.7, the consolidation pressure was $35kN/m^2$ and the sample thickness was 30 mm with a degree of saturation of about 80%. The bubbles appear to be uniformly distributed throughout the sample. In fig2.8, the soil has 80% degree of saturation at $35kN/m^2$ consolidation pressure, but was consolidated under a total stress of $560kN/m^2$ and has a final thickness of 15mm. Again, the bubbles are well distributed, although the

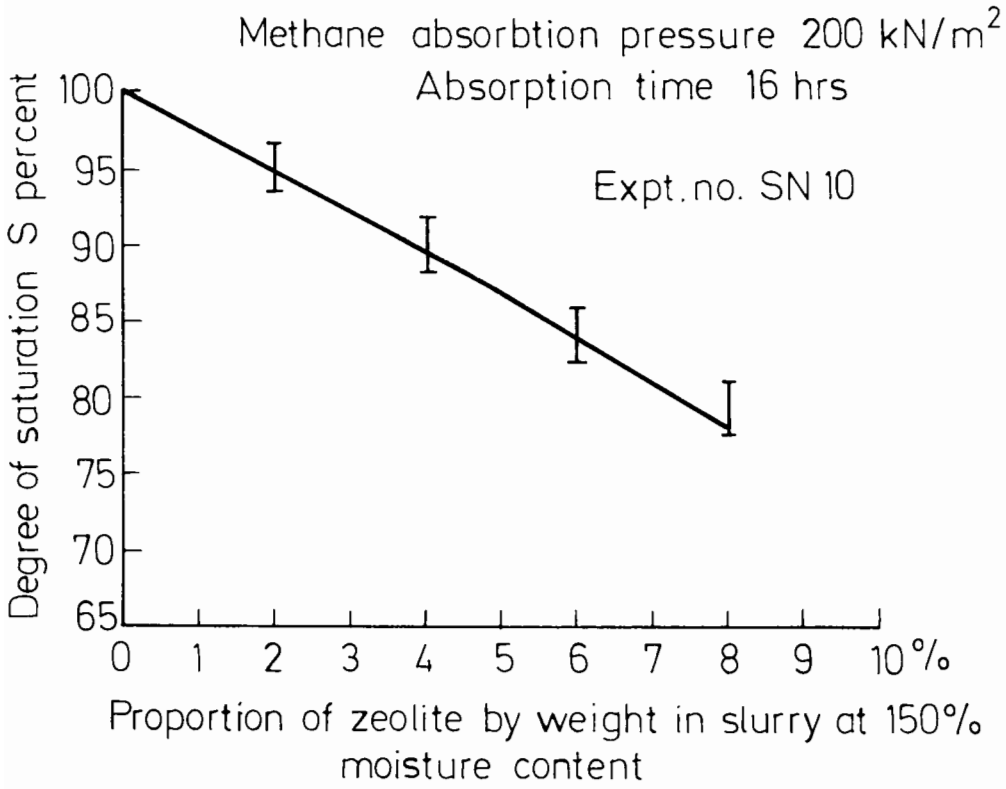

Fig 2.6 Relationship between zeolite content and degree of saturation of soil achieved at atmospheric pressure

Fig. 2.7 Appearance of gassy soil, magnified X 6
Degree of saturation 80% Compressed to 35 kN/m^2

Fig 2.8 Appearance of gassy soil, Magnified X 6,
Degree of saturation 80%, Compressed tO 560 kN/m^2

compression of the sample has squeezed some gas bubbles out of the sample and flattened the remaining bubbles. Fig 2.9 shows the same soil, consolidated under 560kN/m^2 without any gas bubbles, with a final thickness of 15mm. This photograph is therefore directly comparable with fig 2.8.

Fig 2.10 shows the appearance of gas bubbles in a very soft soil (voids ratio between 4.5 - 5) which has been settled from a slurry of density 1.05g/cc in a long perspex tube. The bubbles are generally spherical due to the low stress level in the soil.

2.8 EFFECT OF ZEOLITE ON THE PROPERTIES OF SOIL.

The addition of large quantities of zeolite to the soil is not desirable because of its thixotropic nature. Thixotropy is defined as the property of a material that enables it to stiffen in a relatively short time of standing, but upon agitation to change to a very soft consistency. The lowest degree of saturation obtained using this method is limited to 80% and this slurry will contain zeolite of weight equal to 7% of the slurry weight. This corresponds to a zeolite proportion of the total solid phase of the soil of about 17% by weight.

Fig 2.11 shows the effect of saturated zeolite on the stress-strain (voids ratio-effective stress) curve of saturated soils. These plots are the results of oedometer tests on saturated soils with different amount of water

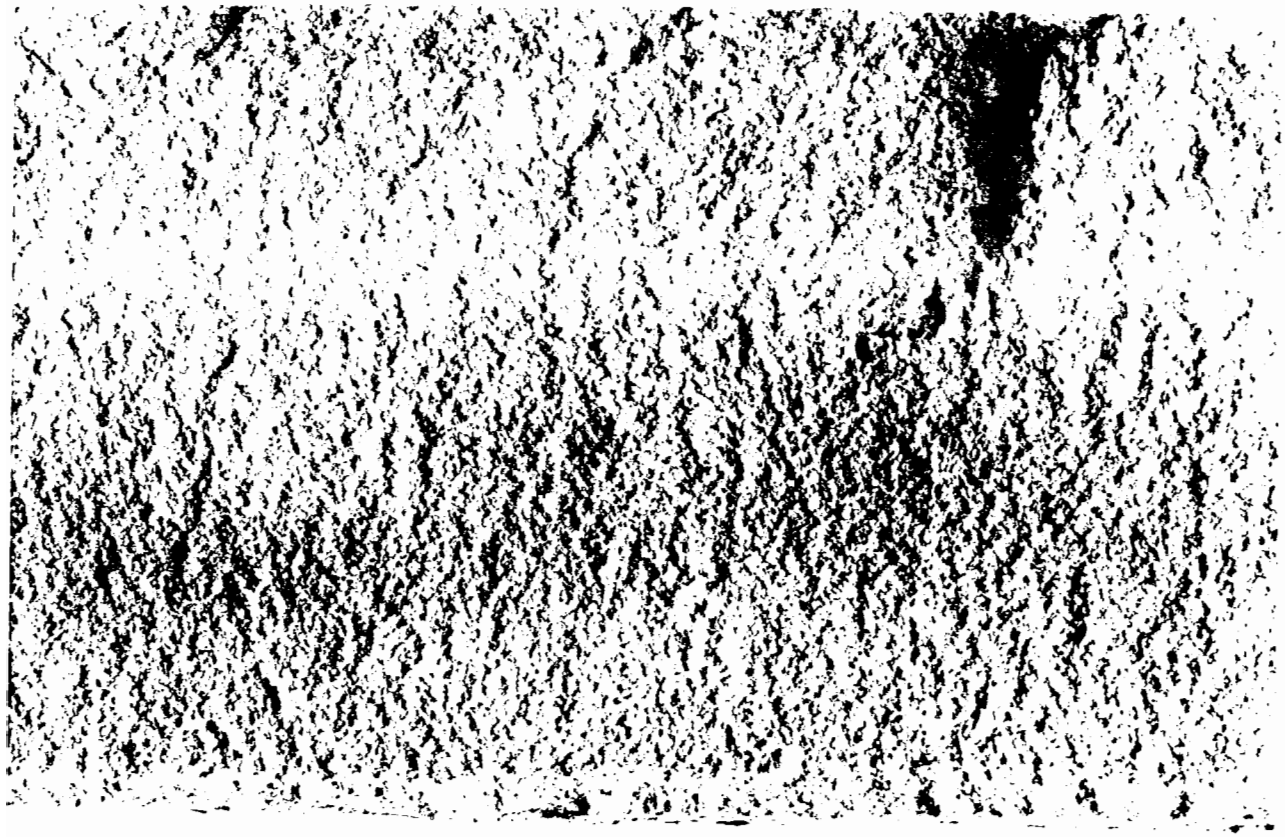

Fig 2.9 Appearance of fully saturated soil, magnified X 6
Compressed to 560 kN/m^2

Fig 2.10 Appearance of gas bubbles in soft sediment.

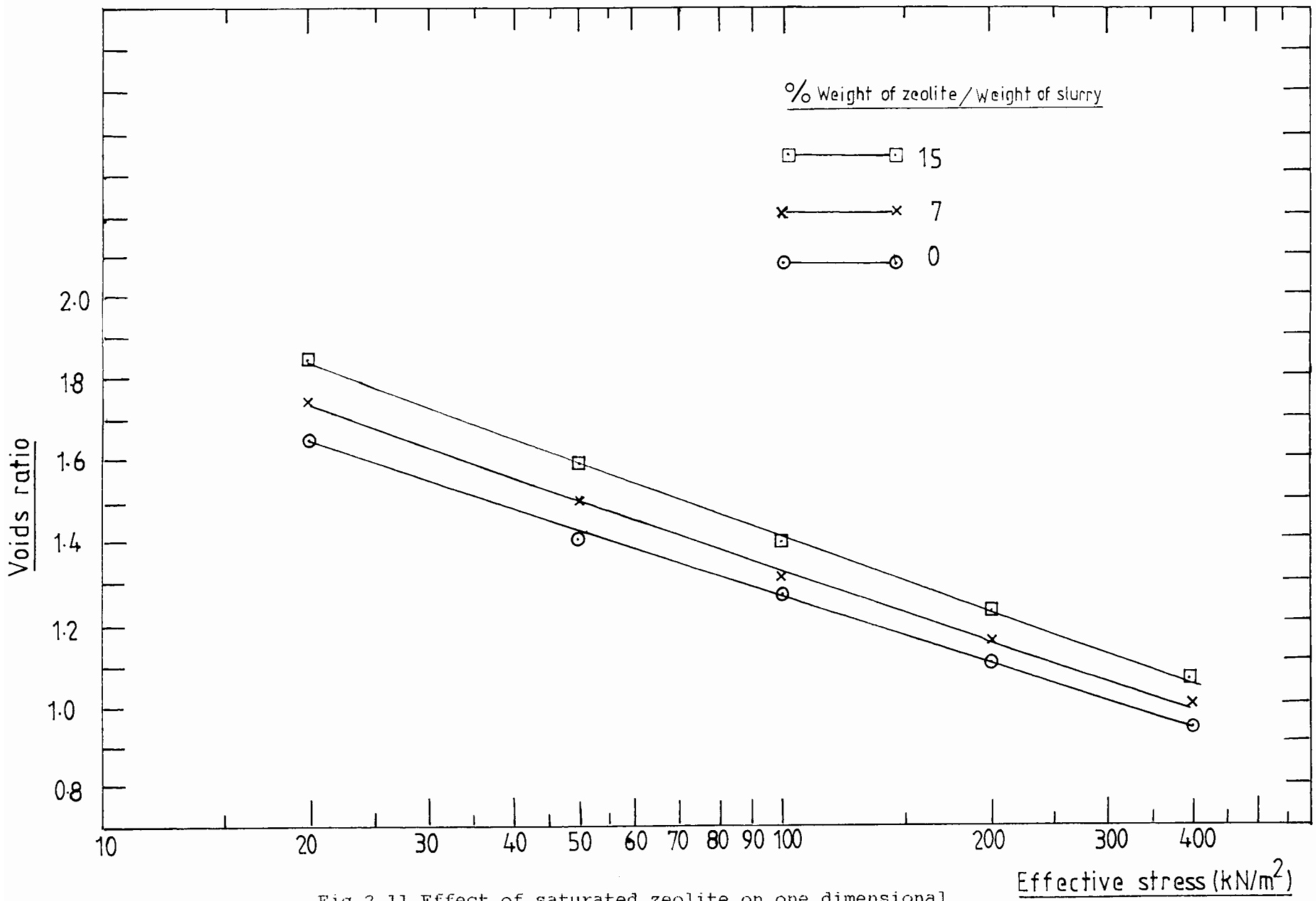

Fig 2.11 Effect of saturated zeolite on one dimensional consolidation (stress-strain) behaviour of soil.

saturated zeolite. The void ratios are calculated from the final moisture content obtained by drying the soil samples at 105^{0}c for 24 hours. Drying will remove not only the free water in the voids, but also the water absorbed by the zeolite since it absorbs water as it liberates gas and this water can not be expelled by consolidating the soil. Therefore the moisture content of the soil sample containing zeolite will be higher than that of the soil sample without zeolite, but consolidated to the same pressure. The shift in the voids ratio - effective stress curves results primarily from the error caused by the measurement of final moisture.

When comparing the properties of gassy samples (which contain zeolite) with those of the saturated sample, it is necessary to eliminate the effect of zeolite on the properties of soil. This could be achieved by adding water saturated zeolite to all the samples in order to make the total zeolite content the same. Control samples of saturated soil are prepared by adding 7% water saturated zeolite. By comparison, an 80% degree of saturation gassy soil contains 7% methane saturated zeolite. Dry zeolite normally contains air and water vapour, therefore full saturation of zeolite is achieved by soaking it in water for 24 hours.

CHAPTER 3

EFFECT OF GAS BUBBLES ON THE VOLUME CHANGE BEHAVIOUR OF SOIL

3.1 Introduction

3.2 Self weight consolidation.

3.3 Stress controlled consolidation (oedometer) tests.

3.4 Experimental observations.

3.5 Discussion of the results.

3.6 A model to describe the volume change behaviour of gassy soil.

3.7 Conclusion.

CHAPTER 3

EFFECT OF GAS BUBBLES ON THE CONSOLIDATION BEHAVIOUR OF SOIL

3.1 INTRODUCTION

Marine sediments containing undissolved gas bubbles are frequently underconsolidated and possess excess pore water pressures under equilibrium conditions. Several factors such as wave action, rapid sedimentation, presence of gas bubbles or a combination of all these may contribute to the above state. The contribution of gas bubbles to these effects is examined in this chapter by carrying out one dimensional consolidation tests on a gassy soil starting from a very soft slurry stage. This is an approximation of the formation of the sea bed by deposition of sediment. The consolidation of the soil is carried out by settling the soil from a suspension (self weight consolidation) or by applying external stresses (oedometer tests). The suitability of the effective stress law for predicting volume change behaviour of gassy soil is also examined.

SECTION 3.2

SELF WEIGHT CONSOLIDATION.

3.2 SELF WEIGHT CONSOLIDATION OF GASSY SOIL

The effect of gas bubbles on the consolidation behaviour of very soft soil consolidating under its own weight is examined in the following experiment. A comparison is made between soils with degrees of saturation 80% and 90%, with the fully saturated soil (100%).

3.2.1 Experiment:

A soil water slurry at a density of 1.1g/cc is made from a natural estuarine clay slurry by adding water to obtain the required density. Different quantities of gas bubbles are introduced in the slurry by the addition of different amounts of zeolite treated with methane (ref:chapter two). The amount of zeolite added to 800ml soil slurry is as follows:

Degree of saturation%	Amount of zeolite
80	60g treated
90	30g treated + 30g saturated
Saturated soil(100)	60g water saturated

The above figures are obtained from the calibration curve showing degree of saturation against the amount of zeolite used, fig(2.5), even though this curve is strictly applicable to a soil of density 1.5 g/cc. Each sample is mixed with the required amount of zeolite and the suspension is allowed to settle in perspex columns of 50mm

diameter, 450mm height. The process is performed quickly to avoid gas escape from the suspension. The samples were allowed to settle until they reached equilibrium and the final height of the samples and their dry solid weights were measured.

3.2.2 Observations:

Except in the saturated soil, gas bubbles started to appear in the suspensions as they settled. Fig(3.1) shows the settlement time behaviour of these samples. The suspensions with gas bubbles did not start to settle immediately because the settlement was hindered by the release of gas bubbles from the zeolite. The final heights were measured after two months when all the movements had stopped and were different in each sample even though the dry solid volume of the samples were the same. The settled sample thickness increased with the increase in the amount of gas in the samples as shown in the photograph fig(3.2). The table below shows the variation in voids ratio (measured at the end of the experiment) with the gas content.

Type of soil (Degree of saturation)	Average voids ratio (e)
82%	6.1
89%	5.2
saturated(100%)	4.2

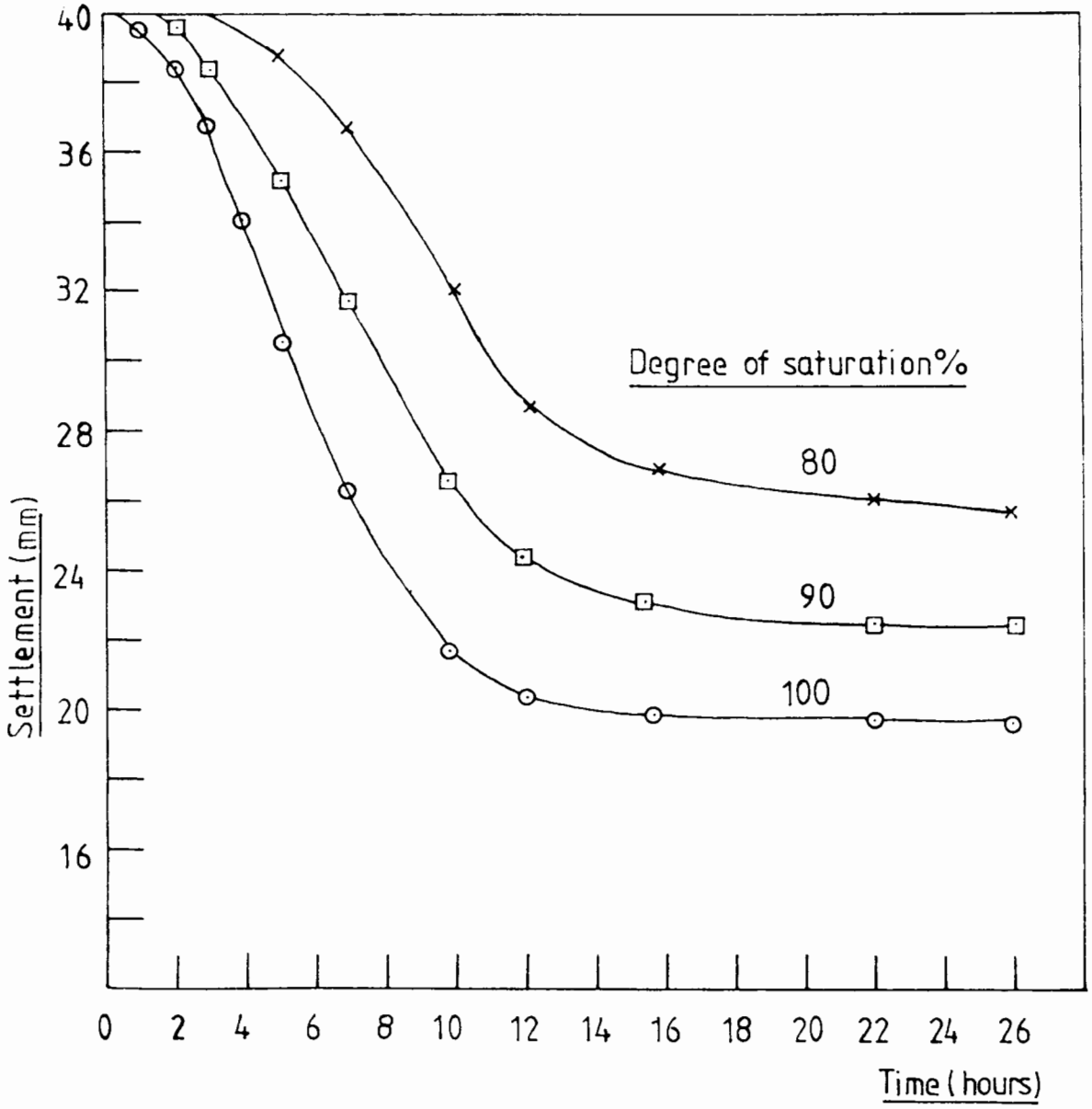

Fig 3.1 Surface settlement vs time, Experiment No. SN-S1

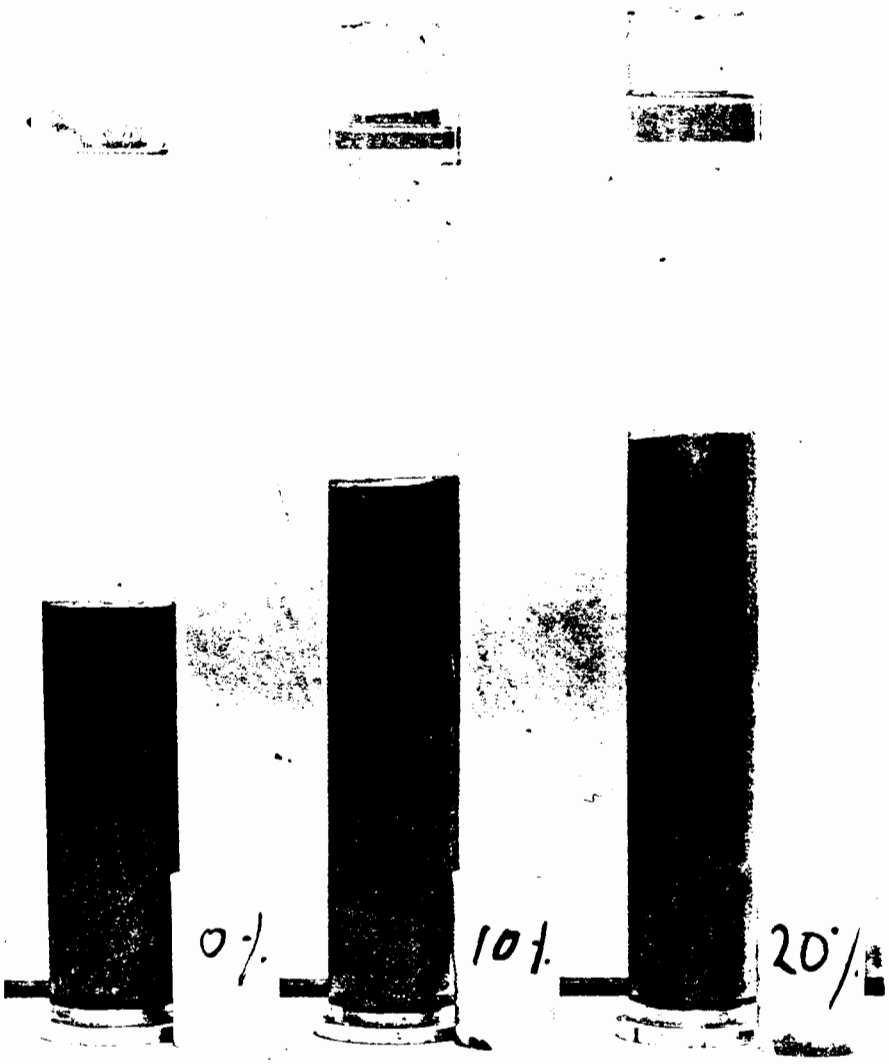

0% gas content----- 100% degree of saturation
10% gas content----- 90% degree of saturation
20% gas content----- 80% degree of saturation

Fig 3.2 Effect of gas bubbles on the settlement behaviour of soft soil.

3.2.3 Discussion of the results:

The above qualitative experiment suggests that the presence of gas bubbles affects the settling behaviour of the soil. The difference in the final heights indicates that the gassy soils have not attained the same degree of consolidation as the saturated soil even though the samples all reached equilibrium stage with no further settling. The voids volumes associated with gassy soils are higher (more loosely packed) than that of saturated soil. The following experiments are carried out in order to investigate these effects in detail.

SECTION 3.3

STRESS CONTROLLED CONSOLIDATION TESTS ON GASSY SOIL.

3.3.1 Description of the oedometer.

3.3.2 Preliminary tests.

3.3.3 Effect of porous stones on the measurement of pore fluid pressures.

3.3.1 DESCRIPTION OF THE OEDOMETER.

3.3.1.1 A brief discription of the oedometer and its mode of operation

Consolidation characteristics of gassy soil under the application of one dimensional stresses (K_o condition) is studied in a special oedometer which enables soil to be consolidated from a slurry stage to a stiff soil. The design and the instrumentation of the oedometer is based on the following considerations:

(a) It should be capable of handling a very soft gassy soil and the large strains associated with it.

(b) It should measure applied total stress, pore pressures and deformation of the soil during consolidation.

(c) It should allow free drainage of water and gas from the sample face and be able to monitor their volumes separately.

Fig (3.3) shows a schematic diagram of the oedometer. This comprises a cell, a piston and its bearing, a base and a top platen. In this oedometer gassy soil slurry is placed between the top platen and the piston and loaded from underneath. The gassy soil sample can be moulded directly from a slurry as soon as it is prepared and allowed to stand for 24 hours for all the gas bubbles to

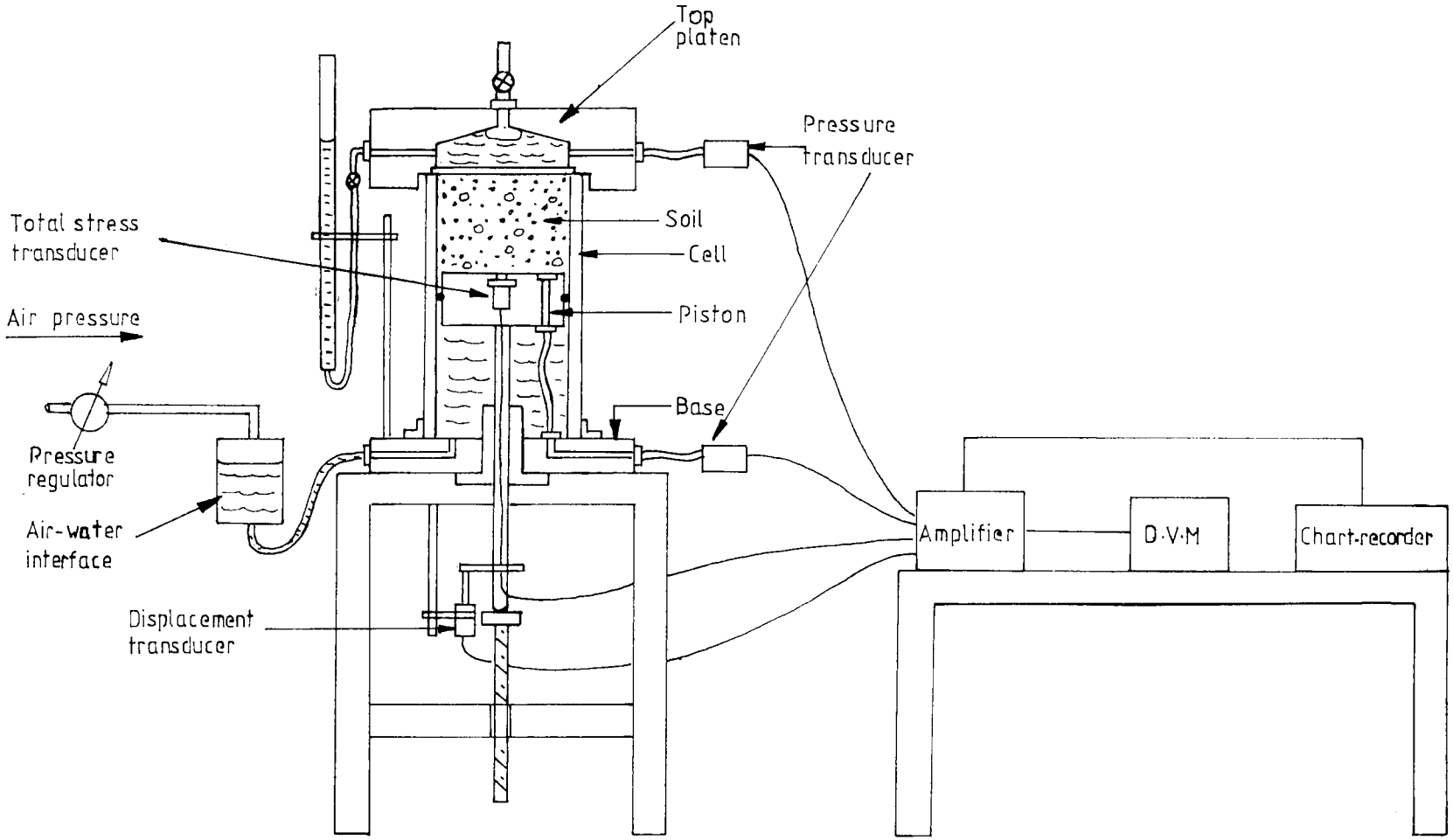

Fig 3.3 A schematic view of the oedometer and the measuring system.

develop without applying any external load on it (particularly the weight of the piston).

The piston is instrumented with a total stress transducer and a pore pressure probe. It is guided by a ram carrying the signal cables from the total stress transducer and the deformation of the sample is monitored by measuring the movement of the ram by a displacement transducer. A plain bush seated in the base is used to guide the ram for a smooth and linear movement. The part of the space in the cell underneath the piston is filled with water which connects through the base to an external pressure source used to drive the piston.

The space above the piston is filled with soil slurry and a highly porous bronze disc (air entry value 10 kN/m^2) is placed on top of the cell which acts as the drainage face. A domed shape top platen is placed over the disc and secured in place by three clamping rods which are threaded to the base. The above arrangement allows the sample to drain only from the top face. The bottom face remains undrained and the total stress and excess pore fluid pressures are measured on this face.

3.3.1.2 The oedometer

A diagram of the oedometer is shown in fig (3.4) in which each part has been numbered for identification. These numbers will be referred to in brackets when the corresponding parts are described in the following

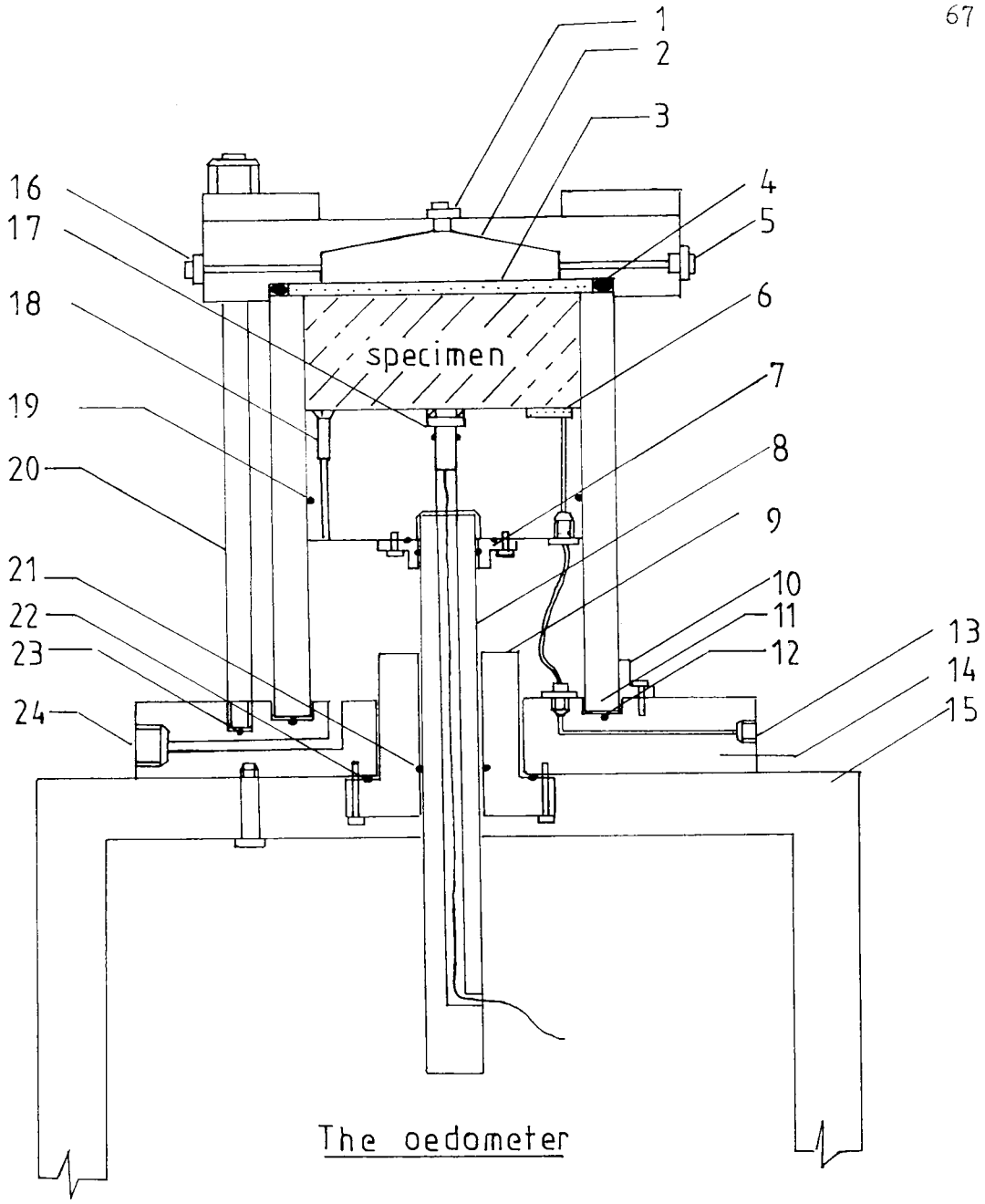

1. Drainage port
2. Perspex top cap
3. Porous plate
4. O- ring
5. Pore pressure port
6. Porous stone
7. Flange seal
8. Ram
9. Plain bush
10. Bracket
11. Cell
12. O-ring
13. Pore pressure port
14. Base
15. Table
16. Drainage port
17. Total stress transducer
18. Bleeding port
19. O-ring seal
20. Tie rods
21. O-ring
22. O-ring
23. O-ring
24. Pressure port
25. Piston

Fig 3.4 Oedometer.

paragraphs. A photograph of the complete assembly is shown in fig(3.5).

The Cell:

The cell(25) is made out of a stainless steel tube of 100mm internal diameter with 10 mm thick walls and 250 mm high. Three brackets(10) at 120^{o} to each other are welded near the lower end of this, and these are used to bolt the cell on to the base in the initial assembly.

The Base:

The base(14) is machined from a 25mm thick stainless steel plate to an overall diameter of 200 mm. A 50mm hole is cut in the centre of this to accommodate a plain bush(9). Further out there is a concentric groove(11) cut to act as a recess to accept the cell and an O-ring groove(12) is also provided within this to seal against the cell pressure. Outside this groove there are three threaded holes to which the cell can be bolted, and there are also three larger threaded holes(23) which are used to bolt the top platen to the base. Two outlets have been provided in the base, one for connecting to the cell pressure(24) and the other to the pore pressure transducer(13). The base is bolted to a main frame which is fixed to the floor.

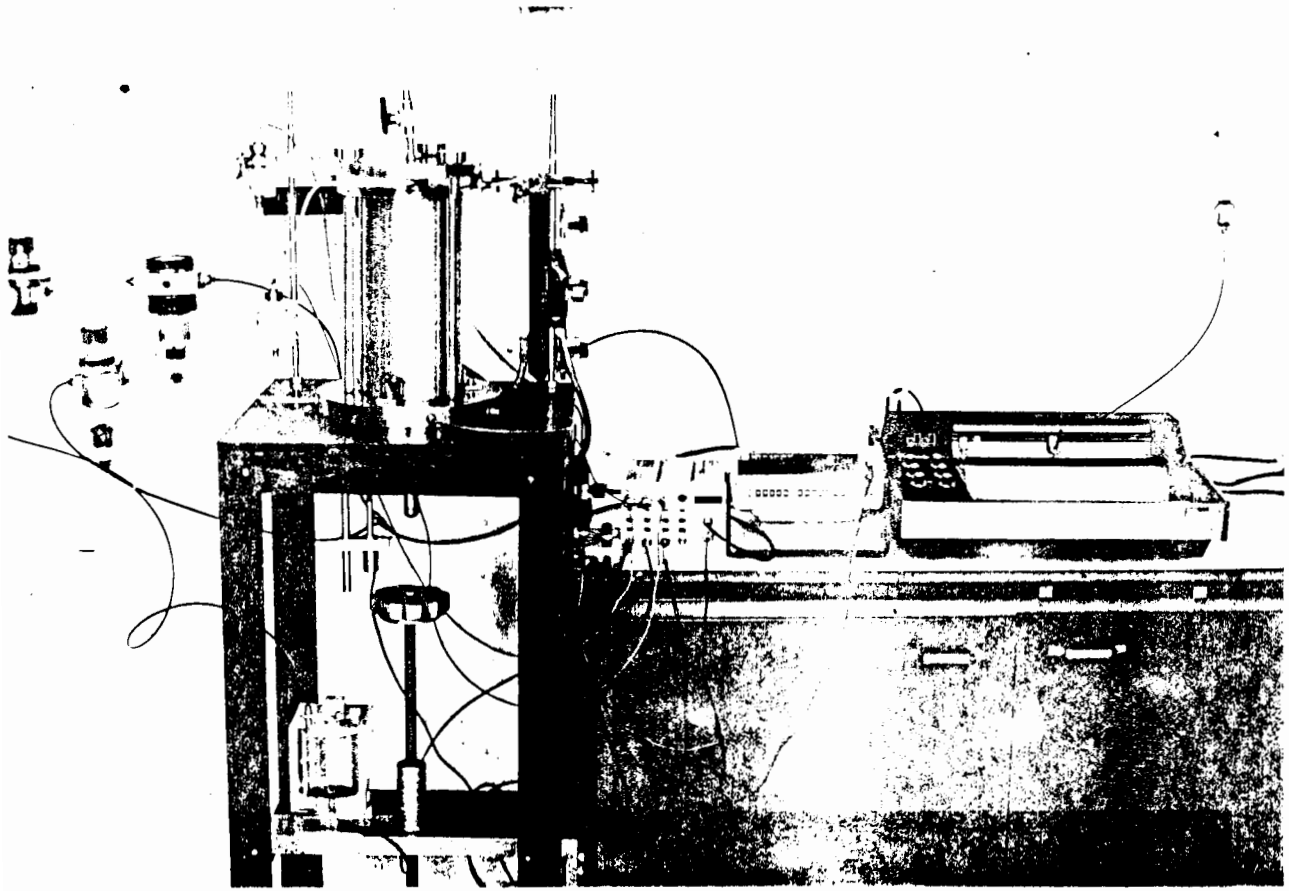

Fig 3.5 Apparatus used in the consolidation experiments.

The Piston:

The piston(26) is machined from a solid block of brass to give a radial clearance of 0.5mm to the wall of the cell. Sealing of this piston is achieved by the use of an O-ring(19). On the specimen side of the piston there is a centre hole to house a total stress transducer(17) and an eccentric recess to house a 3mm thick porous stone(6). A clearance hole of 6mm is cut in the centre of the piston to provide an outlet for the signal cable from the total stress transducer. Threaded connections are provided in the cell pressure side of the piston for connecting the ram(8) and the pore pressure probe. Sealing between the ram and the piston is provided by a flange(7) with O-rings.

The Ram and the Plain Bush:

The ram(8) is made out of stainless steel tube of 19mm outside diameter with 3mm thick wall and an overall length of 200mm. This is guided by a plain bush(9) machined from a solid block of brass. Sealing against the cell pressure is achieved by an O-ring in the bore(21) and another O-ring (22) pressed between the base of the bush and the base of the cell.

The Top Platen:

The top platen(2) is made out of 35mm thick 150mm diameter perspex disc. The side facing the specimen is machined to provide a 100mm diameter and 15mm deep hollow space. The top surface of the hollow space is domed at 15° to horizontal. Three outlet connections, two from the side(5,16) and one from the top(1), at the centre, are provided.

3.3.1.3 Instrumentation.

Total stress measurement:

The load applied to the piston by the cell pressure is not transferred fully to the soil specimen due to the O-ring friction. Therefore the total stress acting on the sample is directly measured by a total stress transducer mounted in the piston. It is an integrated silicon chip pressure transducer (10mm diameter active face) manufactured by Druck Limited, with a range of 0-700kN/m^2. The combined nonlinearity and hysteresis is less than ±0.1% of best straight line.

Pore pressure measurement:

The pore fluid pressures at the undrained and the drained faces of the sample are also measured by silicon chip pressure transducers manufactured by Druck Limited. Both transducers have a range of 0-350kN/m^2, with combined nonlinearity and hysteresis less than ±0.1% of best

straight line. They are housed in perspex blocks and connected to the pore pressure ports in the oedometer by water filled nylon(4mm) tubings.

Total and pore pressure transducers are calibrated using a digital calibrator manufactured by Druck Limited. The output of each transducer is amplified in such a way that the electrical output is converted directly into appropriate engineering units (using the calibration appropriate to each transducer), so that 1mv electrical output is equal to $1kN/m^2$. The above procedure allows the chart recorder output to be read directly in engineering units. The signals are also checked by a digital voltmeter.

Displacement measurement:

The sample displacement is measured by an induction type displacement transducer manufactured by Sangamo Limited. It has a range of 10mm travel, with ±0.1% nonlinearity. It is calibrated by a precision micrometer and the output is again converted to engineering units (1volt=1mm) by a differential amplifier.

Flow measurement:

Fig (3.6) shows the arrangement used for the separate measurement of volumes of water and gas flow from the gassy soil. A water filled domed shaped transparent top cap is used on top of the sample to trap the gas flow out

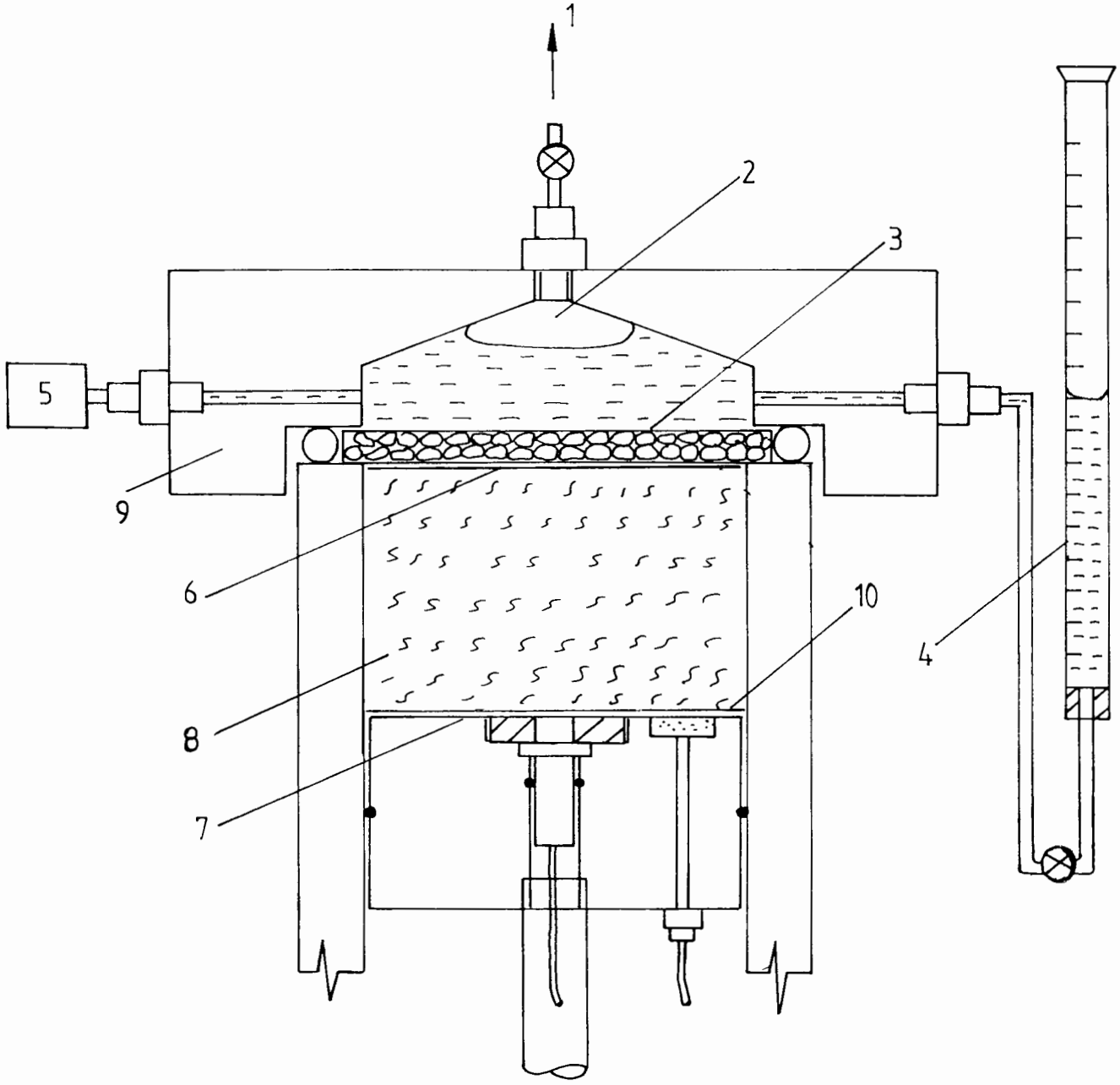

1. Drainage port
2. Gas
3. Porous plate
4. Burette
5. Pore pressure port
6. Filter paper
7. Piston
8. Soil sample
9. Perspex top cap
10. Filter paper

Fig. 3.6 Volume measuring system.

during consolidation. A highly porous stone (10 kN/m^2 air entry value) is used on top of the sample to allow water and gas flow into the top cap. The top port(A) is closed in order to trap gas during consolidation and the side port(B) is connected to a burette which measures the total flow (both of water and gas volume). At the end of each load increment when all the consolidation is over port(A) is opened and the gas is flushed out by allowing the water from the burette to flow into the top cap. The port(A) is closed as soon as all the gas is flushed out. The drop in burette readings gives the volume of gas and the difference in the final and the initial reading will give the water volume. The above method will not provide a continuous reading but does measure the total water and gas flow out of the sample during each load increment. This measurement is used to calculate the degree of saturation at the end of the consolidation corresponding to each stress increment.

Pressure system:

Compressed air pressure with a pressure regulator is used to pressurise the cell. The cell is filled with water and an air water interface is used in the pressure line. The maximum pressure obtainable with this arrangement is $1000kN/m^2$ with a pressure regulation of $13kN/m^2$. The total stress measured by the transducer drops as soon as the drainage valve is open and then gradually rises back to the initial value as the

deformation rate reduces. The error caused in the application of total stress to the sample to a predetermined value is $\pm 5 kN/m^2$ which is due to the friction of the O-ring in the piston and the sensitivity of the regulator.

3.3.1.4 THE INITIAL PREPARATION FOR A TEST

Preparation of the oedometer:

The piston is adjusted to give an initial sample thickness of 35mm and prevented from further downward movement by resting the guide ram on the head of a lead screw, fig(3.3), which can be raised independently from a base below the ram. The sample space is initially filled with deaired water which is used to transfer the porous stone (deaired by boiling under vaccuum) under water to the undrained face pore pressure port on the piston. A fine filter paper is placed over the piston to prevent soil particles clogging the stone and to facilitate the removal of the final sample. The deaired water is then syphoned from the sample space until 2mm depth of water is left over the piston to prevent the porous stone from drying.

Preparation of the soil sample:

The gassy and saturated samples are prepared by the method described in chapter two. The amount of zeolite added to the soil to obtain the required degree of

saturation is calculated from the calibration curve given in fig 2.5 in chapter two. 450g of the soil slurry (including the zeolite) is poured in to the cell as soon as the required amount of zeolite has been mixed in. The top level of the slurry is trimmed by a pallette knife to make it flat with the cell top. A greased O-ring (5.4mm thick) which is subsequently used to seal the top cap and the cell is placed on top of the cell and deaired water is poured to fill the space above the slurry. A filter paper and the top porous platen are placed over the sample. The space above the platen and the O-ring is again filled with deaired water to prevent the porous platen drying. Finally the top perspex cap is placed and secured to the base of the cell. The top cap is deaired by flushing water from the side port and the dome shaped top enables complete dearing.

The sample is allowed to stand for 24 hours for all the gas bubbles to develop before any testing is done. The top drainage port is open and the volume of the sample is kept constant (using the lead screw to prevent the piston movement) during this period. As the gas is generated in the sample, free water from the sample voids is displaced since the total volume of the sample is kept unchanged. If the drainage port is closed during this period, a pore pressure increase is registerd in the sample due to the gas release from the zeolite and this is normally avoided by draining the sample.

3.3.2 PRELIMINARY TESTS.

The samples are consolidated in the oedometer to 450kN/m^2 total stress from a slurry stage in three vertical stress increments. The first increment is applied after allowing 24 hours for the gas bubbles to be released from the zeolite. The stress increments used are 60, 140, 250kN/m^2 and for each stress increment, the sample is allowed 24 hours to attain full consolidation. The deformation of the sample, the pore fluid pressures on the drained and undrained faces of the sample and the volume of flow are monitored during the application of each stress increment and during the consolidation stages. At the end of the 250kN/m^2 increment, the sample is unloaded in stress decrements of 100kN/m^2 and finally the sample is removed from the cell and its height, wet weight, moisture content and the degree of saturation are measured.

The deformation measurement:

The fig(3.7) shows the observed deformations of the samples with different degrees of saturation. Three load increments of 60, 140, 250kN/m^2 are applied, with time in between to allow settlement to occur. Gassy samples show an initial deformation as soon as the stress is applied and then they consolidate to different heights (sample thickness) even though all the samples started with the same thickness. The higher the gas content, the larger

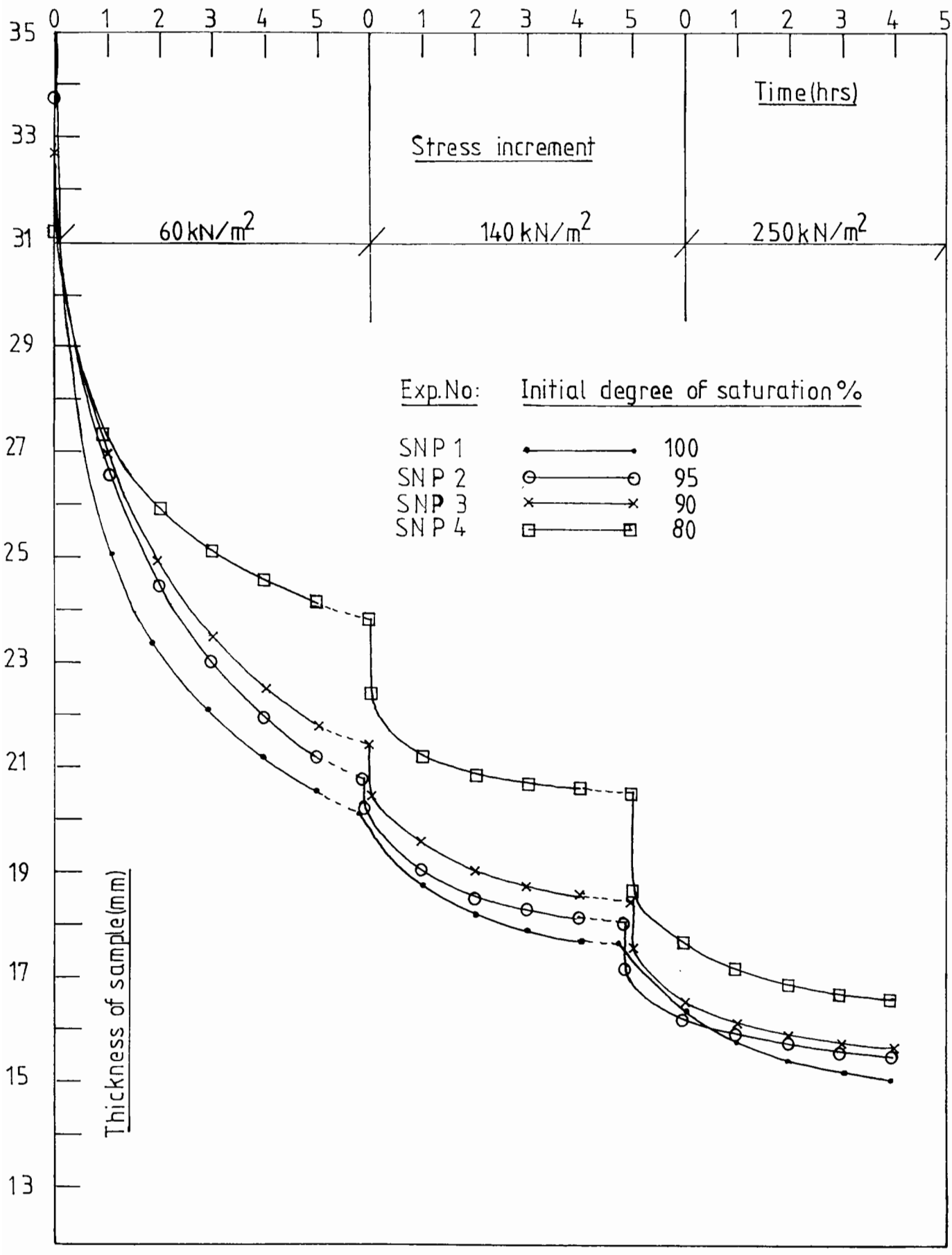

Fig 3.7 Sample deformation

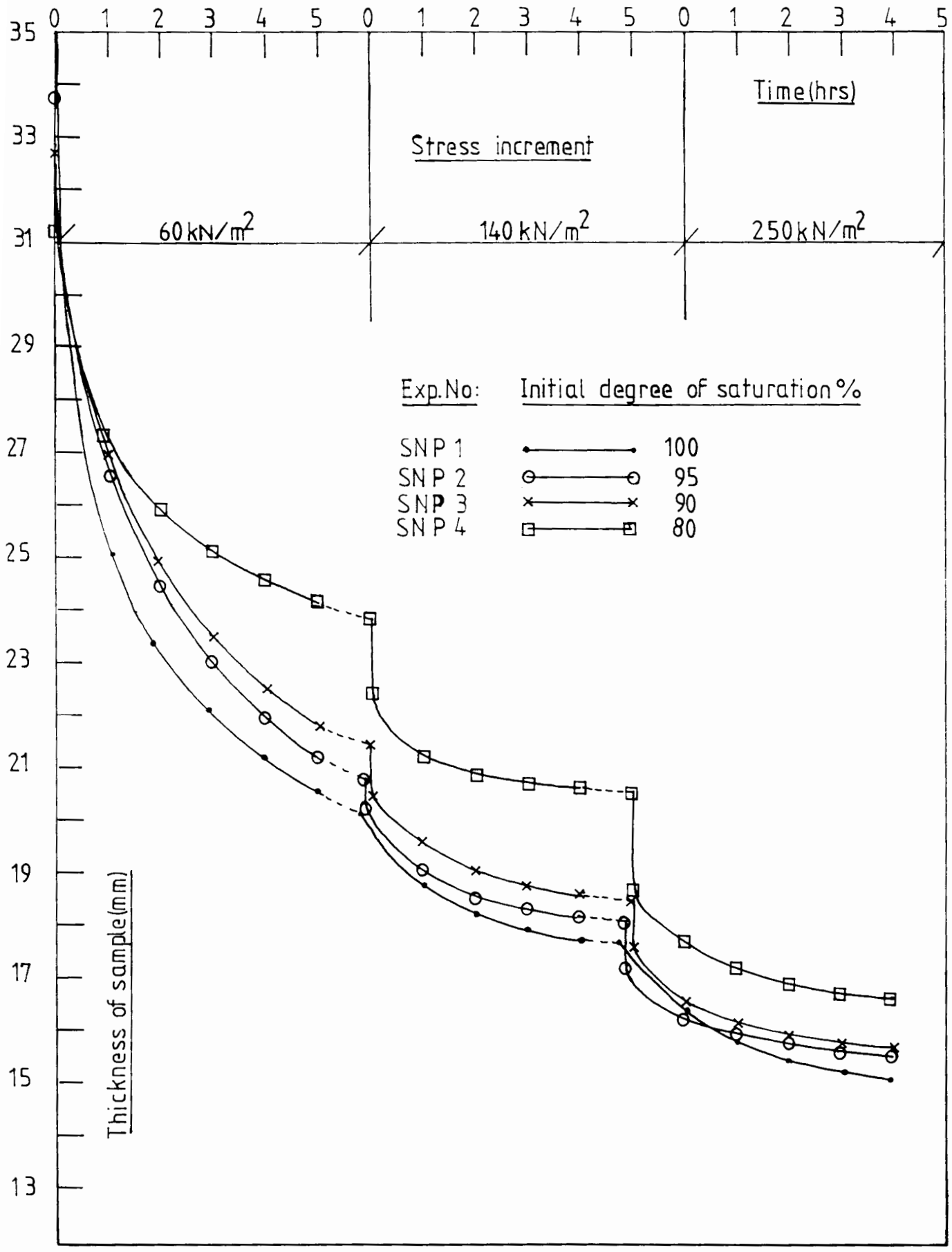

Fig 3.7 Sample deformation

the sample thickness. The saturated soil showed no initial deformation, but reached the smallest sample thickness after consolidation. The solid volumes are slightly different in the samples, therefore comparison of the samples with different degrees of saturation is carried out in terms of voids ratio change (deformation for unit solid height) instead of the deformations of the samples. Fig(3.8) shows the changes in voids ratio for different total stress increments. The gassy soils are associated with high voids ratio (greater sample thickness) when compared to saturated soils at the same total stress level. This observation confirms the behaviour observed in the settling experiment in the previous section.

The pore fluid pressure measurement:

The pore fluid pressures are measured at the undrained and the drained faces of the sample. The drained face pore pressure transducer monitors the back pressure which is zero for most of the tests. The undrained face pore pressure transducer measures the increase in pore fluid pressure during the application of stress increment (undrained stage) and the subsequent dissipation during the consolidation stage. The pore fluid pressure in a gassy soil has two components, pore water pressure and pore gas pressure. The undrained face pore pressure measured by a no flow type pressure transducer

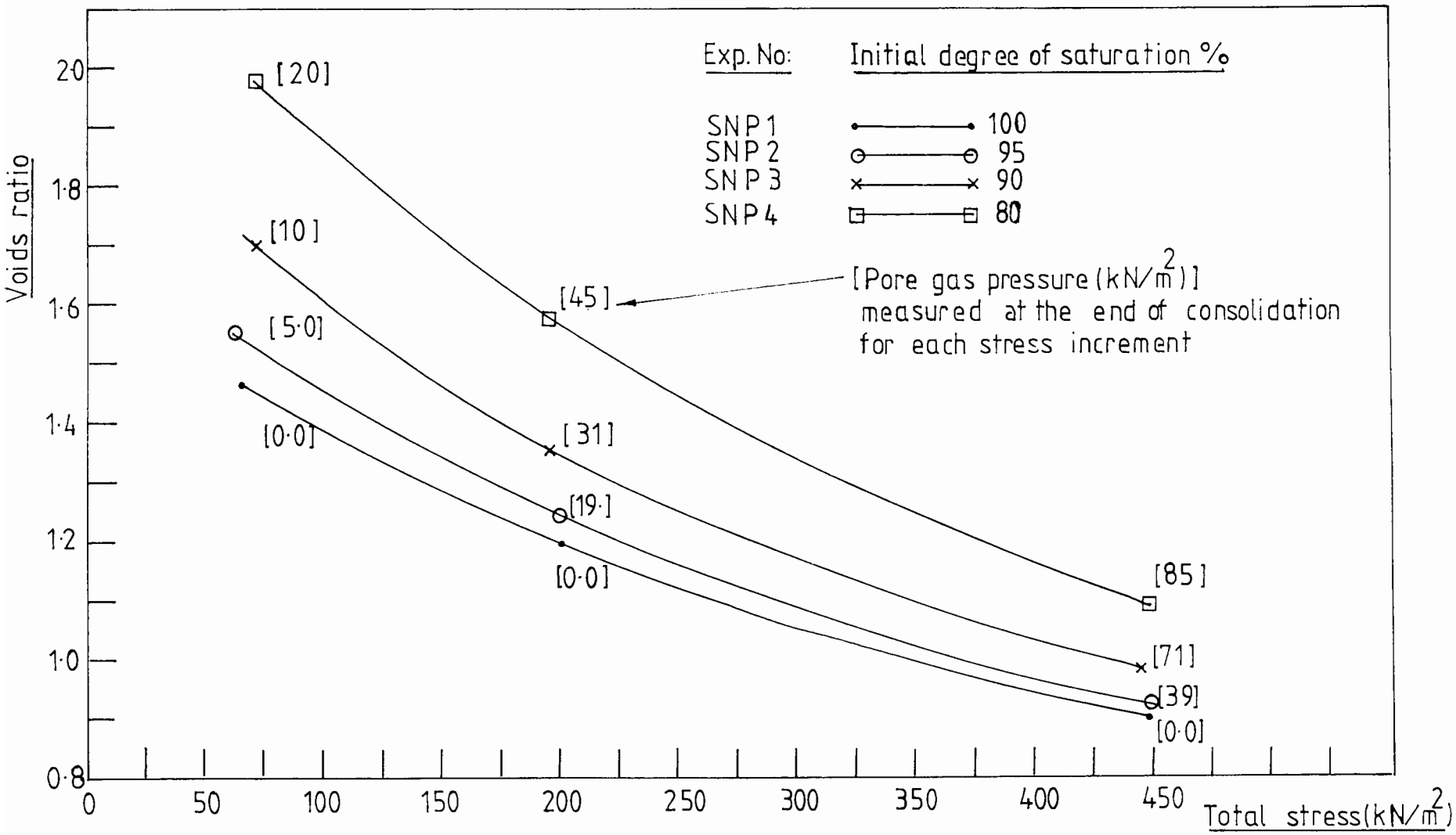

Fig 3.8 Voids ratio - Total stress relationship.

with a completely deaired porous stone system (incompressible system) was initially believed to measure only the pore water pressure for the following reasons.

In order to measure pore gas pressure there should be a physical link between the transducer and the gas inside the bubbles. The gassy soil used here is believed to contain discrete gas bubbles and the pore pressure measuring system is initially gas free. The only direct link to the transducer is with the pore water, which would therefore be expected to measure pore water pressure. During the consolidation stage, gas flow can occur into the measuring system and provide a link between the bubbles and the transducer but this possibility was considered to be comparatively unlikely since the direction of fluid flow is away from the undrained face. In the experiments carried out in partially saturated soils (Bishop 1964) pore air pressure is measured by creating a direct link between the transducer and the air voids by filling the measuring system with air instead of water. Most of the voids are connected in partially saturated soils and flow of air to pressurise the measuring system is provided through a low air entry value porous stone. Selecting a high air entry stone and initially filling the measuring system with deaired water enabled the measurement of pore water pressure in partially saturated soils. However, in the gassy soils, where the gas continuity is poor, the water saturated

measuring system is likely to measure pore water pressure, if the above arguments are correct.

Fig(3.9) shows the measured undrained face pore fluid pressures following a particular load increment(140kN/m^2) and during the subsequent consolidation stage for a saturated soil and for gassy soils with approximately 95%, 90% and 80% initial degrees of saturation. The undrained face pore pressure measured in the saturated soil increases when the stress increment is applied (the pore pressure increment is equal to the total stress increment) and dissipates to the back pressure level (zero) as the fluid drains. In the case of a gassy soil, the pore pressure again increases during the application of the total stress increment, but the pore pressure increment is less than the total stress increment due to the compressibility of the pore fluid. The pore pressure then dissipates to a value which is higher than the back pressure. This excess pore pressure remains at this level for at least for four days even after no further sample deformation is noted.

The undissipated excess pore pressure value depends on the gas content and the total stress level in the sample. The higher the gas content and the higher the total stress level, the higher is the excess pore pressure registered. The air entry value of the stone used for the pore pressure measurement is 10 kN/m^2. Fig(3.10) shows

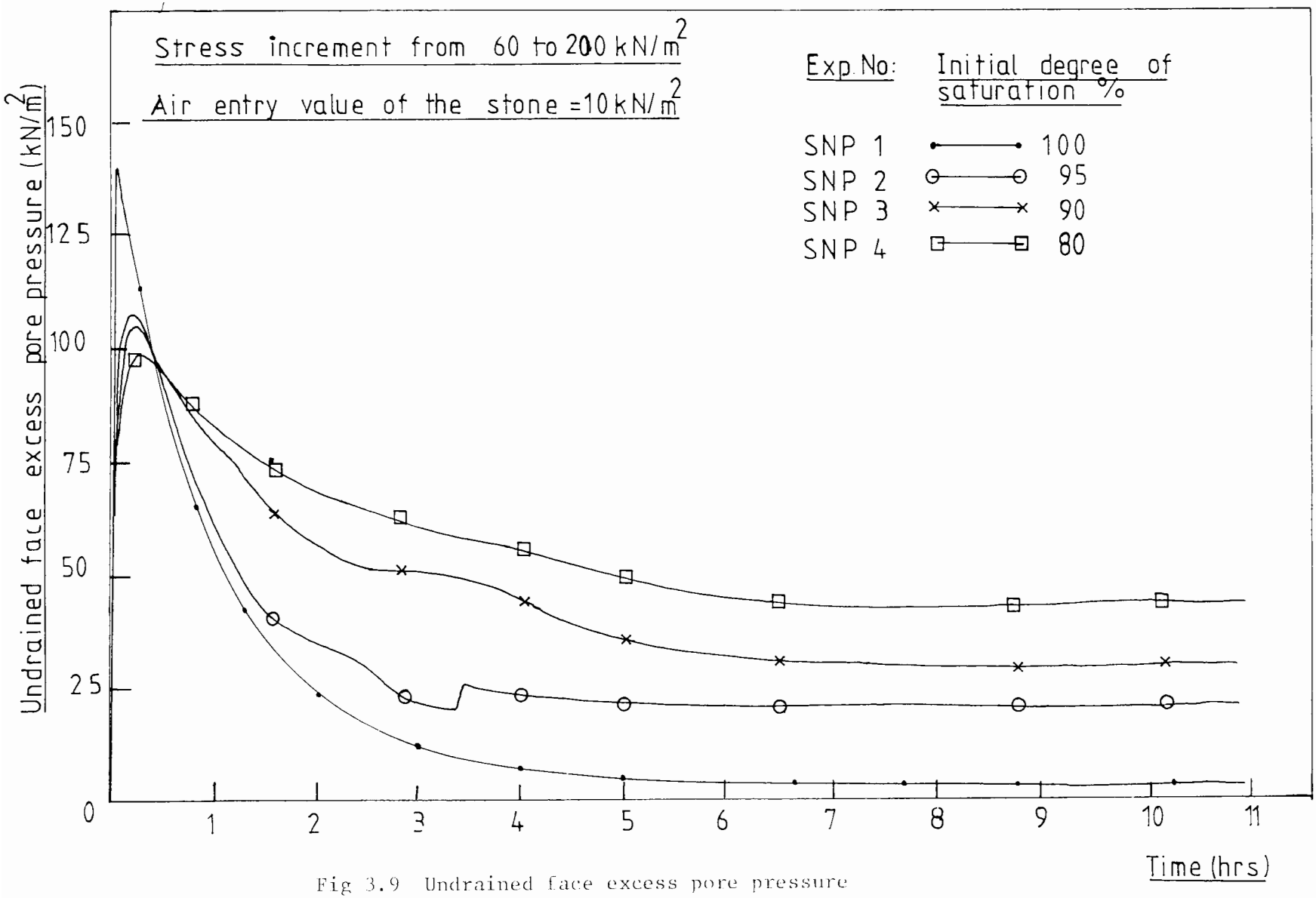

Fig 3.9 Undrained face excess pore pressure

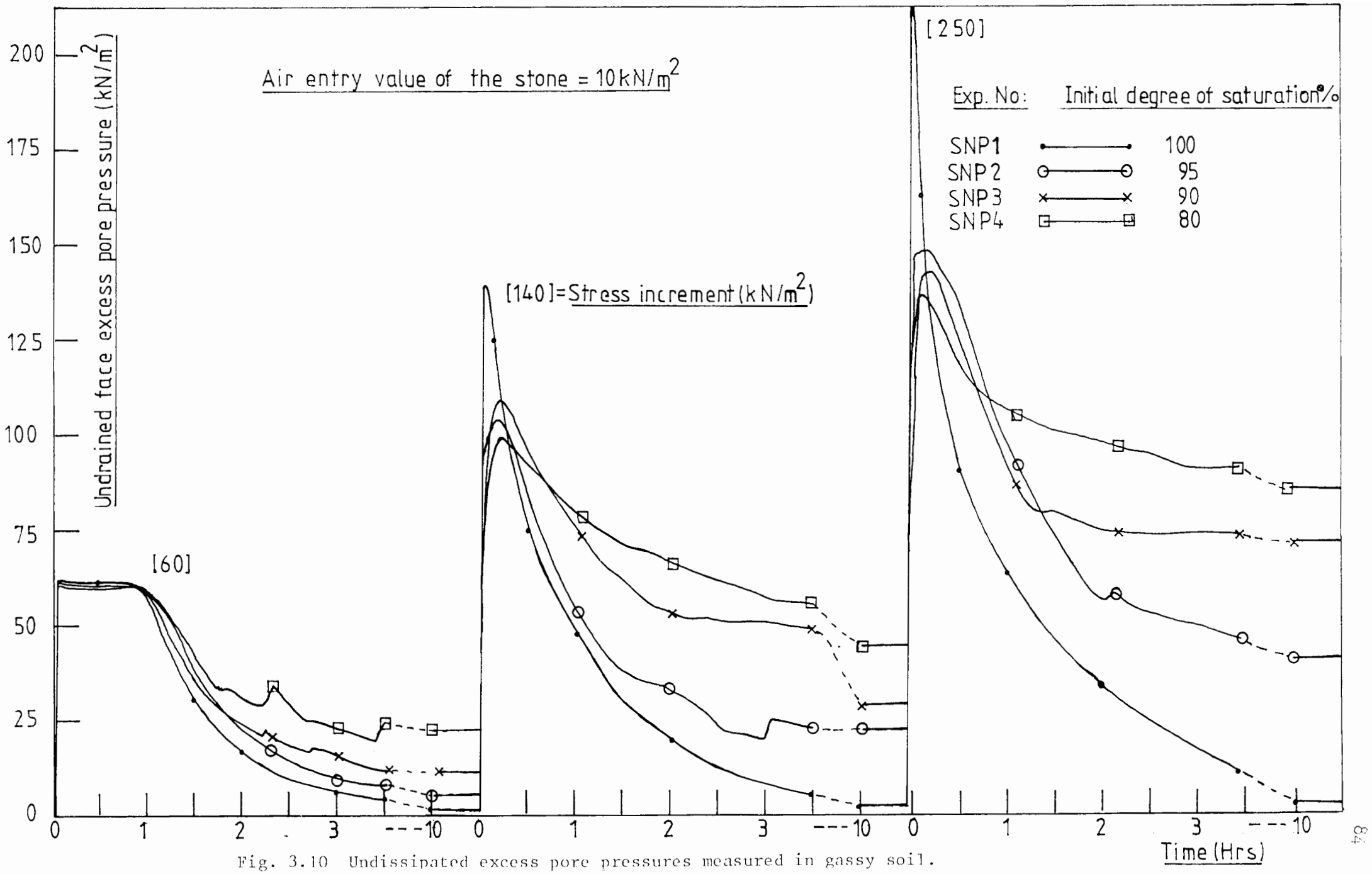

Fig. 3.10 Undissipated excess pore pressures measured in gassy soil.

the measured excess pore pressures in gassy soils with initial degrees of saturation 95, 90, 80% and at different total stress levels (60, 200, 450 kN/m^2). These undissipated equilibrium excess pore pressures associated with gassy soil are consistent with the similar field observations indicating the existence of excess pore pressures in a gassy sea bed (Fig 1.5, SEASWAB 1977). However the pore gas pressure in the gassy soil is greater than the pore water pressure due to surface tension effects and this suggests that the measured pore fluid pressure could contain some part of pore gas pressure whereas the pore water pressure has dissipated to the back pressure level as in the case of saturated soil. The repeatability of the experiments and the effect of porous stone on the measurement of pore fluid pressure are examined before any conclusion is reached.

THE EFFECT OF POROUS STONES ON THE MEASUREMENT OF PORE GAS PRESSURE.

The pore fluid pressure is measured on the undrained face or the sample at two different locations in this experiment (SNAS1) using two different air entry value porous stones (100, 250 kN/m^2) in order to study the effect of the air entry value of the stones on the pore fluid pressure measurement. Fig(3.11) shows the arrangement used in the oedometer to mount the porous stones. Apart from the air entry value, the two measuring systems are identical. Gassy soil with 90% initial degree

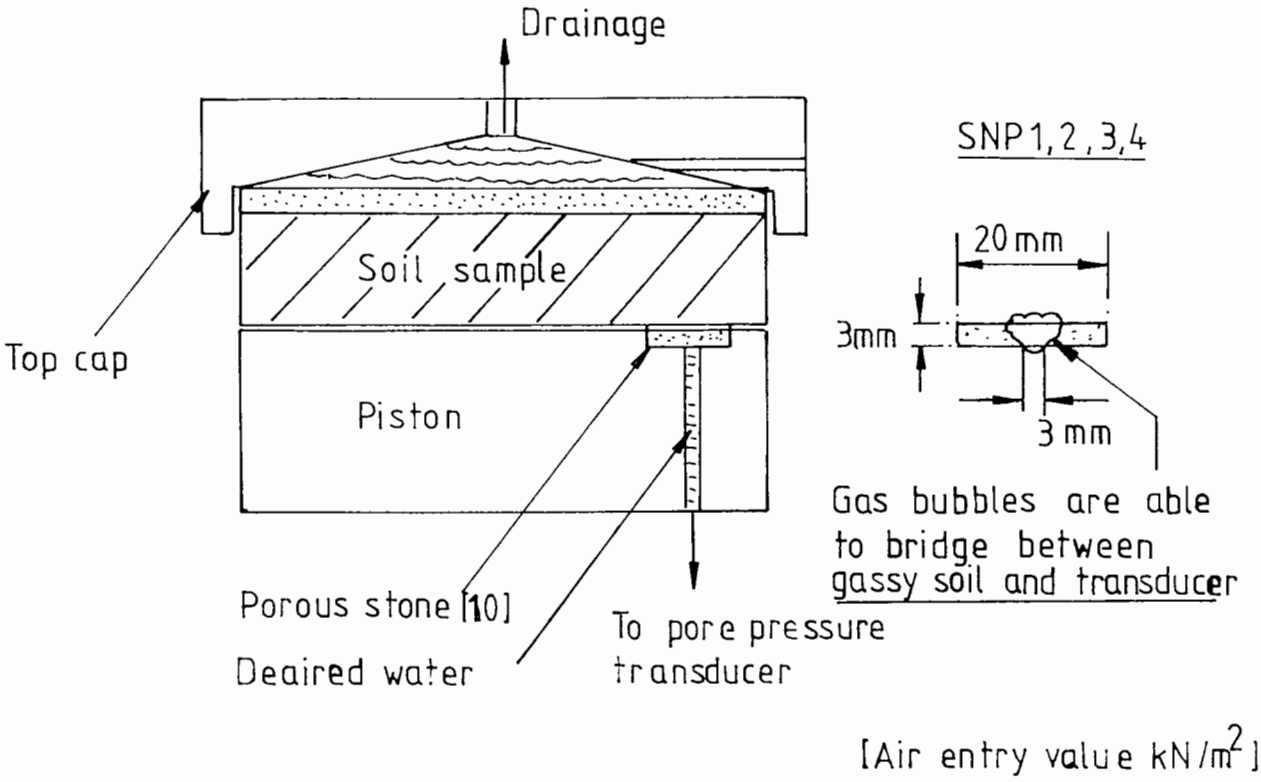

Measuring system used in the preliminary tests.

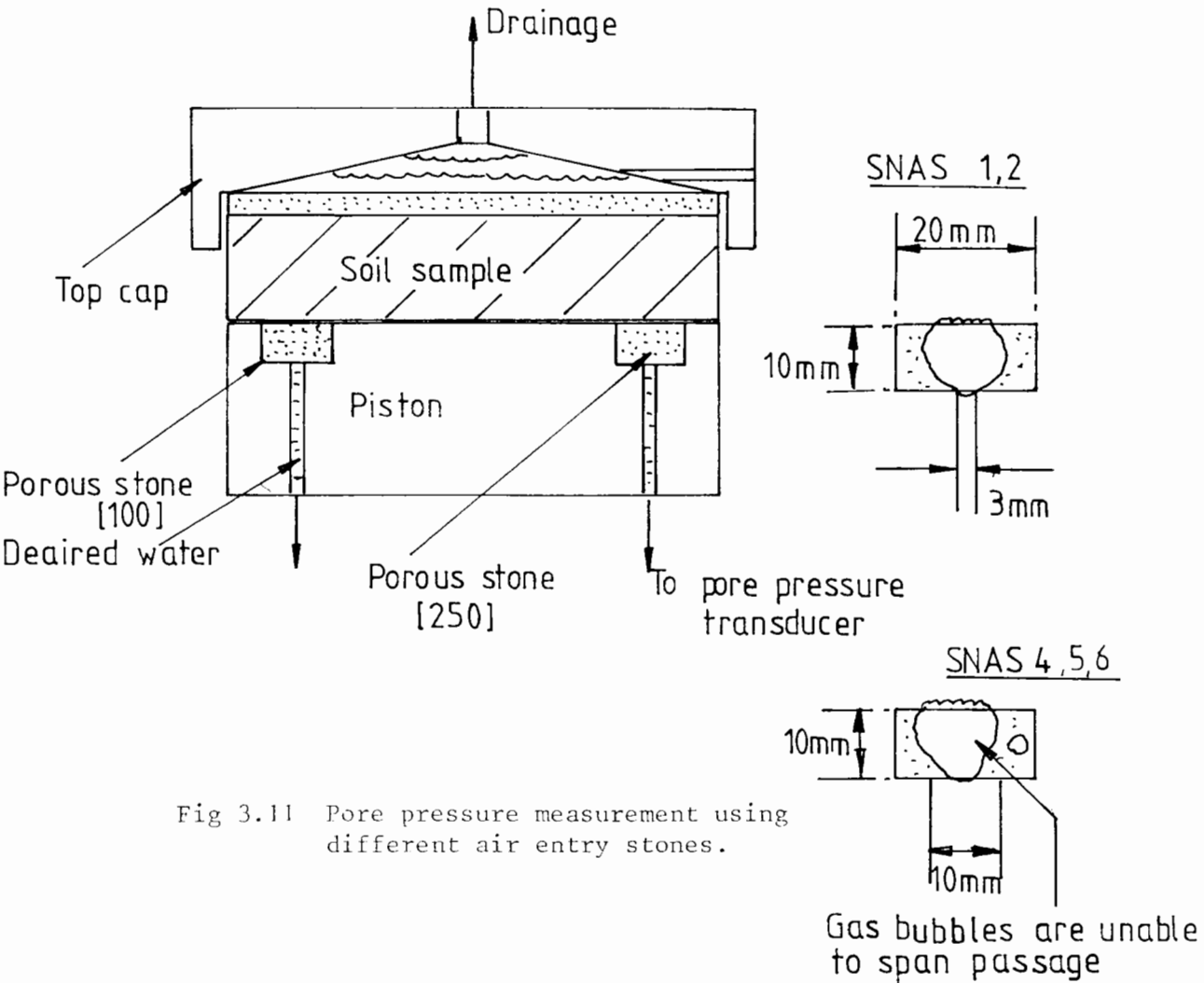

Fig 3.11 Pore pressure measurement using different air entry stones.

of saturation is consolidated in the cell with 40, 60, 100 and 200 kN/m^2 total stress increments. This experiment is repeated(SNAS2), keeping all the variables identical to the previous test to examine the repeatability of the measurements. Pore fluid pressures using the two different stones and the deformations are measured for the comparison.

Fig(3.12) shows the measured excess pore pressures in both tests using different air entry stones (100, 250 kN/m^2) in a gassy sample of 90% initial degree of saturation. For the first two increments (40,60 kN/m^2) all the pore pressures dissipated to the back pressure level (atmospheric pressure). During the following increment (100 kN/m^2) the pore pressure measured by both stones dissipated to the back pressure level, but the pressure behind the low air entry stone started to increase slowly to a higher level, indicating an excess pore pressure, whereas the high air entry stone remained at the back pressure level. After the final load increment (200 kN/m^2) the pressures associated with both stones showed the same undissipated excess value. Repeated experiments showed similar behaviour (high air entry stone shows the excess pore pressure later than the low air entry stone), but the magnitudes were not the same (a maximum difference of 35kN/m^2 was recorded). When the deformations in terms of voids ratios of the samples are compared, both tests showed very good repeatability even

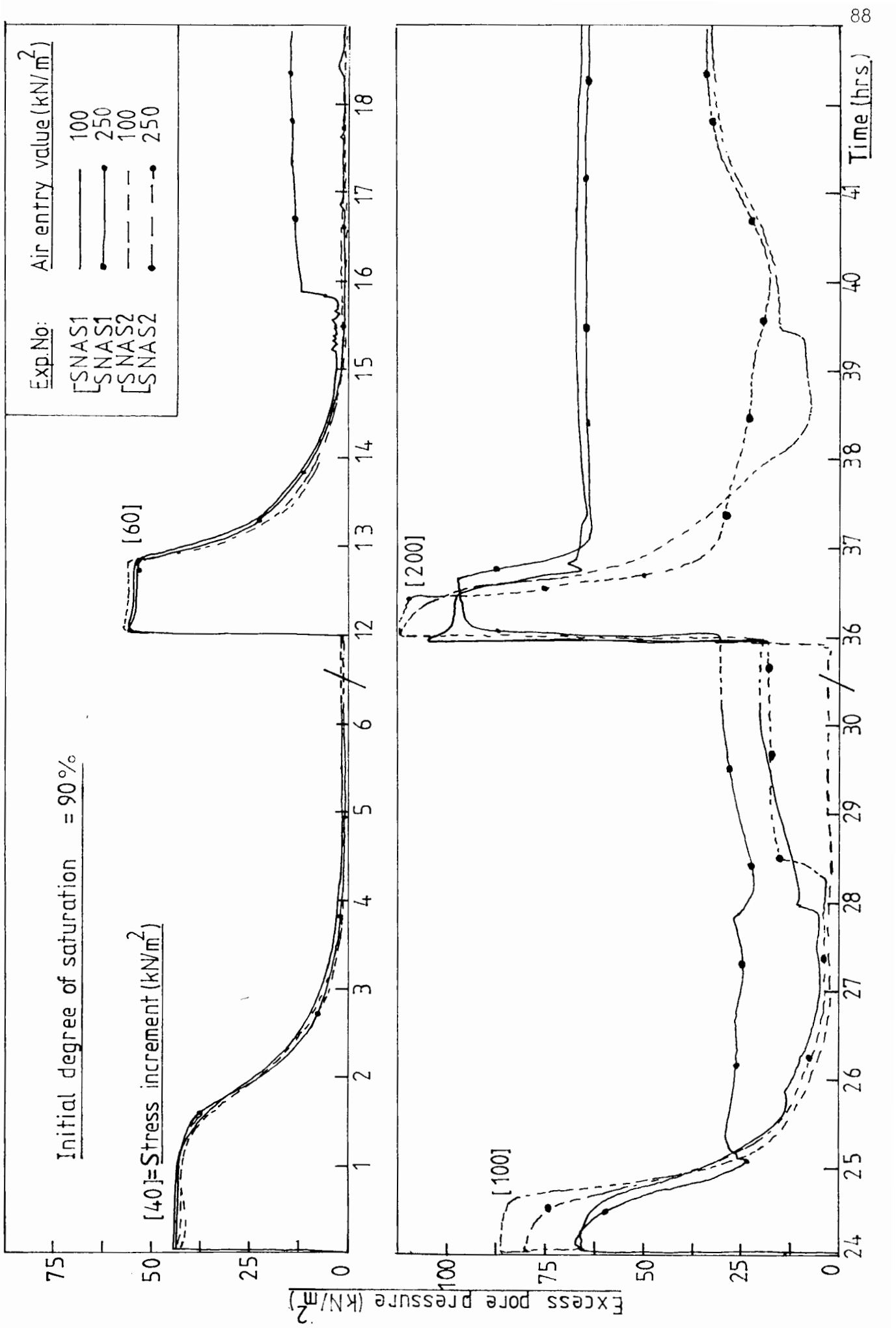

Fig. 3.12 Effect of the air entry value of the stone on the measurement of pore pressures in gassy soil

though the pore pressures were not the same. Fig(3.13) shows the voids ratio-logarithimic stress relationship of the sample in those tests. The stones were found dry at the end of the test, having initially been carefully deaired, suggesting gas movement into the stone. If gas movement is possible into the stone, the measured pore pressure may represent the pore gas pressure. The movement of gas into the pore pressure measuring system is investigated in the following experiment.

The direction of drainage is reversed, thus the sample is drained from the piston end and the undrained face is now the top cap. The undrained face pore pressure is therefore measured through the top cap. The transparent perspex top cap enables the movement of gas through the porous top platen to be seen fig(3.14). The top perspex cap is deaired and a pore pressure transducer is mounted in the side port. Gassy soil with an initial degree of saturation of 90% is consolidated in the cell (thus repeating the earlier tests) and the undrained face pore pressure and the deformation of the sample are measured. Fig(3.15) shows the observed excess pore pressure for each stress increment. For all the stress increments (40, 60, 100, 200 kN/m^2) the undrained face pore pressure dissipated to back pressure level, indicating no excess equilibrium pore pressure unlike the earlier experiments. But gas appeared in the measuring system (in the top cap) initially at the end of the first

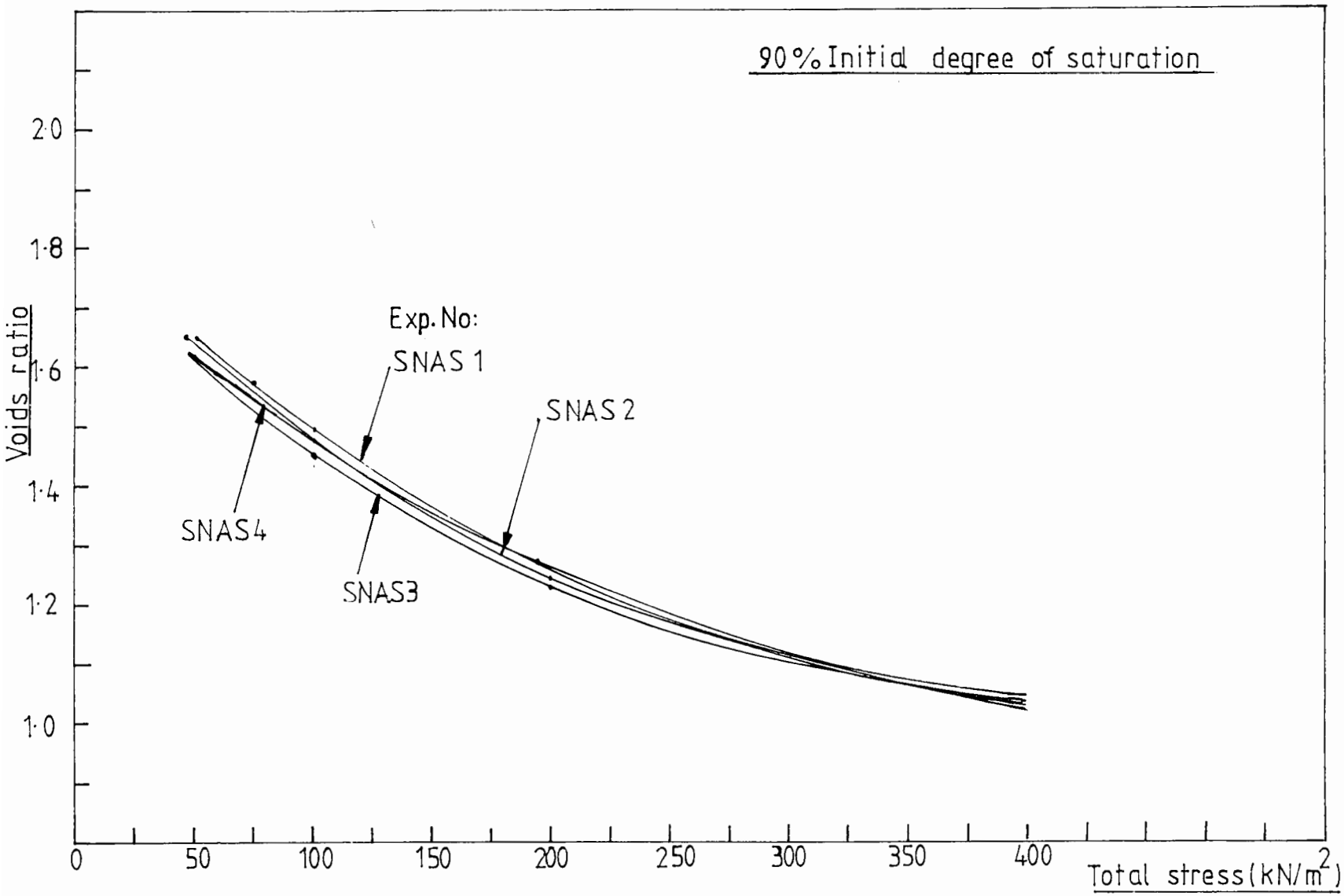

Fig 3.13 Voids ratio- total stress relationship

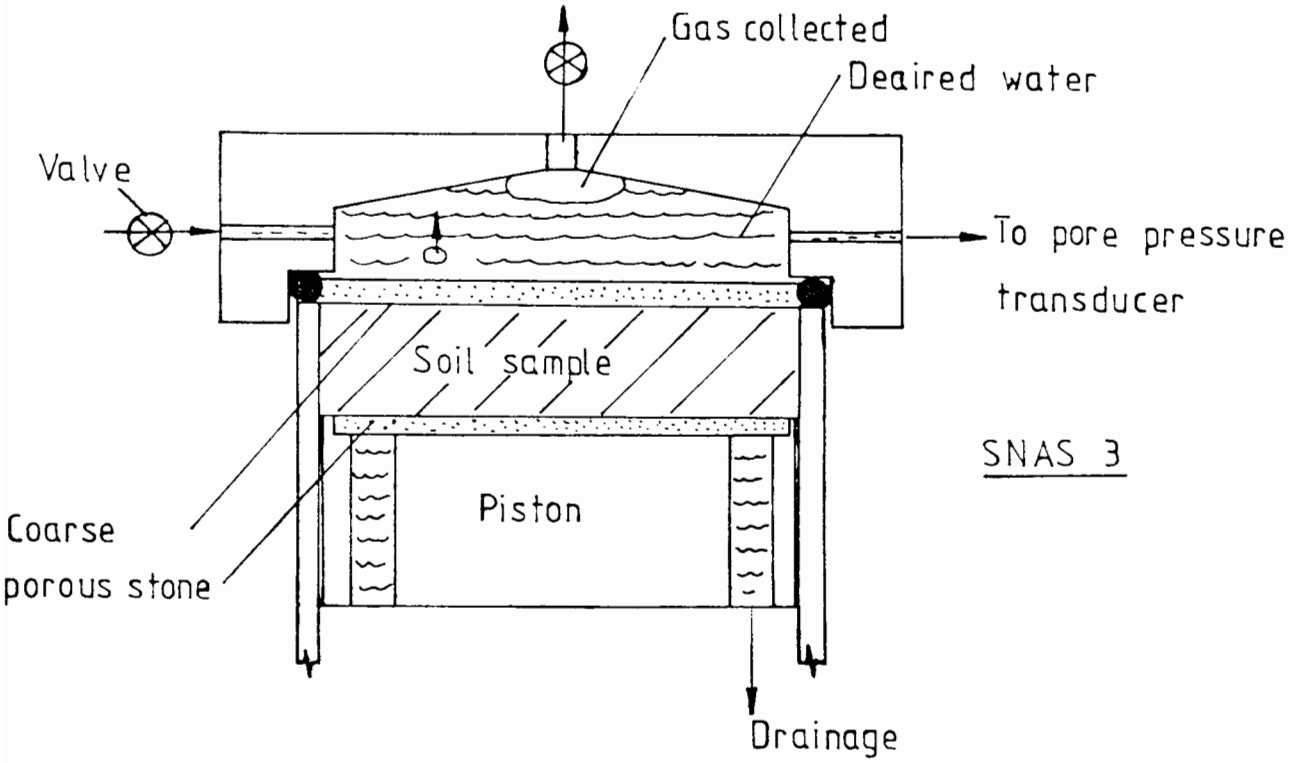

Fig 3.14 Pore water pressure measuring system in gassy soil

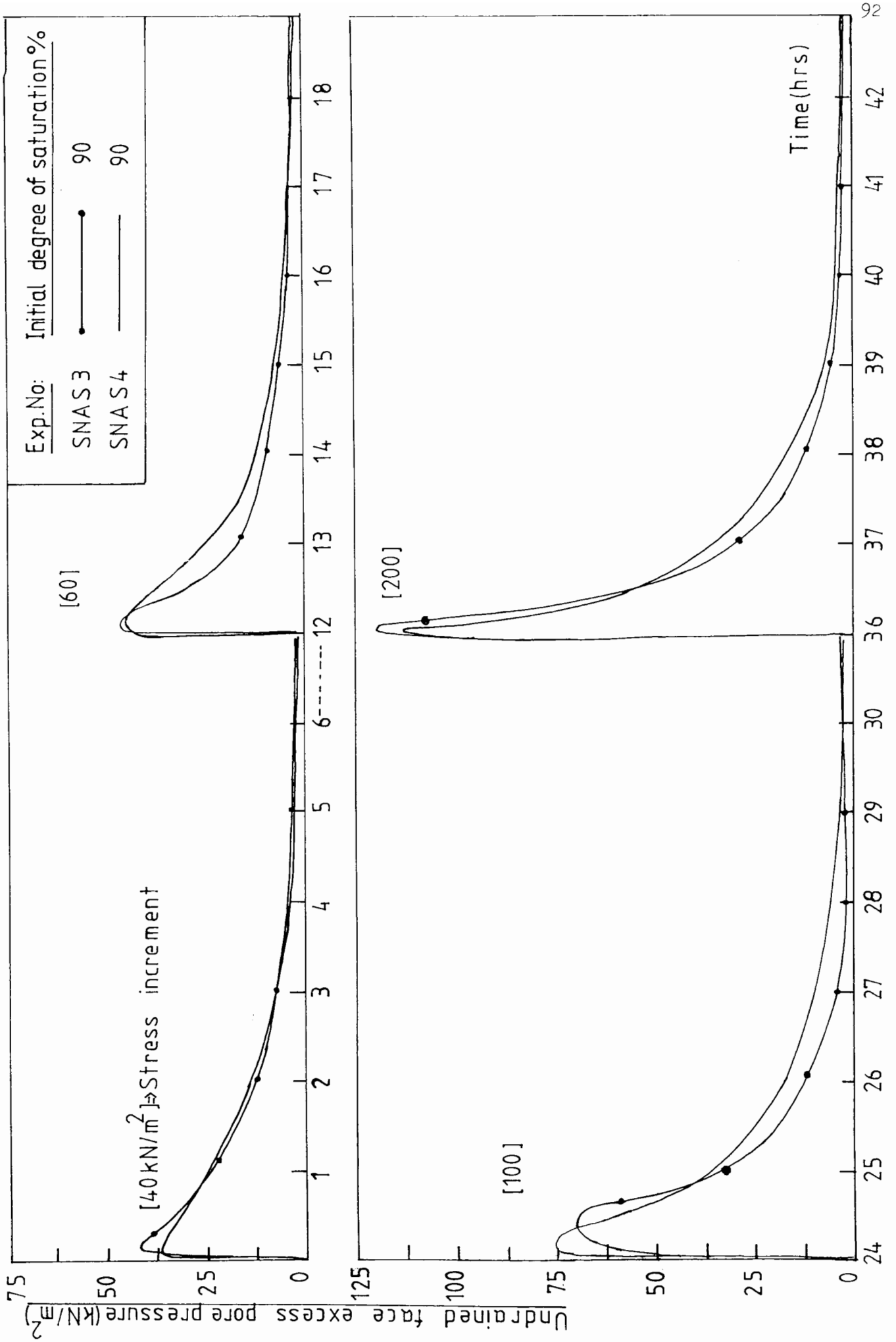

Fig 3.15 Excess pore pressure measured using the arrangement shown in fig 3.14

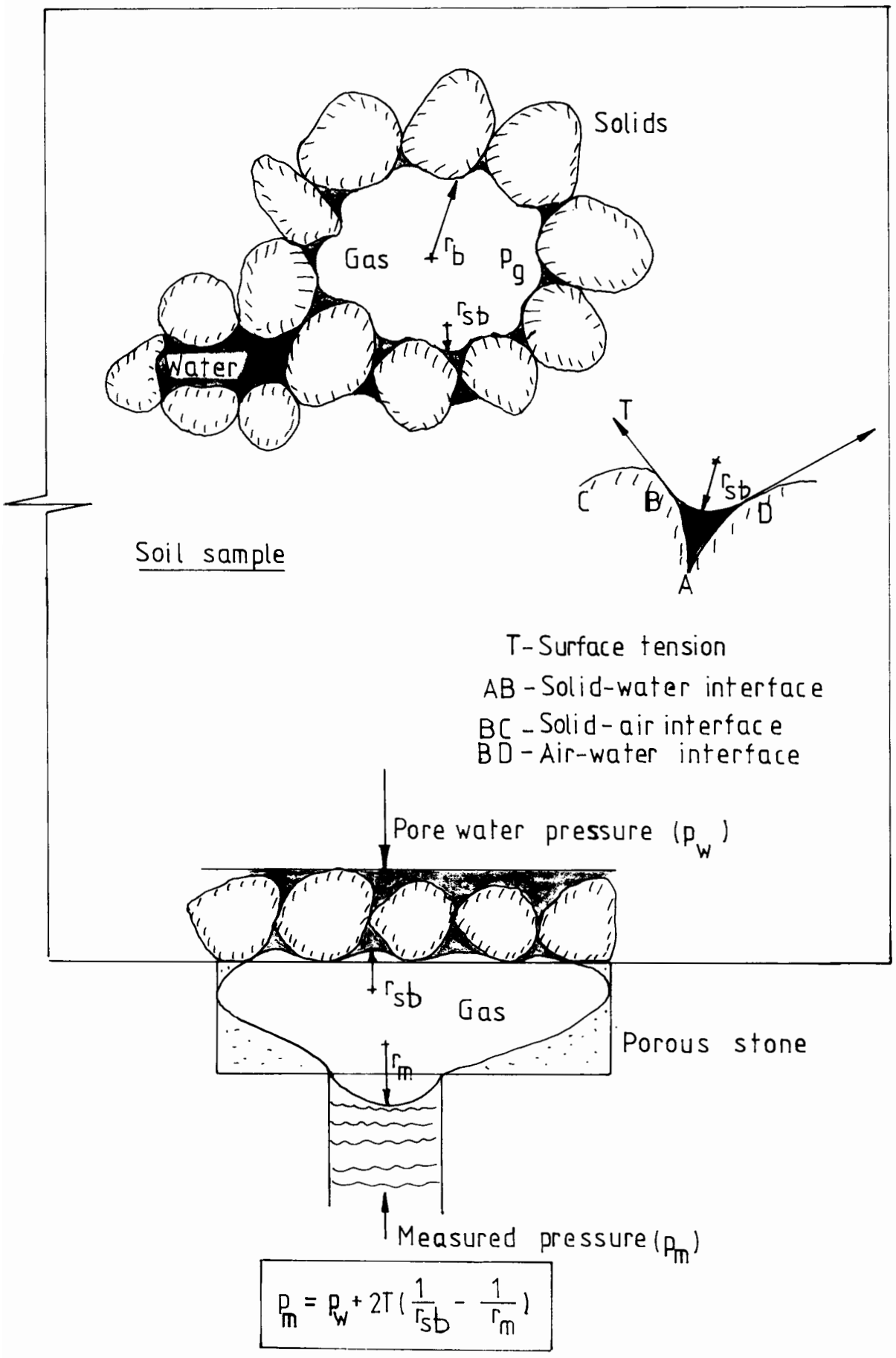

Fig 3.16 A mechanism to register poregas pressure.

stress increment. At the end of the final stress increment about 14ml gas volume was measured in the top cap. This experiment suggests that gas could diffuse in the initially incompressible pore pressure measuring system even though the direction of water flow is away from it.

Therefore a mechanism to register the undissipated pore pressure in the tests could be proposed as follows. If a sufficient amount of gas enters the stone and makes the water link between the transducer and the soil discontinuous as shown in fig(3.16), assisted by the narrow opening behind the stone, the transducer will register a higher pressure than the pore water pressure. Considering the equilibrium of the gas bubbles in the stone fig(3.16), the pore pressure (p_m) measured by the transducer is given by

$$p_m = p_w + (2*T/r_{sb}) - (2*T/r_m)$$

where p_w is the pore water pressure in the soil,

T- surface tension

r_{sb}- radius of curvature of menisci inside the soil which is of the order of a few microns in size.

r_m-radius of curvature of the bubble in the measuring system which is a few millimeters in size.

$r_{sb} <<< r_m$, Hence $p_m > p_w$

The above equation suggests that the pore pressure registered by the transducer is higher than the pore water pressure in the soil because of the surface tension effects due to the small radii of curvature of the bubble menisci in the soil. In the experiment where the pore fluid pressure is meaured at the top end, the gas bubbles were able to pass through the stone because of the high porosity ($10kN/m^2$ air entry pressure) of the stone and the nature of the housing which allow the gas to be collected in the top cap, leaving a continuous water passage between the transducer and the soil fig(3.16). If the water passage is discontinued at the soil-stone interface gas pressure is measured.

One of the factors assisting the collection of gas in the stone in the earlier experiments is the narrow path behind the stones fig(3.11), which enabled the collection of gas in the stone and discontinued the water passage quickly even for a small quantity of diffused gas. An experiment carried out with an enlarged opening increased from 3mm diameter to 10mm, using 90% saturated soil, showed complete dissipation of measured pore pressure. But this arrangement failed with 70% saturated soil, registering an excess pore pressure at the end of the consolidation as shown in fig(3.17). In 70% saturated soil the amount of gas diffused into the stone is sufficient to make discontinuous water passage whereas in the 90% saturated soil only a small amount of gas

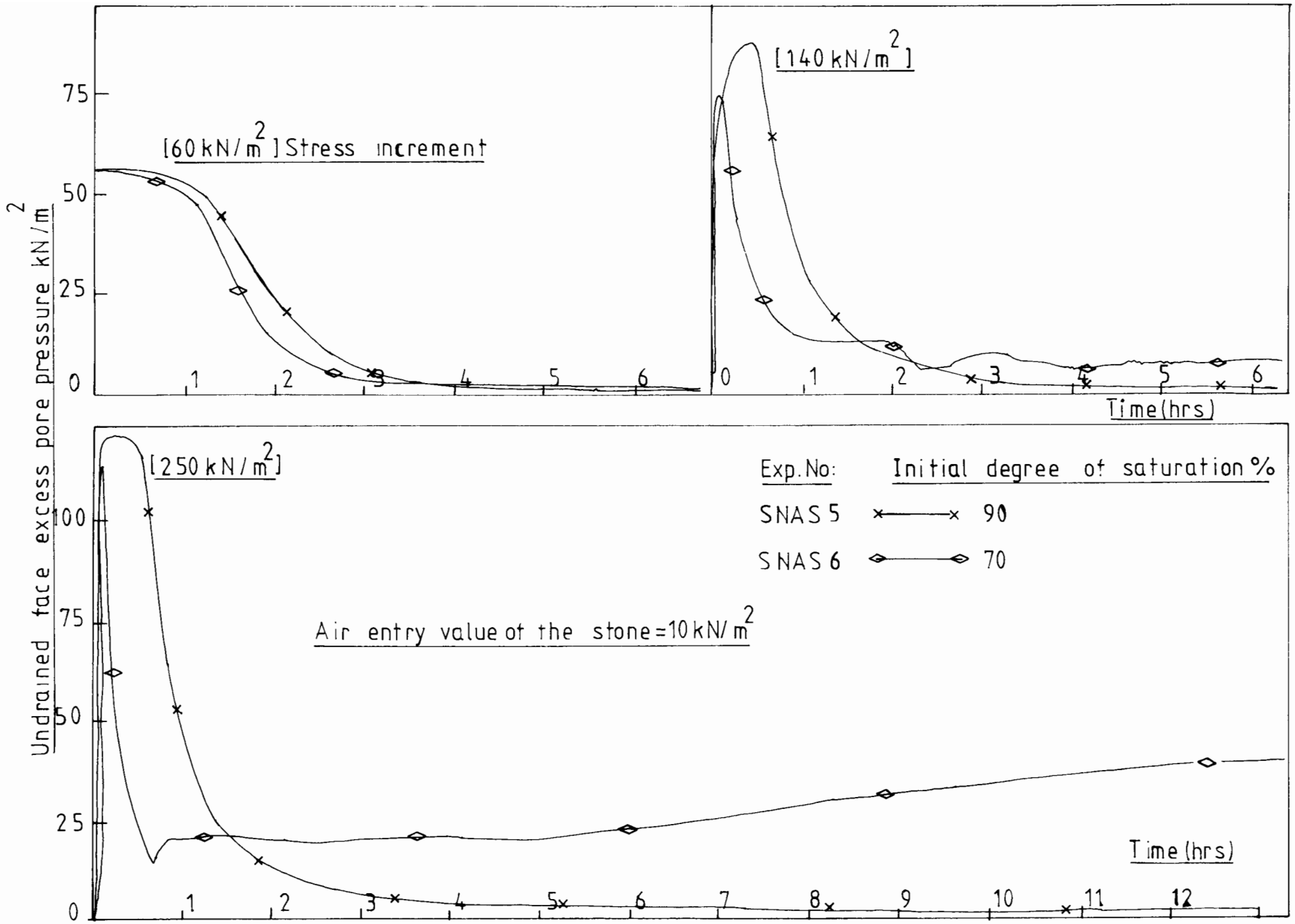

Fig 3.17 Excess pore pressure measurement using the arrangement shown in fig 3.11

entered the stone. Diffusion of gas is a slow process and depends on the gas content in the soil, but cannot be prevented by using a high air entry stone.

A modified arrangement shown in fig(3.18) is used in the following experiments in order to measure the pore water pressure in the soil. The pore water pressure is measured at the top cap end of the sample using the domed shape perspex cap. This time a smaller diameter(20mm diameter, 2mm thick) low air entry ($10kN/m^2$) stone is used instead of the larger diameter porous plate which was initially designed to act as a drainage stone. Using the smaller stone the amount of air entering the perspex cap is reduced. The pore pressure transducer is connected to the side port of the top cap. Fig (3.19) shows the measured pore water pressures using the above arrangement in soils with degrees of saturation 95, 90, 80%. All the excess pore pressures dissipated to the back pressure level at the end of the consolidation, indicating the absence of undissipated excess pore pressures in gassy soils. This system is satisfactorily used with different gassy soils. The gas collected in the top cap is flushed out before each stress increment is applied in order to observe the undrained pore pressure response of the sample for the following stress increment. The presence of gas bubbles in the top cap (pore pressure measuring system) gives very low B values where B is equal to the ratio of excess pore pressure to the total stress increment.

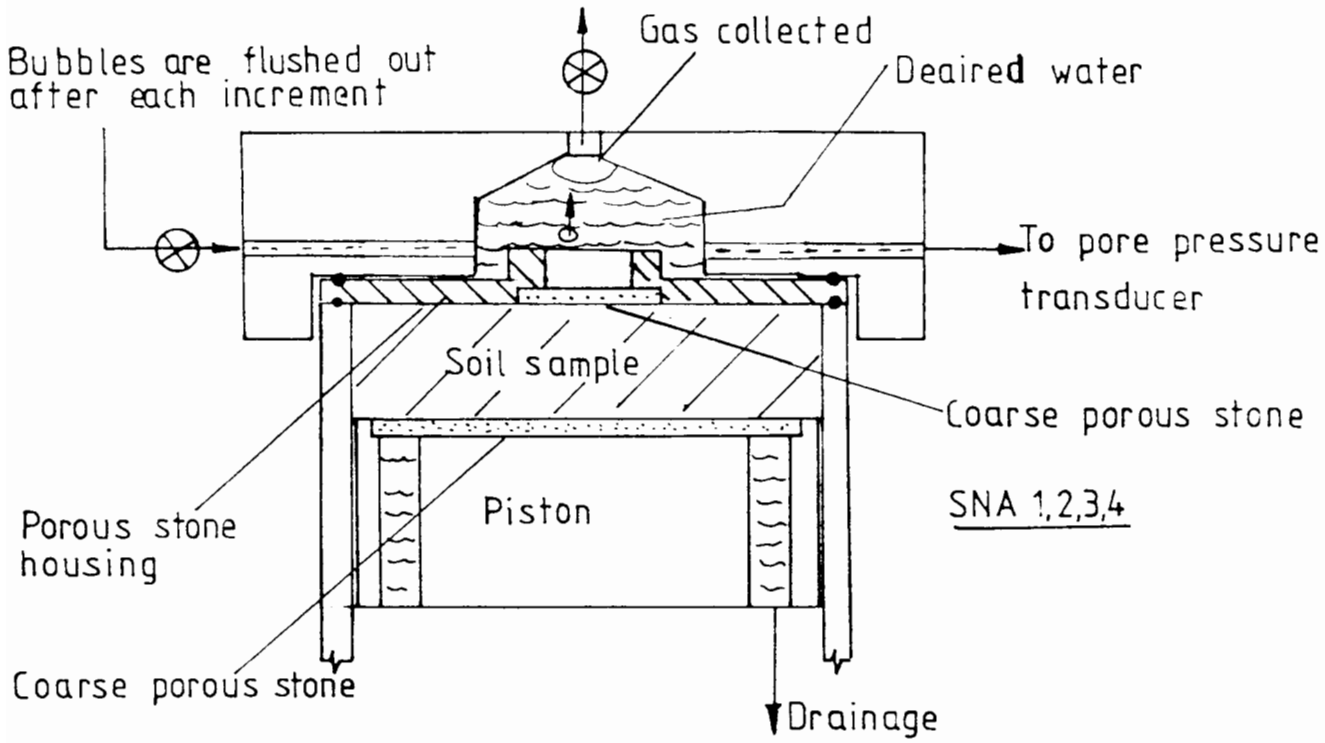

Fig 3.18 Pore water pressure measuring system in gassy soil.

Discussion:

The measurement of pore water pressure in a gassy soil is difficult. Gas could diffuse into the measuring system even if it is initially incompressible. Once sufficient amount of gas has entered the stone to break the water link, the measured pressure is influenced by the presence of the gas. It is possible that it may be in some way representative of the pore gas pressure. The above experiments indicate that there are no real excess equilibrium pore water pressures in the gassy soil, but the influence of gas pressure, which is higher than the pore water pressure may give rise to misleading interpretation of the results. The pore pressure measuring systems with high air entry stones do not always ensure the measurement of pore water pressure. If the stone is left in contact with the gassy soil for a long period, the readings are likely to be influenced by the gas movement into the stone. The measured high gas pressures are not assumed to be the pore gas pressure inside the bubbles due to the non-repeatability of these measurements. Therefore the pore water pressures only are measured in the following experiments using the arrangement shown in fig(3.18).

Section 3.4.

Experimental observations in the modified oedometer.

3.4.1 Single face drainage tests

3.4.2 Two face drainage tests

3.4.3 Effect of back pressure on the volume change behaviour of gassy soil

3.4.4 Structure of gassy soils

TABLE OF EXPERIMENTS

Series A:- 100%, 95%, 90%, 80% degrees of saturation sampes were one-dimensionally consolidated by 25, 25, 50, 100, 200kN/m² stress increments using single face drainage. Undrained face excess pore pressures and deformation of the samples were monitored. Voids ratio-stress relationships of gassy soils were derived from these experiments.

Series B:- 100%, 95%, 90%, 85%, 80%, 70% degrees of saturation samples were consolidated by 25, 25, 50, 100, 200kN/m² stress increments using single face drainage. Gas and water flow from the samples and deformation of the samples were monitored. Degree of saturation - stress relationships were derived from these experiments.

Series C:- 100%, 90%, 80%, 70% degrees of saturation samples were consolidated by 35, 25, 50kN/m² stress increments using single force drainage. Gas and water flow from the samples and the deformations were monitored. These results were used to check the relative position of voids ratio-stress curves obtained in Series A.

Series D:- 100%, 95%, 90%, 80%, 70% degrees of saturation samples were consolidated by 25, 25, 50, 100, 200kN/m² stress increments using double drainage. Samples were unloaded and reloaded at 100kN/m² stress level to study the swelling behaviour of gassy soils.

3.4 CONSOLIDATION TESTS WITH PORE WATER PRESSURE MEASUREMENT:

The following experiments are carried out in the modified oedometer allowing the measurement of excess pore water pressures during the consolidation. The pore water pressures dissipated to the back pressure level at the end of the consolidation in all these tests. The samples are consolidated from a slurry of initial thickness 40mm using 25, 25, 50, 100, 200 kN/m^2 stress increments and unloaded in steps of $100kN/m^2$ stress decrements. The back pressure in these tests was kept at atmospheric pressure.

3.4.1 CONSOLIDATION WITH SINGLE FACE DRAINAGE.

Test series A: Samples with 100, 95, 90, 80% initial degree of saturation.

The consolidation behaviour of gassy soils is compared with that of saturated soil by allowing single face drainage. Samples are drained from the bottom face through the piston and the excess pore water pressure in the sample is measured at the top undrained face using the configuration shown in fig (3.18) in these tests. The deformation of the sample, the excess undrained face pore water pressure and the total stress on the sample are measured during the test and at the end of it, the final thickness of the sample, the total wet weight of the sample and the degree of saturation are also measured. Each test took approximately 10 days.

The dissipation of undrained face excess pore water pressures with time is shown in fig (3.19a, 3.19b) for soils with different degrees of saturation. The pore water pressure increases during the application of the stress increment and dissipates when the drainage valve is open. The initial increase in pore water pressures due to the total stress increments depend on the gas content of the soil. The ratio of the pore water pressure increment to the total stress increment (B value) is unity in the saturated soil and less than unity in gassy soils. The lower the B value, the lower the degree of saturation in the soil. In all these tests the undrained face excess pore pressure dissipated to back pressure level indicating no undissipated excess pore water pressures.

Fig (3.20) shows the displacement-time behaviour of gassy soils and a saturated soil. The vertical axis is taken as the sample height. The sample heights of gassy soils after each consolidation are different from that of the saturated soil even though the initial heights and the solid volumes are the same. The presence of gas bubbles in the soil prevents the samples consolidating to the height of the saturated soil. The higher the gas content the greater the sample height. An initial elastic deformation occurs in gassy soils during the application of a stress increment due to the compressibility of gas bubbles in the soil and this initial deformation is not observed in the saturated soil. When the drainage valve

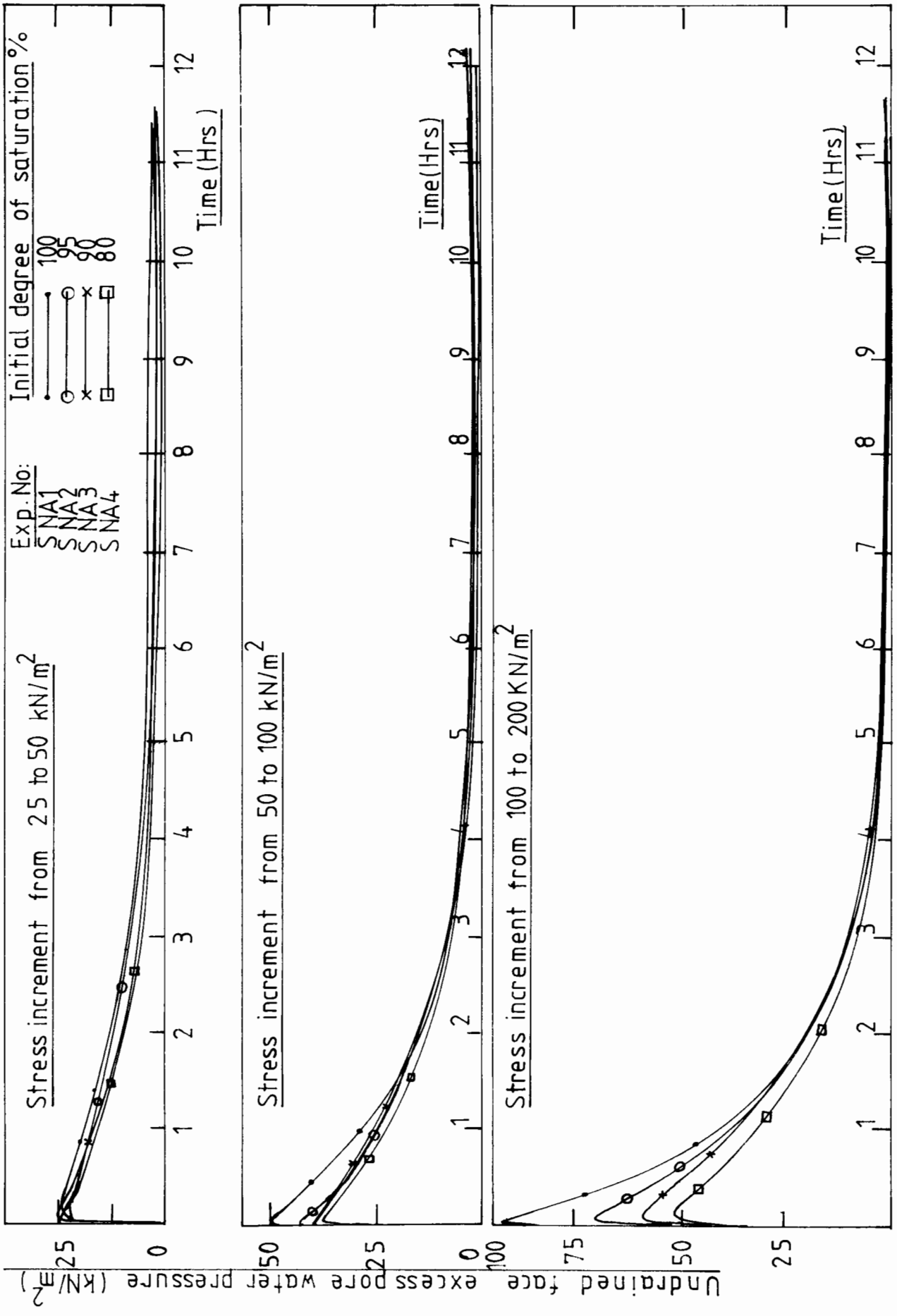

Fig 3.19a Excess pore water pressure measurement

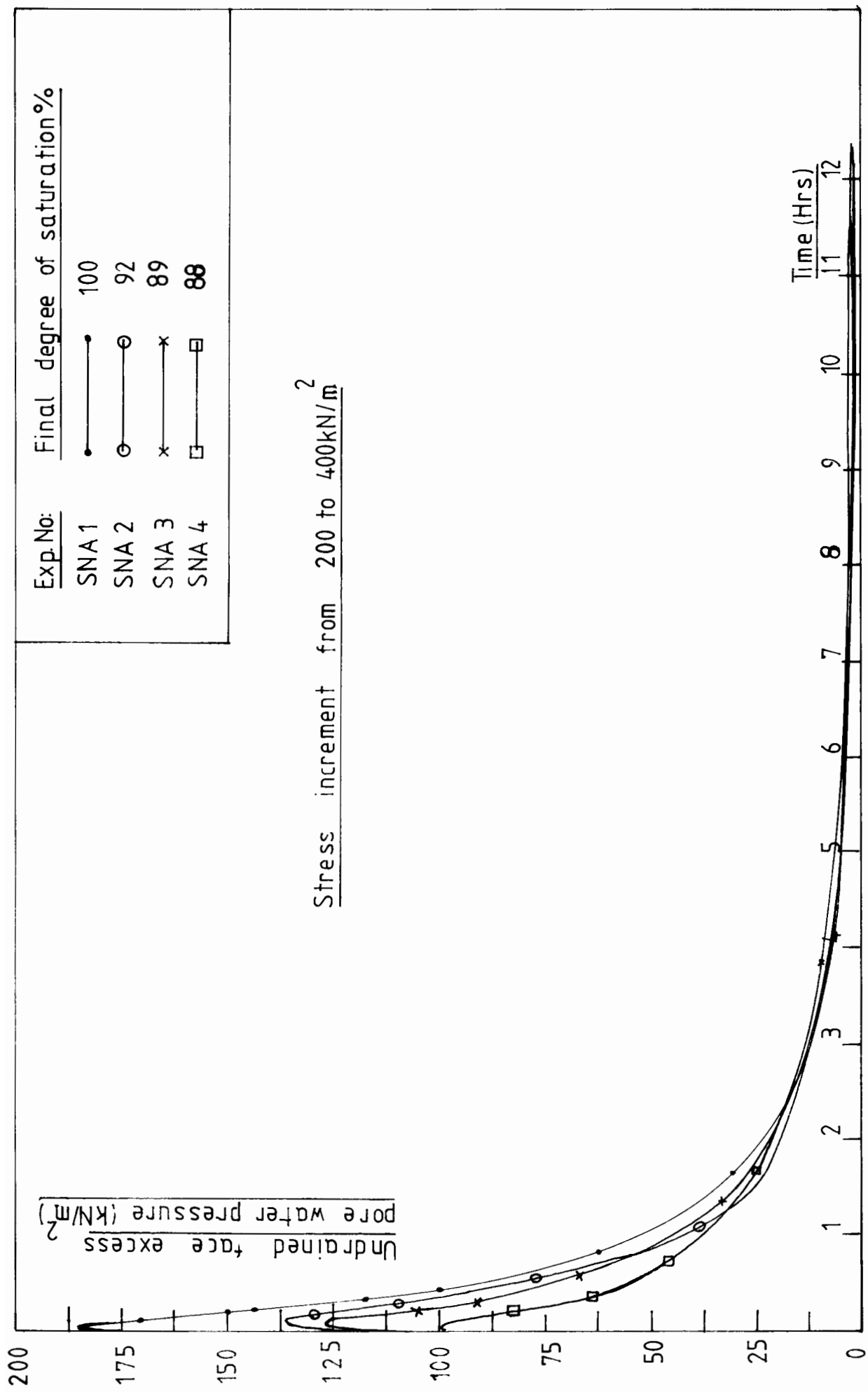

Fig 3.19b Excess pore water pressure measurement

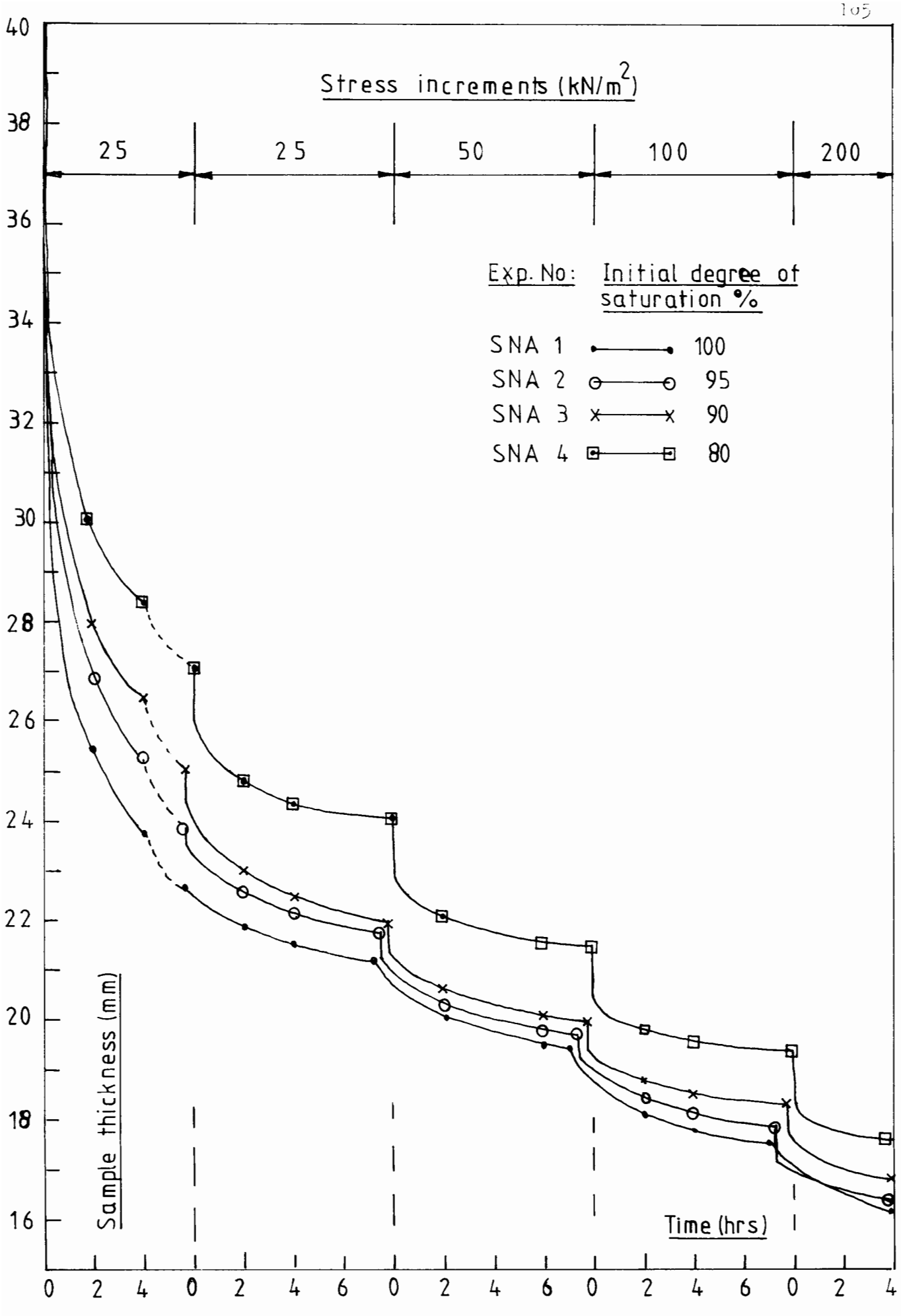

Fig 3.20 Sample displacement during consolidation

is open deformation due to consolidation takes place as the pore fluid drains in all the samples. The initial elastic deformations as well as the total deformations of the samples depend on the gas content. The higher the gas content the higher the deformation.

Fig 3.21 shows the settlement-square root time curves for gassy and saturated soils for each stress increment. Larger deformations are measured in gassy soils compared to that in saturated soil. The total settlement increases with the increase in gas content. However the time taken to achieve 90% settlement from these curves for different gassy soils shows no significant variation from that of the saturated soil. The effect of gas bubbles on the settlement rates (or on the coefficient of consolidation) of soil is examined in chapter four and the rest of this chapter examines the effect of gas bubbles on the voids ratio-stress relationship of the soil.

Void ratio- logarithm of stress relationships are shown in fig(3.22). The stress is taken as the difference between the total stress and the pore water pressure which is the effective stress in the saturated soil. The same stress parameter is used even in the gassy soil due to the difficulties involved in measuring the pore gas pressure which is not repeatable and may vary from bubble to bubble. The effect of gas bubbles in the $e-\ln(\sigma-u_w)$ relationship is remarkable. Void ratios associated with gassy soils are higher than those of saturated soils for a

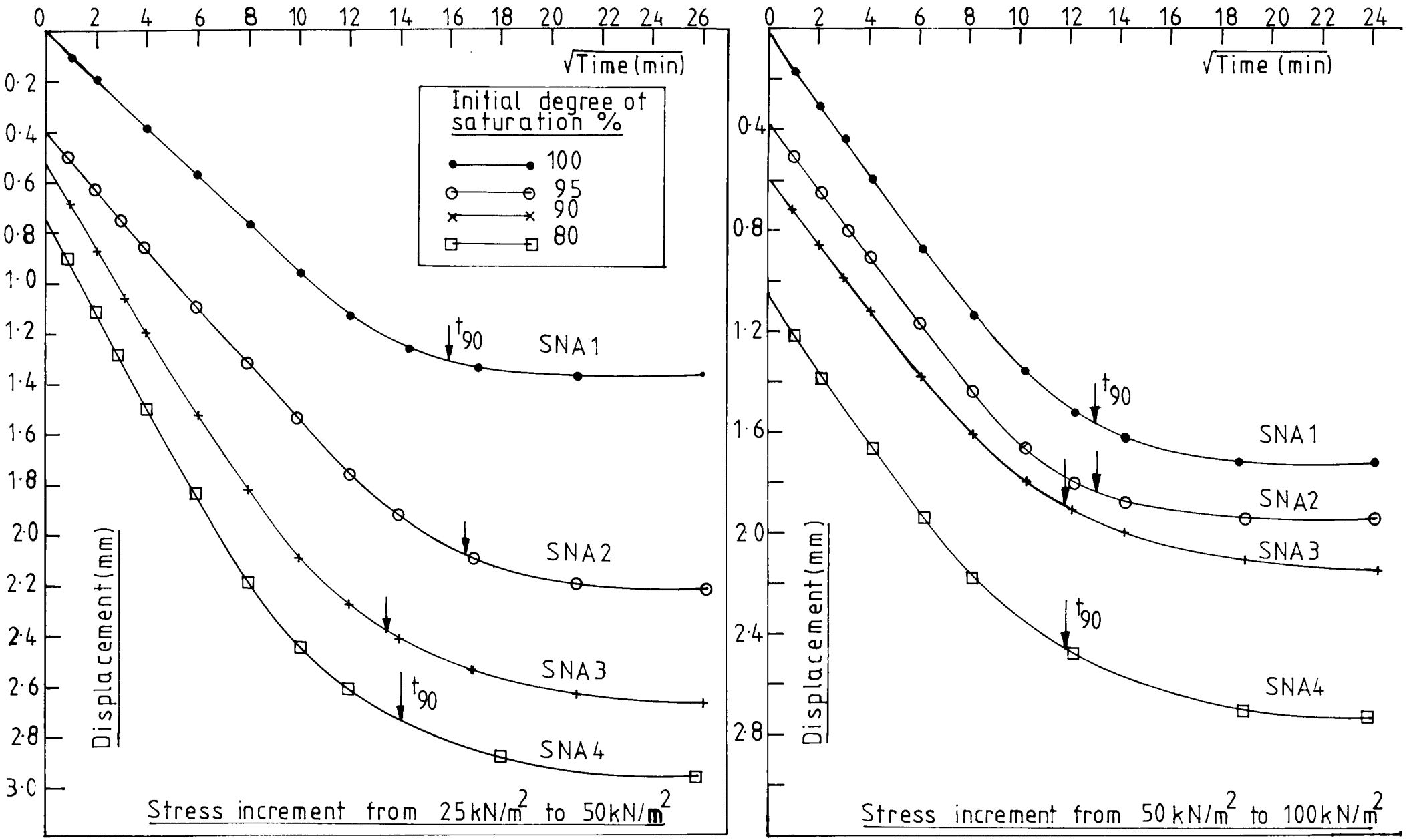

Fig 3.21a Settlement - time behaviour of gassy soil

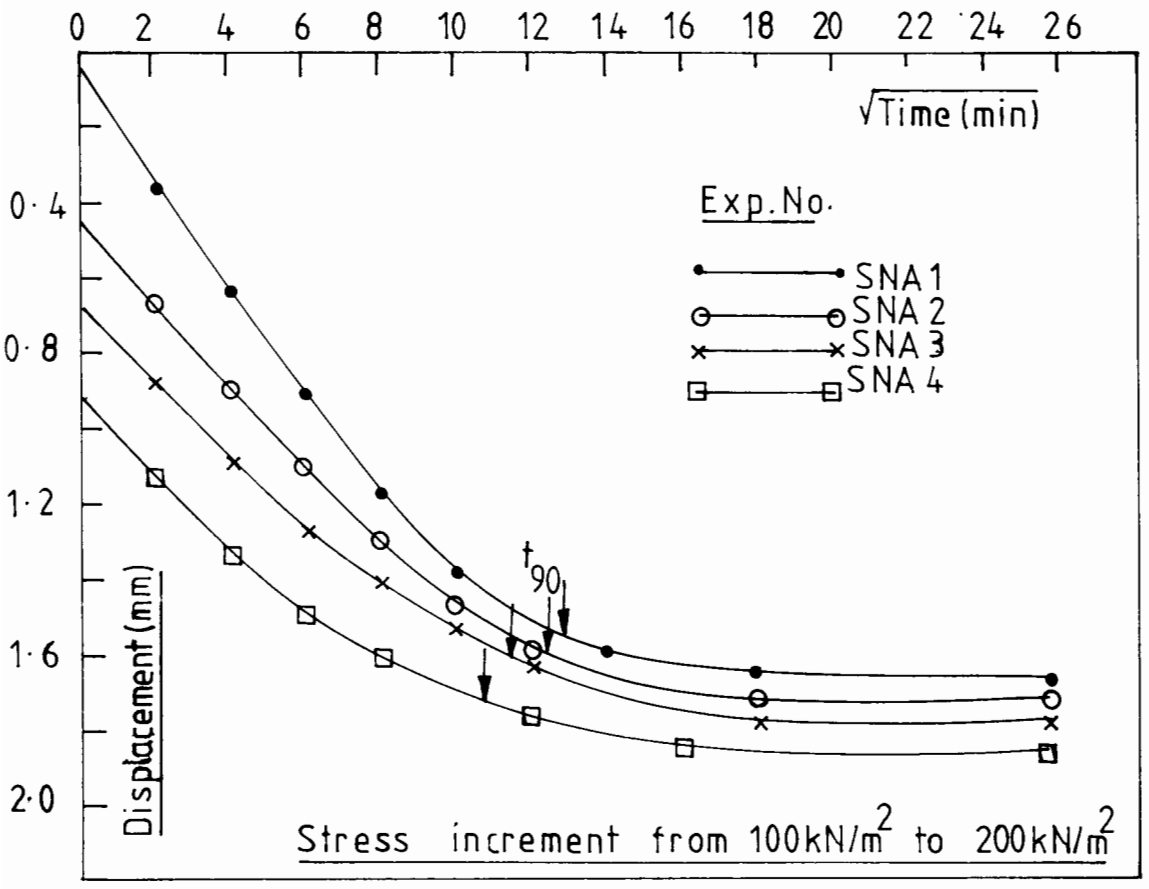

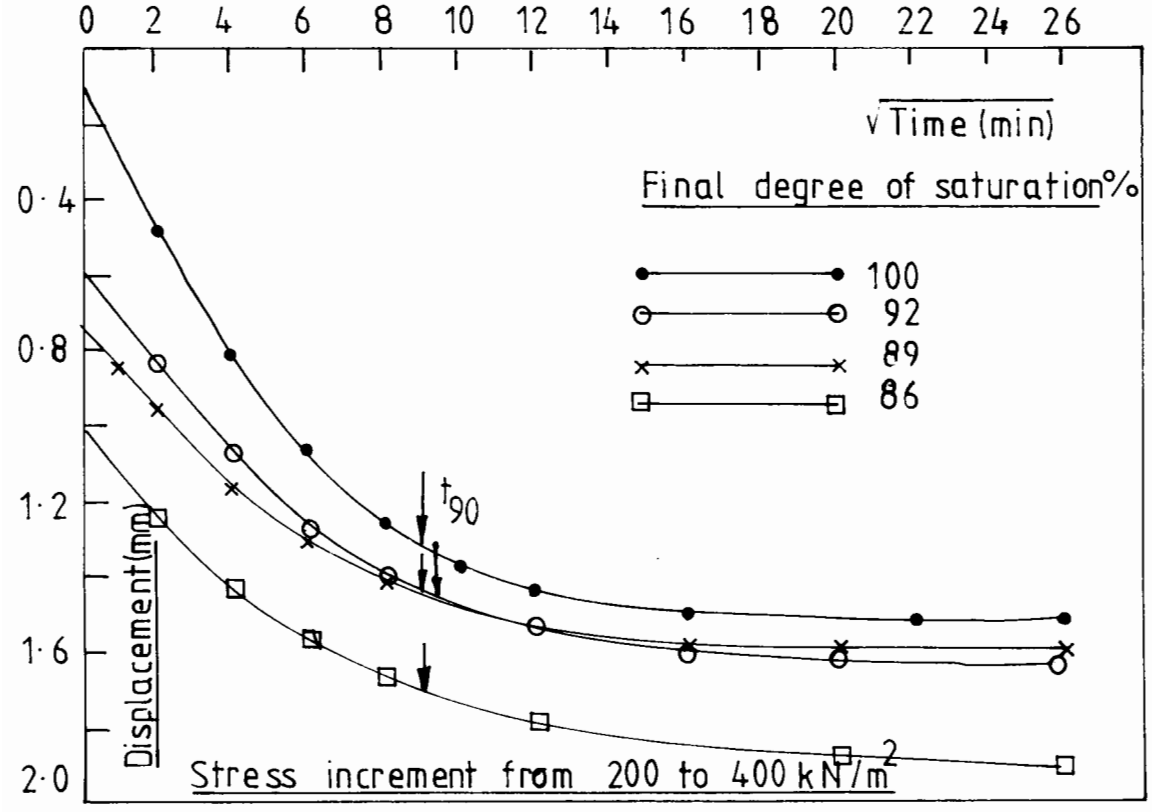

Fig 3.21b Settlement-time behaviour of gassy soil

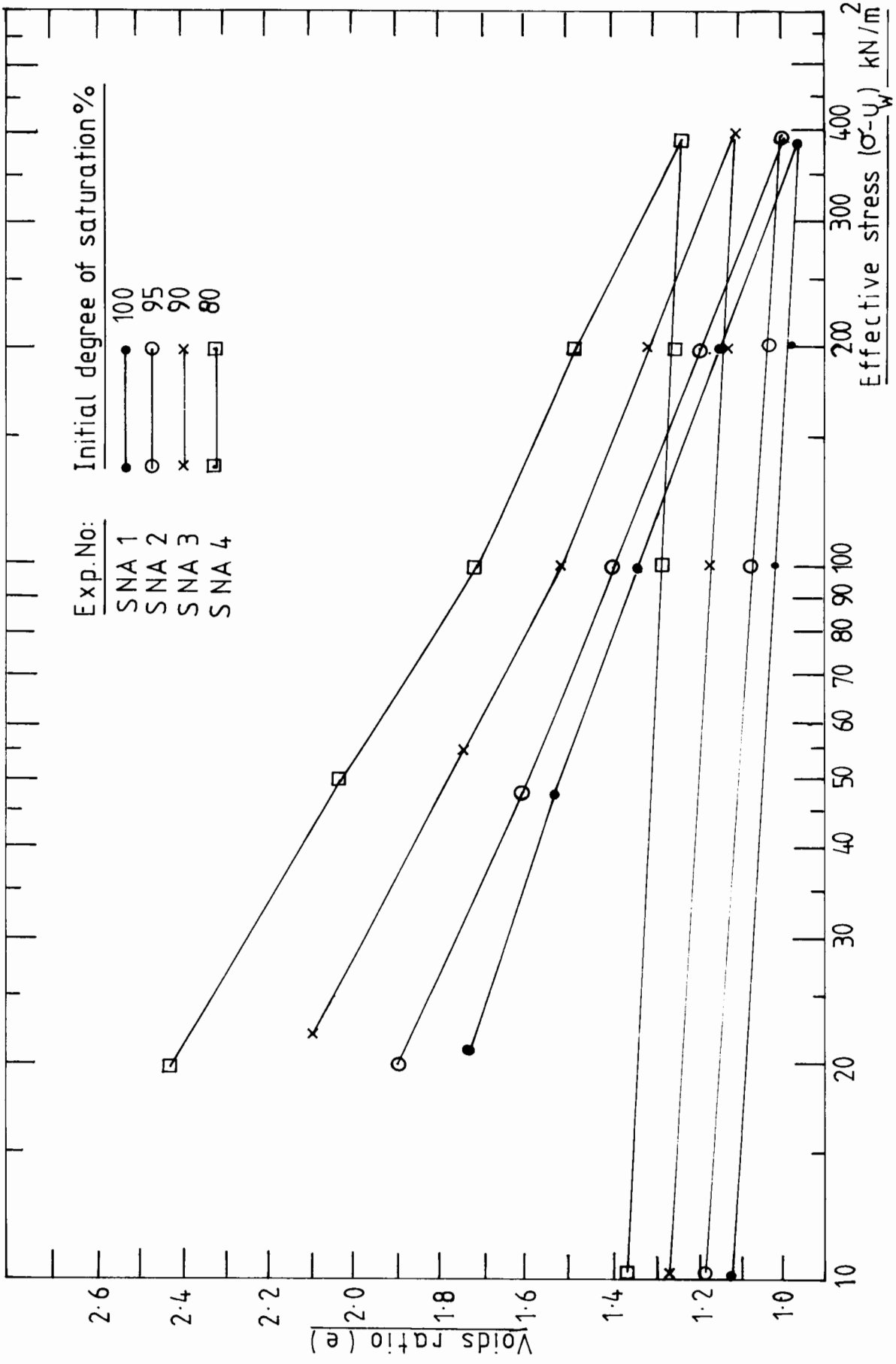

Fig 3.22 Voids ratio- effective stress relationship.

given consolidation stress. The higher the gas content, the higher the voids ratio. The shift in the e-logarithm of stress curves increases with the increase in gas content. The minimum degree of saturation (maximum gas content) used in these experiments is 80%. In the following experiments the voids ratio-logarithm of stress curves for samples of different degrees of saturation are compared instead of the sample heights or the deformations since the latter depend on the initial thickness and the initial density of the samples.

Test series B: Samples with 100, 95, 90, 85, 80, 70 % initial degree of saturation.

The measured final degree of saturation differed from the initial degree of saturation (estimate from the zeolite content) indicating changes in saturation during the consolidation process. Therefore the correlation of the above consolidation properties with gas content requires the value of degree of saturation of the soil corresponding to that particular stress state. This is achieved in the following tests by measuring the gas and water flow separately as explained in section(3.3.1.3) of this chapter. These tests allowed a check on the repeatability of the voids ratio-logarithm of stress curves obtained in the previous set of tests. The degree of saturation at the end of each load increment is calculated from the final degree of saturation measured at

the end of the test using the measured gas volume and the water volume outflow during each increment. The samples are drained from the top end and the gas displaced is collected in the perspex cap. At the end of consolidation for each increment, the gas volume is measured. It is assumed that all the gas displaced from the sample flows through the high porosity disc without getting trapped. Gas movement into the pore pressure measuring system is avoided by sealing the pore pressure port so that no measurement of pore water pressure is made in these experiments.

Fig (3.23) shows the displacement-square root time curves obtained from these tests. Gassy soil undergoes immediate settlement as soon as the load increment is applied. This immediate settlement depends on the gas content as well as the soil stiffness. The higher the gas content, the higher the immediate settlement. However, the time taken to attain 90% of the total settlement in gassy soil is similar to the saturated soil. Settlement-time behaviour of gassy soil is studied in detail in chapter 4.

Fig (3.24) shows the voids ratio-logarithm of stress curves obtained for different degrees of saturation. The repeatability of these curves is reasonable (compared with test A) and shows again the higher voids volume associated with gas bubbles. The shift in e-ln(σ-u_w) curves

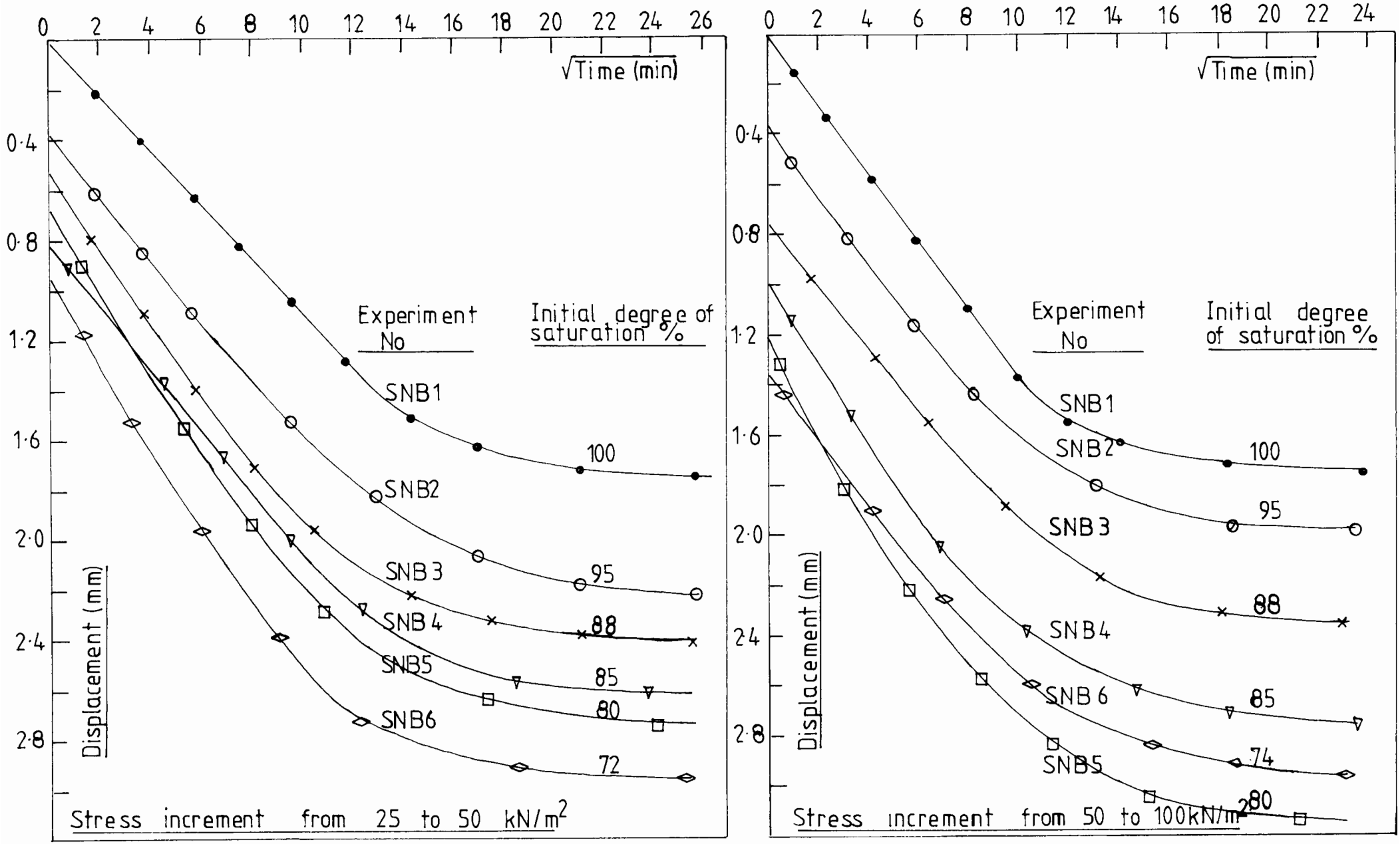

Fig 3.23a Settlement-time behaviour of gassy soils.

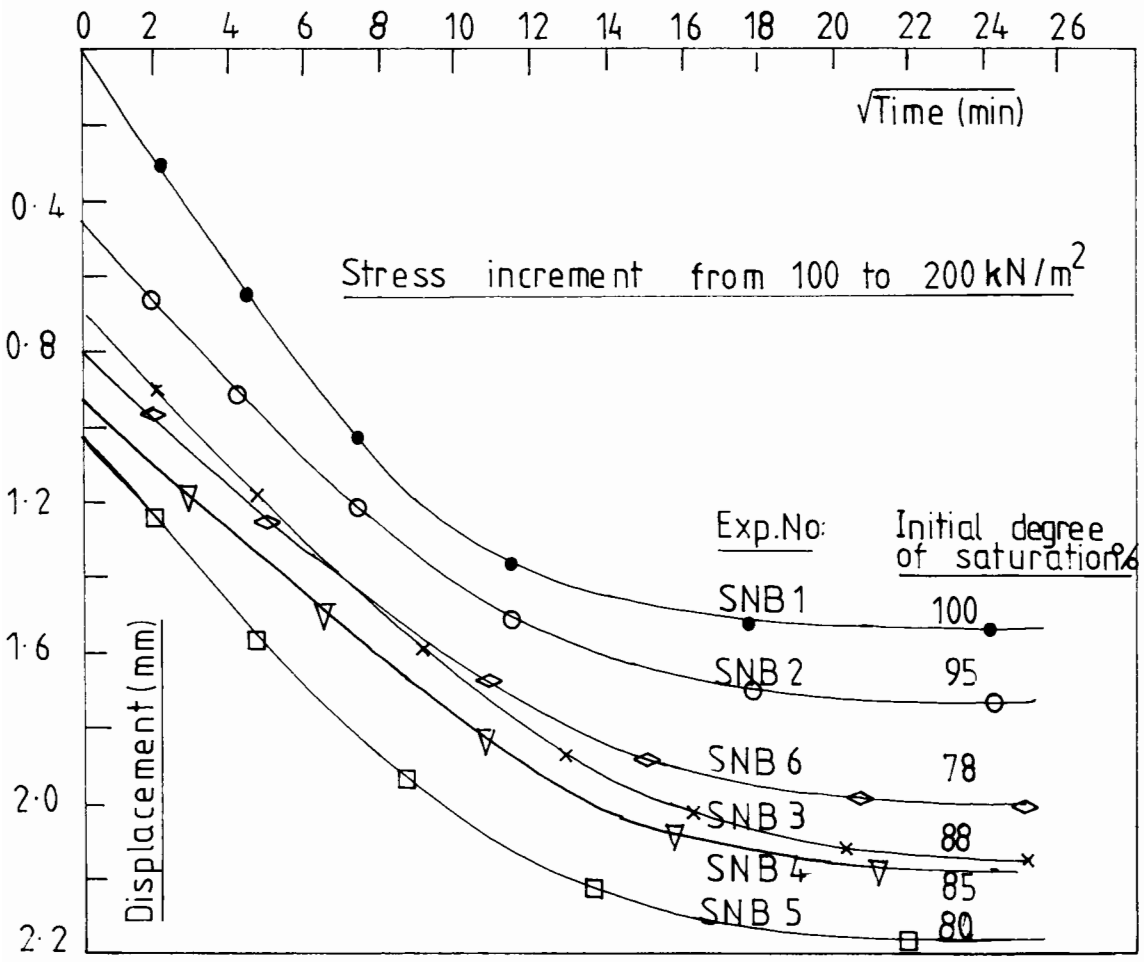

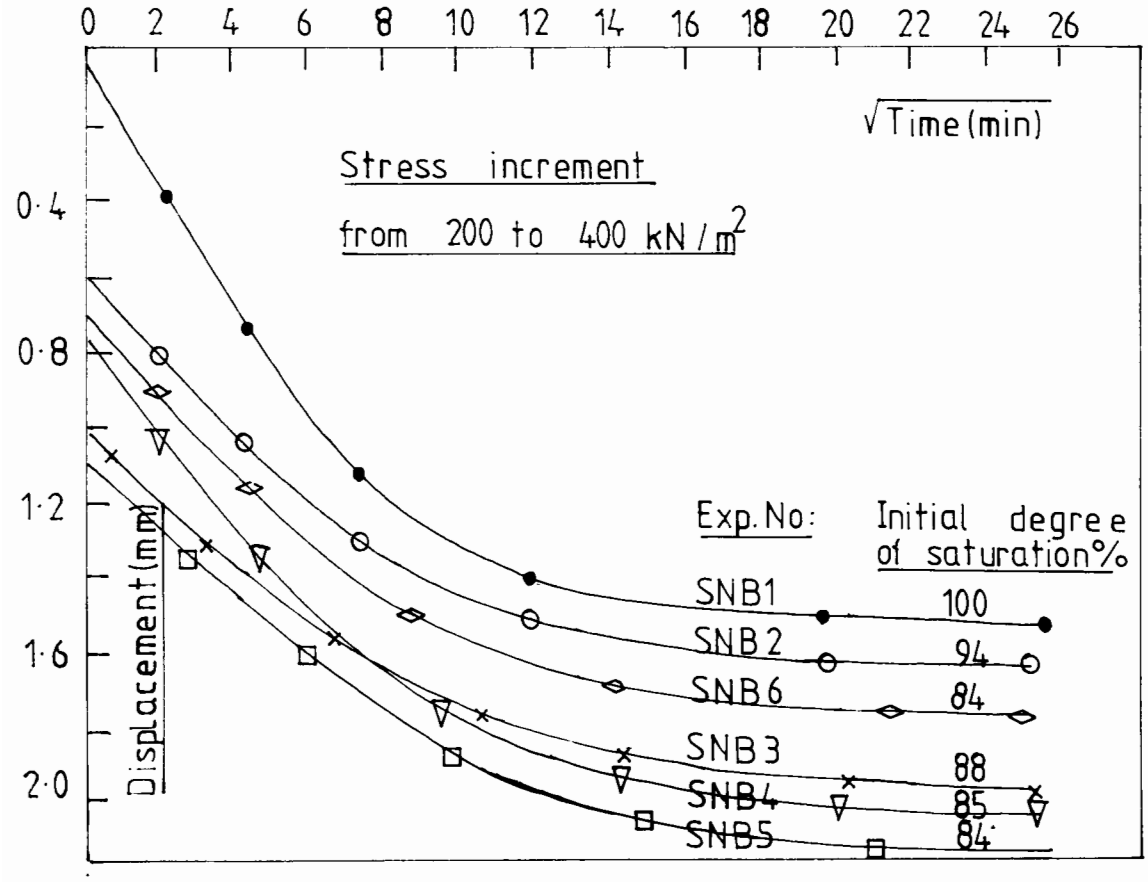

Fig 3.23b Settlement - time behaviour of gassy soils.

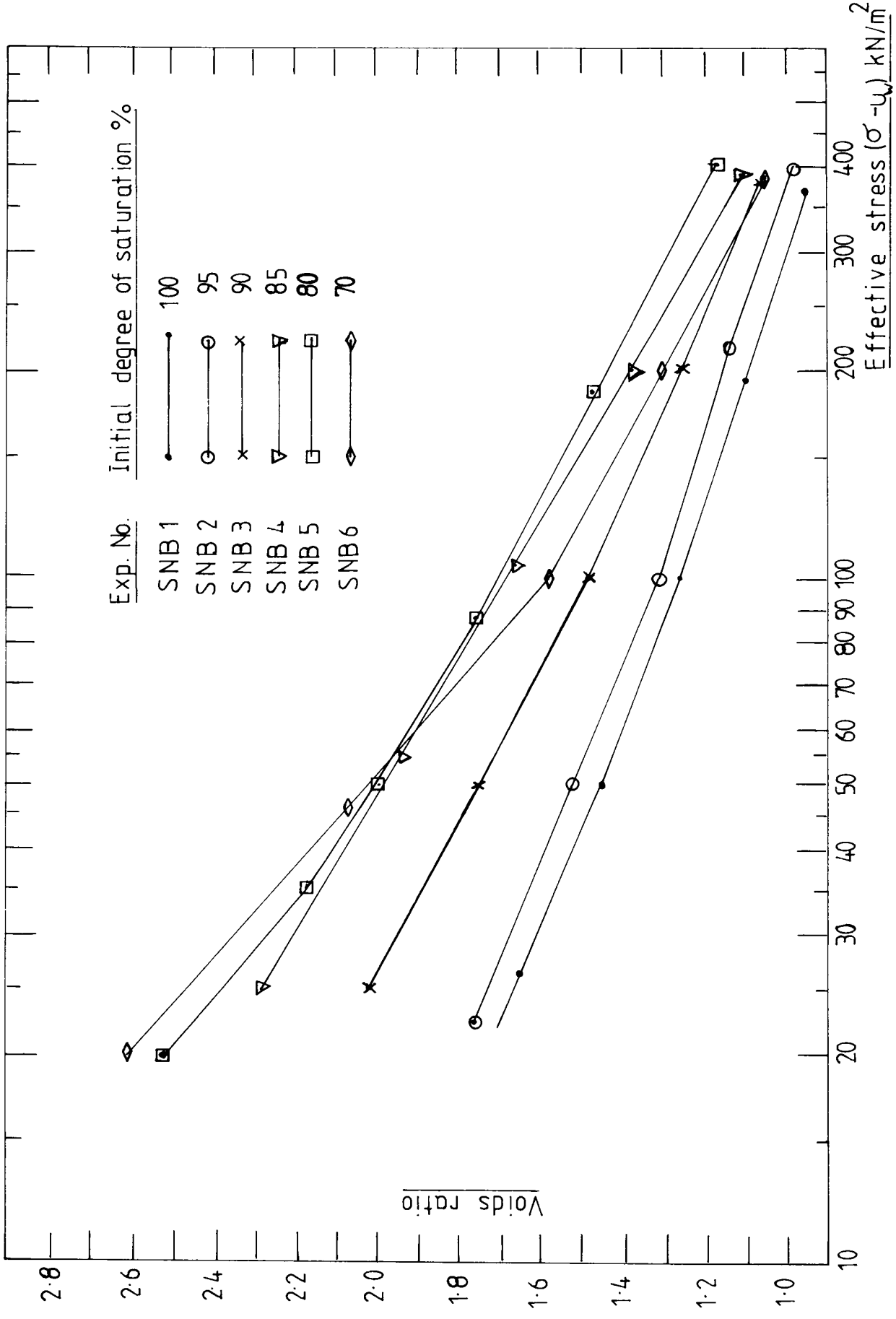

Fig 3.24 Voids ratio - effective stress relationship.

increases as the degree of saturation decreases from 100% to 85%. The sample with 80% initial degree of saturation shows only a small variation from that of the 85% sample and a further decrease in degree of saturation to 70% showed a decrease in the shift of e-ln(σ-u_w) curve .

Fig(3.25) shows the changes in degrees of saturation during consolidation. Each point corresponds to the degree of saturation (at atmospheric pressure) at the end of each stress increment when the consolidation for that increment is over. The degree of saturation of the soil with 95% initial degree of saturation decreases with subsequent stress increments indicating a higher water flow compared to the gas flow. Thus bubbles remained in the soil and no gas outflow is observed from the soil with 95% degree of saturation. In the case of the soil with 80% initial degree of saturation, the saturation increases with stress increment, indicating more gas flow compared to water flow, suggesting that bubbles are connected and gas permeability is comparatively high. Soils with initial degree of saturation 90% and 85% show no changes in saturation with stress increments, suggesting that the proportions of gas and water in the drainage fluid are the same as those in the soil. The test carried out with 70% initial degree of saturation shows no further shift in e-ln(σ-u_w) curve compared to that of 80% soil, but the degree of saturation rapidly increased (from 70% to 88%) with stress increments.

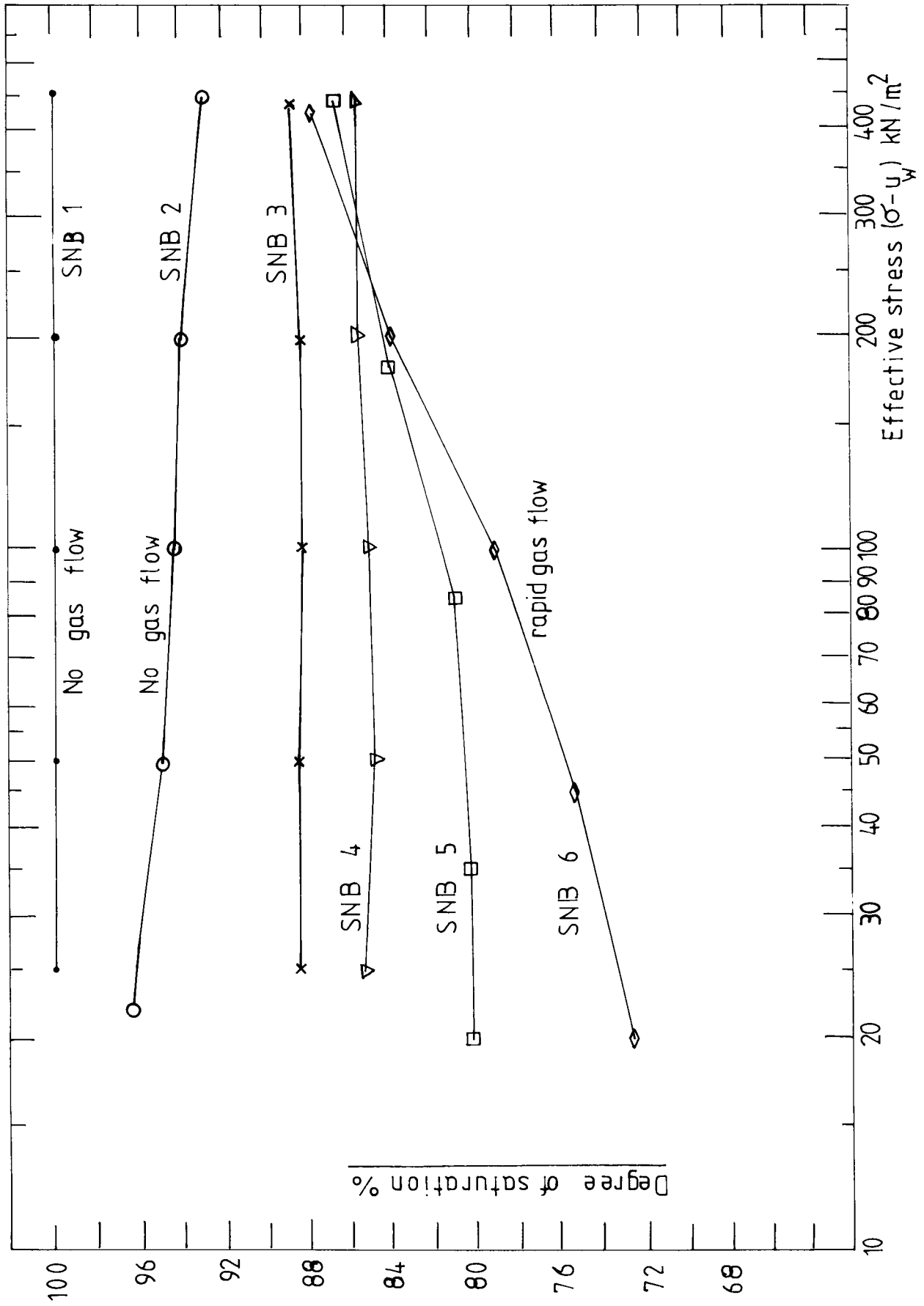

Fig 3.25. Variation in degree of saturation during consolidation.

Test series C: Samples 100, 90, 80, 70% degree of saturation.

The voids ratio e- $\ln(\sigma-U_w)$ curves for all the tests (series A, B, C and D) are plotted from the final voids ratio measured at the end of the tests and the displacement measured for each stress increment. The absolute position of the curves depends on the accuracy of the measurement of the final voids ratio. However the gradient of each curve is not sensitive to the final voids ratio calculation and is found to be the same for samples with the same degree of saturation. In order to check the absolute position of the e-$\ln(\sigma-U_w)$ plots for different degree of saturation, the following tests are carried out. Instead of consolidating the samples to 400kN/m^2 vertical stress as in the previous tests, samples are consolidated to 100kN/m^2 stress and then unloaded. Fig(3.26) shows the e-$\ln(\sigma-U_w)$ curve for the above tests which when compared with that for the results of the earlier tests, fig(3.24), show similar behaviour, ie.high voids ratio occur in gassy soils.

Fig (3.27) shows the variation in degree of saturation during consolidation. The degree of saturation of the soil with 90% initial degree of saturation remains constant, whereas that of the soil with 80% and 70% initial degrees of saturation increases with stress increments.

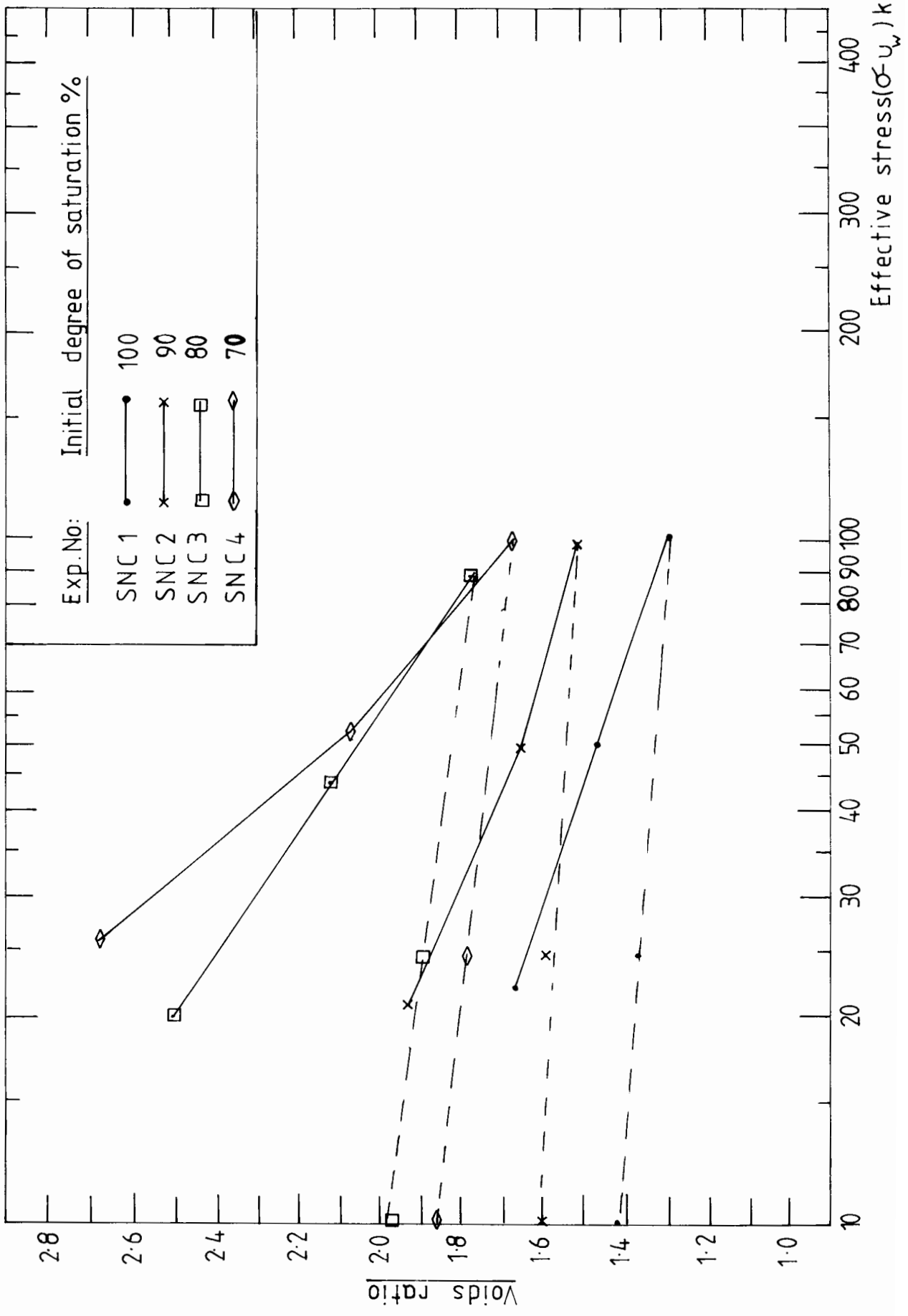

Fig. 3.26 Voids ratio - effective stress relationship.

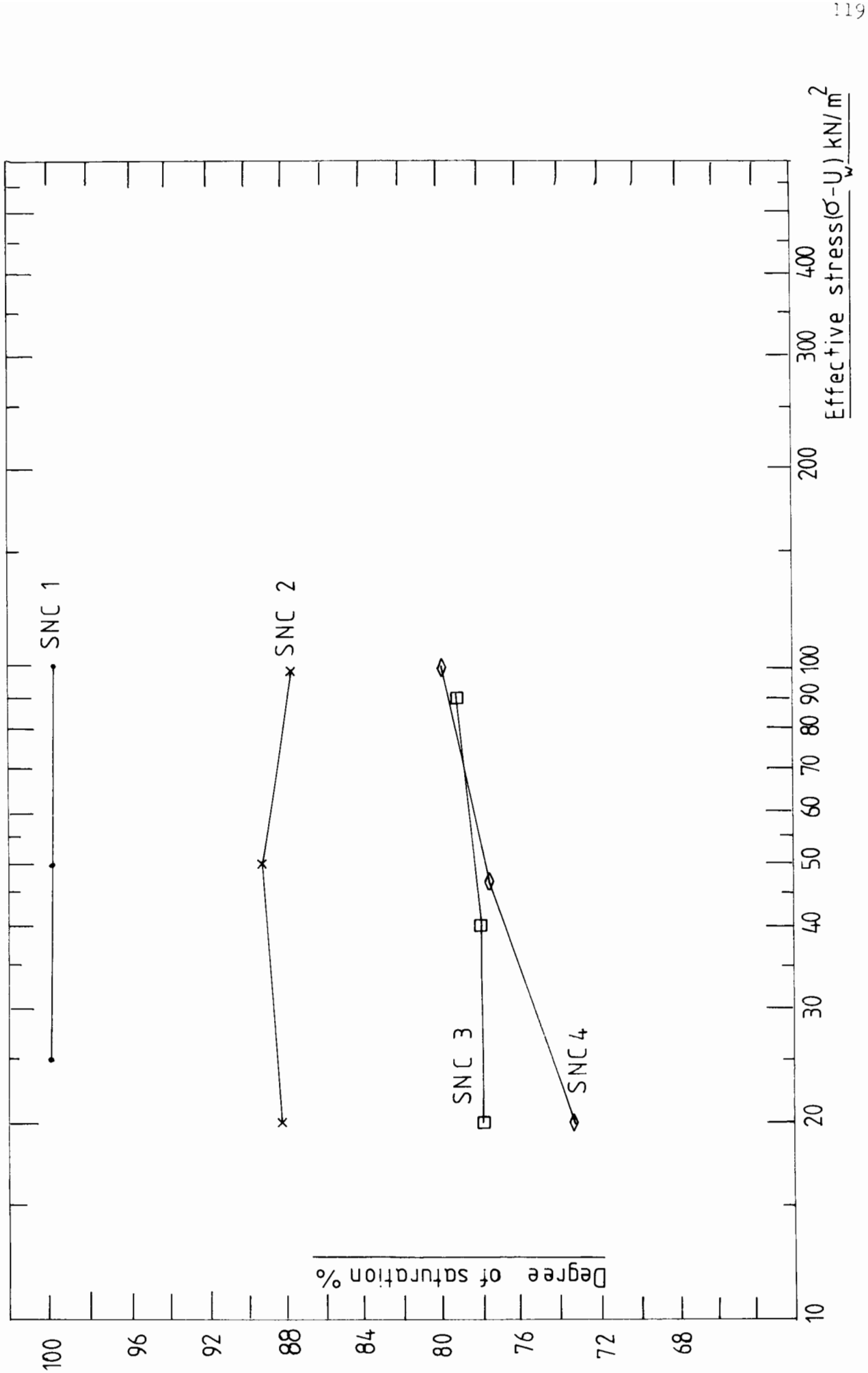

Fig 3.27 Variation in degree of saturation during consolidation.

3.4.2 DOUBLE DRAINAGE CONSOLIDATION:

Test series D: Samples with 100, 95, 90, 80, 70% initial degree of saturation.

Soil samples with different initial degrees of saturation were consolidated using top and bottom face drainage. Fig (3.28) shows the voids ratio-logarithmic stress relationship for these tests. The behaviour is similar to that of the single drainage tests, demonstrating the shift in the curves depending on the degrees of saturation. The shift in the curves (compared to the saturated soil curve) increases with decrease in degree of saturation down to 80%. A further decrease in the degree of saturation down to 70% shows a reduction in the shift. The swelling behaviour of gassy soils is also examined by unloading the samples at 100kN/m^2 stress level to 10kN/m^2 stress and then reconsolidating them to 400 kN/m^2 stress level fig (3.28). No remarkable variation in the swelling gradients is observed in the soils with different degrees of saturation even though the gradients of the loading curves are different.

3.4.3 THE EFFECT OF BACK PRESSURE ON THE CONSOLIDATION BEHAVIOUR OF GASSY SOILS.

The above experiments were carried out without back pressure and the amount of gas content is varied using different amounts of methane-saturated zeolite. In these tests the gas content is varied using different back

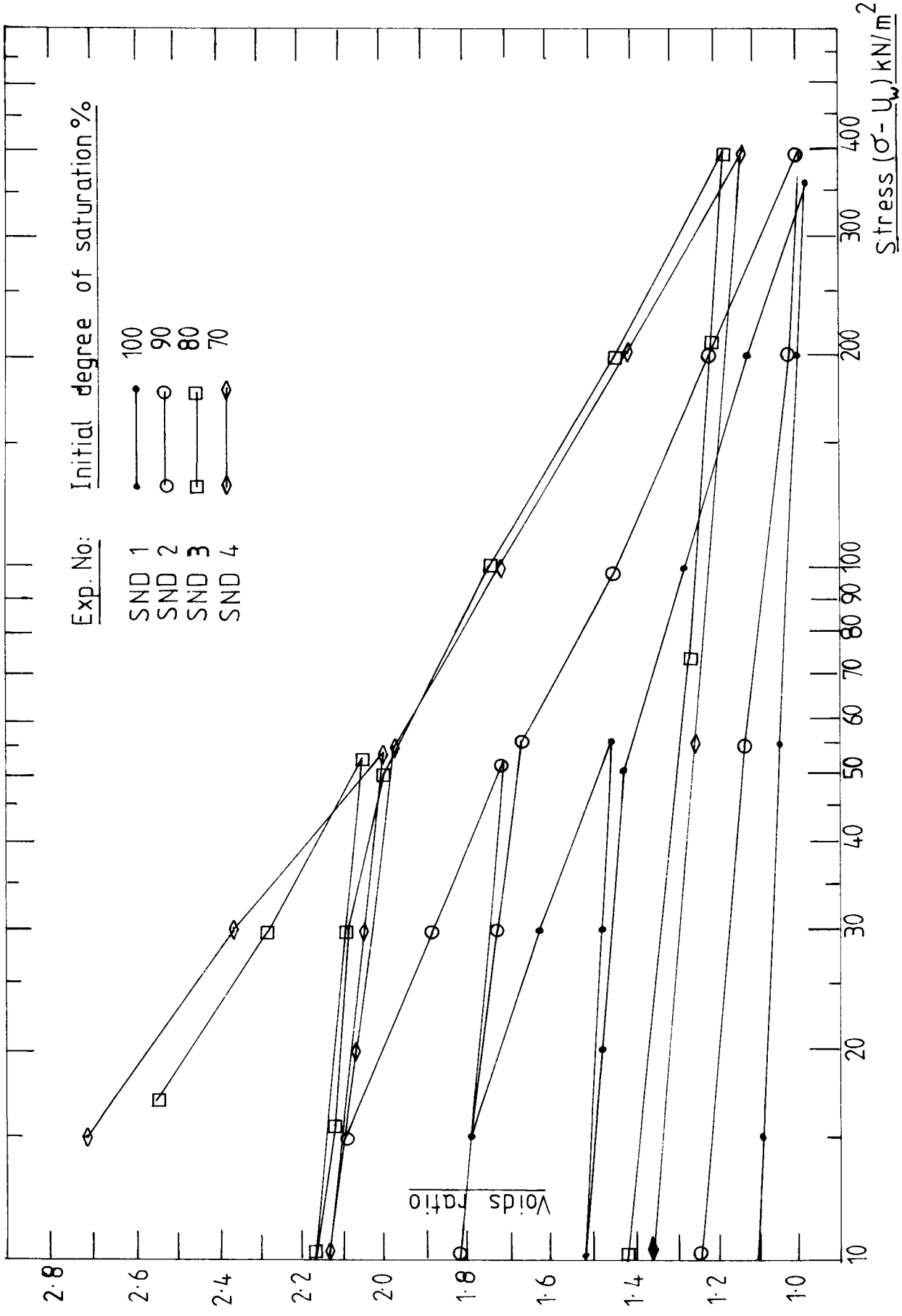

Fig 3.28 Voids ratio- stress relationship in two face drainage tests.

pressures. The following experiments are carried out using 50 kN/m^2 back pressure. The back pressure is applied after the gas bubbles have been released from the zeolite. The table below shows the changes in degree of saturation due to the application of the back pressure, calculated using Boyle's and Henry's laws.

Degree of saturation at atmospheric pressure estimated from zeolite content.	Degree of saturation after the application of the back pressure 50 kN/m^2
80%	87%
90%	93%
100%	100%

The fig (3.29) shows the voids ratio-logarithm of stress relationship of the tests with back pressure and those without back pressure. The shift in the $e-\ln(\sigma-u_w)$ curves increases with the decrease in degree of saturation in both set of experiments. The application of back pressure reduces the amount of shift when compared to the test with the same initial degree of saturation at atmospheric pressure because the amount of gas in the soil is reduced by the back pressure increase. These experiments show that the increase in back pressure reduces the shift in voids ratio-logarithm of stress relationship and suggest that this shift is due to gas volume.

Another set of experiments are carried out to investigate whether the e lnσ curve for a given degree of saturation (eg.80%) could be brought down to coincide with that of the saturated soil if sufficient amount of back pressure

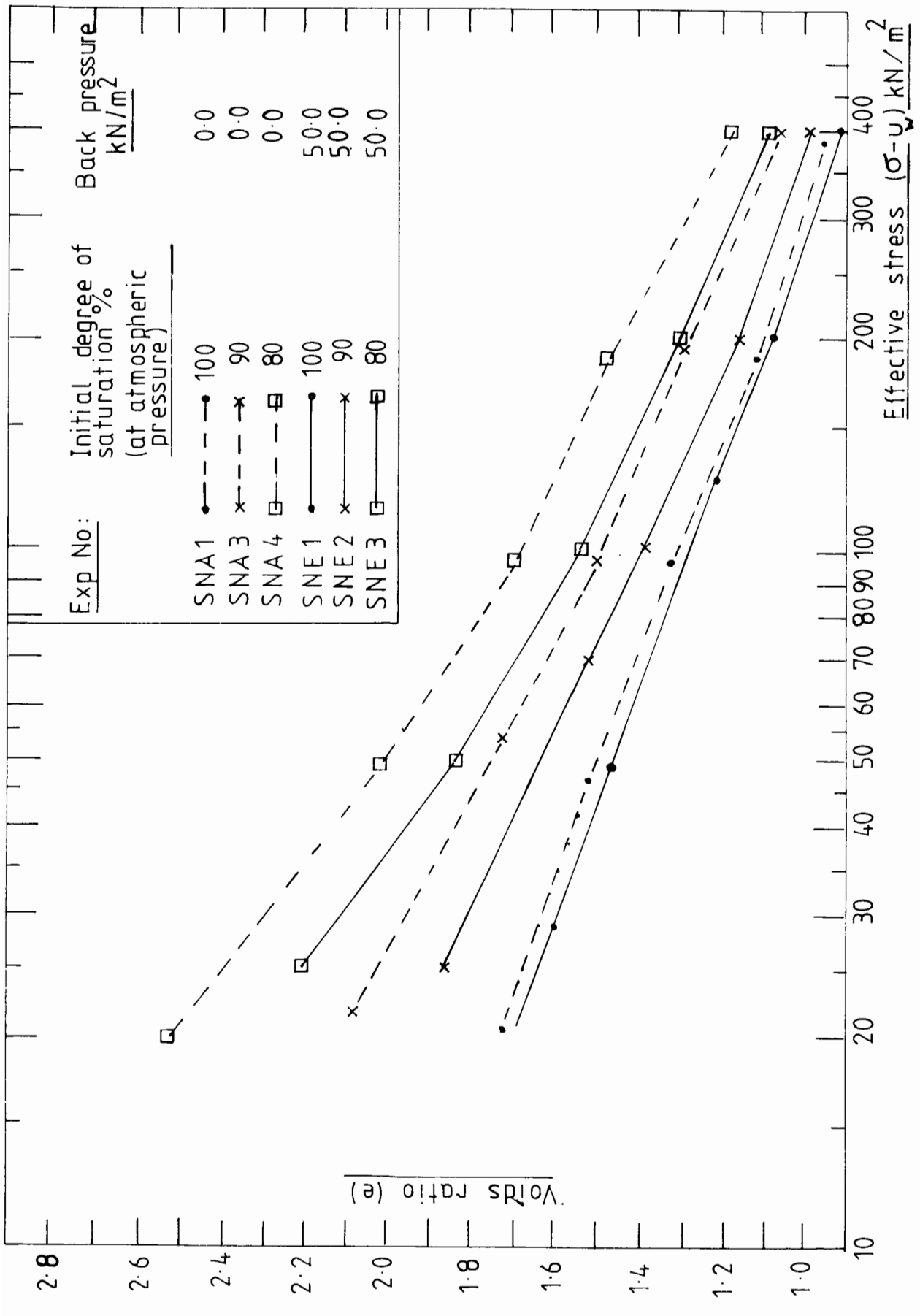

Fig 3.29 Effect of back pressure on the voids ratio-stress relationship.

is applied. In these tests the soil samples with initial degree of saturation of 80% are prepared and consolidated to a particular vertical total stress (50, 100kN/m^2) using no back pressure. At this stress state the back pressure and the total stress are increased either by 100 or 400 kN/m^2 (keeping $\sigma-u_w$ constant) and then the consolidation tests are carried out by increasing the total stress, keeping the back pressure constant. Fig (3.30) shows the e-ln($\sigma-u_w$) curves for these tests. The increase in back pressure and the total stress either by 100 or400 kN/m^2 show an immediate reduction in voids ratio as the bubble size decreases. The shift in the e-logarithm of stress curves for 100 and 400 kN/m^2 increase in back pressures becomes curves corresponding to a gassy soil with degree of saturation between 90% and 95% without back pressure. The calculated degree of saturation, using Boyle,s and Henry's laws, due to the back pressure increase of 100 and 400kN/m^2 are 90% and 96% respectively. However the e-ln($\sigma-u_w$) curve for 400 kN/m^2 back pressure is closer to a 90% saturated soil with zero back pressure. This curve is expected to fall between the curves for 95% and 100% saturation, if the shift is due directly to the gas volume. This unexpected behaviour may be due to some structural effects caused by the presence of gas bubbles in the soil which are not removed by the reduction in gas volume by the application of the back pressure.

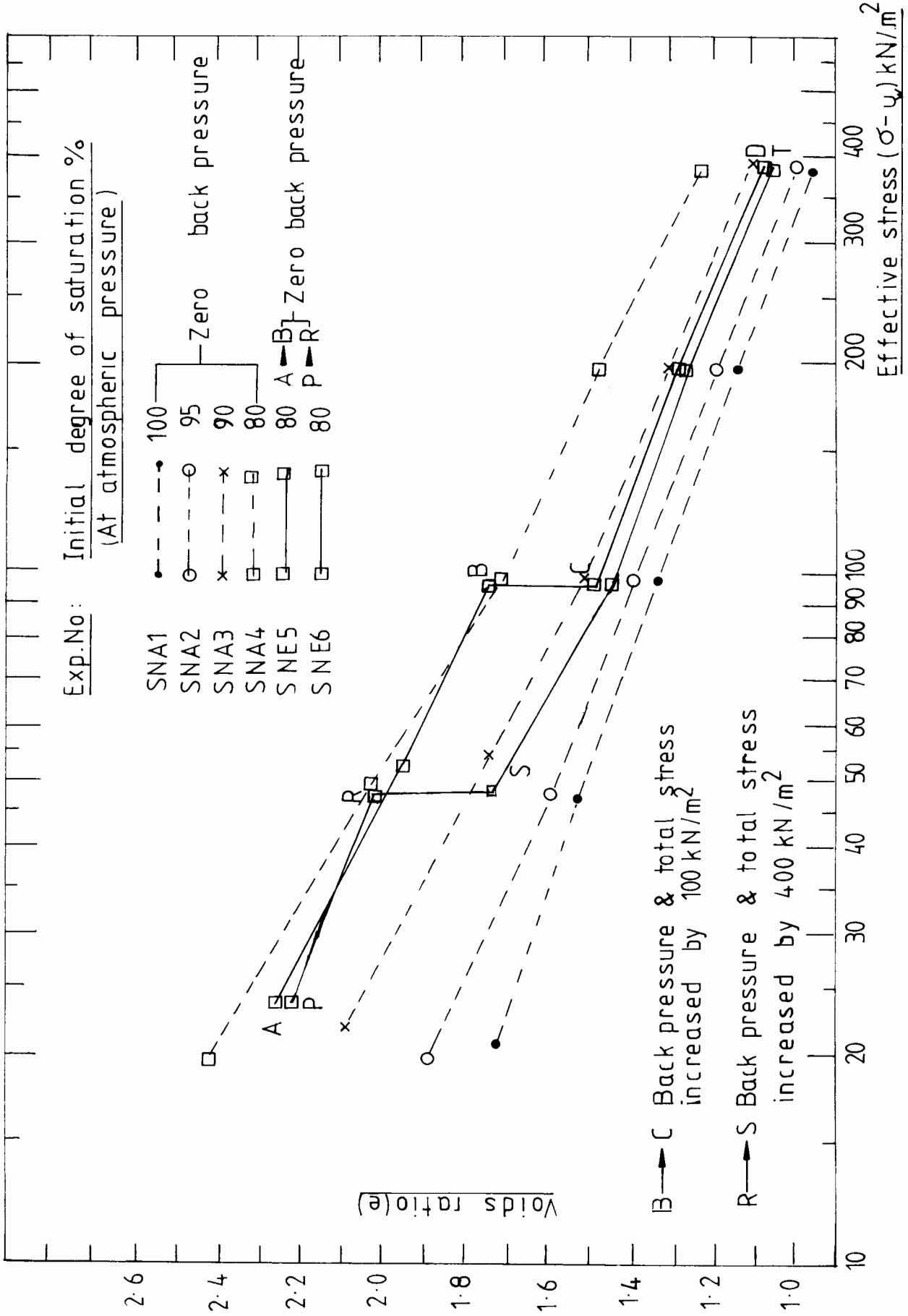

Fig.3.30 Effect of back pressure on the voids ratio - stress relationship.

3.4.4 STRUCTURE OF GASSY SOILS.

Fig (3.31) shows the photographs of the samples with different degrees of saturation, consolidated to 400 kN/m^2 pressure in the test series A. The photographs provide a six times magnification of oven dry samples. The bubble sizes are significantly larger (1-3mm) than that of the clay particle size. The bubbles sizes are estimated from the photographs. A continuous structure is seen in the saturated soil even after drying it, since the magnification is not enough to reveal the water voids. This is useful to separate the water voids from the gas voids. Gas bubbles are squashed to an oval shape during consolidation and these photographs shows the possibility of bubble interconnection when the degree of saturation is as low as 50%.

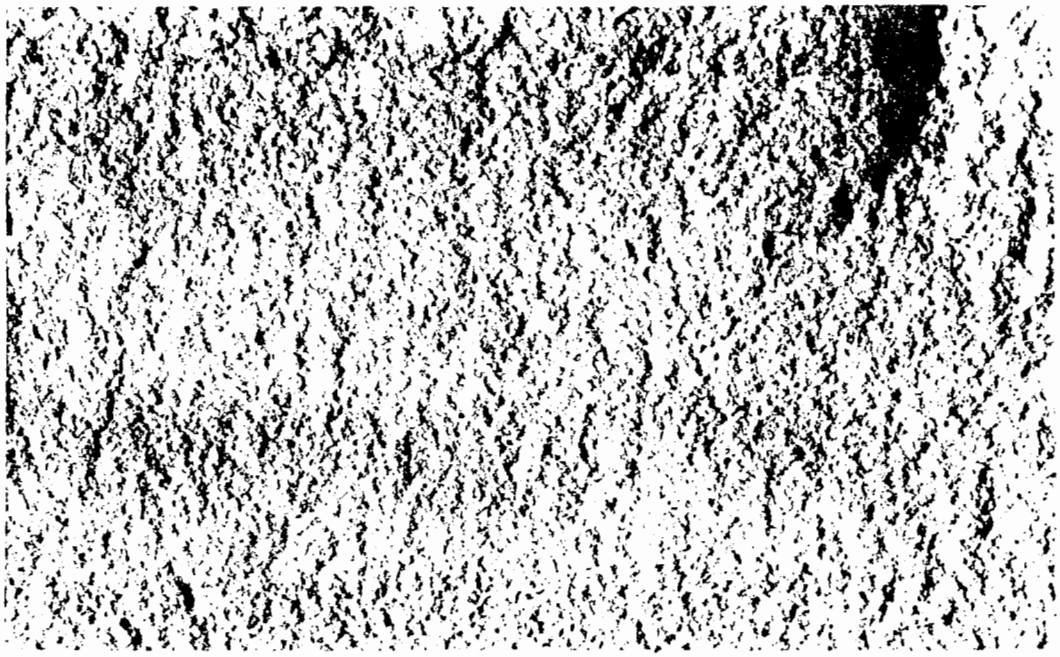

Saturated soil.

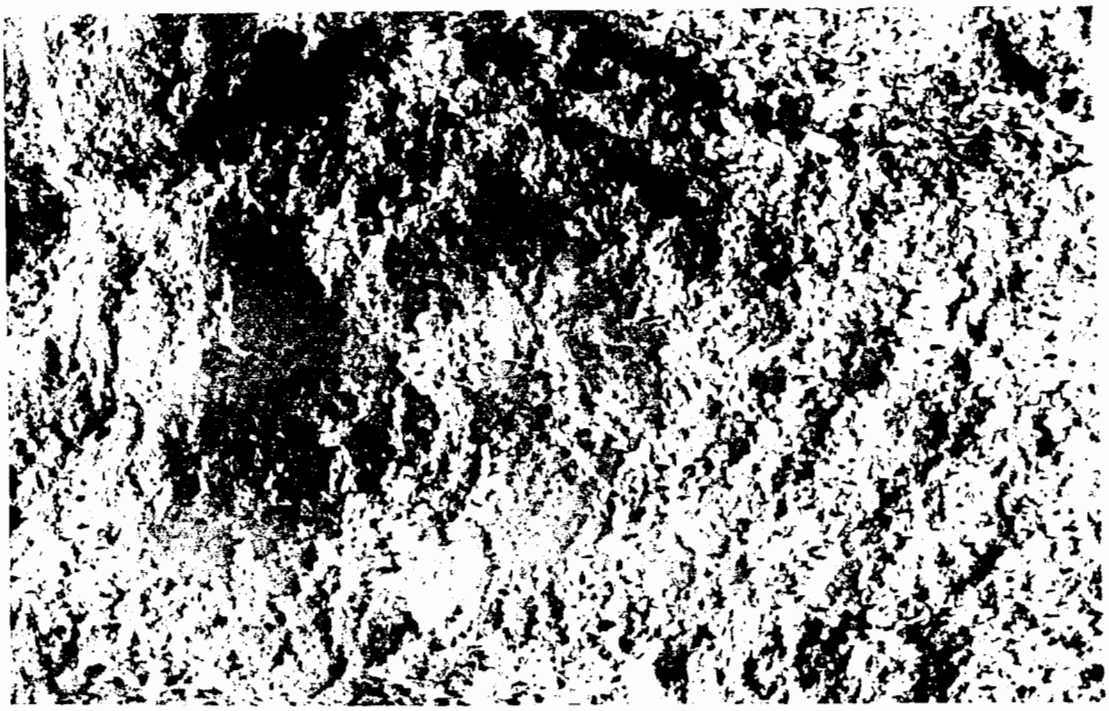

Gassy soil. Initial degree of saturation 95%.
Final degree of saturation 92%.

Fig 3.31 Appearance of soil samples subjected to 400kN/m^2 consolidation stress.

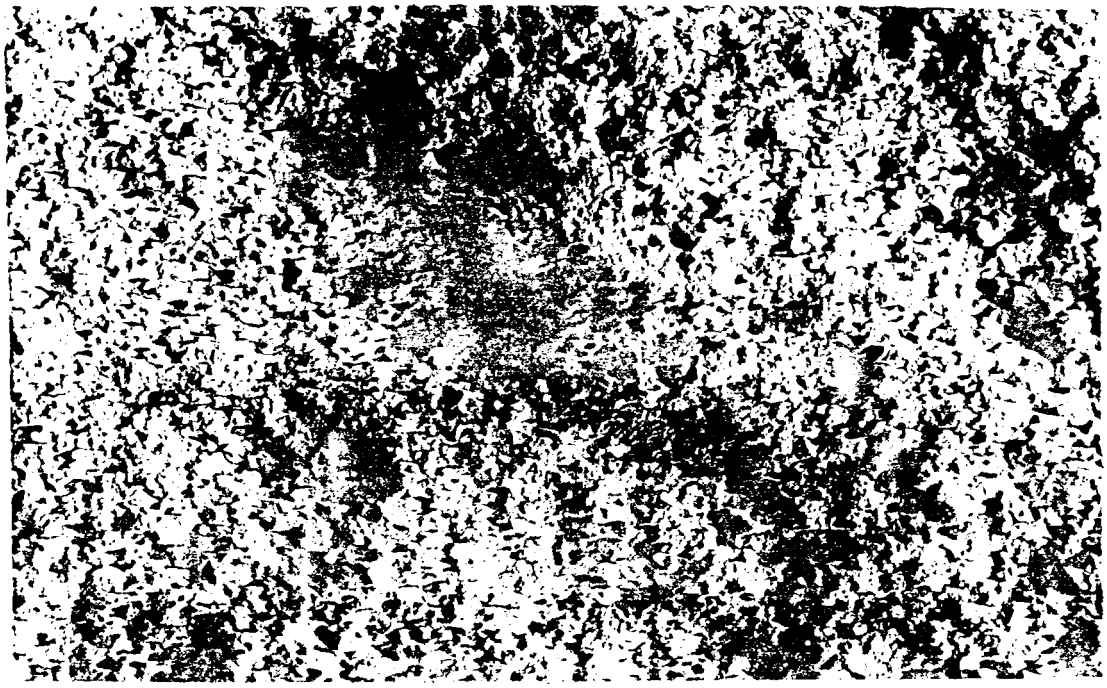

Gassy soil. Initial degree of saturation 85%
Final degree of saturation 85%

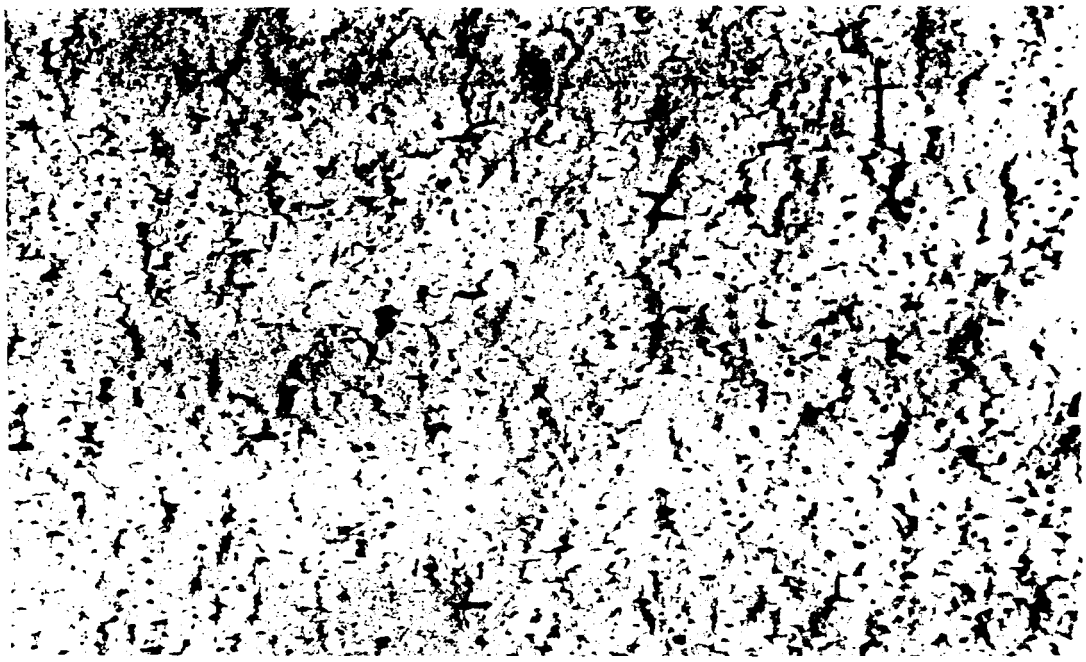

Gassy soil. Initial degree of saturation 72%
Final degree of saturation 88%

Fig 3.31

Appearance of soil samples subjected to 400 kN/m^2 consolidation stress.

3.5 DISCUSSION OF THE RESULTS:

(a) Pore fluid pressure:

The measurement of pore water pressure in gassy soil is hindered by the gas movement into the measuring system. Pore pressure measurement is affected, if sufficient amount of gas enters the system and becomes trapped between the porous stone and soil as suggested in fig(3.16). Positive excess pore pressures are measured in these circumstances and this can be avoided by allowing the gas to pass through the stone rather than be collected in the pressure measurement system. Higher air entry porous stones may prevent the movement of gas in the form of bubbles, but do not prevent the gas diffusion. The highest gas pressure registered in the experiments is 85kN/m^2 which is measured in 80% saturated soil at 400kN/m^2 stress level. The fig(3.32) shows the voids ratio-logarithm of stress relationship for gassy soil. The stress parameter used in this particular plot is the effective stress defined as:

$$\sigma' = \sigma - \chi u_w - (1-\chi) u_a \quad \text{----------(a)}$$

by Bishop(1963)

and the factor χ is assumed to be equal to the degree of saturation (χ=S/100) and

u_a is the pore gas pressure. The elevated pore pressures registered in the experiments, SNP series, are assumed to be the pore gas pressure in this analysis.

The e-In(σ') curves are still different for different

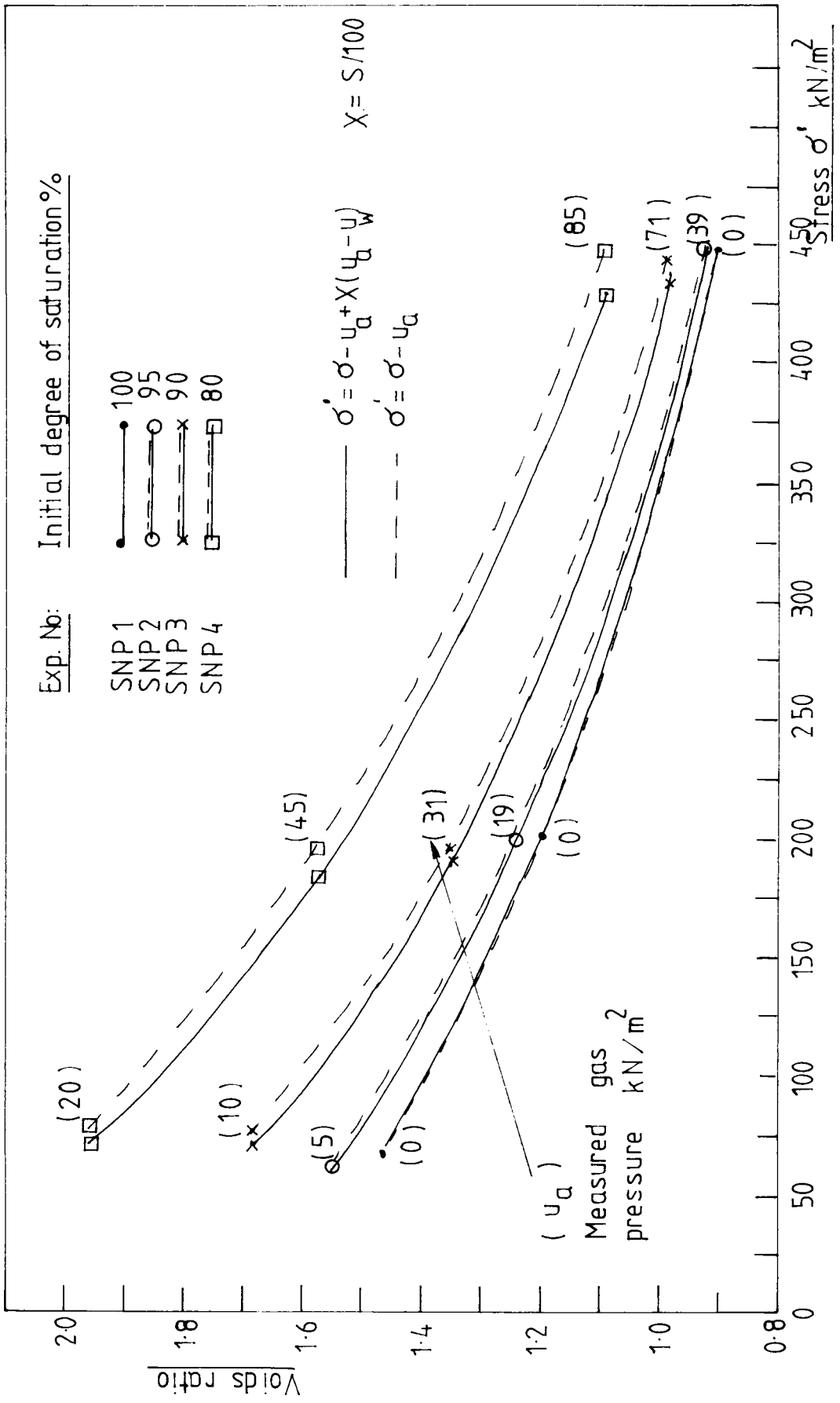

Fig 3.32 Effect of pore gas pressure on the voids ratio-stress relationship

gassy soil and this observation suggests that behaviour of gassy soil can not be described by the effective stress law(a) or that the measured excess pore gas pressure in the experiments do not represent true pore gas pressure values. These measured gas pressures were not found closely repeatable and hence are believed to be unreliable. A model to describe the volume change behaviour of gassy soils is developed later which uses only the pore water pressure and does not require the measurement of pore gas pressure.

The measured pore water pressure using the modified measuring system fig(3.18), increases during the undrained application of the stress increment and then dissipates and reaches the back pressure level in all the gassy soil samples. The magnitude of the initial pore water pressure increase depends on the gas content of the soil as well as on the soil stiffness and this undrained behaviour is studied in detail in chapter four.

Degree of saturation:

The degree of saturation in the soil varies as gas and water flow occurs during consolidation. Fig(3.25) shows that soils with initial degree of saturation 95% and 90% behave differently to that of 80% and 70% saturated soils. When the gas content is low (S=95, 90%), larger proportion of water flow occurs compared to the gas flow. This behaviour decreases the degree of saturation of the

soil. When the bubbles are interconnected at low degrees of saturation (S=80, 70%), the gas permeability is higher and a larger proportion of gas flow occurs compared to the water flow. Therefore the degree of saturation of the soil increases. There is a transition stage between 90% and 80% degree of saturation where the proportion of the water and gas in the drainage fluid is the same as in the soil. The degree of saturation remains constant in this stage and for this particular soil it is around 85%.

Voids ratio-logarithm stress relationship:

The effect of gas bubbles on the soil formation as reflected in the consolidation behaviour can be clearly and consistently seen in the voids ratio-logarithem of stress relationship. The relative position and the slope of the voids ratio-logarithm stress (σ-u_w) curves depend on the gas content in the soil. Gassy soils contain high void volumes compared with the saturated soil. This causes greater sample thicknesses for gassy than for saturated soil with the same solid volume. The shift in voids ratio-logarithem stress curves increases rapidly with increase in gas content up to 85% degree of saturation. Further increase in gas content is associated with interconnecting gas bubbles and the behaviour of these soils differs from that of gassy soil with discrete bubbles fig(3.24). The void volume is increased in gassy soils primarily due to the trapped bubbles in the soil. Most of the isolated bubbles are unable to move out of the

soil. Application of the consolidation stress expels larger proportion of water due to its continuity and the remaining bubbles are squashed. The photographs in fig(3.31) show the existence of larger bubbles when compared to the water voids, even at very high stress levels. The exact mechanism which enables the gas to exist as larger bubbles and to be associated with increased voids volume is not known. However the following proposals are useful to understand the behaviour of gassy soils.

(a) Structural effects:

The formation of the soil structure during the initial stage of consolidation (first stress increment from slurry state) is likely to be affected by the presence of gas since the soil is in a very soft state while the bubbles are released from the zeolite. The arrangement of the soil particles is therefore controlled by the position and the size of the bubbles. Before any load is applied a soil structure is formed to accommodate these bubbles and this structure is subsequently broken by the large consolidation stresses. The collapse of the open structures gives large deformation in gassy soil fig(3.20) compared to saturated soil. If the bubbles are created in a very stiff soil, the open structure cannot occur and the soil structure may be less affected. Therefore an important factor is the stage at which the bubbles are created in the soil, ie.

before or after the soil structure is formed. The open structures associated with the formation of the bubbles at a soft stage cannot be completely broken by decreasing the bubble volume by the application of the back pressure. Fig(3.30) shows the effect of an increase in back pressure by 400 kN/m^2, applied to a gassy soil with initial degree of saturation 80%. Although the degree of saturation was increased to 96%, the new voids ratio was more typical of an initial degree of saturation of 90%. However the measurements of the degree of saturation are not exact and these apparent differences may not be significant. Nevertheless, it may be that the open structures created in the very soft soil by the bubbles have not been completely destroyed even though the gas volume has been reduced. Therefore the existence of possible initial structural effects can not be totally neglected in understanding the behaviour of the gassy soil.

(b) Pore gas pressure:

The pore gas pressure in the gassy soil is higher than the pore water pressure, hence the effective stress in the soil is affected by it. The effective stresses in the gassy soils are lower than those in the saturated soil, for the same total stress and pore water pressure, due to the higher pore gas pressure in the gas voids. The parameter controlling the gas pressure

is not the mean bubble radius, but the radii of curvature of the gas-water interfaces in the soil skeleton as shown in fig (3.17). This interface inhibits the gas movement from the pores and increases the pore gas pressure for each stress increment. The magnitudes of these radii are very small (of the order of the soil particle size, ie. a few microns) and these give very high pore gas pressures compared to those calculated using the bubble radii. The table below shows the difference between the pore gas and the pore water pressures calculated from the typical bubble radius and from the interface radii.

$u_g = u_w + 2*T/r$

where T is the surface tension and r the bubble radius.

Bubble radius(mm)	Pore gas pressure(kN/m^2)
2.0	0.07
1.0	0.14
0.1	1.4

Interface radii(mm)	Pore gas pressure(kN/m^2)
0.06 (silt size)	2.33
0.006	23.3
0.002(clay size)	70

The interface radii are assumed to be the same as the solid particle size.

Surface tension = 70 kN/m

This high pore gas pressure in the isolated bubbles maintains the gas voids against the applied stress.

This model can be explained by the following analogy. Let us assume that the gassy soil is made by mixing small rubber bags containing gas, with saturated soil. The size of the rubber bags is larger than the clay particle size. The stresses in the rubber skin represents the surface tension term in the real soil. When this soil is subjected to a consolidation stress, some of the rubber bags which are broken or dissolved, flow with the draining water. The remaining bags are squashed and they carry a part of the applied total stress. The void volume of this soil is greater than the saturated soil because of the volume of the remaining rubber bags and reduction in effective stress caused by the high pore gas pressure. Suppose if we replace these bags by water, the voids occupied by these rubber bags will reduce as the water flows out of the soil. This analogy shows the trapped gas bubbles increase the void volume of the saturated soil.

When the gas content increases, the bubbles become interconnected and a stage is reached where the bubbles are able to move as freely as the water. At this stage the soil behaviour changes as shown in fig(3.24). The shift in e-logarithm stress curve decreases in the soil with 70% degree of saturation when compared to that of 80% saturated soil.

The higher voids volumes associated with gassy soils can be misinterpreted as underconsolidation (higher voids ratio due to excess pore water pressure) of the soil, but the nonexistence of the excess pore water pressures suggests that the gassy soils have attained full consolidation and the effect is due to the presence of trapped gas bubbles.

3.6 A MODEL TO DISCRIBE THE ONE DIMENSIONAL CONSOLIDATION BEHAVIOUR OF GASSY SOIL.

One dimensional stress-strain behaviour of a fully saturated soil under K_o conditions can be described in terms of the total stress and the pore water pressure by the following equation.

$$e=e_1+A\ln(\sigma-u_w) \quad \text{---------(3.1)}$$

where e_1 corresponds to the voids ratio at unit stress $(\sigma-u_w)$ and A is a constant.

Thus, in general,

$$e=F(\sigma,u_w)$$

In order to describe the behaviour of a gassy soil an additional parameter is necessary and traditionally (in partially saturated soils) the pore gas pressure is used with total stress and pore water pressure. It is found that the measurement of a meaningful pore gas pressure to represent the gas pressures in individual bubbles is difficult. Therefore the degree of saturation which is an average parameter to represent the whole soil sample is used instead of the pore gas pressure and

$$e=F(\sigma,u_w,S)$$

The possibility of expressing the behaviour of gassy soil mathematically is explored by making a few idealisations. The gassy soil used in the experiments contains high water voids volume compared to gas voids volume since the degree of saturation is above 80%.

Therefore it is reasonable to assume that the voids which are saturated in a gassy soil to behave like the voids in a fully saturated soil. This assumption requires the gas voids to be comparatively few, large compared to the soil particles and isolated as shown in fig(3.33). The voids ratio of the saturated part of the gassy soil is equal to the volumetric water content (eS) where e is the overall voids ratio of the gassy soil and can be determined if the degree of saturation of the soil at each stage is known. This is measured in the experiment. The behaviour of saturated soil can be expressed by the equation(3.1) modified to represent the saturated portion of gassy soil as;

$$eS = e_1 + A\ln(\sigma - u_w) \qquad (3.2)$$

The validity of the above equation is examined from the experimental results by plotting eS against $\ln(\sigma - u_w)$ instead of e against $\ln(\sigma - u_w)$, thus combining fig(3.24) and fig(3.25). The curves for different gas contents are much closer to that of saturated soil in eS-$\ln(\sigma - U_w)$ space fig(3.34), indicating that the saturated portion in the gassy soil may well behave according to the equation(3.1). In the case of soil with 70% initial saturation the curve differs very much from that of saturated soil suggesting the assumption is not valid when gas content is high. Soil with a saturation greater than 85% could be modelled as outlined above. This limit of 85% may well be different for different soils. The above equation suggests that if the e-$\ln(\sigma - u_w)$ relationship is known for a

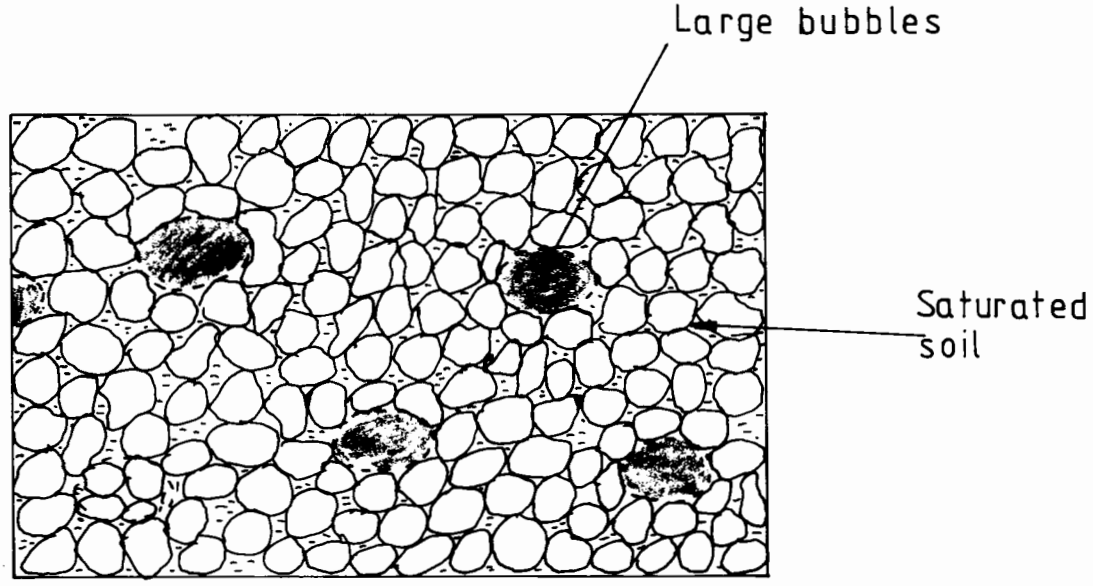

Total soil = Saturated soil + Large bubbles

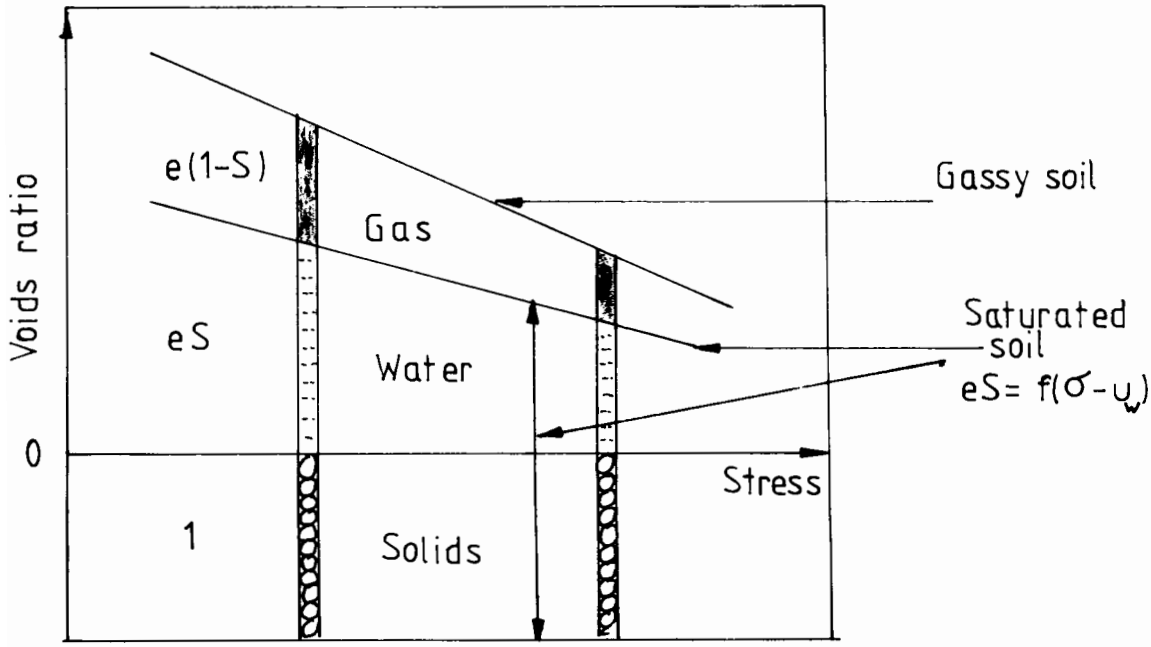

Fig 3. 33 Idealised gassy soil.

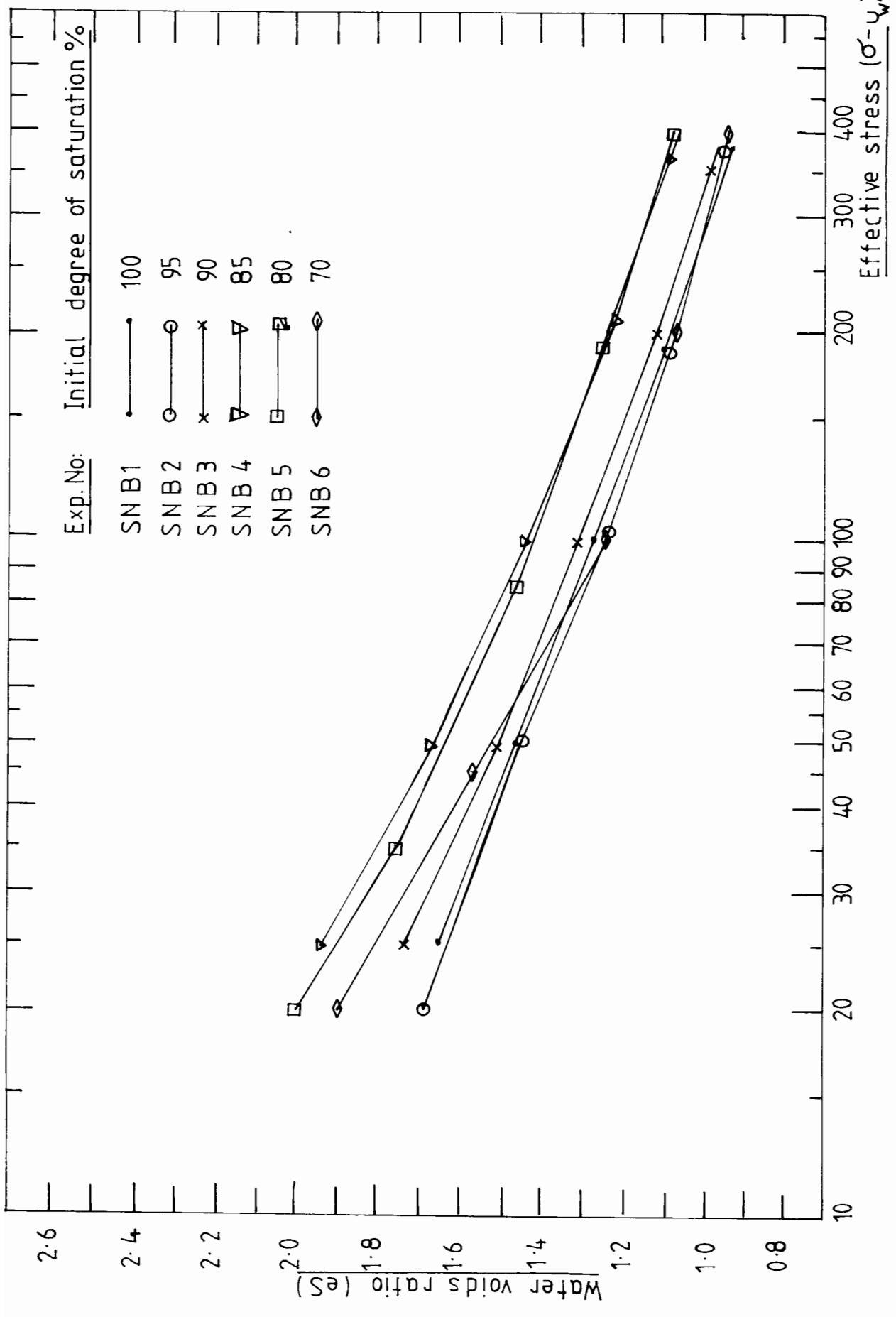

Fig 3.34 Water voids ratio - stress relationship.

saturated soil, the stress-strain behaviour of a gassy soil with a known degree of saturation can be predicted.

However a single representation of the curves for soils with different degrees of saturation can be better established, if the points are plotted in vS-ln(σ-u_w) space where v-is the specific volume of the soil, as shown in fig(3.36). The justification for this type of modelling is as follows. The behaviour of the soil particles surrounding the gas bubbles is expected to be controlled by the effective stress which locally is the difference between the total stress and the pore gas pressure instead of pore water pressure. Similarly the behaviour of soil particles surrounded by water is controlled by the saturated effective stress (σ-u_w). Therefore the gassy soil is divided into two phases, one being saturated soil (solids and the water voids associated with them) and other being gassy soil (bubbles and the solids surrounding them) as shown in fig(3.35). In the earlier model all the solids are associated with water voids with the second phase being the bubbles. The assumption made in the second type of model is that the division of solids associated with gas bubbles and the water is based on the same ratio as the gas to water volume (100-S :S).

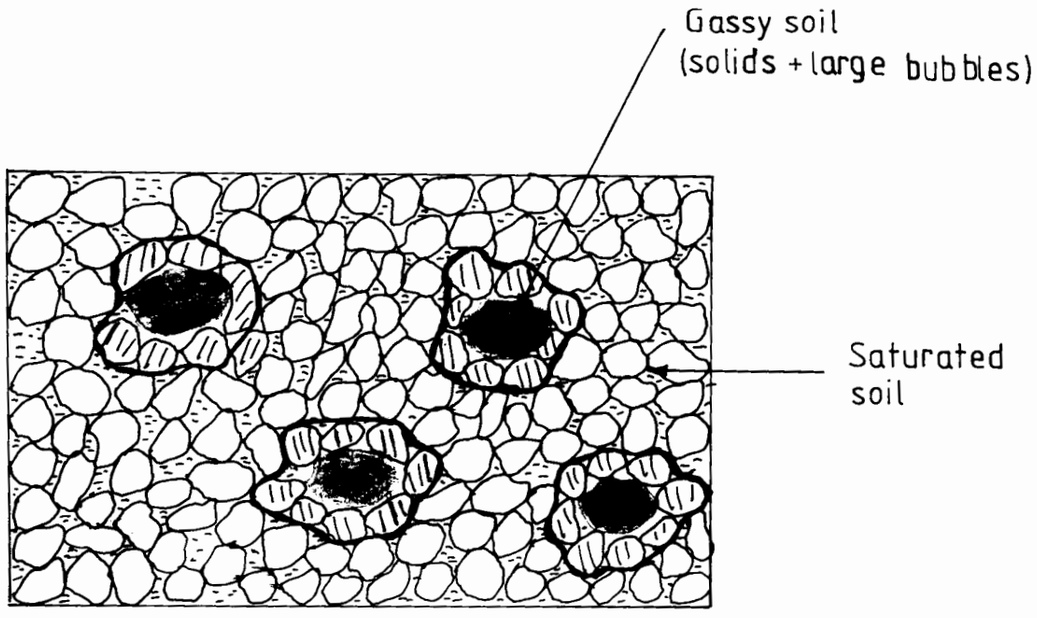

Total soil = Saturated soil + Gassy soil

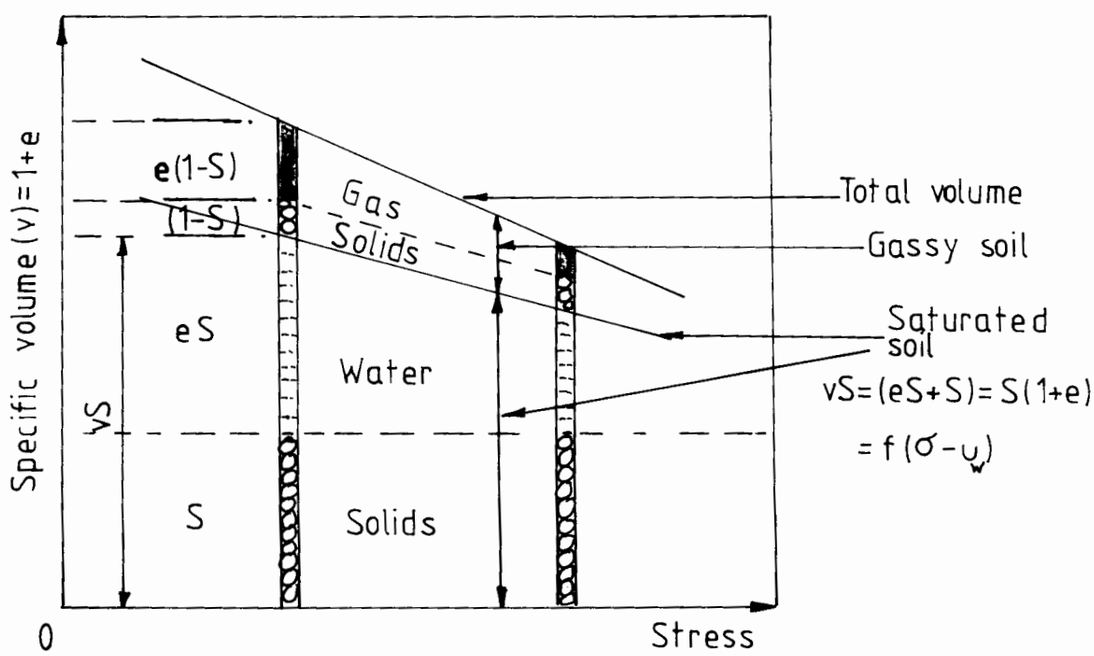

Fig 3.35 Idealised gassy soil.

0
Stress

Fig 3.35 Idealised gassy soil.

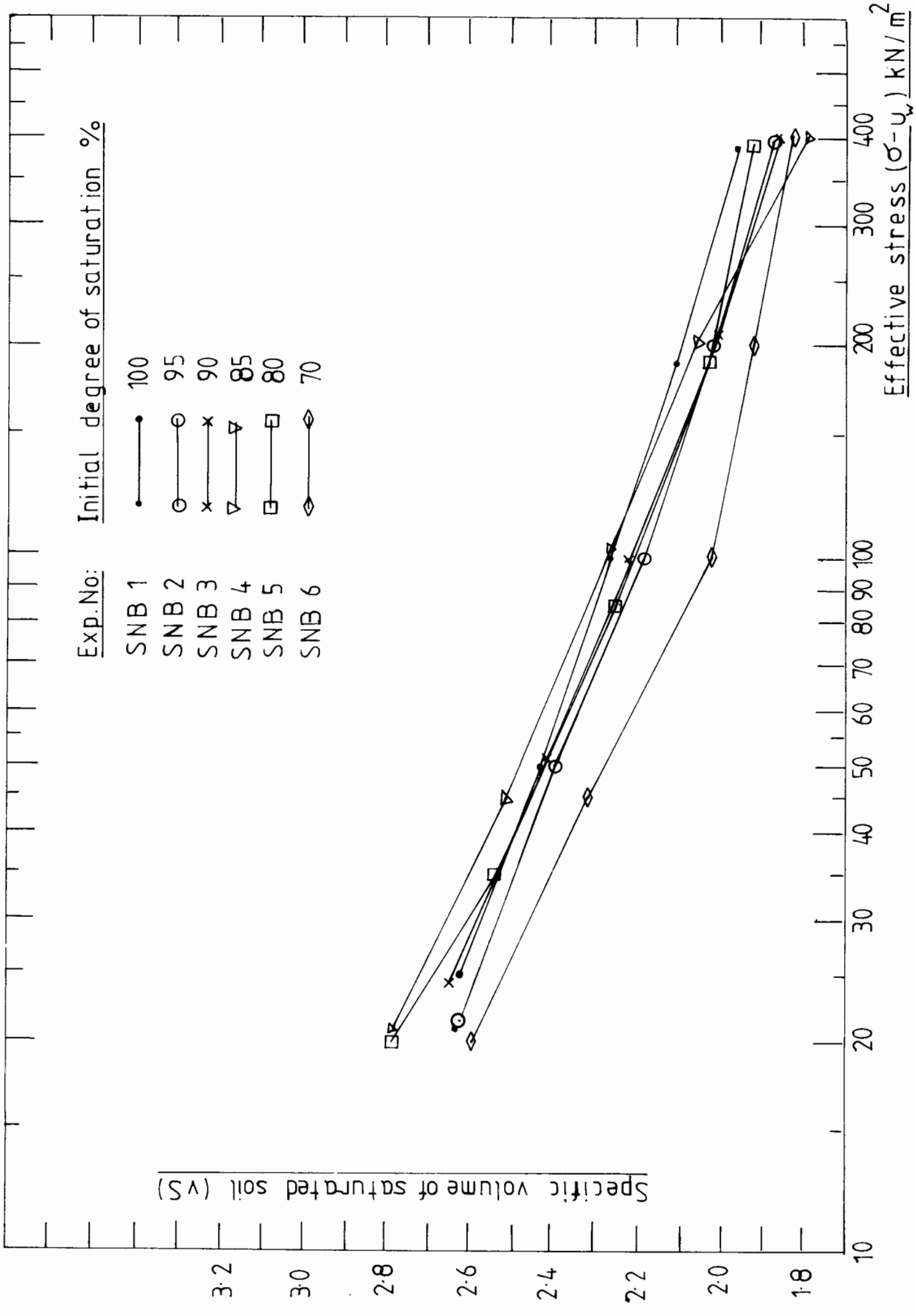

Fig 3.36 Specific volume of saturated soil Vs stress

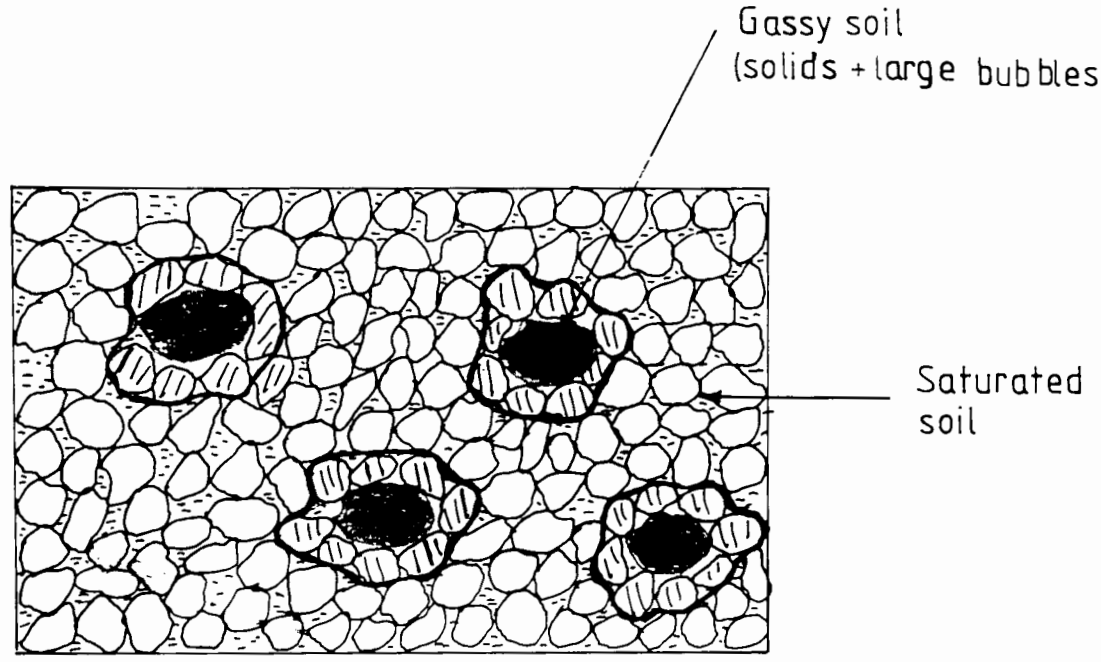

Total soil = Saturated soil + Gassy soil

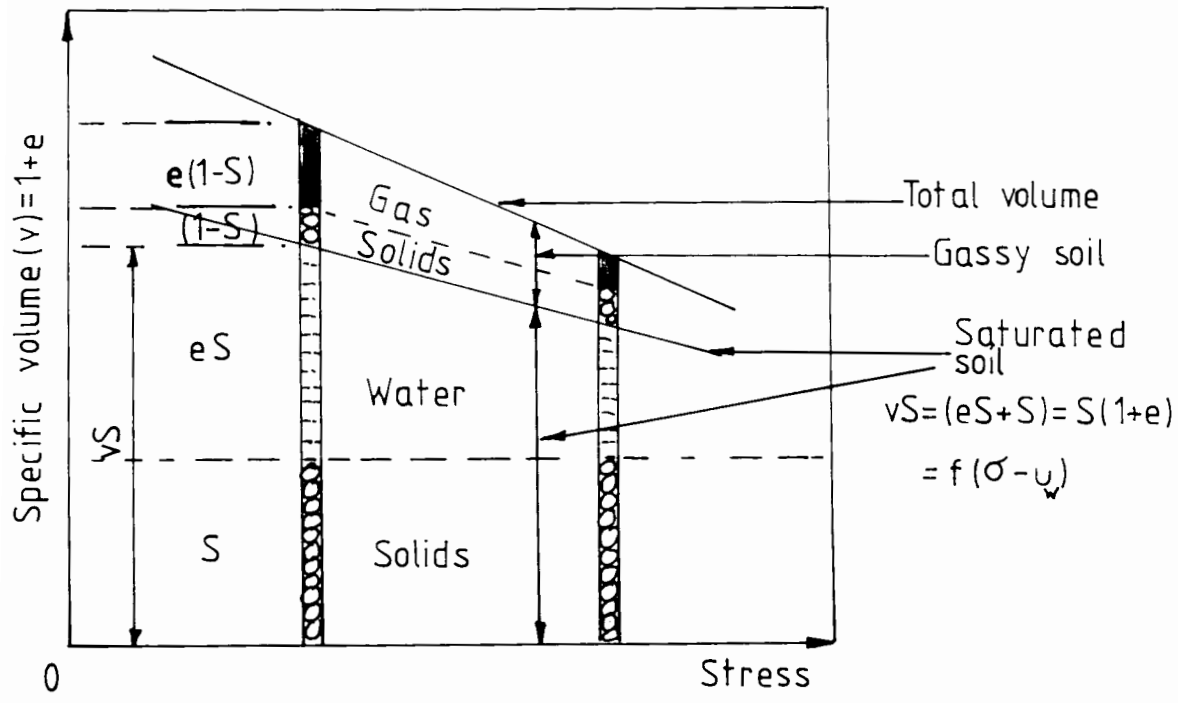

Fig 3.35 Idealised gassy soil.

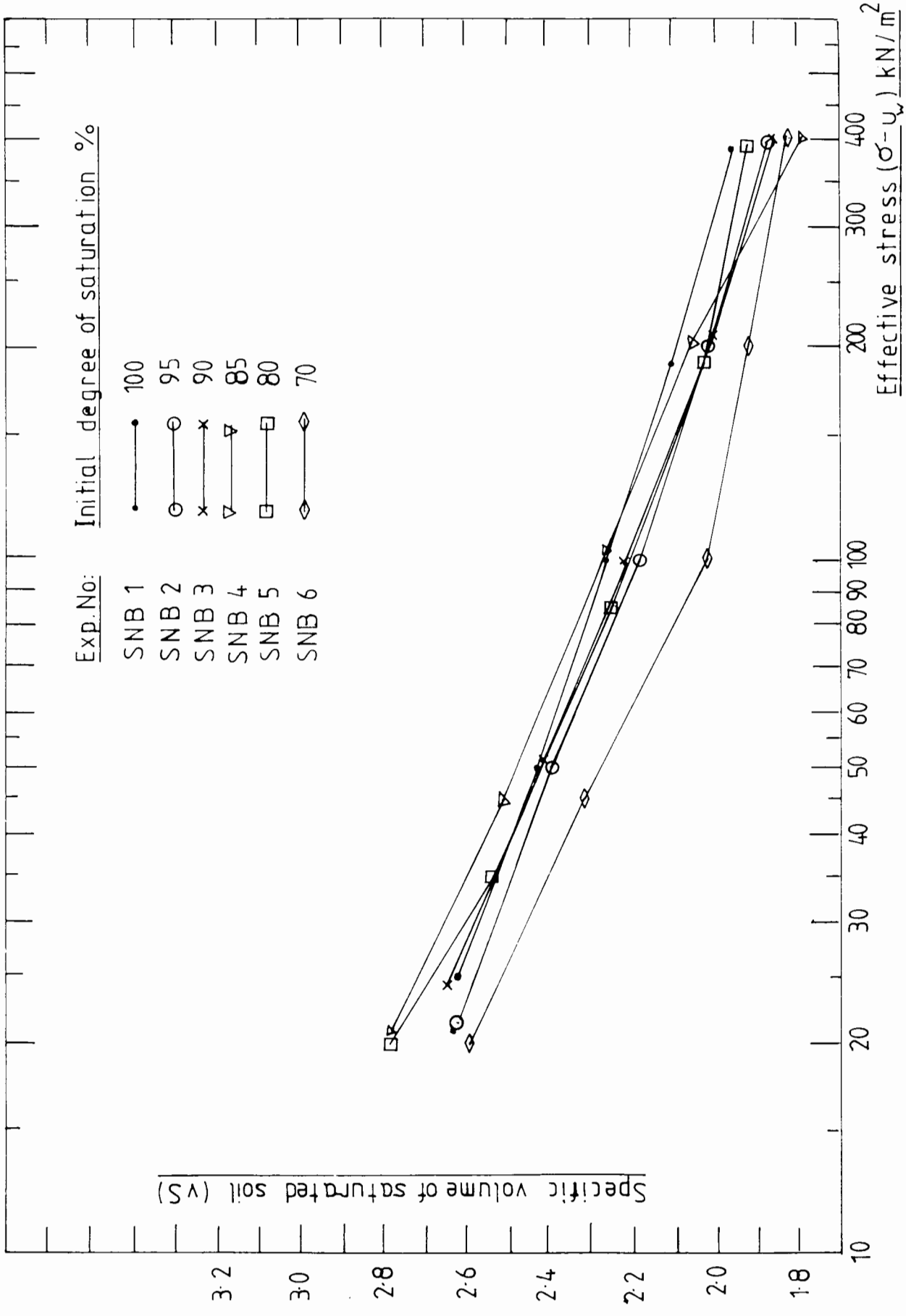

Fig 3.36 Specific volume of saturated soil Vs stress

Considering a unit volume of solids , the volume of voids associated with it is by definition the voids ratio(e). The water volume in this soil is eS and according to the proposed assumption the solids associated with the water is S. Therefore the volume of the saturated soil controlled by the saturated effective stress $(\sigma-u_w)$ is (1+e)S which is equal to vS. Then the modified equation is as follows:

$$vS=v_1+A\ \ln(\sigma-u_w) \qquad (3.3)$$

Fig(3.36) shows the curves for different gassy soils when plotted in vS, $\ln(\sigma-u_w)$ space. The curves for different gas content are much closer to that of saturated soil in this space than those plotted in eS, $\ln(\sigma-u_w)$ space. However the soil with 70% initial degree of saturation does not obey the above model. Therefore the model is restricted to gassy soil with high degrees of saturation (for the soils with degrees of saturation greater than 85% for this type of clayey soil). As the degree of saturation decreases, the gas bubbles are interconnected and no longer discrete and the behaviour cannot be modelled by this simple model.

A choice of a suitable model (eq 3.2 or 3.3) largely depends on the accuracy in the measurement of the degree of saturation in the experiments. Therefore both models can be considered, with reasonable accuracy, to represent the behaviour of gassy soils.

3.7 CONCLUSIONS:

The effect of gas bubbles on the consolidation behaviour of soil, including the formation of the soil structure is examined in this chapter. The gassy soils have higher equilibrium voids volume than those of a fully saturated soil under the same vertical stress in one dimensional confined conditions. The voids ratio of the gassy soil at a given consolidation stress increases with the decrease in degree of saturation up to a critical saturation level. Soils with lower degrees of saturation (less than 85%) behave differently to soil containing discrete gas bubbles since the bubbles are then interconnected and can move more freely. The critical degree of saturation will depend on the soil type and for this type of clayey soil it is around 85% degree of saturation. The volume change behaviour of a gassy soil with a degree of saturation higher than the critical degree of saturation, can be modelled using the following equation.

$$e = e_1 + A\ln(\sigma - u_w)$$

where the constant A and e_1 are obtained from an oedometer test on a fully saturated soil and e_1 is the voids ratio of the saturated soil at unit stress $(\sigma - u_w)$.

CHAPTER 4

COMPRESSIBILITY AND DEFORMATION OF GASSY SOILS.

CHAPTER 4

COMPRESSIBILITY AND DEFORMATION OF GASSY SOILS

4.1 INTRODUCTION

In the majority of engineering calculations involving soil behaviour, the soil can be idealised as a two phase material, a porous skeleton saturated with incompressible water. The initial, undrained response of the soil to a stress increment occurs virtually without volume change. However, if the soil contains undissolved gas bubbles, then this initial incompressibility no longer exists and the undrained response is a compressible one. A simple theoretical model is developed to predict the initial undrained response and the subsequent consolidation behaviour following a total stress increment for soils containing a compressible pore fluid. The validity of the model is examined by comparison with laboratory experimental observations in this chapter.

The above model is then applied to analyse a practical problem. In harbours and estuaries, the deposition of cohesive sediment can cause substantial maintenance dredging programmes, based on a requirement for a minimum navigable depth. The presence of gas bubbles here could cause sufficient compressibility to change the elevation of the sea bed measurably during a tidal cycle, with the mud surface moving as the gas bubble volumes change with the changing total water pressure. An upper bound value for the changes in seabed surface

elevation for cyclic water pressure changes (eg. a tidal cycle) is predicted using the theoretical model and compared with small scale laboratory slow cyclic experiments on gassy soil in the K_o condition.

4.2 THEORETICAL MODEL:

4.2.1 INTRODUCTION:

A theoretical model to describe the undrained response and the consolidation behaviour of gassy soil under K_o conditions is developed. This model is then used to predict the behaviour of gassy soil for the following cases:

(a) The undrained soil deformation and pore water pressure changes for a one dimensional total stress increment in the K_o state:

When a gassy soil is subjected to a total stress increment under undrained conditions, the volume of the soil changes immediately. This is not observed in a saturated soil. With the volume change, there is an immediate effective stress change in the gassy soil and only a part of the total stress increment is carried by the pore fluid sothat the B value (defined as the ratio between pore pressure increase and the total vertical stress increment) is less than unity. The amount of initial sample deformation and the effective stress changes are calculated using the model.

(b) The pore water pressure dissipation and the consolidation behaviour of gassy soils, simulating an oedometer test: The bubbles expand, changing the pore fluid density as the pore water pressure dissipates during consolidation. The traditional consolidation theories assume constant density for the pore fluid during consolidation. Therefore a suitable model which accounts for the changing pore fluid density is used to study the consolidation behaviour of gassy soil.

(c) Deformation of a gassy sea bed for a cyclic water pressure change: This simulation combines the effects studied in the two previous cases and has some practical importance. The sea bed elevation changes when the undissolved gas bubbles are compressed in an undrained loading when the water pressure over the sea bed varies. The pore fluid pressure change will be less than that of the water head change. This imbalance in the fluid pressures induces fluid movement and consolidation (or swelling) in the soil during a tide cycle. Sea bed movement and the effective stress changes are calculated for the changing water levels over the bed. This one dimensional analysis is suitable only for tide changes since the change in water head over the sea bed is required to occur slowly and over a large area so that only mean normal stress changes. No excess pore

pressures are generated due to shear forces as in the case of waves.

Notations

a_v Coefficient of compressibility of the saturated soil skeleton $=\frac{\partial e}{\partial \sigma}$ where $\sigma' = (\sigma - u_w)$

a_{vg} Coefficient of compressibility of the gassy soil

C_{vs} Coefficient of consolidation of saturated soil

C_{vf} Coefficient of consolidation of gassy soil

C_g Compressibility of gas $=\frac{\partial V}{\partial P}$

C_{go} Compressibility of gas at $P=P_o$

e_g Overall voids ratio of the gassy soil

e_s Voids ratio of the saturated soil

n Porosity of the gassy soil

k_w Permeability of water

k_g Permeability of gas

k_f Permeability of gas water mixture

P Absolute pore fluid pressure

P_o Initial absolute pore fluid pressure

S Degree of saturation at fluid pressure P_o

α Gas volume to water volume ratio at pressure P_o

T Time factor $=C_{vs}\ t/H^2$

Δu Excess pore fluid pressure

4.2.2 IDEALISATION:

Gassy soils can be generally modelled by a three phase system, made up of gas, water and solid particles. However, in the following analysis, further simplifications are made. The idealisations used are as follows:

(a) The gassy soil is modelled as a two phase material, made up of incompressible solid particles and a compressible pore fluid. The properties of the compressible pore fluid are derived from the properties of the small compressible bubbles which are well distributed in the soil and from the incompressible water. Fig(4.1) shows the schematic view of the idealised soil with small and well distributed gas bubbles compared with the reconstituted gassy soil prepared in the laboratory with comparatively large bubbles (up to 2-3mm diameter). The volume of undissolved gas will change in two ways if the pore gas pressure changes. Thus the amount of gas in solution will change according to Henry's law, in direct proportion to the total gas pressure, while Boyle's law, stating that the product of absolute gas pressure and its volume is constant for a given amount of gas, describes the gas bubble behaviour. The effect of surface tension is neglected so that the pore gas pressure and the pore water pressure are taken to be equal. The main reason for

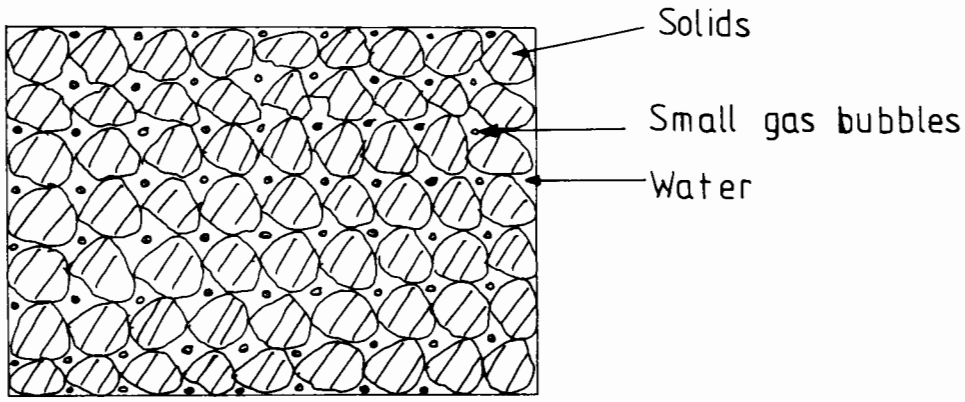

Idealised soil (compressible pore fluid)

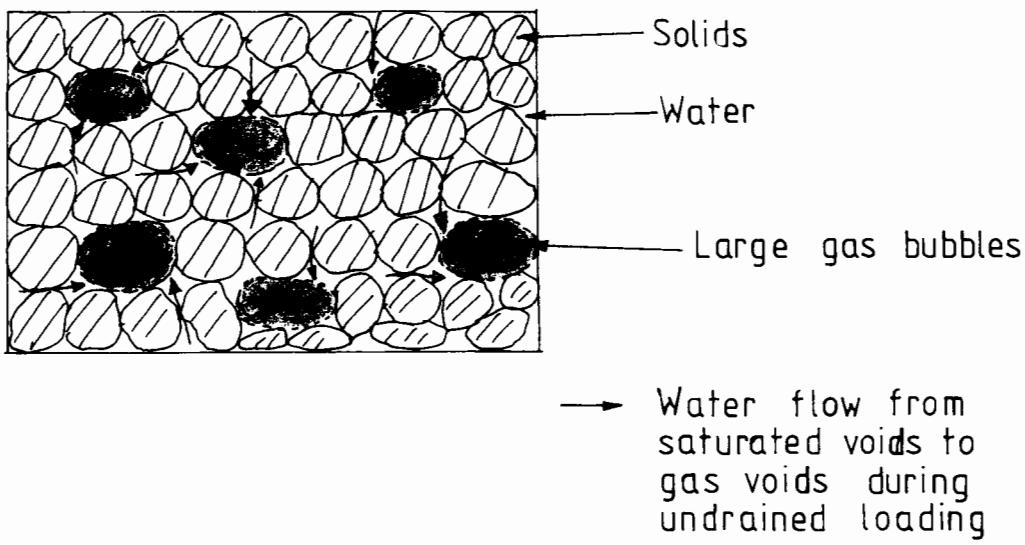

Reconstituted gassy soil

Fig 4.1 Idealisation used in the numerical model.

this is the difficulty in determining the pore gas pressure. The effective stress is defined in terms of pore water pressure. Thus $\sigma'=\sigma-u_w$

(b) The one dimensional stress-strain curve used for the analysis is derived from the experimental results (chapter three) and it is expressed as

$e_g=e_1+A_g\ln(\sigma-u_w)$

and for small strain consolidation this is further idealised as a straight line in e-σ space:

$\Delta e_g=a_{vg}\Delta(\sigma-u_w)$

where e_g, a_{vg} are the voids ratio and the coefficient of compressibility of gassy soil respectively.

(c) The degree of saturation before the vertical stress increment and the final degree of saturation at the end of the consolidation corresponding to that increment is assumed to be the same. This is reasonable for a gassy soil with a degree of saturation above the critical degree of saturation fig(3.25). If the initial saturation is less than the critical degree of saturation (85%) a larger proportion of gas flows out of the soil, thus increasing the degree of saturation. The degree of saturation during consolidation is calculated from the initial degree of saturation using Boyle's law and Henry's law. The saturation increases as soon as the load is applied (due to the pore pressure increase)

and then decreases to the initial value as the water pressure dissipates.

The above idealisations are valid for soils with comparatively high degrees of saturation, i.e. above 85%.

Governing equations.

The equations governing the one dimensional consolidation of clayey soil with a compressible pore fluid are derived by modifiying the equations derived for saturated soil by Gibson and Hussey (1967). In the derivation , an element of soil skeleton of unit cross-sectional area normal to the direction of flow, which at time t=0 lies between planes embedded in the soil skeleton at distances a and (a+δa) from an embedded datum plane is considered, fig(4.2). At some subsequent time t these same planes will be located at unknown distances $\xi(a,t)$ and $\xi(a+\delta a,t)$ from this datum plane. This co-ordinate system is known as a Lagrange co-ordinate system. The chosen co-ordinate element always encloses the same solids.

The vertical equilibrium of the soil grains and the fluid currently occupying the cylinder ABCD fig(4.2) requires that

$$\frac{\partial \sigma}{\partial a} + [n\rho_f + (1-n)\rho_s]\frac{\partial \xi}{\partial a} = 0 \qquad (4.1)$$

where the total stress is σ, n is the volume porosity and ρ_f, ρ_s are the densities of the fluid and the solid phase.

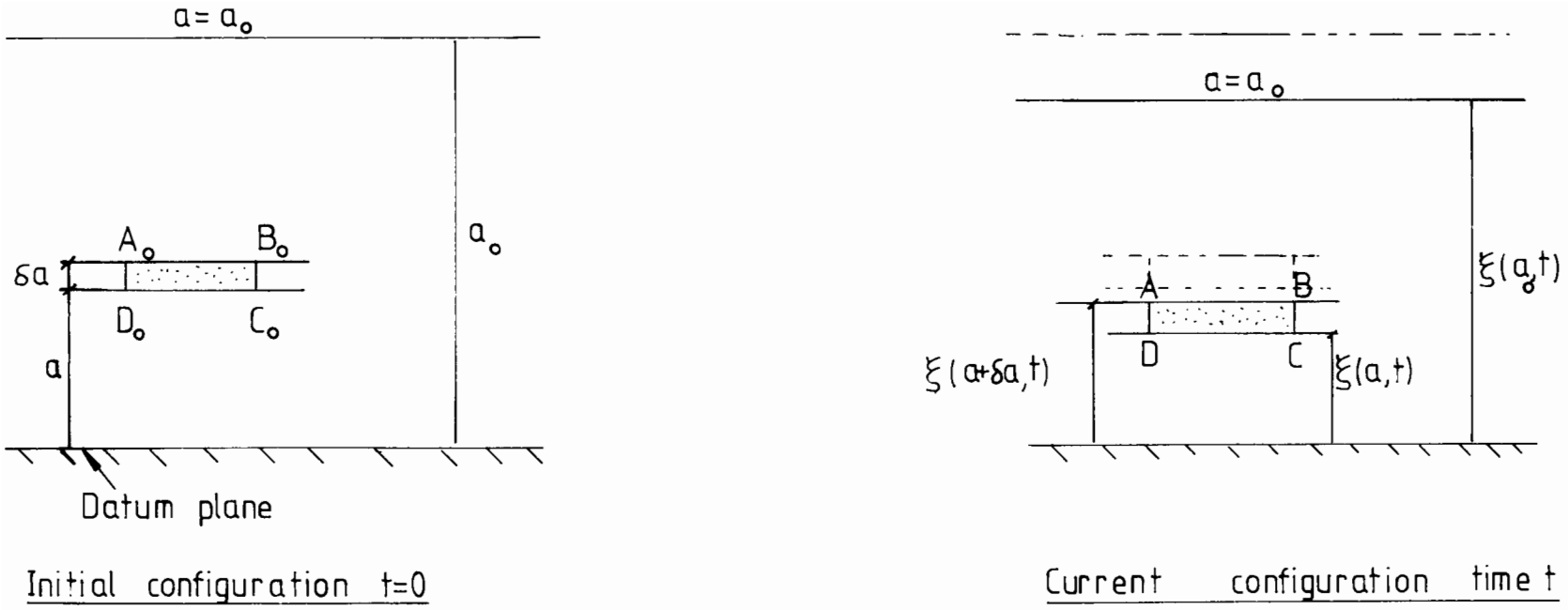

Fig 4.2. An element of soil at time t=0 and t=t.

The solid density is assumed to remain constant in the following analysis, while the fluid density will change with pressure.

The solid continuity requires:

$$\rho_s[1-n(a,0)]=\rho[1-n]\frac{\partial \xi}{\partial a} \qquad (4.2)$$

The fluid phase continuity requires

$$\frac{\partial}{\partial a}[n\rho_f(V_f-V_s)]+\frac{\partial}{\partial t}[n\rho_f\frac{\partial \xi}{\partial a}]=0 \qquad (4.3)$$

where V_s, V_f are the solid and the fluid velocities.

The fluid flow is assumed to obey Darcy's law which relates the relative velocity of the pore fluid and the soil skeleton to the excess pore pressure gradient.

$$n\rho_f(V_f-V_s)=-k_f\frac{\partial p}{\partial \xi} \qquad (4.4)$$

k_f is the permeability of the pore fluid and depends on the viscosity of the fluid and the soil porosity. During consolidation, both gas and water flow out of the soil skeleton, so that the fluid permeability used in this analysis should include both phases. When the gas voids are interconnected the gas permeability is very high by comparison with the permeability of water in a saturated soil due to the low viscosity of the gas. However in this analysis the pore fluid permeability is assumed to be equal to the pore water permeability. This is acceptable for a comparatively high degree of saturation (greater than 85%) and is also necessary due to a lack of experimental evidence to modify the pore fluid permeability to suit the degree of saturation in clayey

soils. As the gas content increases the gas permeability increases rapidly and the soil consolidates faster. Therefore this analysis is restricted to degrees of saturation greater than the critical degree of saturation (85%).

$k_f = \Phi[k_w, k_g, S]$

When the degree of saturation is greater than the critical degree of saturation

$k_f = k_w$ (4.5)

The pore fluid density varies with pressure and the governing equation is obtained as follows:

$\rho_f = [M_w + M_g]/[v_w + v_g]$

where v_w, v_g are the water and gas volumes in the pore fluid, M_g, M_w are the mass of gas and the water in the pore fluid and the mass of gas is neglected subsequently. At time t=0, the degree of saturation is S_o and the pore fluid pressure is p_o

Using Boyle's law and Henry's law the volume of gas at time t, (when the pore fluid pressure is p) is given by

$v_g = [v_w p_o (\alpha + H)/p] - Hv_w$

where $\alpha = (100/S_o) - 1$ = Volume of gas/volume of water

and H=coefficient of solubility, and the dissolved gas volume=Hv_w

Therefore the pore fluid density:

$\rho_f = \rho_w / [1 + (\alpha + H) p_o / p - H]$ (4.6)

When α and H are zero (no gas in the pore fluid)

$\rho_f = \rho_w$

The above equation represents the change in pore fluid density with pore pressure. As the pressure increases, the volume of the gas decreases, more gas goes into solution and the density increases. When all the gas bubbles are dissolved the density approaches the water density. The saturation pressures necessary to dissolve all the methane gas bubbles can be obtained by equating the denominator of the equation (4.6) to unity. This pressure depends on the initial degree of saturation and the solubility coefficient.

In addition, some simplification results from working in terms of the voids ratio

$$e=n(1-n)^{-1} \qquad (4.7)$$

rather than the porosity n.

The equations 4.2, 4.3, 4.4, 4.5, 4.6 ,4.7 and the stress strain relationship ($e-\sigma'$) are combined to give the following equation which governs the consolidation behaviour of the gassy soil.

$$\frac{\partial^2 u}{\partial a^2} = A\left[\frac{\partial u}{\partial t} - B\left(\frac{\partial \sigma}{\partial t}\right)\right] \qquad (4.8)$$

where $$A = \frac{1}{C_{vs}}\left[1+\frac{(\alpha+H)\, e_o\, P_o}{P^2\left(1+\frac{\alpha P_o}{P}-H\right)}\right] = \frac{1}{C_{vf}}$$

$$B = \frac{1}{1+\frac{(\alpha+H)\, e_g\, p_o}{a_{vg}\left(1+\frac{\alpha p_o}{p}\right) p^2}}$$

and C_{vs} is the coefficient of consolidation $\frac{k\,(1+e_o)^2}{\rho_w\, a_v\,(1+e)}$ of the saturated soil.

The voids ratio and the slope of the e-σ' curve of a gassy soil are greater than those of the saturated soil. From the experimental observations in chapter three

$e_s = Se_g$ where S is the degree of saturation

and

$a_v = Sa_{vg}$

threfore

$e_g/a_{vg} = e_s/a_v$

The parameter B contains a term e_g/a_{vg} and this can be replaced by e_s/a_v.

$$B = \frac{1}{1 + \dfrac{(\alpha + H)\, e_s\, p_o}{a_v\,(1+\frac{\alpha p_o}{p})\, p^2}}$$

The new parameter B now contains only the properties of a saturated soil and the gas content of the soil. Therefore the equation(4.8) can be solved for a gassy soil of known gas content using the consolidation properties, i.e the coefficient of compressibility and the coefficient of consolidation, of a saturated soil.

pressure increment to stress increment (the parameter B) and the ratio of the undrained deformation to the final deformation (δ_i/δ_f) of the soil are as follows:

$$B = \frac{\Delta P}{\Delta \sigma} = \frac{1}{1 + \dfrac{e_o\,(\alpha + H)\,P_o}{a_v\,P^2\,(1+\alpha)}} \quad \text{and} \quad \frac{\Delta_i}{\Delta f} = \frac{a_v\,\Delta(\sigma - u)}{a_v\,\Delta\sigma} = (1-B) \qquad \text{----------(4.9)}$$

$$C_g = e_o(\alpha+H)p_o/(1+\alpha)/p^2$$

Therefore

$$B = 1/(1+C_g/a_v)$$

The above set of equations suggest that the undrained response of the soil depends on the gas compressibility (C_g) and the soil skeleton compressibility (a_v). The gas compressibility depends on the amount of gas in the soil and the current pore gas pressure which is assumed to be same as the pore water pressure. The soil skeleton compressibility decreases with the increase in the consolidation stress (σ_v'). As the soil becomes stiffer in a consolidation test (a_v decreases) the B value decreases for a given initial gas content as shown in the fig(4.3). During the initial stress increment from 25 to 50 kN/m^2 when the soil is soft the undrained B value for an 80% saturated soil is 0.8 and this decreases to 0.58 when the stress is increased from 100 to 200 kN/m^2 when the soil is stiffer.

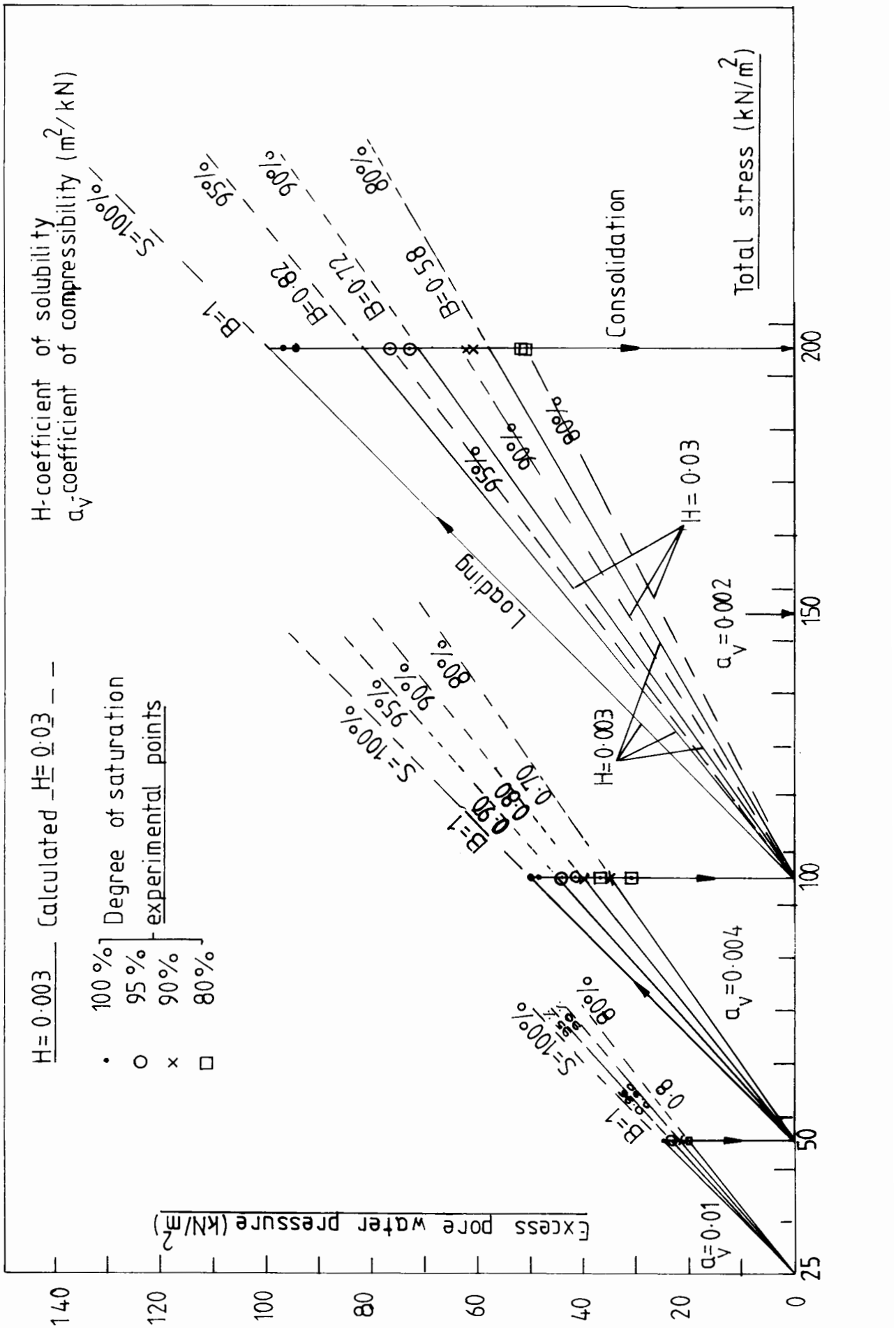

Fig 4.3 Calculated and measured B values at different stress levels.

The B value depends on the gas content too. It decreases with the increase in gas content for a given soil skeleton compressibility. These values of B match reasonably well with the values obtained from the experimental results.

4.3.2 CONSOLIDATION BEHAVIOUR:

The behaviour of gassy soil during consolidation also depends on the soil stiffness as well as the gas content. The behaviour of a soft soil and a stiffer soil are analysed to illustrate the importance of the soil stiffness in the consolidation behaviour of gassy soil. Fig(4.4) and fig(4.5) show the comparison between the numerical results obtained by solving the equation and the experimental observations made in the oedometer tests. The coefficient of consolidation of the saturated soil, sample heights, coefficient of compressibility of the soil skeleton and the degrees of saturation for the numerical analysis are obtained from the experimental results.

Fig (4.4) shows the dissipation of the undrained face pore water pressure in gassy soils with different degrees of saturation and with different soil skeleton compressibilities obtained by the previous consolidation at different stress levels. The parameter a_v given in the diagrams indicates the different soil compressibilities. The initial undrained face excess pore water pressure for a particular load increment decreases with the increase in

Fig 4.4 Calculated and measured excess pore water pressures during consolidation.

gas content, but increases with the increase in the soil compressibility. The stiffer the soil, the lower the B value for a given gas content.

Fig(4.5) shows the deformation-time behaviour of gassy soils with different gas content and soil skeleton compressibilities. The deformation of the soil (at time t) is normalised by dividing it by the total deformation attained by the soil sample. This is done for the following reason. The ratio of the initial deformation (at t=0) to the total deformation is equal to (1-B) which provides an alternate method of determinig the value B. The gradient of the deformation-square root time curves decreases with the increase in gas content indicating the lower settlement rates in gassy soils. However the immediate settlement increases with the increase in gas content. These two opposing effects results in similar settlement times to achieve 90 to 95% settlement in gassy and saturated soils. Defining a coefficient of consolidation for a gassy soil in the traditional way (eg. from 'time fitting method using t_{90}) is meaningless. The equation(4.8) suggests that the coefficient of consolidation of a gassy soil

$$C_{vf} = C_{vs} \frac{1}{1 + \frac{(\alpha + H)\, e_o\, P_o}{P^2 \left(1 + \frac{\alpha P_o}{P}\right)} - H}$$

where $$C_{vs} = \frac{k\,(1+e_o)^2}{\rho_w\, a_v\, (1+e)}$$

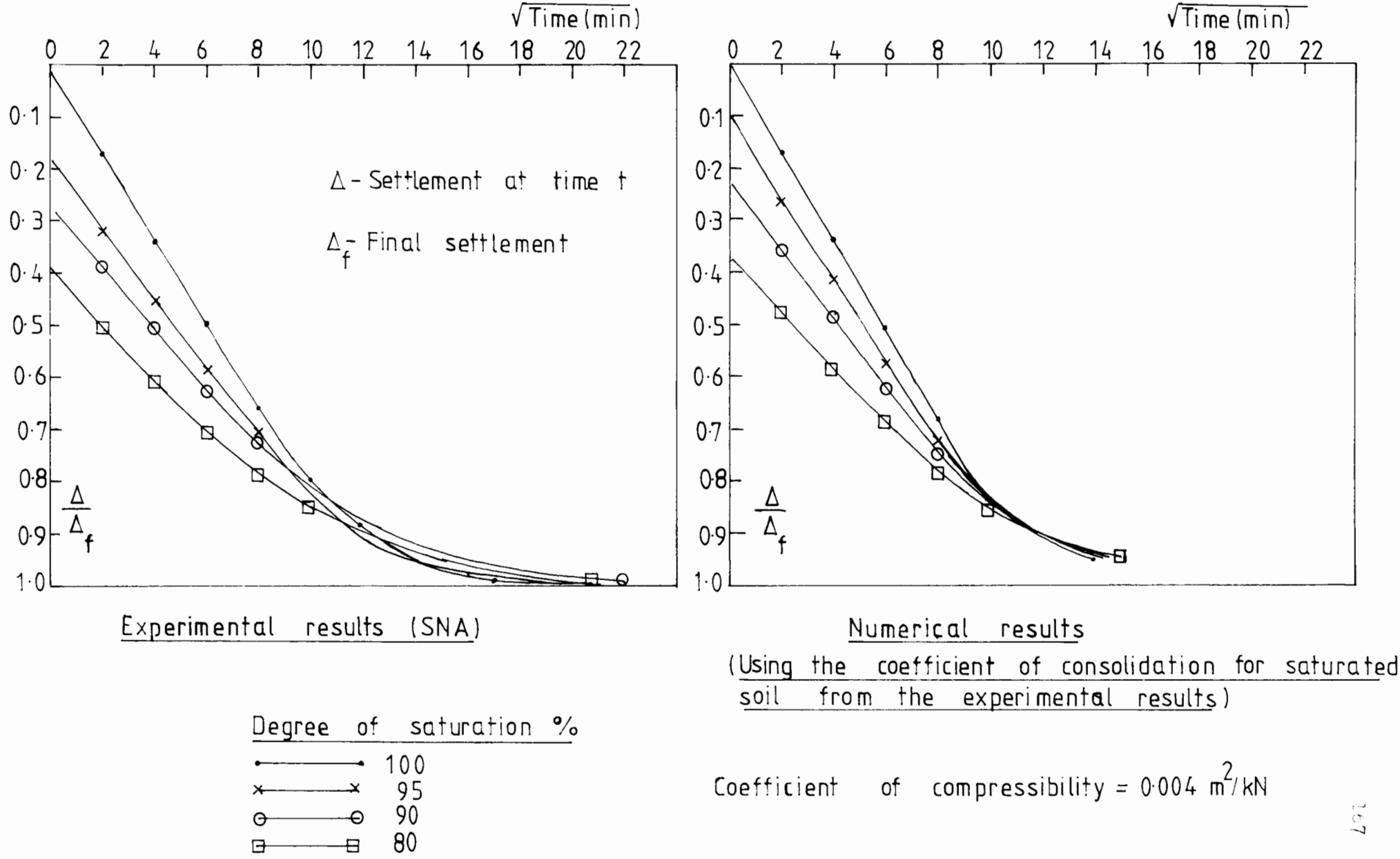

Fig 4.5 Calculated and measured settlement-time behaviour of gassy soils with different gas content

depends on the pore fluid pressure and it varies during consolidation. It decreases as the pore fluid pressure decreases during consolidation by a large factor depending on the gas content and the soil stiffness (for 80% saturated soil the factor is 1.8 as the pore fluid pressure decreases from 200 to 100 kN/m^2) and this reduction cannot be neglected. However the traditional saturated soil consolidation theories assume a constant coefficient of consolidation since the variation is small for a small strain deformation.

Fig(4.6) shows the effect of soil skeleton compressibility (a_v) on the consolidation behaviour of gassy soil with different degrees of saturation. A soft soil with a coefficient of compressibility 0.01 m^2/kN and a relatively stiffer soil with a coefficient of compressibility 0.002 m^2/kN are compared. The undrained degree of settlement of a gassy soil increases with the decrease in soil compressibility. However the following settlement rate (slope of the curves) decreases with the decrease in the soil compressibility. Therefore the consolidation time to attain a particular degree of settlement depends on the stiffness of the soil as well as the gas content.

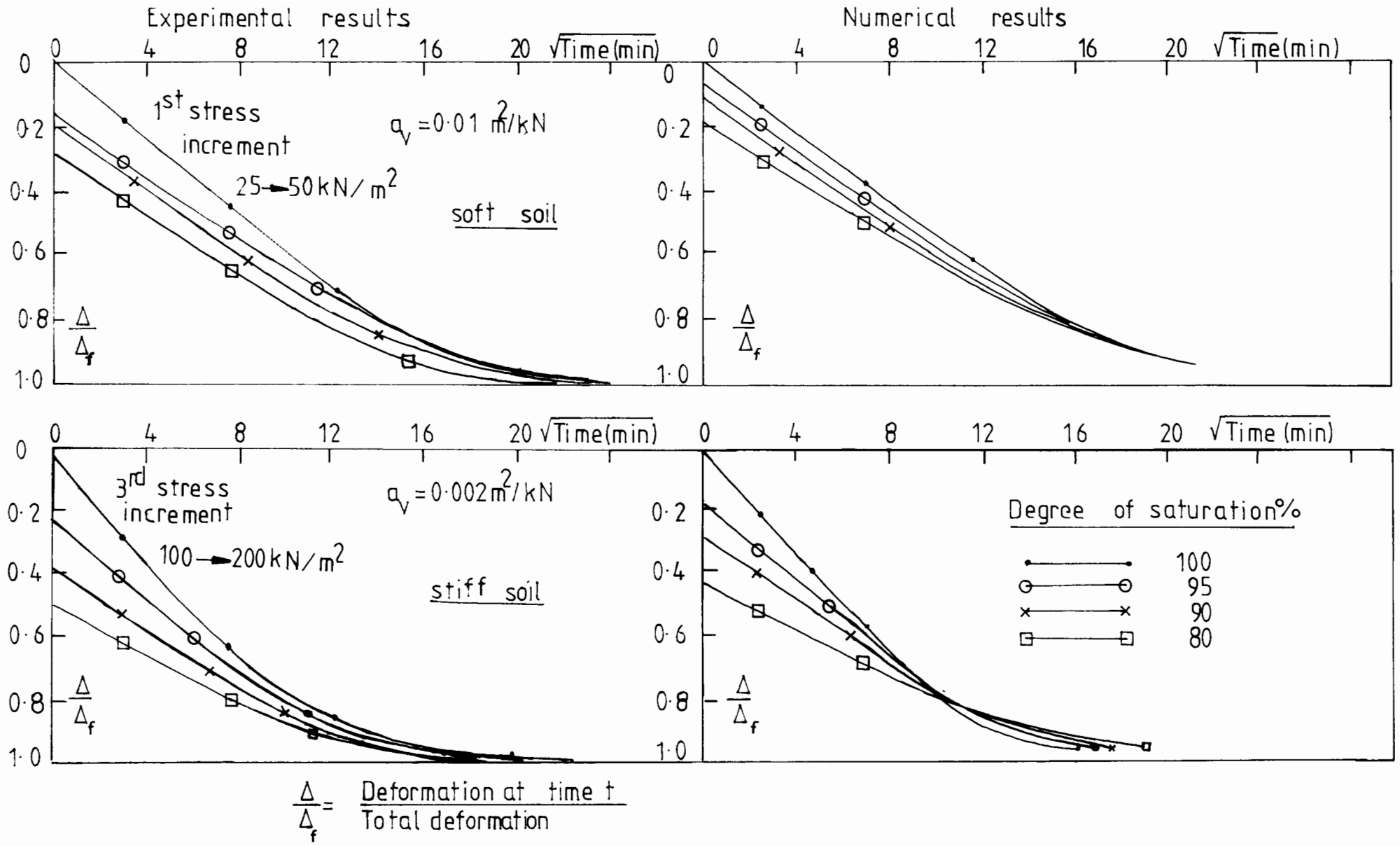

Fig 4.6 Effect of soil compressibility (a_v) on the settlement-time behaviour of gassy soils.

Remarks

The settlement-time behaviour of gassy soil has two different characteristics.

(a) The undrained settlement: This depends on the gas content and the stiffness of the soil. For a given stiffness, the lower the degree of saturation, the higher the settlement. No immediate settlement is observed in saturated soils.

(b) The settlement due to pore fluid drainage: The settlement rates due to fluid drainage are reduced as the degree of saturation decreases. This is reflected as shallow gradients for gassy soils in square root time vs settlement curves.

These two opposing effects give similar settlement times to achieve 90-95% of the total settlement in gassy and saturated soil. The settlement vs time curves given in fig(4.7) are useful to calculate the time to reach a particular degree of settlement in gassy or saturated soils. The time factors used in these plots are calculated using the coefficient of consolidation of saturated soil. Each plot corresponds to a particular soil skeleton compressibility and a non-dimensional parameter $a_v p_o / e_o$ is used to indicate the compressibility effect. This is thus a relative compressibility term.

$$a_v p_o / e_o = a_v / (e_o / p_o)$$

$$= \text{soil compressibility} / C_{go}$$

where C_{go} denotes the coefficient of compressibility of

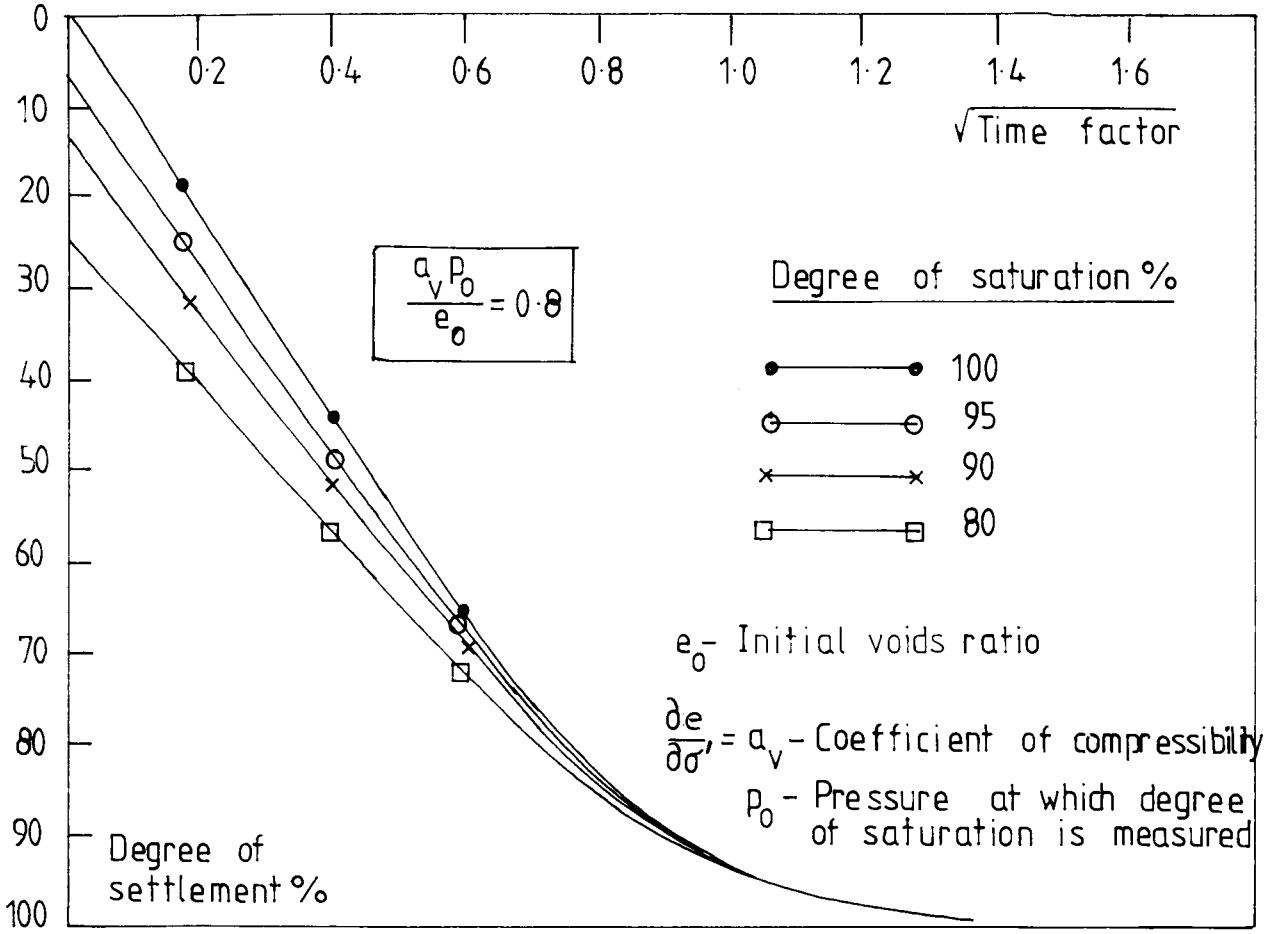

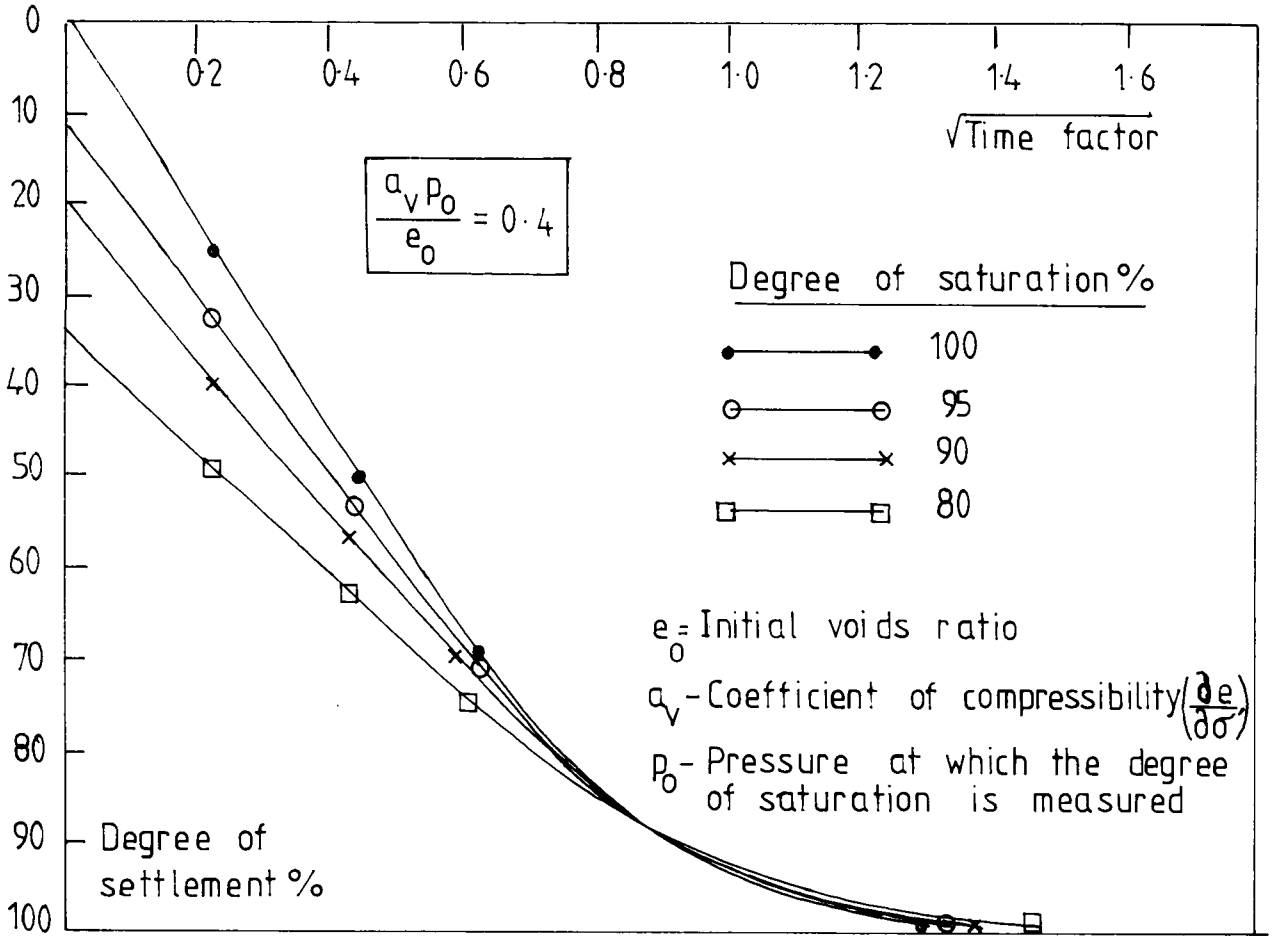

Fig 4.7 Degree of settlement-square root time relationship for gassy solis.

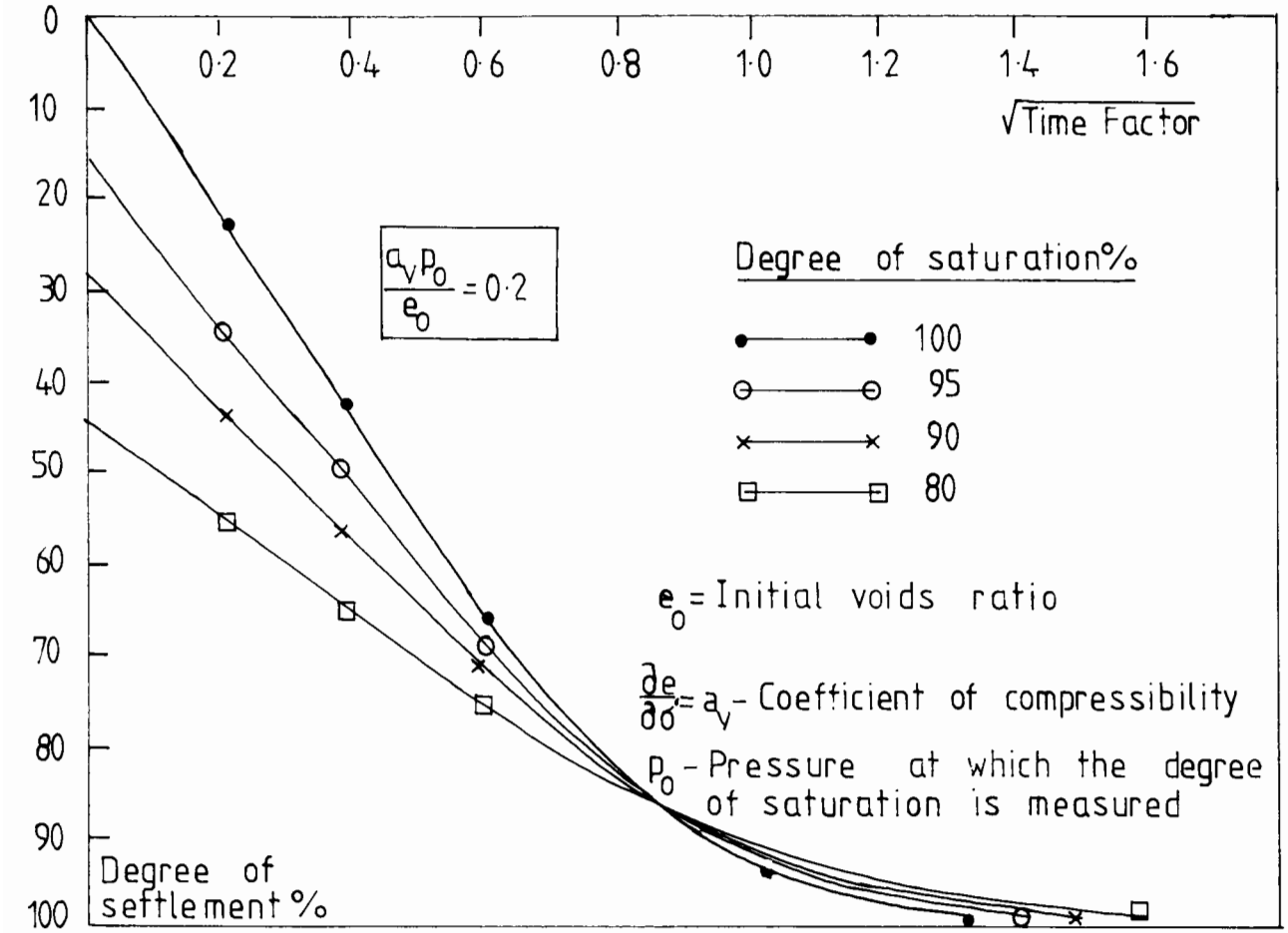

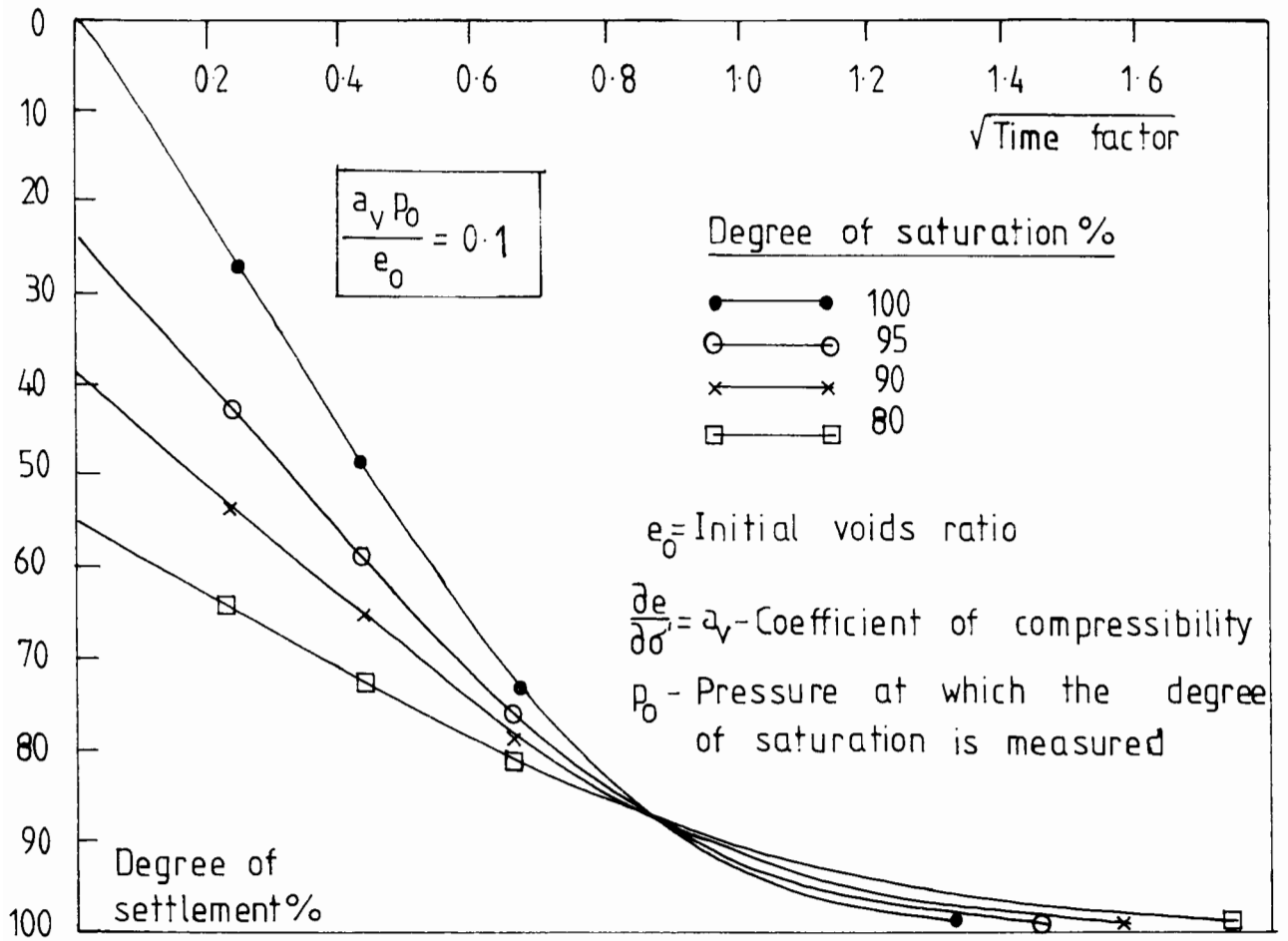

Fig 4.7 Continued.....

a gas phase in a unit volume of dry soil (with a voids ratio e_o) at at pressure p_o.

From Boyle's law: $pV=p_oV_o$

Therefore the compressibility of gas at pressure p

$=-dV/dp=[p_oV_o/p^2]$

The compressibility of gas at pressure $p_o=V_o/p_o$

If the volume of gas in a unit volume of dry soil is e_o, then the compressibility $=e_o/p_o$

4.3.3 SINUSOIDAL LOADING.

This analysis is to simulate the loading of a gassy sea bed by a varying water head such as tide. Variation in the water head (total stress) causes volume and effective stress changes due to the compressibility of the pore fluid. The pore water pressure change will not be the same as the water head change (B≠1), so that water flow (which is governed by the consolidation equation) occurs into and out of the sea bed. The pore water pressure generated in the sea bed and the water head change may also not be in phase due to this water flow. In this analysis the pore pressures generated by the shear stresses are ignored.

$$\Delta u = B[\Delta p + A\Delta\tau_{oct}]$$

If wave loading is analysed instead of tide changes, the above mentioned pore pressures can not be neglected. The equation(4.8) is solved numerically with the following boundary conditions as shown in fig(4.8).

(a) The variation in total stress and pore water

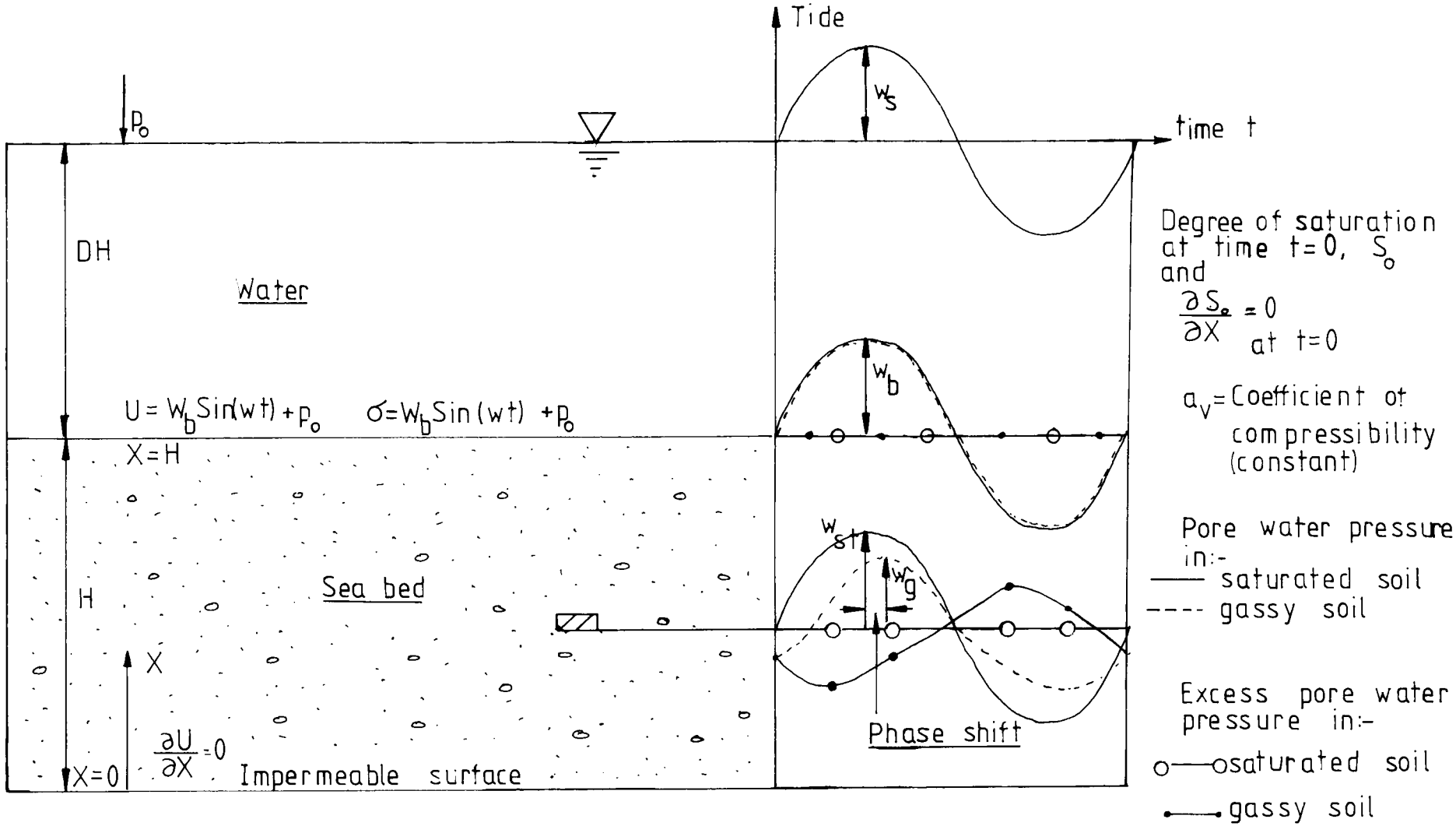

Fig 4.8 Boundary conditions used to model the gassy sea bed behaviour for tide action.

pressure acting on the top boundary (water-soil interface) is assumed to be sinusoidal.

(b) The bottom boundary of the soil layer of thickness H is selected as a fixed datum and it is undrained.

A SENSITIVITY STUDY:

The deformation and the pore water pressure changes of the sea bed depend on the gas content, soil stiffness, the magnitude of the tide amplitude, the water depth and the permeability of the soil. Each of these factors is varied, keeping the others constant, in the following sensitivity study. In this study the pore water pressure generated at 5 m depth in a 10 m thick sea bed and the surface deformation of this sea bed are calculated for the comparison. The deformation of the sea bed and the excess pore water pressures are non-dimensionalised by the thickness of the bed and the tide amplitude respectively. This analysis relates to the use of the differential piezometer described in chapter five.

(a) The effect of gas content in the soil (100,95,90,80% degrees of saturation)

The deformation of the sea bed surface and the excess pore water pressure generated at 5 metres depth in the sea bed increases with the increase in gas content as shown in fig(4.9). The curves are non symmetrical even though the tide pressure is sinusoidal. This is due to the decrease in bubble compressibility with the water pressure increase.

$PV=C$ (constant)

$dV=-[C/P^2]\ dP$ ---------- (4.11)

Bubble compressibility= C/P^2

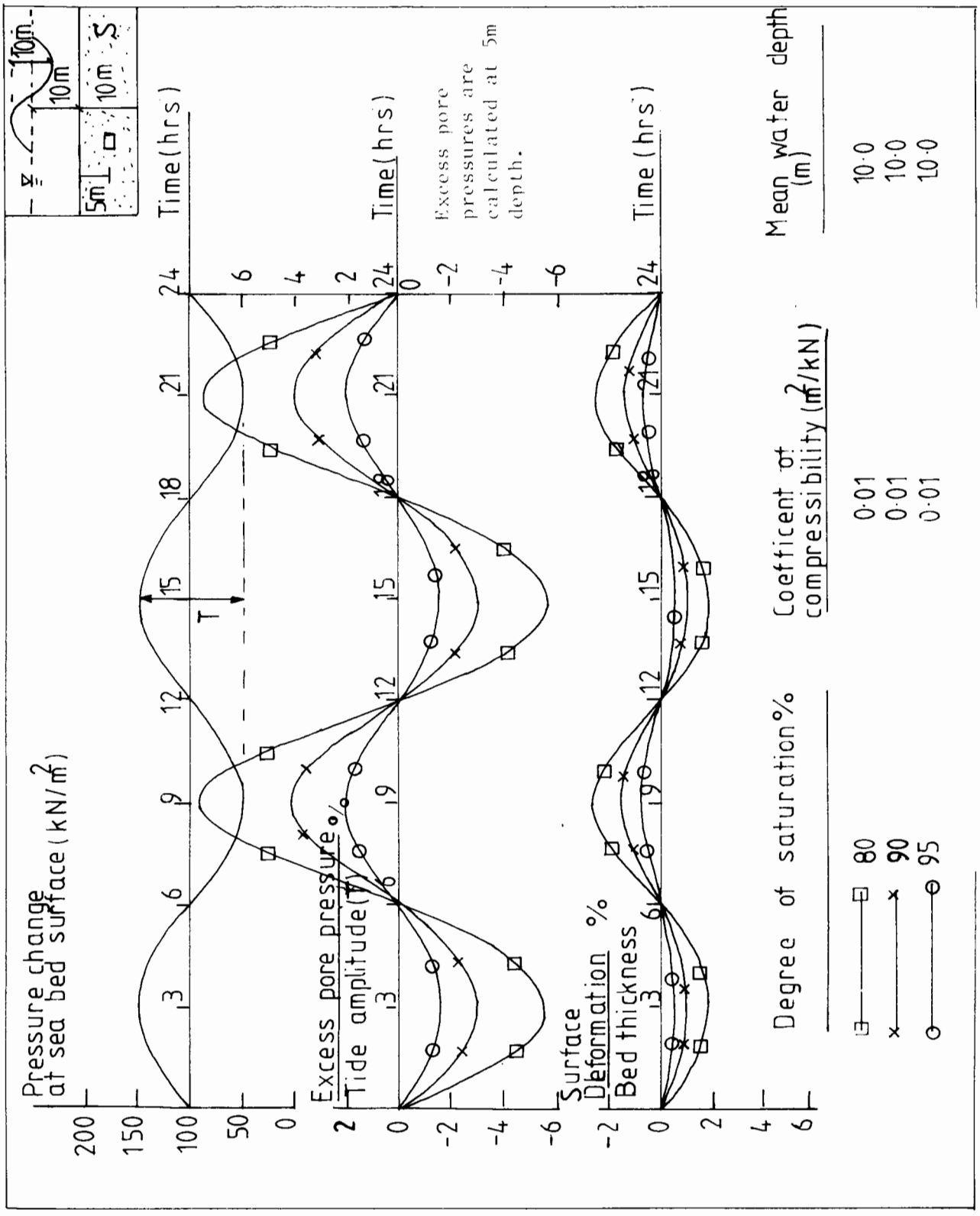

Fig 4.9 Effect of degree of saturation on the behaviour of the sea bed.

where P,V are the absolute bubble pressure and the volume.

(b) The effect of the soil skeleton compressibility (a_v).

The coefficient of compressibility of the soil is defined as the voids ratio change caused by a unit effective stress change in the soil. (eg. 0.01, 0.02, 0.04 m^2/kN). The magnitude of the excess pore water pressure increases as the compressibility of the soil decreases, but the deformation of the soil decreases as shown in fig(4.10).

(c) The effect of the magnitude of the total stress change (tide amplitude 50,100,200 kN/m^2)

The non-dimensionalised values for deformation and excess pore pressures decrease with increase in tide amplitude fig(4.11), but the absolute values increases. As the tide amplitude increases, so does the excess pore pressure response. However, the relationship is not linear due to the non linear decrease in gas compressibility ($p_o V_o/p^2$) with the increase in the fluid pressure. Thus, the non dimensionalised parameters are not constant.

(d) The effect of the water depth above the sea bed. (eg. 10,15,20 metres)

The non-dimensionalised values for deformation and the excess pressures are affected by the mean water depth of

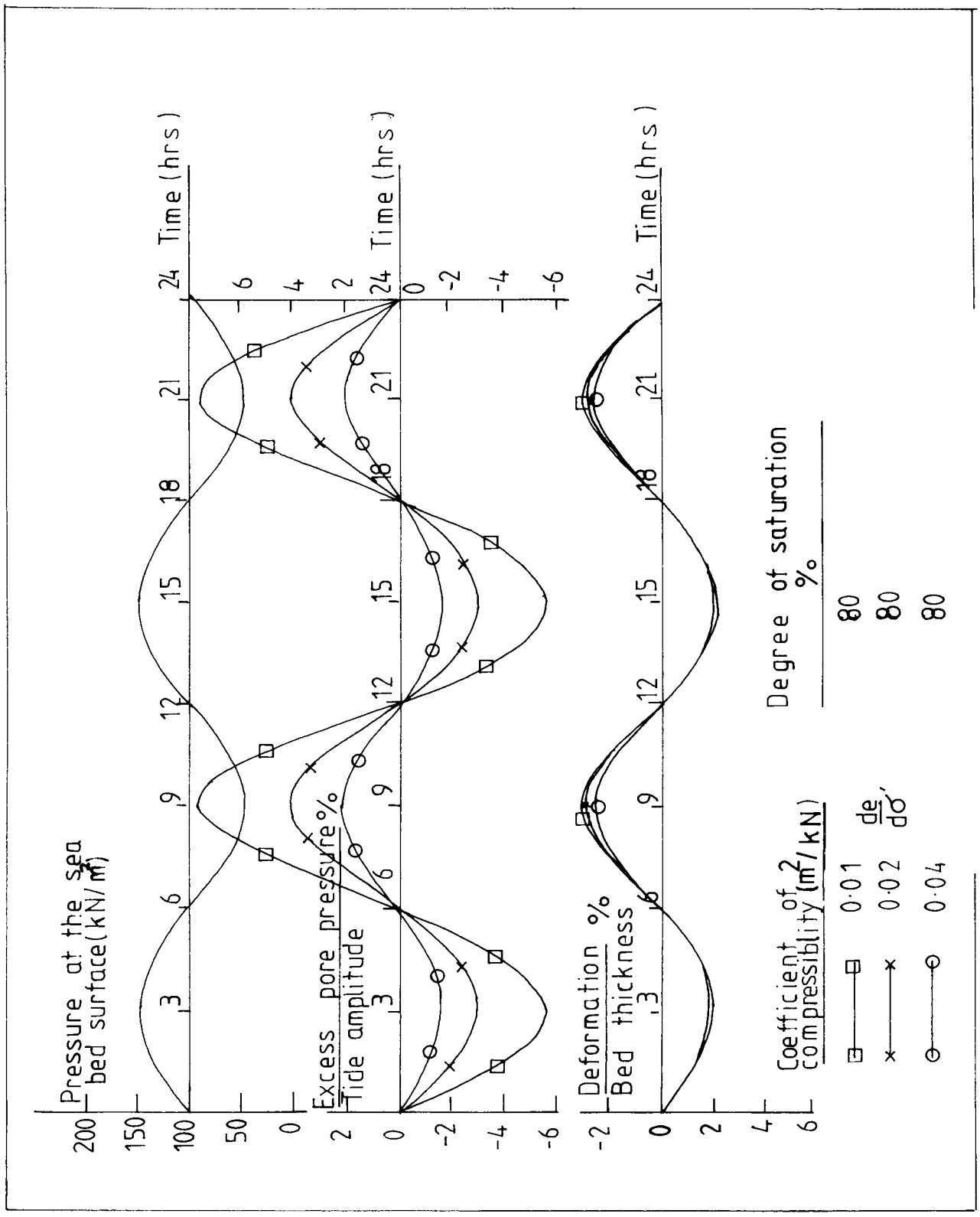

Fig 4.10 Effect of compressibility on the behaviour of gassy sea bed.
(compressibility=1/soil stiffness)

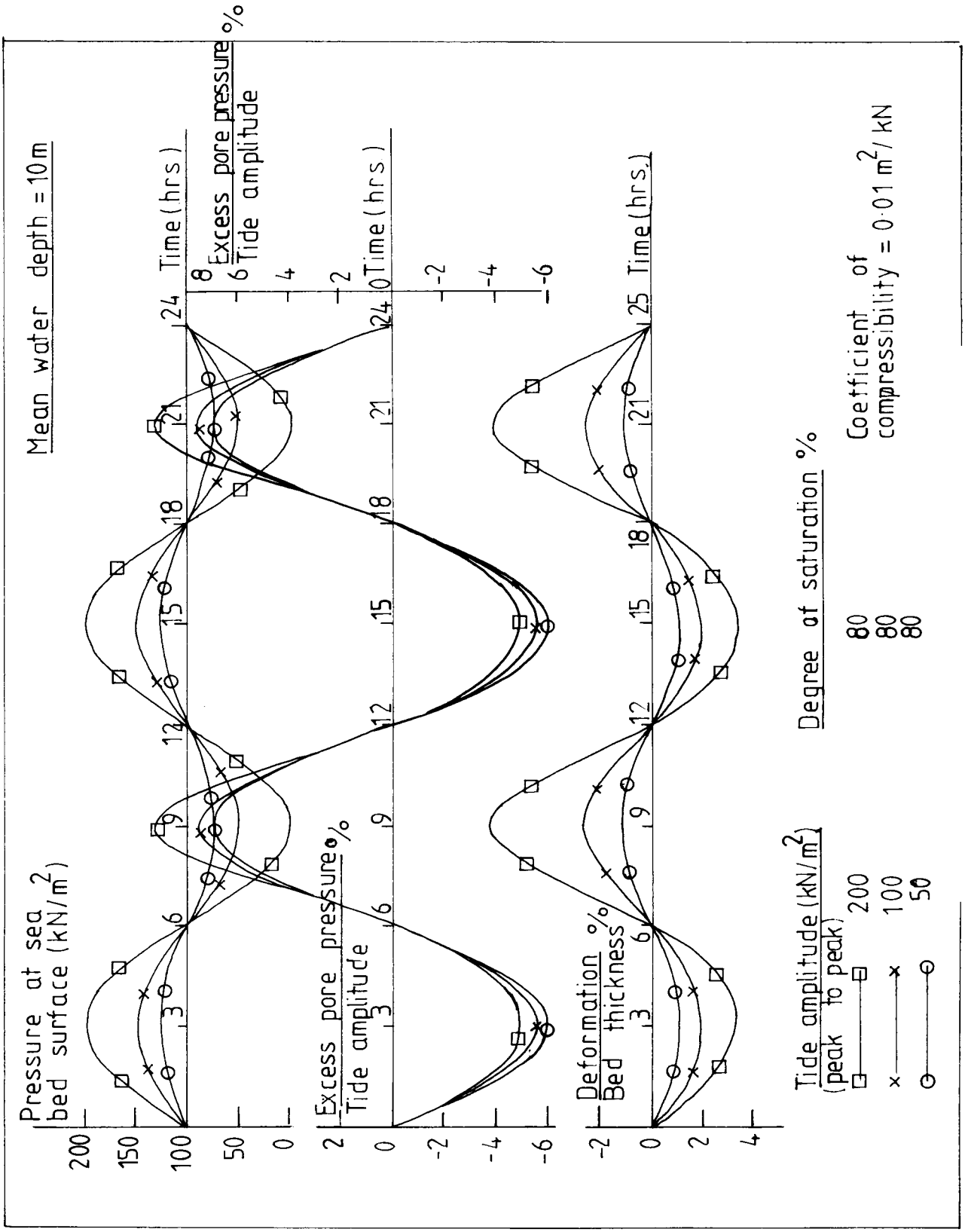

Fig 4.11 Effect of tide amplitudes on the behaviour of gassy sea bed.

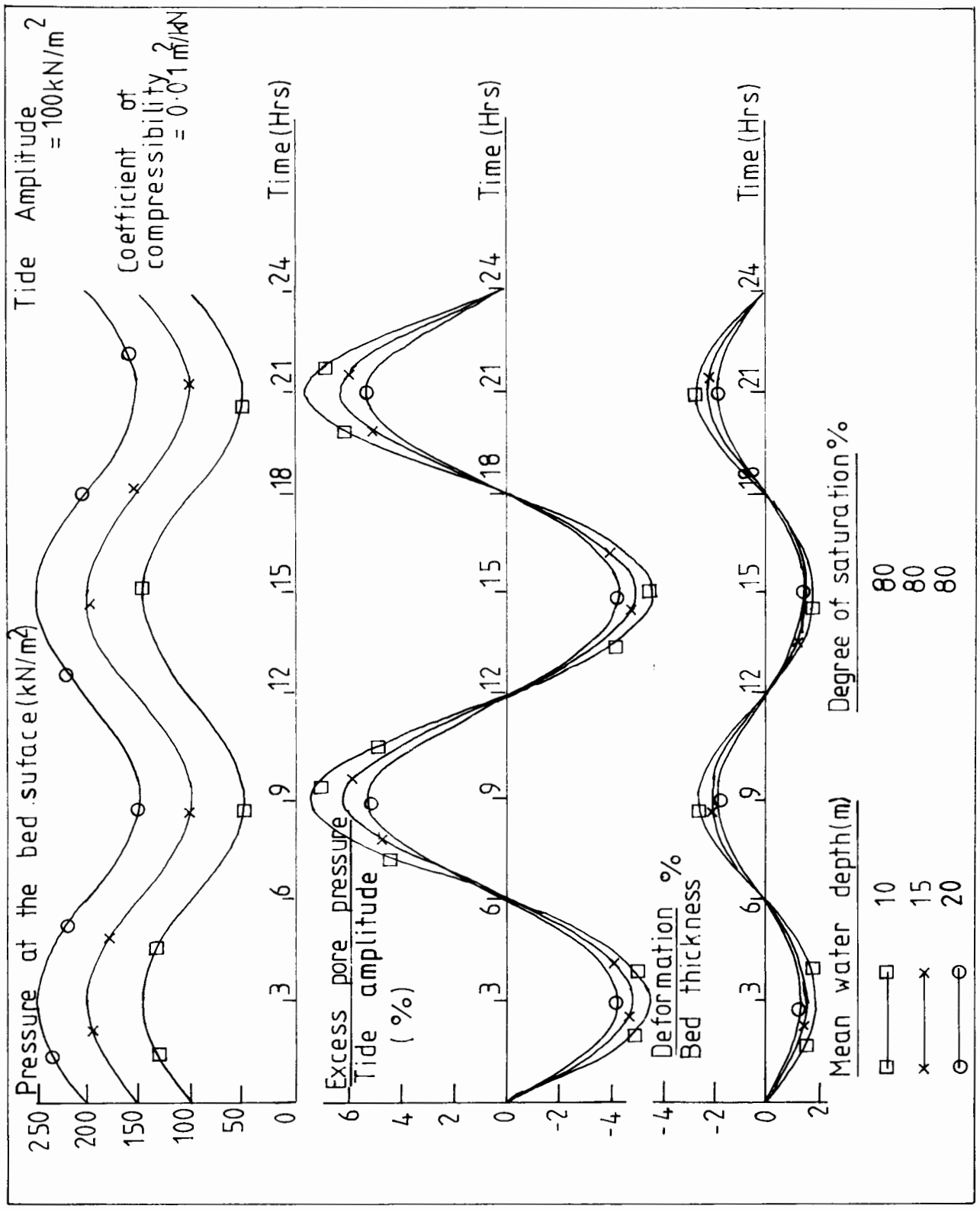

Fig 4.12 Effect of mean water depth on the behaviour of gassy sea bed subjected to tide variations.

the sea bed fig(4.12). The increase in water depth reduces the deformation and the excess pore pressure values.

(e) The effect of the permeability of the soil.

The dissipation of excess pore pressure depends on the permeability of the soil. As the permeability increases, the flow rate of water increases and faster equalisation of pore pressures is achieved. Fig(4.13) shows the effect of permeability on the soil behaviour. The excess pore pressure and the deformation decrease as the permeability increases. The phase shift between the pore pressure and the tide also increases with permeability increase. No phase shift is observed when typical values of clay permeabilities are used, suggesting that soil behaves as though subjected to undrained loading with no water flow.

(f) The pore pressure response with depth.

The excess pore pressures measured in a sea bed depend upon the depth at which they are measured. As the depth increases the flow path to the sea bed surface increases since the consolidation is one dimensional. The top few centimetres of soil in the sea bed will experience virtually no excess pore pressures irrespective of the gas content, since they dissipate very quickly due to the small flow path. Fig(4.14) shows the excess pore

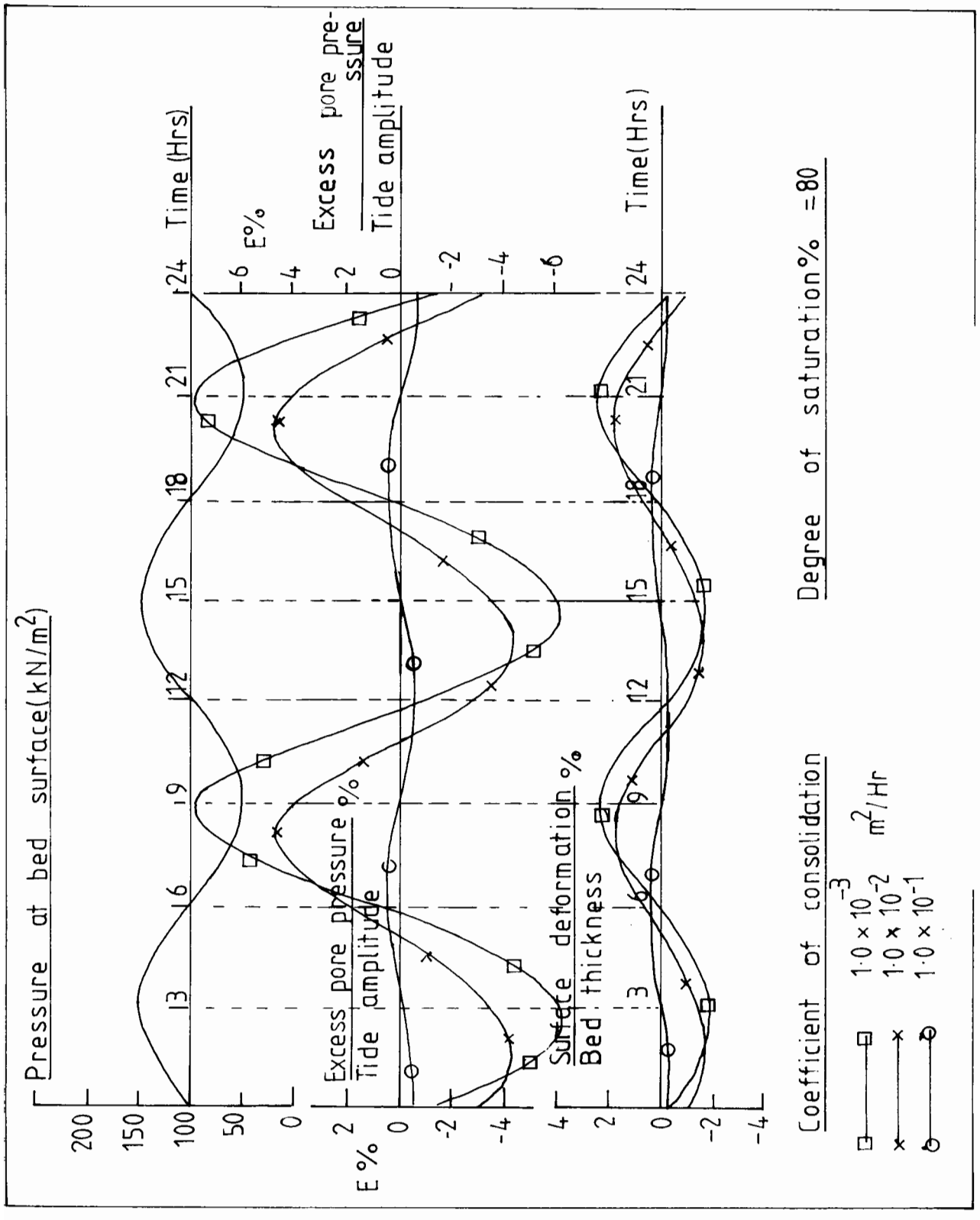

Fig 4.13 Effect of coefficient of consolidation on the behaviour of gassy sea bed subjected to tide variation.

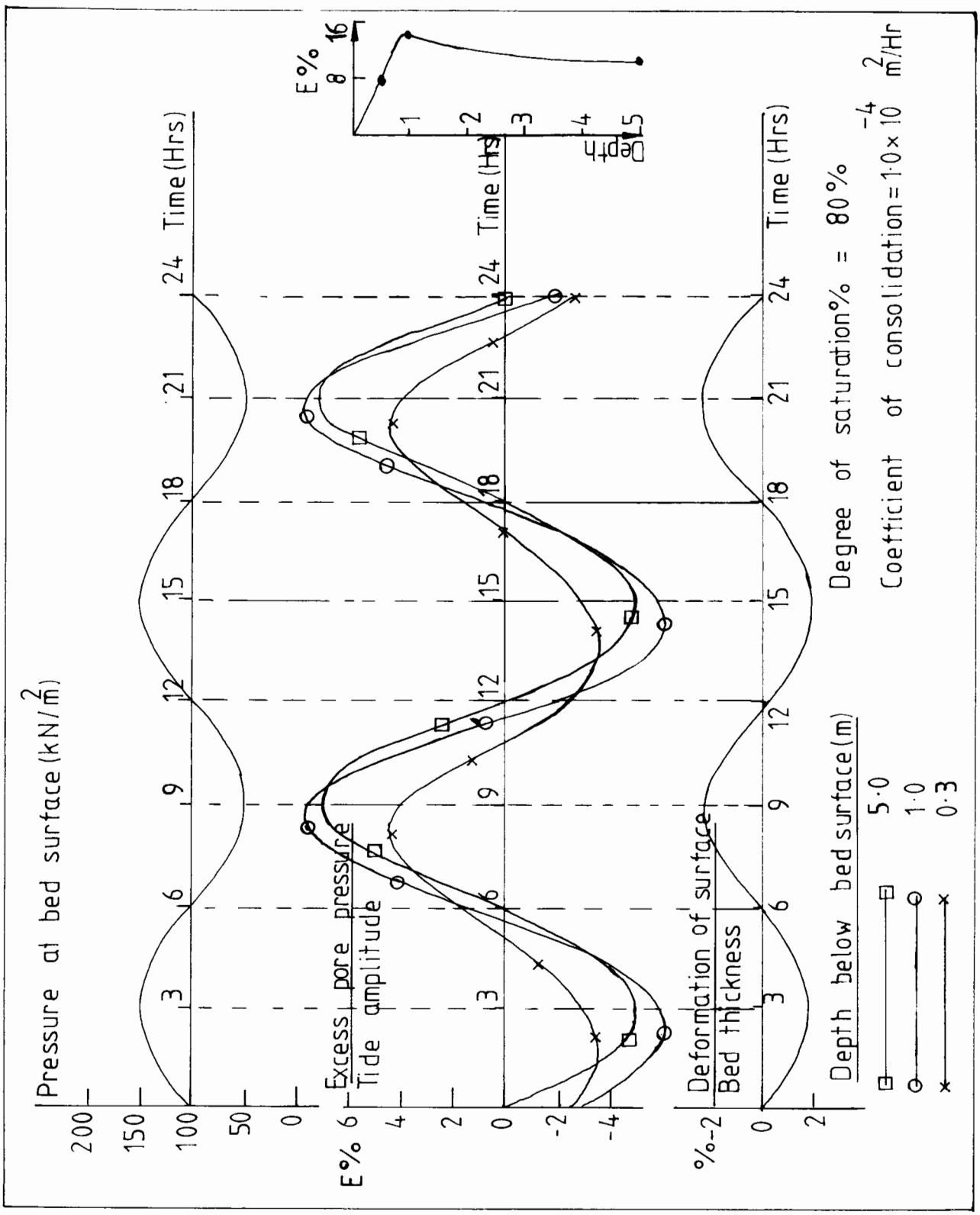

Fig 4.14 Excess pore water pressures at different depths in a gassy sea bed.

pressures at different depths in the sea bed. As the depth increases, the amplitude of excess pore pressure variation increases. For clayey soils the phase shift is observed only in the first few metres of the bed and the rest of the bed experiences no flow of water, ie. it is undrained.

Note:-Initially, the pore water pressure in the sea-bed is assumed to be hydrostatic, with zero excess pore pressure at time t=0. This condition causes some initial oscillation in the pore pressure behaviour during the initial computations, until the new stable conditions are established after a few tidal cycles. The values plotted correspond to the final equilibrium stage.

REMARKS:

The sensitivity study suggests that the pore water pressure generation and the deformation of the gassy soil for a varying water head depend on the gas content as well as the soil stiffness. The deformations and the pore pressure response are non sinusoidal and non symmetric even though the water head change is sinusoidal. For most of the cases no phase shift between the water head change and the pore water pressure variation is noticed. The phase shift occurs because of the fluid flow into the soil (to equalise the pore water pressure differences) which depends on the permeability of the soil. For clayey soils, it is observed only on the top few centimetres of

the sea bed. As the depth increases, the flow path increases and the soil at greater depths only experiences undrained loading as the tide changes. Therefore, the pore pressure response of a gassy soil at greater depths can be predicted using the equation(4.9) rather than solving the consolidation equation(4.8).

4.3.4 THE EXPERIMENTAL VERIFICATION:

The pore water pressure variation in the soil and the total deformation of a 200mm thick soil sample are computed for two different soil conditions, a soft sediment and a stiff soil and compared with the corresponding experimental results.

Description of the experiments:

(a) Soft gassy sediment subjected to sinusoidal stress variation:

The preparation of the soft soil samples is similar to the settling experiment described in chapter three. The soil slurry of density 1.1 g/cc is mixed with the required amount of zeolite to produce gas bubbles and allowed to settle in a 50mm diameter, 500mm long perspex tube. Three different samples, of different initial degrees of saturation (100%, 90%, 80%) are prepared and allowed to settle until they reach an equilibrium state. A sinusoidally varying water head is generated by a mercury pot attached to a rotating arm fig(4.15) and is applied to the samples. The mercury pot is rotated at

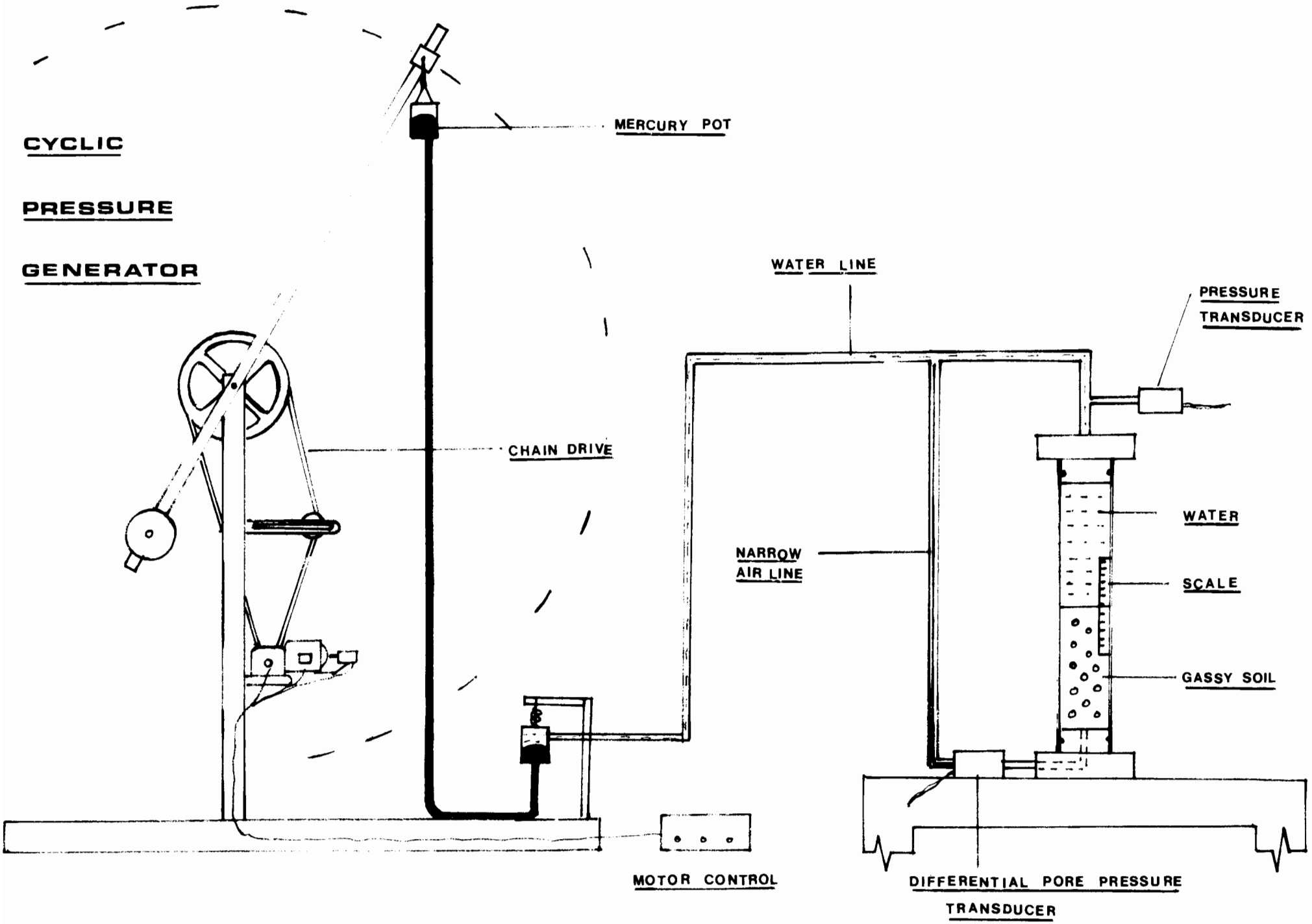

Fig 4.15 Apparatus used to study the compressible response of soft gassy soil.

constant angular speed with a cycle time of 32 minutes and the deformation of the top surface of each sample is measured. The excess pore water pressure at the bottom undrained face of the sample is also monitored. A differential transducer (35 kN/m^2 max range) is used since the magnitude of the excess pore water pressure is very small. The active face of the differential pressure transducer measures the actual pore water pressure in the soil and the back face of the transducer diaphragm is connected to the applied water pressure, so that the net output of the transducer gives the excess pore water pressure. The deformation of the samples and the excess pore water pressures are measured for a cyclically varying water head of $200kN/m^2$ amplitude. This is a 1:50 scale model test to represent the tide action on the gassy seabed of 10 metre thickness. The cycle time should be reduced by a factor 2500 if the scale factor is 50,however due to the experimental difficulties 30min cycle time is used to scale the tide cycle.

The deformation and the excess pore pressures measured in the gassy soils are shown in fig(4.16). They increase with the increase in gas content. A large amount of deformation occurs in the initial part of the cycle, showing non-symmetric behaviour even though the applied water pressure variation is symmetric sinusoidal. No phase shift is measured. The measured deformation of the sample for the initial cycle is greater than that of the

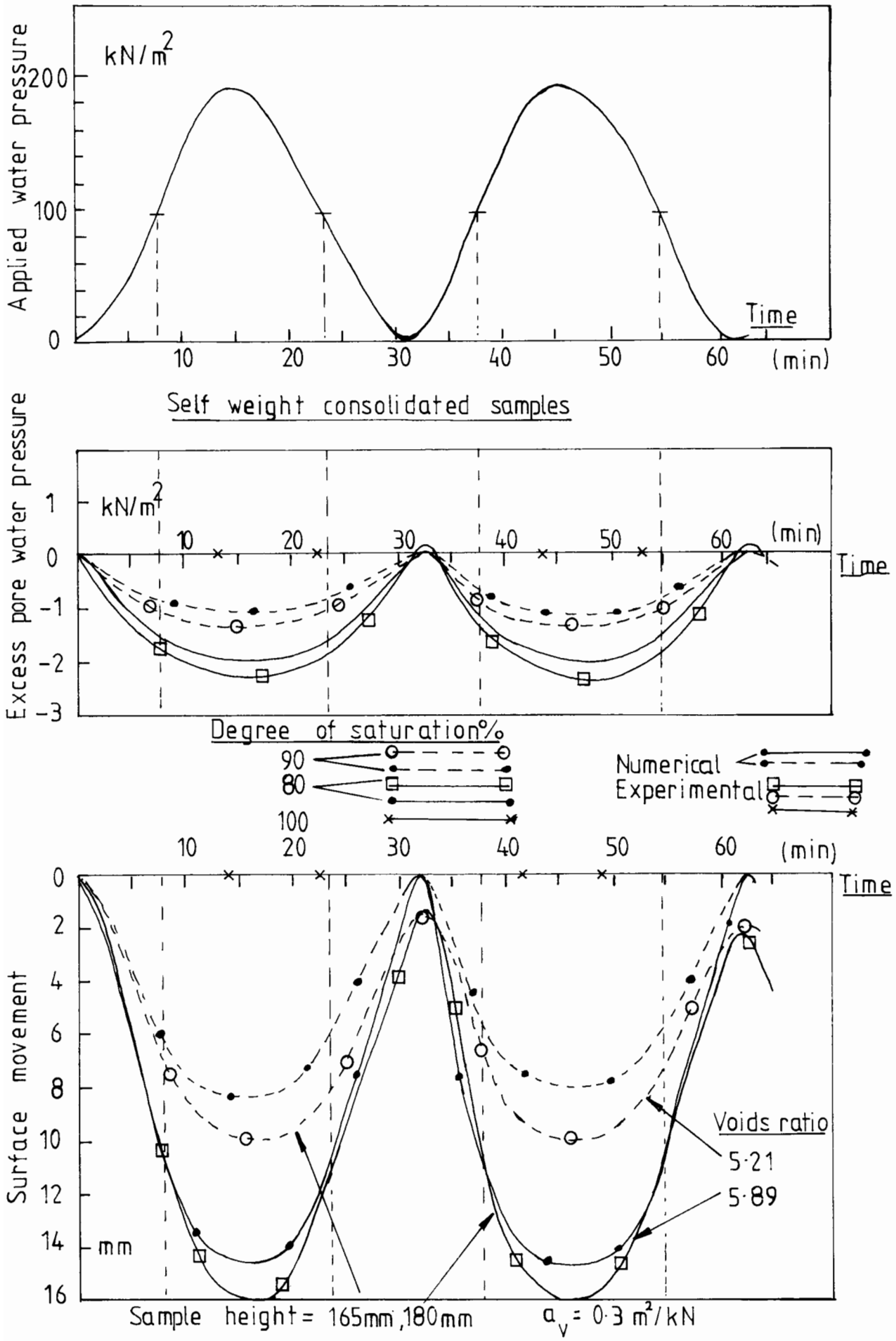

Fig 4.16 Compressibility of soft gassy soil.

following cycles. For the first cycle, soil follows the virgin consolidation line and for the subsequent cycles it behaves as an over consolidated soil, with the effective stress moving up and down the swell back line.

Fig (4.16) also shows the corresponding numerical solution for this problem. The degrees of saturation used in the analysis are obtained from the direct gravimetric measurements from the experimental gassy samples. The deformations and the excess pore pressure response are calculated and they match well with the experimental observation.

(b) STIFF SOIL SUBJECTED TO SINUSOIDALLY VARYING LOADING.

In this experiment, stiff gassy soils (of the order of 200 times stiffer than the soft soil prepared in the earlier experiment) are prepared with different degrees of saturation and tested in order to study the effect of the soil stiffness (1/compressibility) and the gas content on the deformation and the pore water pressure behaviour. These stiff gassy soils are prepared by consolidating a soil slurry (which is mixed with zeolite to give the required amount of gas content) in a 75mm diameter perspex cell, fig(4.17), under a vertical total stress of35 kN/m^2. The final thickness of the samples varies (depending on the gas content), but is around 100mm. The pore water pressure at the bottom face of the sample and the total stress are varied cyclically using the rotating mercury

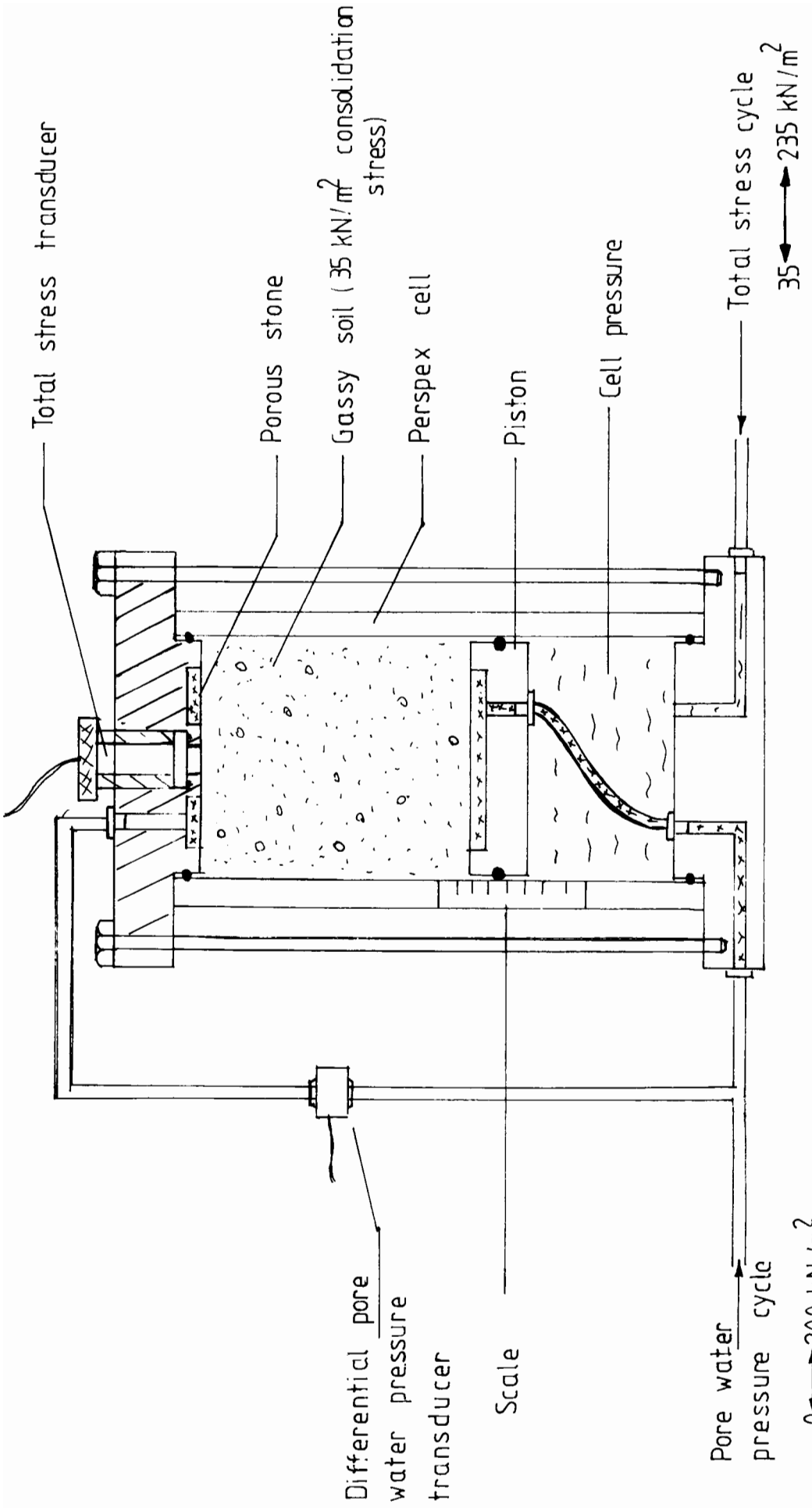

Fig 4.17 Apparatus used to study the compressible response of a stiff gassy soil.

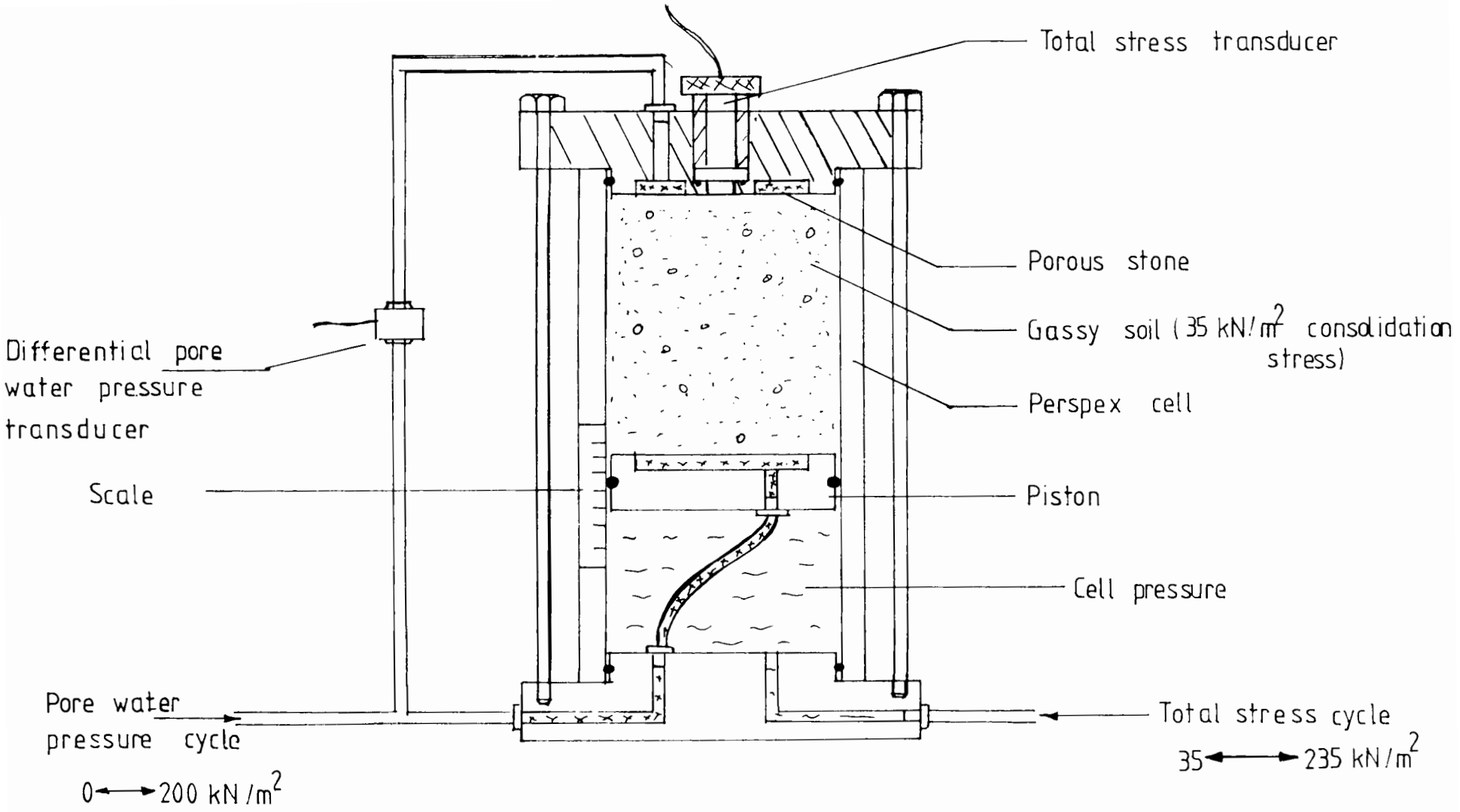

Fig 4.17 Apparatus used to study the compressible response of a stiff gassy soil.

pot system. This time two mercury systems are used, one to change cyclicly the pore water pressure at the bottom face of the sample from zero to 200kN/m^2 and the other to change the total stress from 35kN/m^2 to 235kN/m^2. The deformation of the sample and the pore water pressures at the top end of the sample are monitored. This experiment models an element of soil in the sea bed under 35kN/m^2 total overburden stress and subjected to 200kN/m^2 tide variation. Fig(4.18) shows the experimental results of three samples with degrees of saturation 100, 90, 80%. The deformation and the excess pore pressure increase with increase in gas content and both are non-sinusoidal.

The magnitudes of the excess pore water pressures measured in the stiffer soils are higher than those measured in the soft soils (fig 4.16) with the same gas content. However the sample deformation is lower in the stiffer soils. The above deformation comparison is possible since the solid heights in the stiff and the soft soil samples are the same. This experiment illustrates the importance of the soil skeleton compressibility on the undrained behaviour of gassy soil quite unlike saturated soil behaviour.

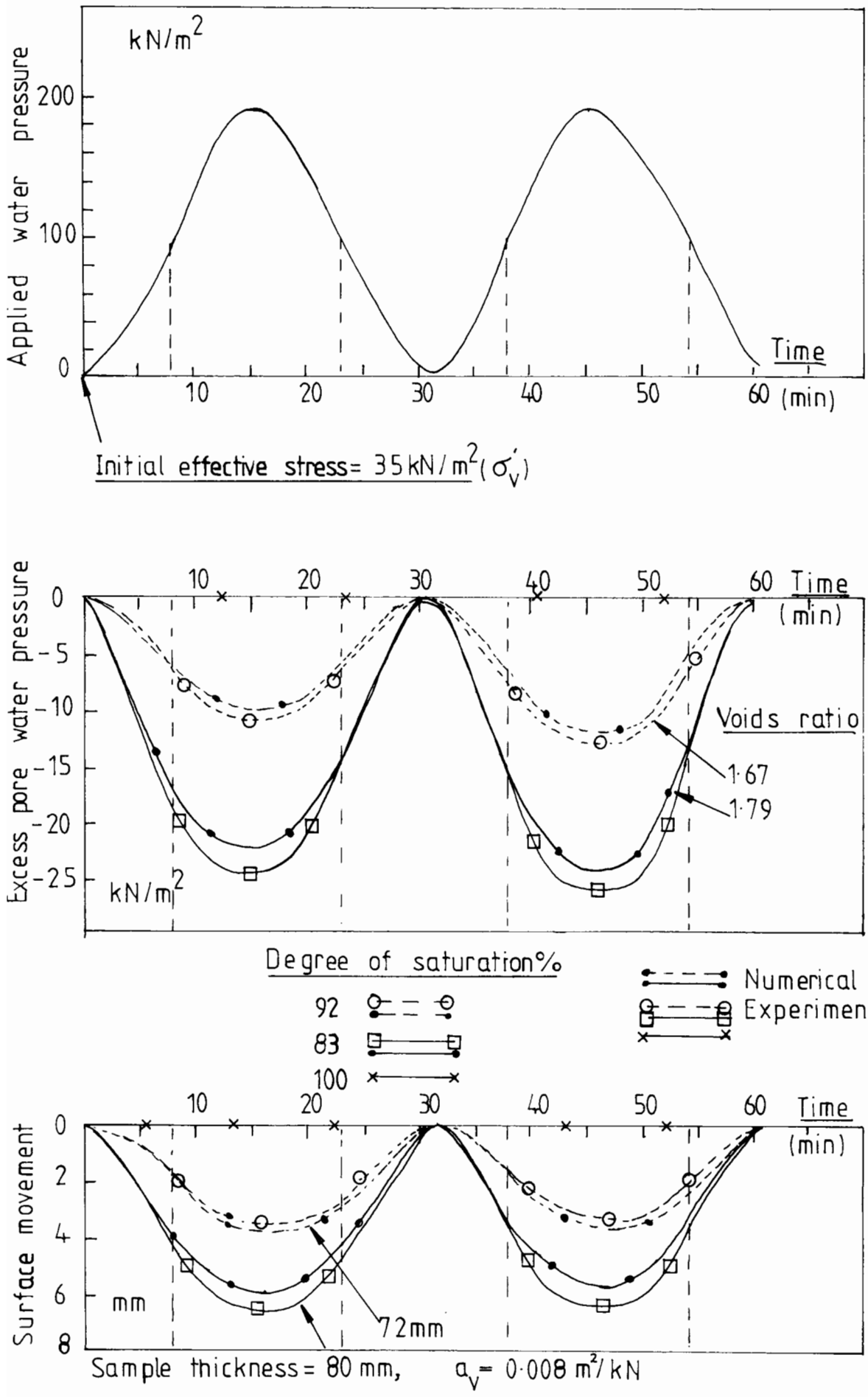

Fig 4.18 Compressibility of a stiff gassy soil.

4.4 CONCLUSION:

The above simple theoretical model predicts the initial undrained and the subsequent consolidation behaviour of the gassy soil reasonably well even though some simplifying assumptions were made. The behaviour of gassy soil depends on the gas content of the soil and the soil stiffness. Immediate undrained volume change occurs in a gassy soil as the gas volume decreases when the total stress is increased, but the subsequent consolidation rate decreases as the gas bubbles expand. In saturated soil no immediate consolidation is observed but subsequent consolidation is faster than that of the gassy soil. The consolidation time (eg for 95% consolidation) for a gassy soil with a degree of saturation above the critical saturation (ie. greater than 85% for this soil) and for the saturated soil are nearly the same due to these two compensating effects. As the gas content increases (below the critical degree of saturation), the gassy soils consolidate much faster than the saturated soil because of the higher gas permeabilities. The above model could be improved by using a suitable permeability-saturation relationship.

The behaviour of a gassy sea bed for tide changes is also predicted and shown to cause surface movement. the magnitude will depend on the soil properties and, as shown in the next chapter, could be significant.

CHAPTER 5

IN-SITU PORE WATER PRESSURE MEASUREMENT IN A GASSY SEA BED

5.1 Introduction

5.2 Brief description of the instrument and the mode of operation

5.3 The differential piezometer

5.4 Calibrating and deairing the piezometer

5.5 Deployment of the piezometer and the measurements

5.6 Observations

5.7 Analysis of the results

5.8 Conclusion

CHAPTER 5

IN-SITU PORE WATER PRESSURE MEASUREMENTS IN A GASSY SEA BED

5.1 INTRODUCTION

In addition to the laboratory study on reconstituted gassy soil, an instrument to measure the in-situ pore pressures in a gassy sea bed has been developed. The presence of gas bubbles, (a) increases the total voids volume, (b) reduces the shear strength (chapter seven), and (c) increases the compressibility of the soil when compared to a saturated soil. Even small quantities of gas bubbles produce a significant compressible response of the gassy soil, affecting the pore water pressure changes and the deformation of the soil for an undrained total stress increment. A differential piezometer to measure the pore water pressure response in a gassy sea bed to tide and wave action has been developed in order to study the behaviour of the gassy sea bed.

The pore water pressure in the sea bed changes for changes in external applied loadings such as the water head variation over the bed caused by tide or waves. With pressure changes of long period, such as tide changes, pore water pressure in a saturated sea bed varies exactly the same way as the hydrostatic head changes. In the case of wave loading, additional pore water pressures are generated due to the shearing of the soil. However in a

gassy soil subjected to a hydrostatic pressure change, the pore water pressure change is less than that of the water head change due to the compressibility of the pore fluid, fig(5.1). The difference between the pore water pressure and the hydrostatic pressure is an indication of the effect of undissolved gas in the sea bed and it is measured using a differential piezometer. An estimate of the amount of in-situ gas can also be predicted, as detailed later, using the differential pressures measured, if the volume change-stress relationship of the soil skeleton can be measured.

5.2 BRIEF DESCRIPTION OF THE INSTRUMENT AND THE MODE OF OPERATION.

This instrument is designed to measure the in-situ pore water pressures in a gassy sea bed. The in-situ pore water pressure changes as the water pressure over the sea bed changes due, for example, to tide and wave action. With a tide change, the sea bed pore pressure and the hydrostatic pressure will be different from each other if the sea bed contains gas, with the difference between them depending largely on the gas content, the magnitude of the water head variation and the soil skeleton compressibility (chapter four). The difference in pressures can be measured by subtracting the measured pore water pressure from the water head change (hydrostatic pressure) using two separate pressure transducers. However, the accuracy in the estimated excess pore pressure would then depend on the measurement of two large pressures including the depth of water, using transducers whose sensitivity would necessarily be restricted by the high range required. The higher the range of the transducer, the lower the sensitivity. As an alternative approach to increase the accuracy, this instrument measures the difference directly using a differential transducer, instead of subtracting the two large pressures to obtain a small difference. The active face of the transducer measures the sea bed pore water pressure and the back face of it is connected to an air filled rubber bladder which lies on the sea bed

surface fig(5.1). The pressure in the bladder is controlled by the water pressure acting on the sea bed surface and the transducer output directly gives the excess pore water pressure in the sea bed.

The piezometer consists of two such differential transducers to measure the excess pore pressures at depths of 2.25 and 3.45 metres below the surface of the sea bed. In addition to the differential measurements, the total water pressure acting on the sea bed is also measured. The instrument is 3.5 metres long, 44mm in diameter and has been pushed into the sea bed using lead weights which are removed soon after the installation. The instrument is then supported by a large mud plate which is attached to the top of the instrument, to prevent it sinking under its own weight in soft mud.

The piezometer is used to measure the excess pore pressures generated by tide and wave in soft sediments in tidal zones. The output of the transducers is amplified and transmitted via electrical cables to the ship or platform for recording, so that the initial driving pressures and the excess pore pressures due to wave and tide actions after the dissipation of the driving pressures can be measured. Undisturbed samples are also obtained using a gravity corer and they provide the one dimensional stress-strain characteristics, i.e.the compressibility of the soil skeleton, which is used to estimate the in-situ gas content.

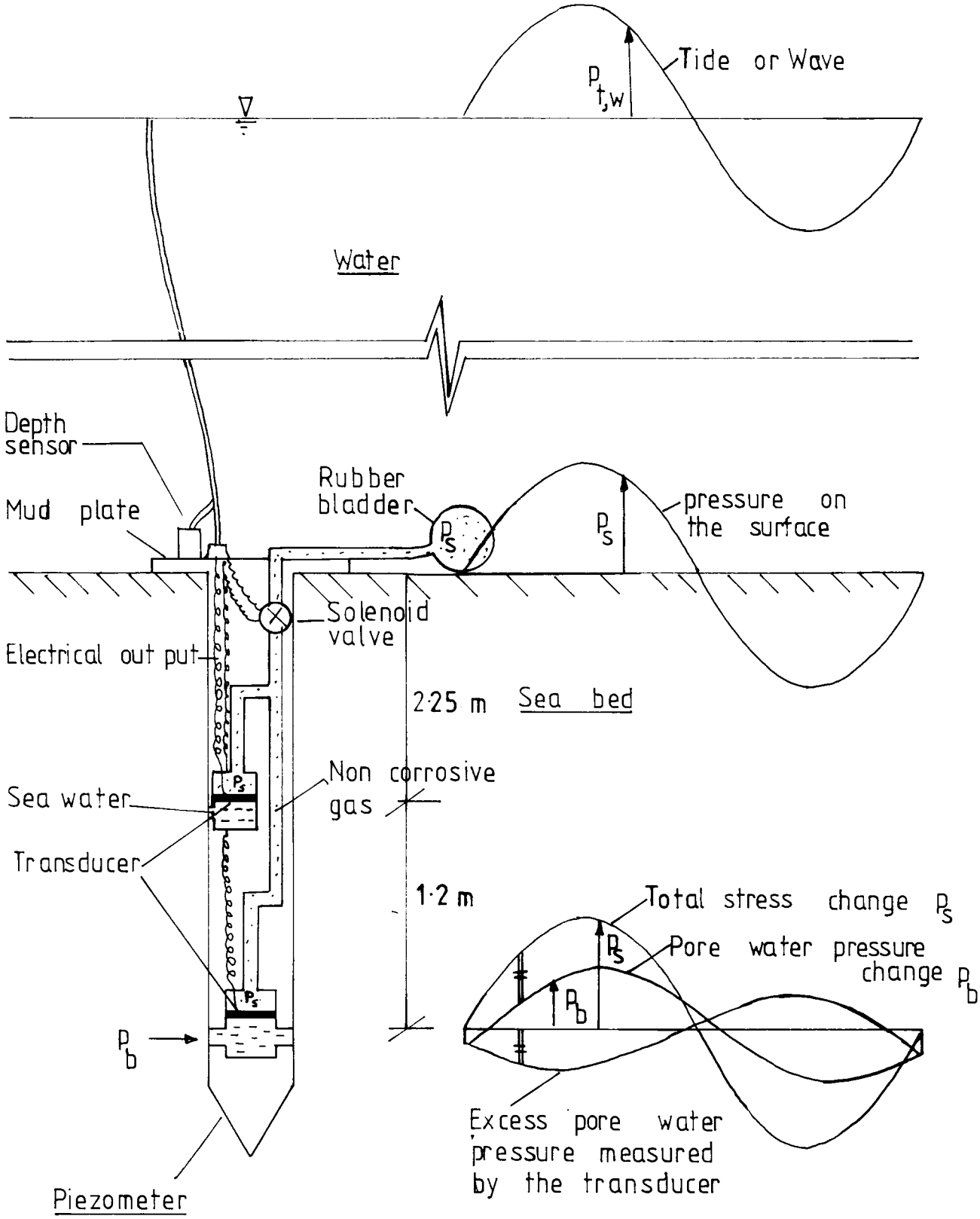

Fig 5.1 Pore water pressure response in gassy sea bed for tide action.

5.3 THE DIFFERENTIAL PIEZOMETER.

The piezometer consists of two differential transducers mounted in housings which are separated by a hollow rod, fig(5.2). The upper transducer housing is connected to another hollow rod which brings the electrical leads and the back pressure line (from the passive side of the transducer diaphrams) to the surface of the seabed. The top end of the piezometer has a larger diameter hollow cylinder in which all the transducer power supply units and the signal amplifiers are mounted. The whole instrument is sealed at atmospheric pressure. The back pressure line is connected to an external rubber bladder via a solenoid valve and the pressure in the back pressure line is monitored by a total pressure transducer. This total stress transducer registers the water head variation acting on the bladder when the solenoid is open. A pressure transducer acting as a depth sensor is also attached to the piezometer to measure the water head variation. The whole instrument is made out of stainless steel to prevent excessive corrosion. The components are numbered in fig(5.2) and these numbers are used in the following text when they are described.

Tip of the piezometer

The tip(1) is machined from a solid stainless steel rod to an overall diameter of 44mm with a 60^{o} cone. The

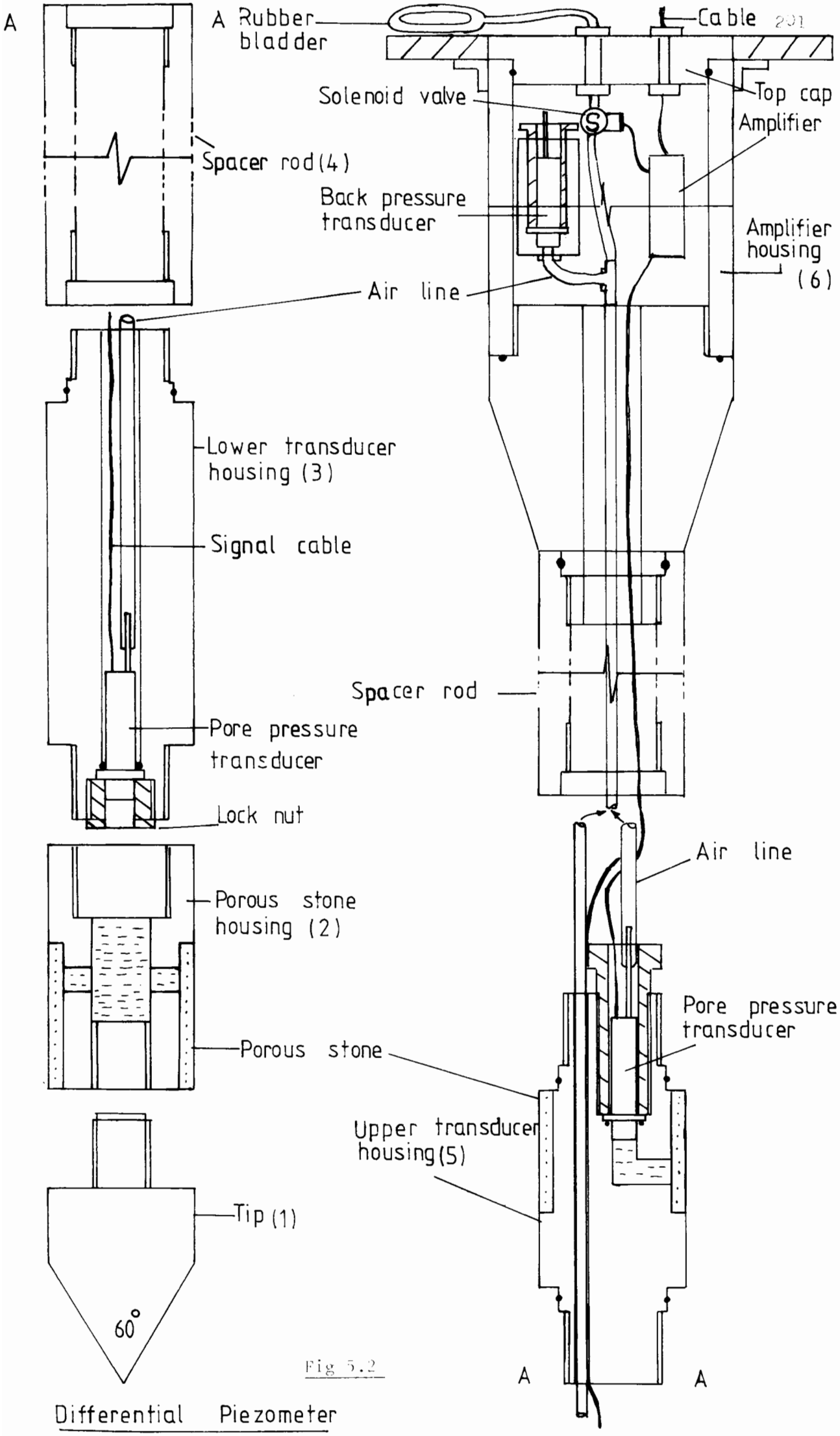

Fig 5.2

Differential Piezometer

other end is threaded to connect to the female end of the porous stone housing(2).

Porous stone housing(2)

The porous stone housing is machined to accomodate a 44mm outside diameter and 3mm thick porous plastic annulus(4) with an air entry value of 10kN/m^2. This housing provides pore water connection from the sea bed to the lower pressure transducer. A central hole of 30mm diameter is drilled and both ends are threaded (female). Four 6mm holes are drilled on the body of the housing to allow pore water connection to the active face of the transducer. One end is connected to the tip section and the other end to the transducer housing.

Lower pore pressure transducer housing

The lower transducer housing(5) is turned out from solid stainless steel to 44mm diameter. Each end is threaded (male 33mm diameter) and a central 20mm hole is drilled. One end is recessed to accommodate a 40mm long and 15mm diameter differential pressure transducer (PDCR22) manufactured by Druck Ltd. The transducer is attached (axially) to the housing by a threaded lock nut and the sealing is provided by an O-ring. This end is connected to the porous stone housing. The electrical connections and the 4mm diameter plastic tubing (connected to the back face of the transducer) are taken from the other end of the housing.

Upper pore pressure transducer housing(7)

Unlike the lower housing, this accommodates the transducer and the porous annulus in the same unit. This is machined to 38mm outside diameter to accommodate a porous annulus of 44mm outside diameter and 3mm thickness. Both ends are threaded (male 33mm diameter) and a 6mm off centre hole is drilled to pass the electrical connection and the back pressure line from the lower transducer through to the top end of the piezometer. The transducer (PDCR 22) is mounted in an axial direction, but at an off centre position. The pore water connection to the front face of the transducer is provided by a 10mm hole which connects with another 10mm hole drilled sideways. The side hole is covered by the porous annulus.

Spacer rods.

The two transducer housings and the housing which accommodates the electrical components are separated by two hollow stainless steel rods of diameter 44mm and length 1.0m and 2.0m respectively. The ends are threaded (female) and the sealing between the connections is provided by O-rings on the male parts of the components. The length of the piezometer and the spacing between the transducers can be varied by selecting different lengths of spacer rods.

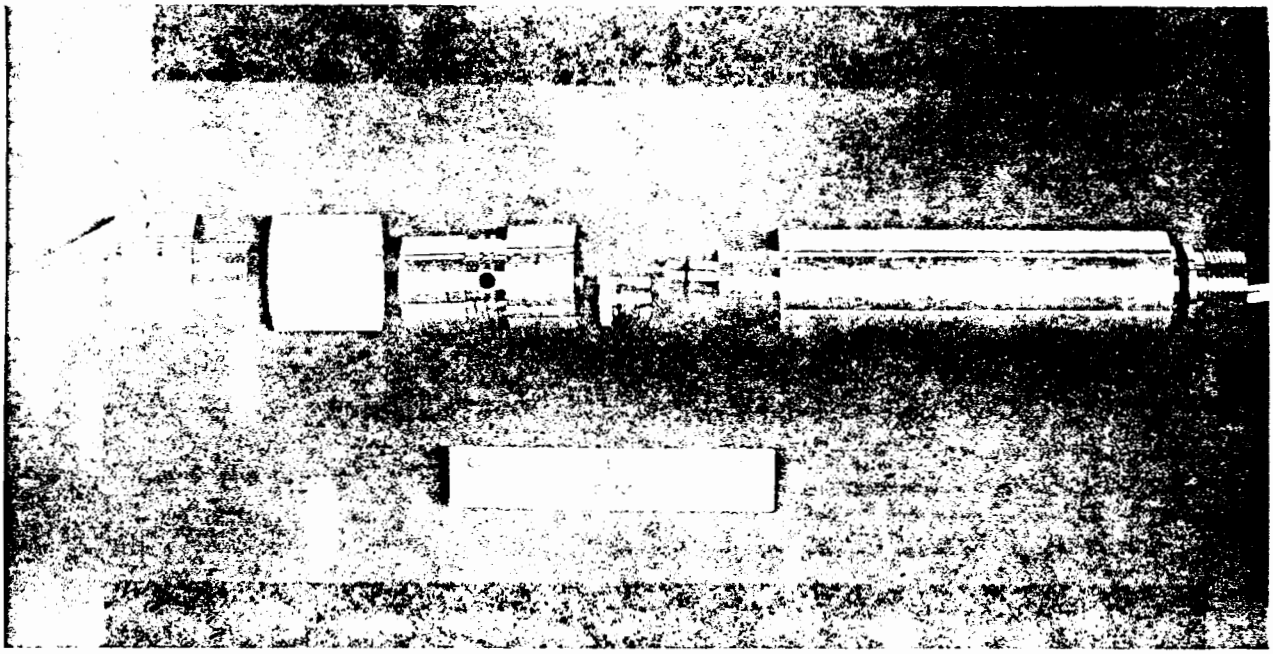

Plate 5.1 Lower transducer housing

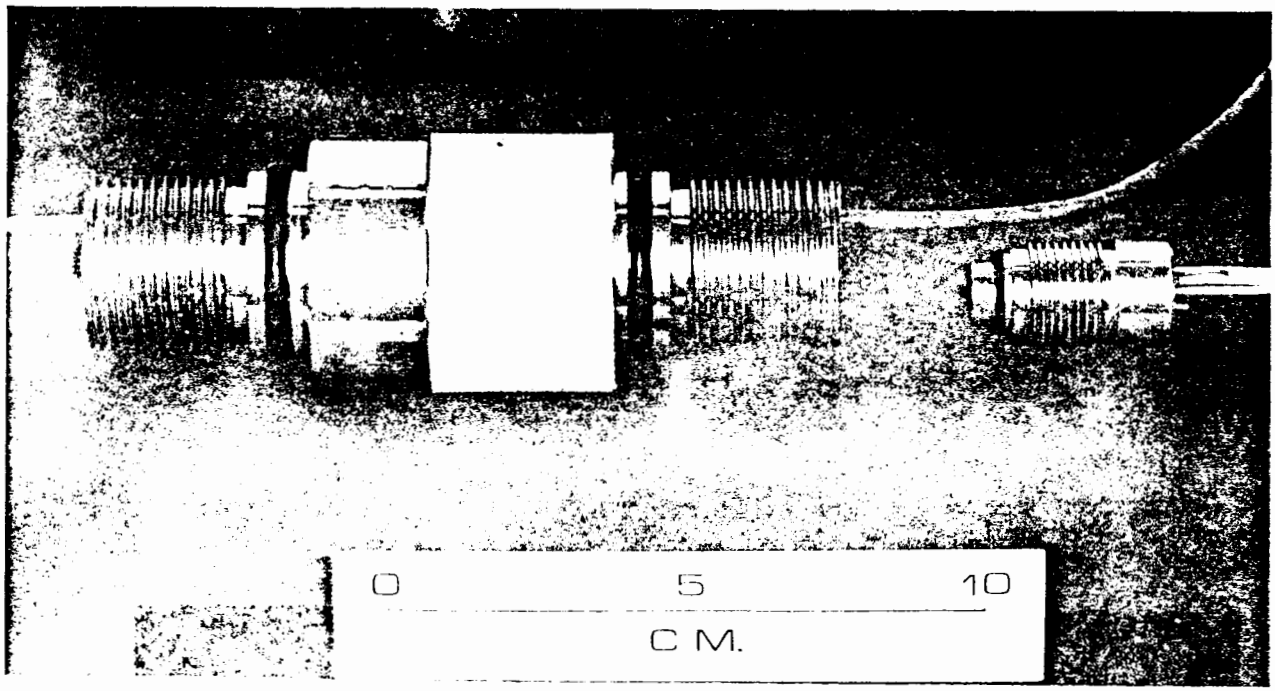

Plate 5.2 Upper transducer housing

Electrical component housing(6).

This housing is larger in diameter than the rest of the instrument due to the bulk of the electrical circuitry and is machined from hollow stainless steel tube to give 60mm outside diameter and 10mm thick wall. The continuity from the 44mm diameter spacer rods and the electrical housing is provided by a cone shaped section machined to vary the diameter from 44mm to 55 mm in a 200mm length. The top end of the electrical component housing is sealed by a stainless steel plug. The electrical leads and the back pressure nylon tube are brought out from the sealed piezometer through watertight connectors.

Mud plate.

A steel plate, 20mm thick and 500mm diameter, is attached to the top end of the piezometer, fig(6.3) in order to support the piezometer in soft soil by distributing the weight to a larger area. The mud plate is bolted to a flange welded on to the electrical housing.

Weight stand.

The piezometer is driven into the sea bed using lead weights (60mm diameter and 50mm thick cylindrical cast units with 20mm diameter central hole). The lead weights are placed on a steel tube stand of 30mm diameter (5mm wall thickness) and 1m high. A flange is welded to the bottom end of the tube to support the weights. A lifting

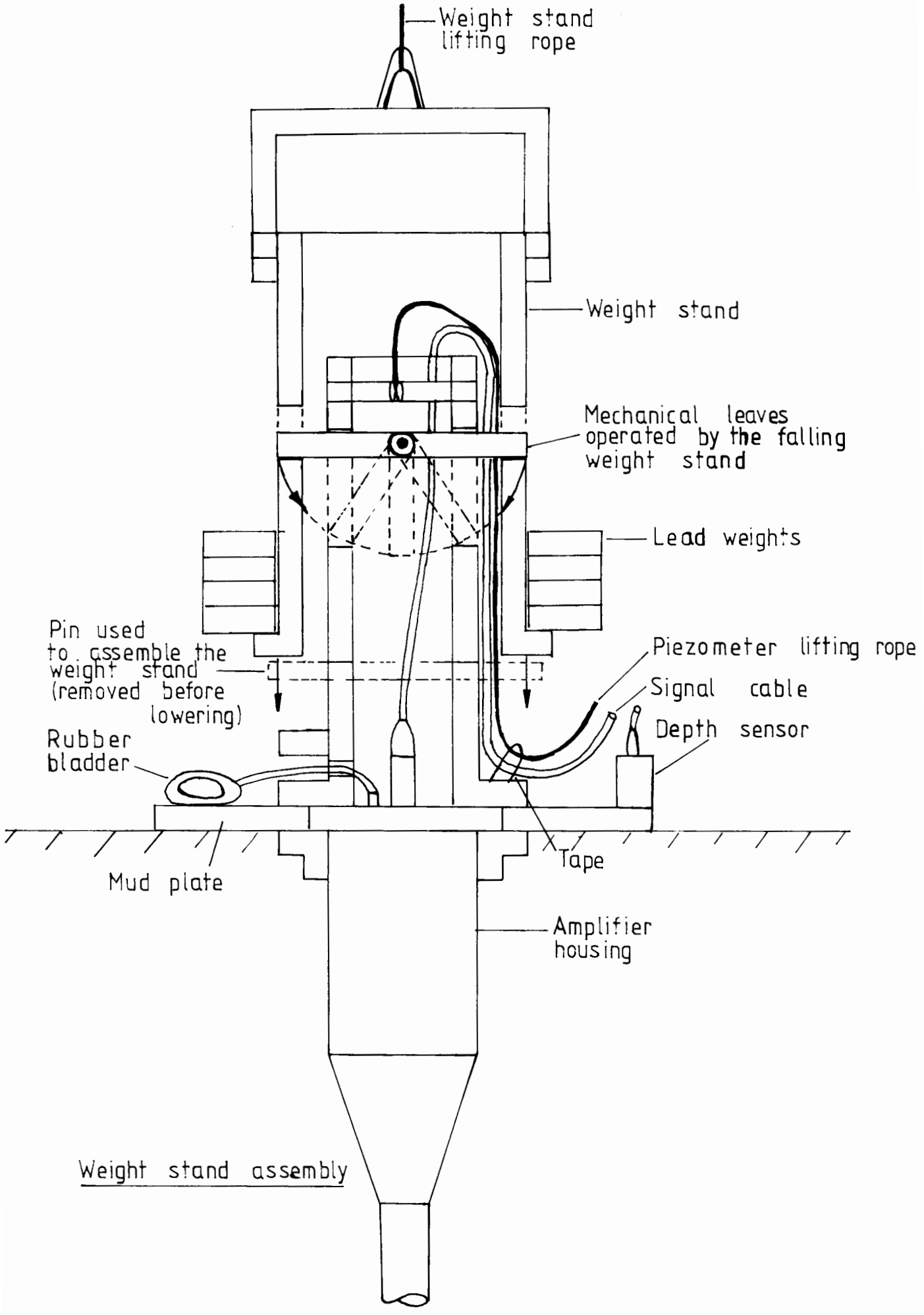

Fig 5.3 Weight stand assembly

(c) Depth sensor

Type:- Druck PTX 110/D

Range:- 600kN/m^2, Non-linearity: ± 0.1% of the best straight line

5.4 CALIBRATING AND DEAIRING THE PIEZOMETER.

All the transducers used are calibrated in the instrument before the installation of the piezometer and again after recovering it. The calibration of the differential pore pressure transducers is carried out after the whole instrument has been assembled. A pressure tight cylinder is placed over the transducer housing and pressurised using a bicycle pump. The transducers are calibrated against a Druck digital pressure indicator. Fig(5.4a) shows the components used for calibration.

The accuracy in the measurements largely depends on the efficiency of dearing of the porous stones and the transducer housing. The presence of a small quantity of air in the system changes the characteristic response of the piezometer, so that poorly deaired piezometer results will show the effect of gas bubbles in the sea bed even if the sea bed is fully saturated. The porous elements are initially deaired by boiling them under vacuum. They are assembled into the transducer housing after they have been filled with deaired water. However during the assembly of the porous element onto the housing some bubbles may become trapped in the system and the system is deaired

again using the following procedure. The piezometer is placed in a water trough with the upper and lower transducer housings submerged. A rubber membrane is placed over each of the porous elements. A water filled nylon tube is inserted through the rubber membrane using a brass connection as shown in fig(5.4b) and the other end of the tube is connected to a vacuum pump via an air water interface. The remaining gas bubbles from the housing are drawn out as the vacuum is applied and they are collected in the air water reservoir. The vacuum is released after a while and water flows into the housing. The vacuum is turned on and off until no air bubbles appear from the transducer housings. The brass connection and the tubes are removed and rubber O-rings are placed over the rubber membrane to keep the porous element saturated. These membranes are pushed away from the porous element, when the piezometer enters the sea bed ,

5.5 DEPLOYMENT OF THE PIEZOMETER AND THE MEASUREMENTS:

The piezometer with the driving weights is lowered into the sea bed with the use of a derrick. The piezometer is hung vertically in the water, fully immersed above the sea bed, for some minutes to obtain the zero reading. The readings obtained from the differential transducer do not change as the water head changes as the piezometer is lowered since there is no excess pore pressure. As the piezometer is lowered into the sea bed, the excess pore pressure increases, measuring the driving

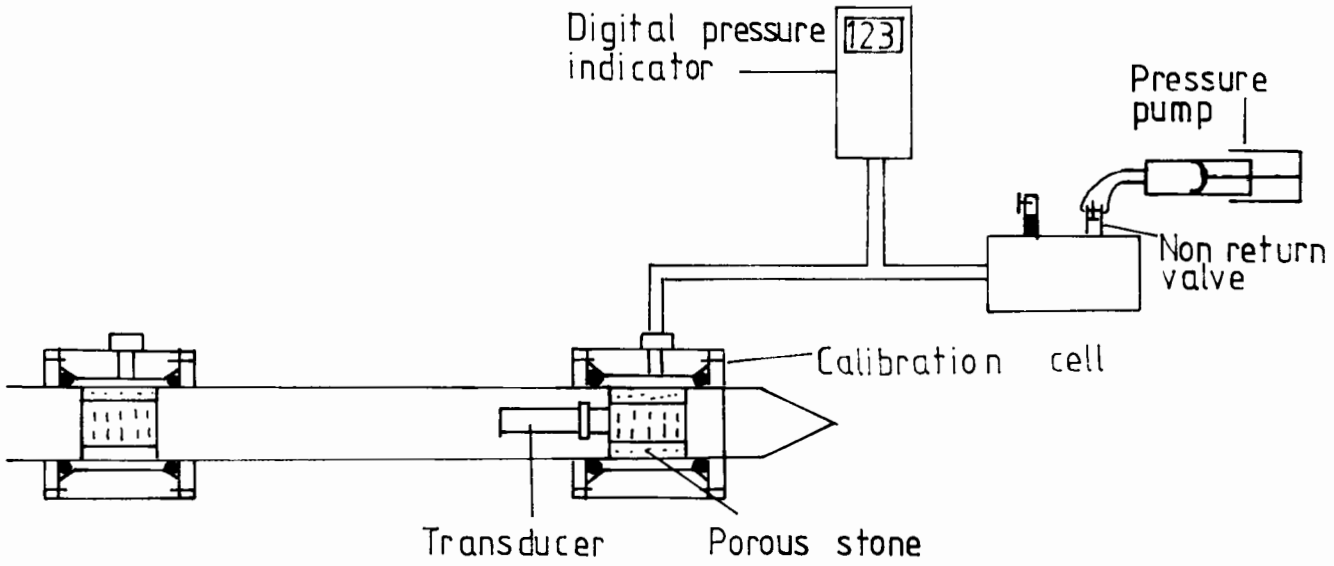

5·4 a Transducer calibration assembly

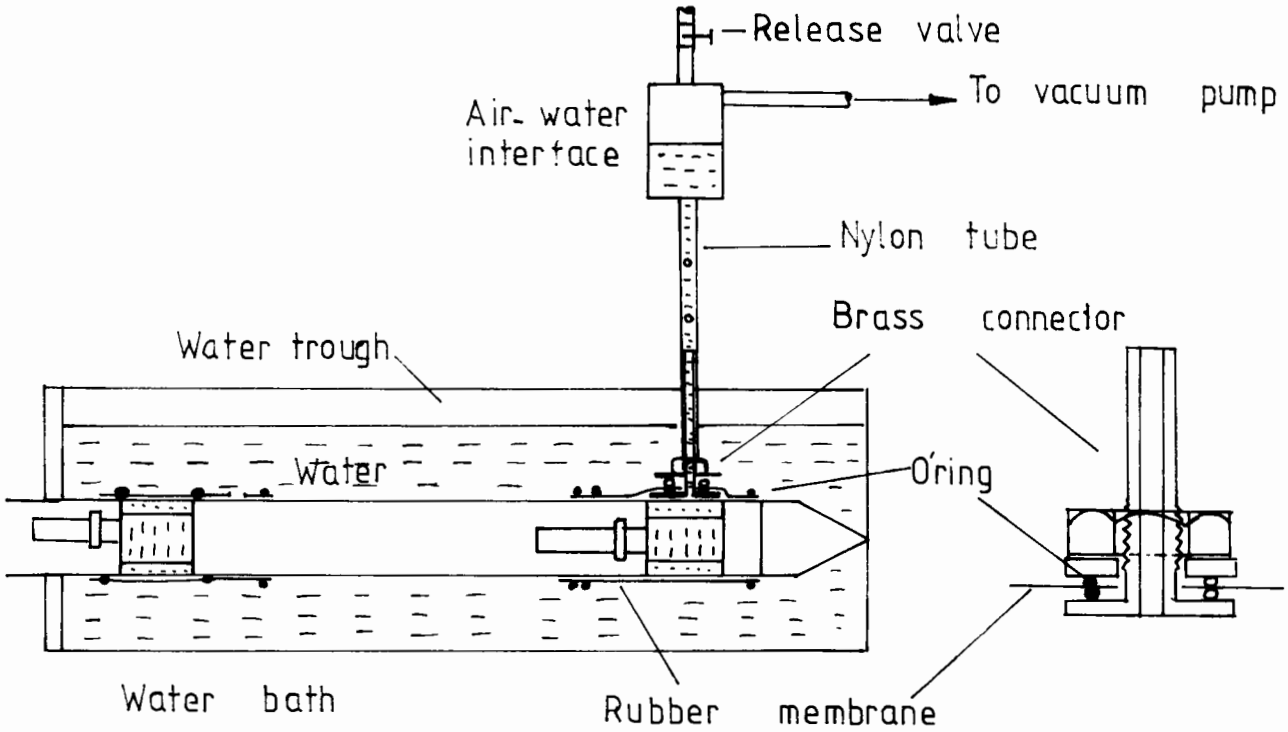

5·4 b Deairing the pore water pressure transducer

Fig 5.4 Deairing and calibrating the piezometer.

pore pressures. A tilt indicator (a mercury switch) attached to the piezometer indicates whether the piezometer is driven vertically. Slackness in the rope which is used to lower the piezometer and a stable reading from the depth gauge indicate the end of the penetration. The amount of weights necessary to achieve full penetration is determined from a trial run, using weights to drive a gravity core barrel (40mm diameter) to obtain a 3.5 metre long core sample before the piezometer is lowered. The depth obtained from an echo sounder in the ship is also compared with the depth sensor reading to ensure the full penetration of the piezometer. The weight stand with the weights is removed from the piezometer as soon as the rope becomes slack as the mechanical latch is released.

The signal output from the transducers and depth gauge are continuously recorded using a six channel analogue chart recorder and also by a Commodore Pet micro computer in digital form. During normal operation the solenoid valve is open to allow the changing water pressure to act on the back face of the differential transducer. The time taken for the pressure variation at the level of the seabed to be transmitted through the back pressure line to the back face of the transducer depends on the compliance of the air filled rubber bladder and on the magnitude of the pressure change. This lag is small in the case of a tide change, since the sea bed pressure

changes slowly. Any time the lag registered by the piezometer is therefore due to the presence of gas in the sea bed. Sudden changes in sea bed pressures caused by waves may not be transmitted through the back pressure line immediately, and hence a lag measured by the piezometer would be a relative quantity. To avoid the lag caused by the rubber bladder in this dynamic case, the solenoid valve is closed and a constant pressure(equal to the head of water at the time the valve is closed) is maintained in the back pressure line during the measurement of wave induced sea bed pore pressures. The phase shift obtained by this method is then the absolute phase shift in the sea bed and may be attributed to the presence of gas bubbles.

5.6 OBSERVATIONS:

The piezometer has been used at two sites, Port Talbot Harbour in South Wales and Holyhead Harbour in Anglesey. The presence of gas bubbles was suspected from the depth measurements observed in Port Talbot Harbour. The apparent sea-bed position at a given location varied between high tide and low tide by up to half a metre and this could be caused by the presence of gas bubbles.

The readings obtained using the piezometer in Port Talbot Harbour are shown in fig(5.5). The maximum driving pressure observed is 14kN/m^2 and its dissipation took 24 hours. The tide amplitude is 50kN/m^2 and the amplitude of

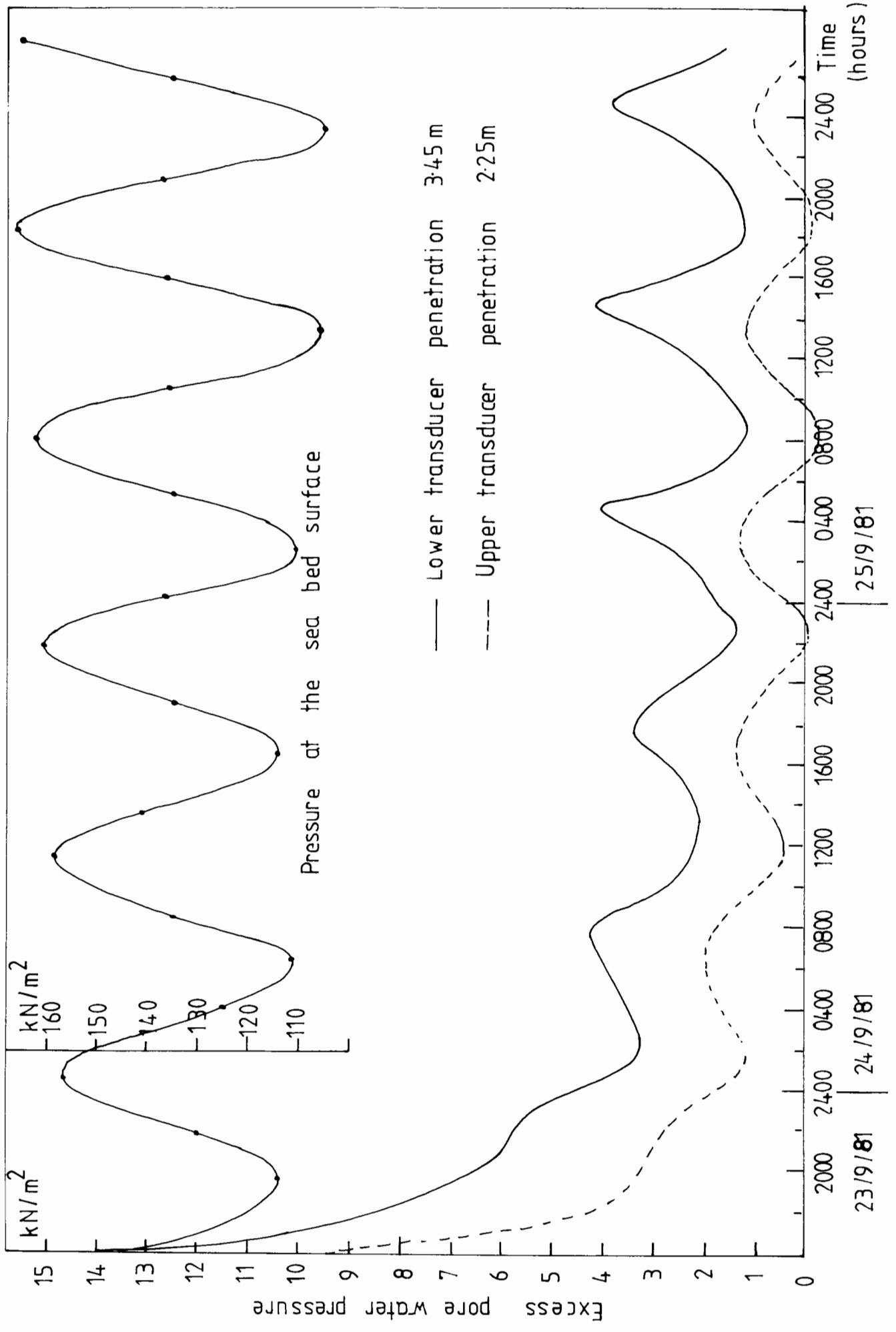

Fig 5.5 Excess pore water pressure induced by tide at Port Talbot Harbour.

the excess pore pressure measured at 3.45m depth into the sea bed is about 3kN/m^2 and at 2.25 metre depth is 2kN/m^2. This indicates the presence of gas in the bed. The piezometer is used to measure the wave induced pressures for a short period. Fig(5.6) shows the chart recorder out put obtained during this measurement. Although the amplitude of the wave pressures is very small, a few points may be noted.

(a) The sea bed surface pressure and the pore pressures were all exactly in phase.

(b) Examining a single wave, the pressure amplitude at the bed surface is 1.50kN/m^2 with the resulting pore pressure at 2.25m being 1.0kN/m^2 and 0.8 kN/m^2 at 3.45m.

Fig(5.7) shows the observation at Holyhead Harbour. No varying excess pressures were observed in either transducer, thus indicating a saturated sea bed.

5.7 ANALYSIS OF THE RESULTS:

The observations in Holyhead Harbour suggest that the sea bed is fully saturated while the observations at Port Talbot suggest the presence of gas. The sensitivity study in chapter four indicates that the following parameters are necessary to estimate the gas content from the measured excess pore water pressure induced by tide changes:

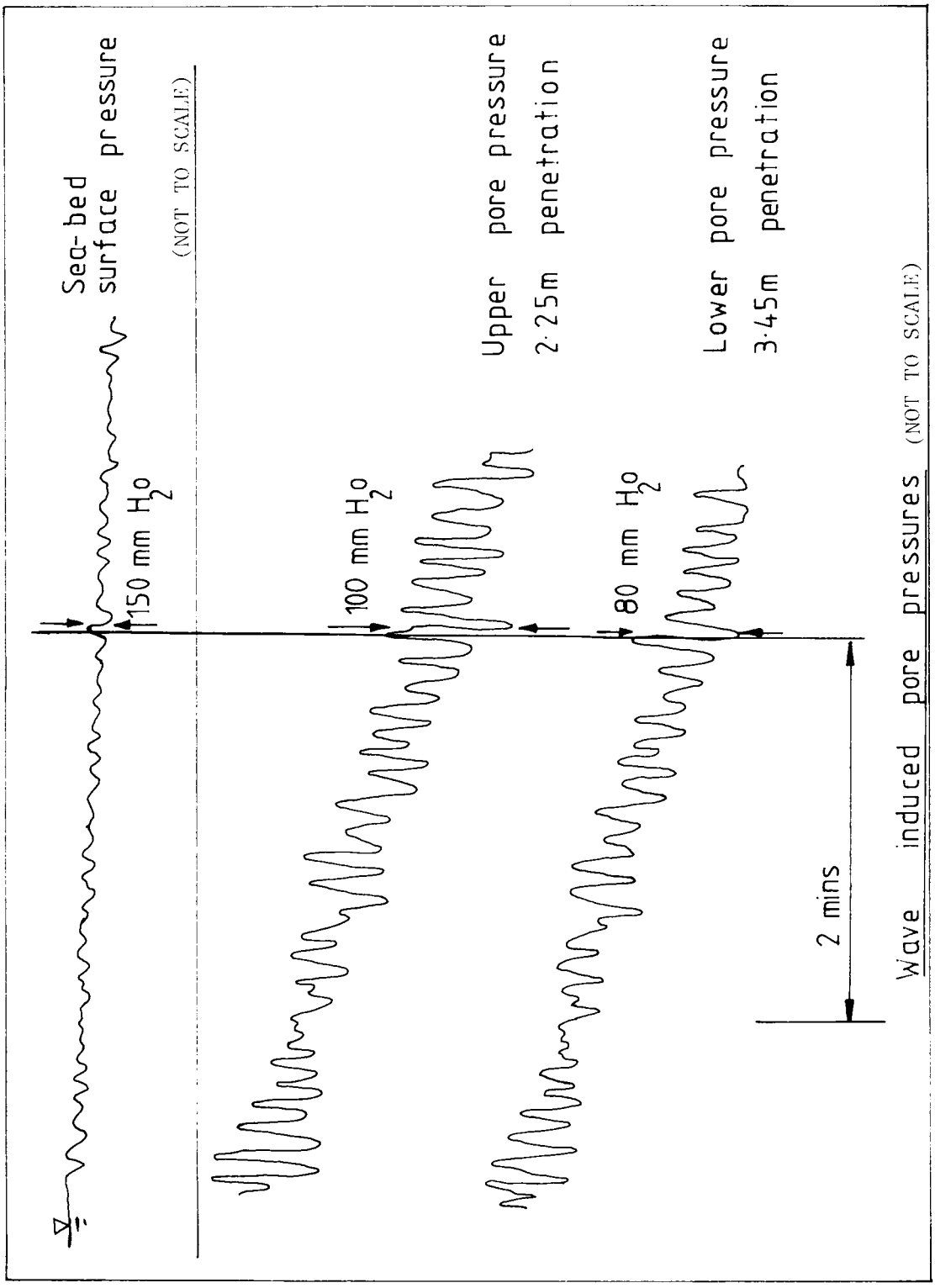

Fig 5.6 Excess pore water pressures induced by waves at Port talbot Harbour.

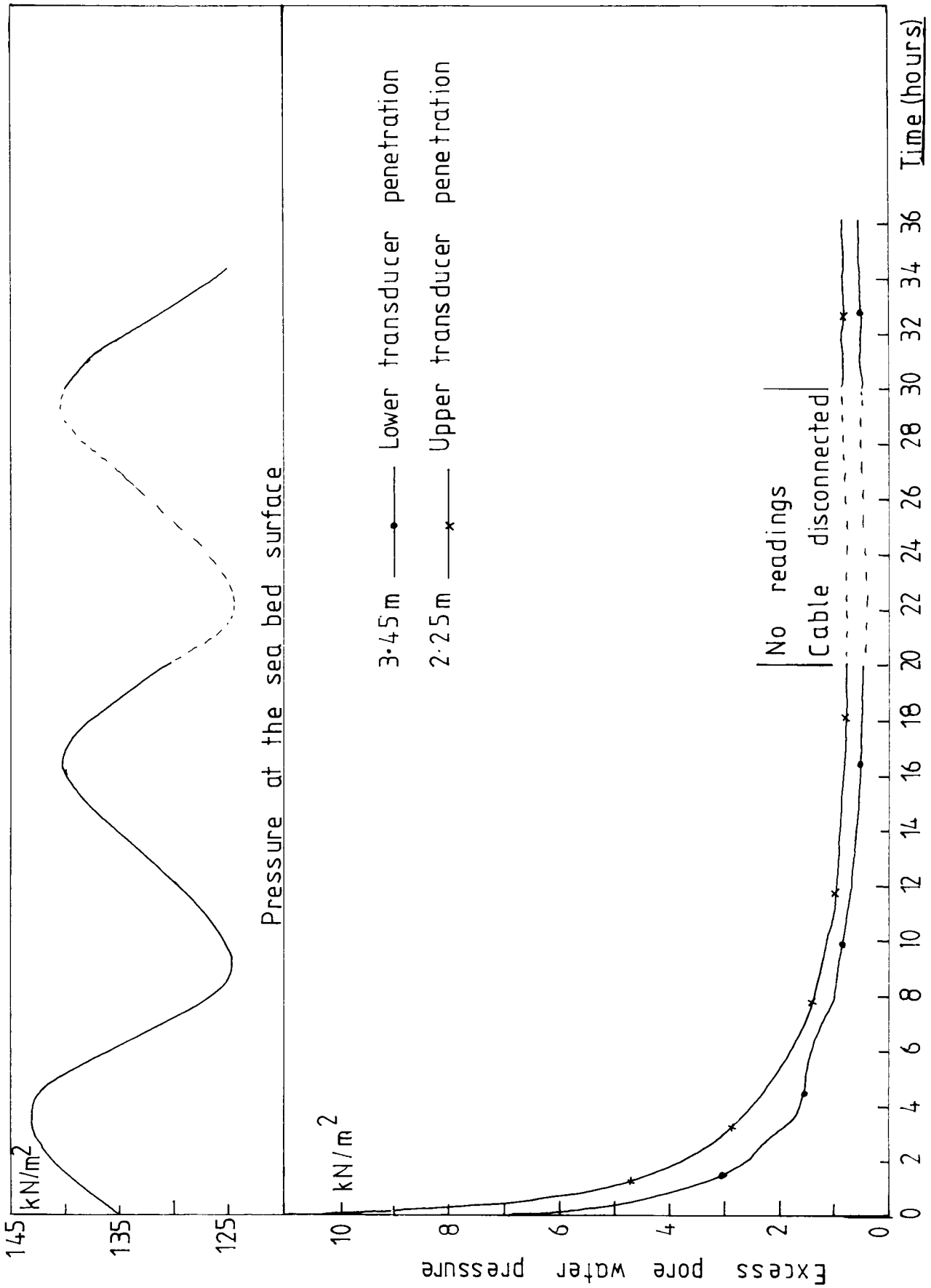

Fig 5.7 Excess pore water pressure measured at Holyhead Harbour.

(a) the tide amplitude,

(b) depth of water above the sea bed at low tide or at high tide,

(c) the compressibility of the soil, and

(d) the coefficient of consolidation of the soil.

The variables (a),(b) are measured by the depth sensor attached to the piezometer and the compressiblity and the coefficient of consolidation of the soil are obtained from laboratory oedometer tests on the core sample. The table below shows the parameters used in the calculations.

Voids ratio (e_o)=2.3

Coefficient of compressibility (a_v)=0.004 m^2/kN

(obtained from the swelling gradient, fig(5.8)

Total stress increment ($\Delta\sigma$)=50kN/m^2 (tide amplitude)

Pore water pressure increment(Δu)=47kN/m^2 at 3.45 m depth

Initial pore water pressure(P_o) =144kN/m^2

Peak pore water pressure (P_{max}) =191kN/m^2

Coefficient of consolidation =$5\times10^{-8}m^2/sec$

The degree of saturation is estimated from the following equation which is derived in chapter four for clayey soils.

$$B = \frac{\Delta u}{\Delta\sigma} = \frac{1}{1+\dfrac{e_o\ (\alpha+H)\ P_o}{a_v\ p^2\ (1+\alpha)}}$$

where and $\alpha=(100/S_o)-1$

$$\frac{1}{p^2} = \frac{1}{p_{ave}^2} = \frac{1}{2}\left[\frac{1}{p_{max}^2} + \frac{1}{p_{min}^2}\right]$$

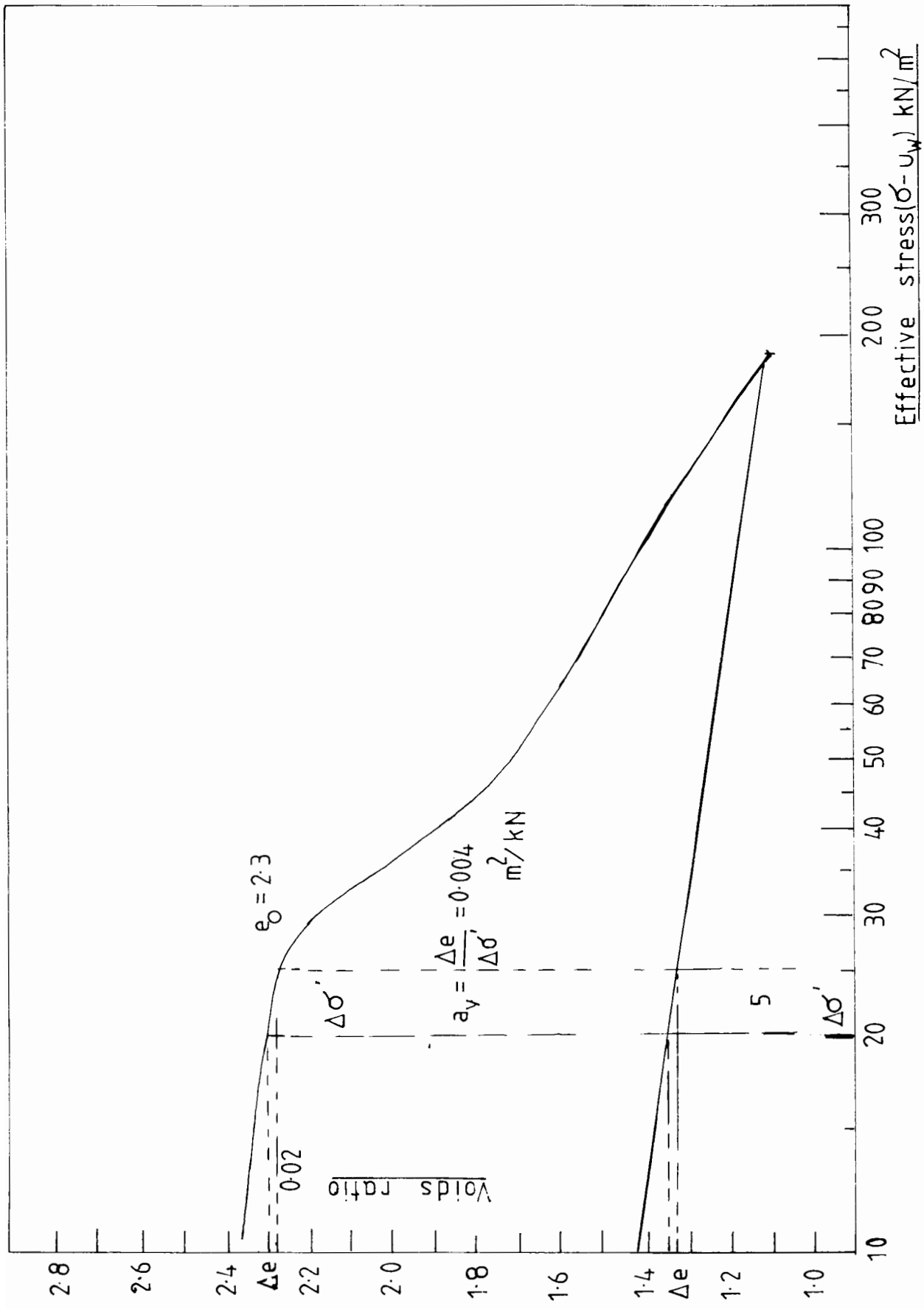

Fig 5.8 Voids ratio-effctive stress relationship of the sample taken at Port Talbot Harbour at 3m depth.

The estimated degree of saturation at Port Talbot is around 98%. The maximum deformation of the surface of a 10m thick seabed is 36mm.

5.8 CONCLUSION:

The differential piezometer is a useful instrument to measure the pore water pressure behaviour in the sea bed. The accuracy in the measurement is higher than a conventional total pressure piezometer because it measures directly the excess pressure above the hydrostatic pressure instead of measuring the total pore water pressure and the hydrostatic pressure separately to evaluate the excess pressure. The reliability of the instrument largely depends on the efficiency in deairing the instrument and keeping it saturated during deployment. The measurement of excess pore water pressures due to tide changes in Port Talbot harbour suggests that the sea bed contains undissolved gas bubbles with a degree of saturation of the order of 98% and the measurements in the Holyhead Harbour suggest no gas bubbles. This instrument can also be used to measure the wave induced excess pore water pressures in a sea bed.

CHAPTER 6

UNDRAINED SHEAR STRENGTH OF GASSY SOIL

6.1 Introduction

6.2 Vane shear tests

6.3 Undrained triaxial compression tests

6.4 Discussion of the results

6.5 Conclusion

CHAPTER 6

UNDRAINED SHEAR STRENGTH OF GASSY SOIL

6.1 INTRODUCTION

Undrained shear strength is one of the important properties of the soil used in geotechnical engineering. The effect of gas bubbles on the undrained shear strength of the soil is examined in this chapter. The experiments in the previous chapter suggest that the soil containing gas bubbles has a higher voids ratio than that of a saturated soil with the same consolidation stress. The shear strength of a soil at a given normal effective stress is largely dependent on the voids ratio (packing of the soil particles), so that the structural differences caused by the presence of gas bubbles in the soil could be expected to change the shear behaviour of the soil. The presence of high pore gas pressures in the soil and the compressibility of the pore fluid add to this effect. The undrained shear strengths of soils with different amount of gas contents are measured and compared with that of the saturated soil using a shear vane. The vane is selected as a measuring device because most of the field data available on gassy soils were obtained either from field vane or laboratory vane tests. In addition to vane shear tests a few unconfined compression tests and undrained triaxial shear tests were carried out to supplement the vane shear measurements.

6.0 VANE TEST

The shear strengths of normally consolidated samples with varying degrees of saturation are measured using a standard laboratory vane shear apparatus. Vane tests are particularly suitable for soils such as soft, sensitive clays from which it would be extremely difficult to prepare undisturbed specimens for other types of test. The gassy soils are prepared in the laboratory by one dimensionally consolidating a soil slurry in a sample preparation mould and they are tested for strength in the mould itself to avoid sampling disturbance.

6.2.1 BRIEF DESCRIPTION OF THE APPARATUS AND THE MODE OF OPERATION:

(i) SAMPLE PREPARATION MOULD:

The sample preparation mould used for the cyclic loading tests in chapter four is used again with a modified top cap. Fig (6.1) shows a schematic diagram of the preparation mould. This comprises a cell, a piston, a base and a top cap. In this cell the soil slurry is placed between the top platen and the piston and loaded from underneath. The soil is drained from both top and bottom ends and the resulting soil is tested for strength.

The new top cap is made out of 150mm diameter and 40mm thick aluminium plate. It has a 40mm diameter hole at the centre (which is sealed by a plug during the

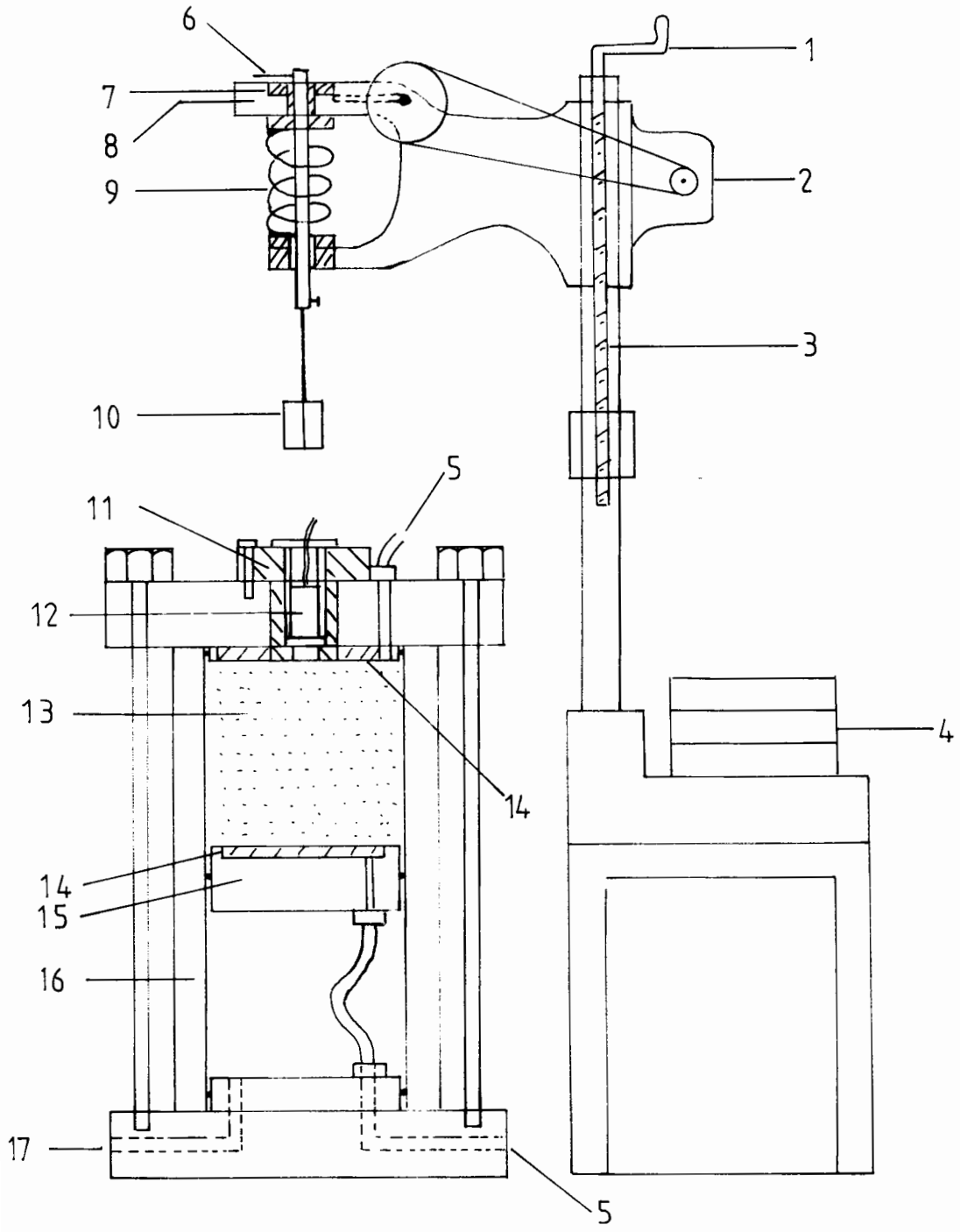

1. Handle for raising and lowering the vane assembly
2. Drive motor
3. Lead screw
4. Counter balance weight.
5. Drainage port
6. Pointer
7. Inner scale
8. Outer scale
9. Spring
10. Vane with four blades
11. Plug to insert the vane
12. Total stress transducer
13. Cassy soil
14. Porous stones
15. Piston
16. Perspex cell
17. Base

Fig 6.1 Laboratory Vane apparatus and the sample preparation mould.

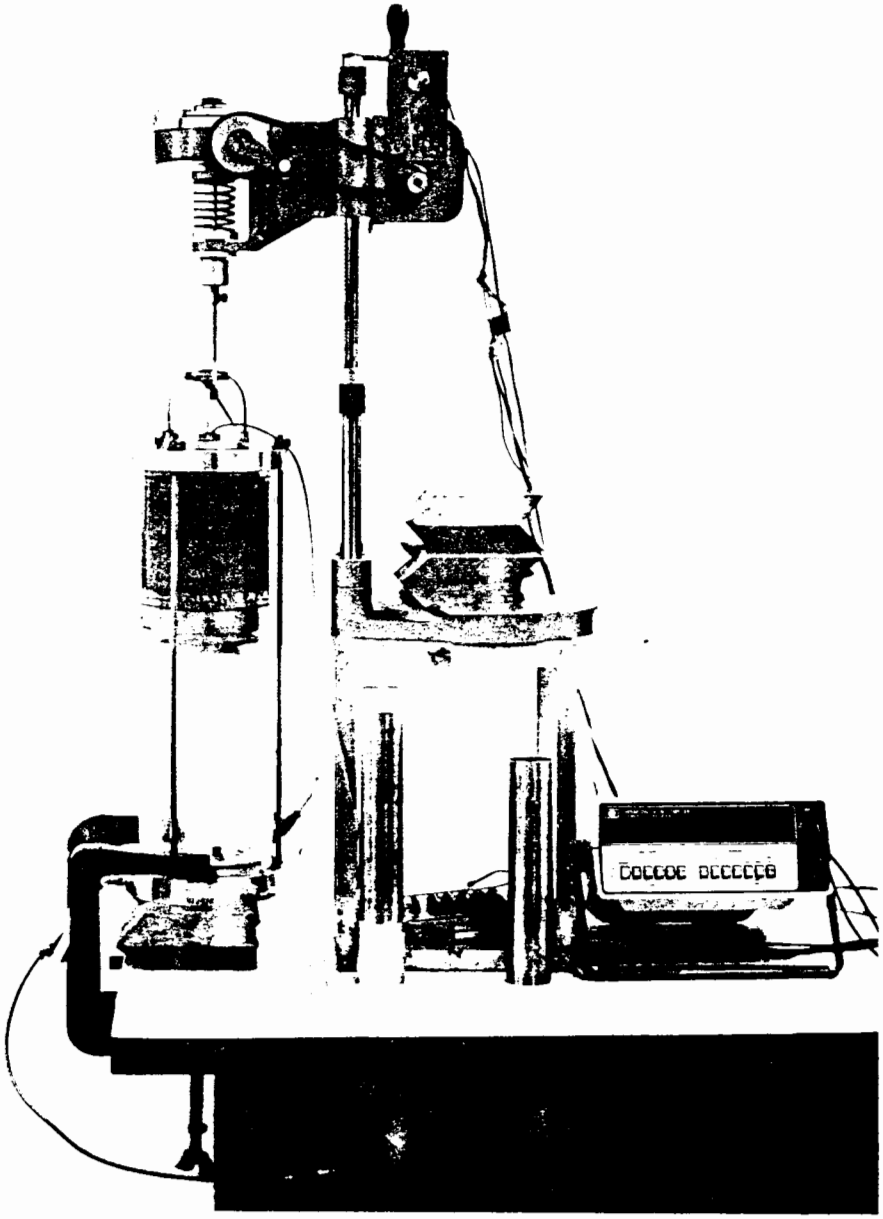

Plate 6.1 Laboratory Vane shear apparatus and the sample preparation mould.

consolidation stage), through which the vane is inserted in to the sample to measure the shear strength without unloading it. The top cap also contains drainage ports like the piston and radial and concentric grooves are cut on both of them to facilitate the drainage. A total stress transducer (Druck PDCR 22) is mounted on the top cap, on the plug,to monitor the consolidation stresses.

6 2.2 THE VANE SHEAR APPARATUS

A standard laboratory vane shear apparatus, fig(6.1), is used and it consists essentially of the following components.

(a) Frame and stand: the frame can be swivelled through 180^{o} to accommodate long sample tubes and counterbalance weights are added to the base plate.

(b) Vane mounting assembly

(c) Handle for raising and lowering the vane assembly by means of the threaded lead screw.

(d) Vane with four blades, 12.7mm wide and 12.7 mm long.

(e) Drive motor to rotate the vane at a rate of 9^{o} per minute.

(f) Graduated scales, marked in degrees, one on the fixed vane head and the other rotating with the vane.

(g) Rotation pointer

(h) Vertical shaft attached to knob fitted with pointer carrier on friction sleeve.

(j)Spring and the calibration chart.

The principle of operation of the apparatus is as follows. If the vane is prevented from rotation as the handle is turned, the inner graduated scale in fig(6.2) rotates through the same angle as the upper end of the spring but the vertical shaft and the pointer remain stationary, so that the pointer reads zero on the outer scale and indicates the torsional rotation, or 'twist', of the spring on the inner scale, from which the torque applied to the spring can be calculated. Therefore at the end of the test, the pointer reading on the inner scale gives the torque and the pointer reading on the outer scale equals the vane rotation provided that at the begining of the test the reading on each scale is set to zero.

6.2.3 TEST PROCEDURE:-

(1) Preparation of samples.

Gassy soil slurries with different degrees of saturation are prepared by adding treated zeolite as described in chapter two. This soil slurry is then poured into the perspex sample preparation mould fig(6.1) and one dimensionally consolidated from an initial thickness of 150mm. Three batches of samples with initial degrees of saturation 100, 90, 80 % are prepared by consolidating them to three different vertical stress levels (30, 50, 100 kN/m^2). No back pressure is used in these tests. All the samples are allowed to attain full consolidation by

draining them from top and bottom ends for 10 days. The final thickness of the sample obtained after consolidation varied between 75 and 90mm which provided adequate cover for the vane.

(2) Measurement of shear strength

The vane shear apparatus is mounted on a platform so that the vane is directly above the sample . The vane scales are set to read zero. The first measurement of shear strength on each sample is performed without unloading the samples (i.e maintaining the consolidation stress acting on the sample) by removing the plug from the central hole on the top cap and inserting the vane. The vane is inserted to sufficient depth to give 30mm cover and rotated at a rate of 9 degrees per minute by the drive motor. The torque and the vane rotation angles are recorded to the nearest 1/2 ^{o}. The torque increases until failure occurs and then decreases, but the pointer remains in position indicating the maximum torque. At the end of the test, the vane is raised steadily and as it emerges from the sample, the soil is pressed gently around it to prevent excessive disturbance due to tearing of the surface. The top cap is then removed, exposing the whole of the soil surface and thereby unloading the sample. The vane is cleaned and the test is repeated at different locations on the samples as shown in fig(6.3). The effective stress states of the samples before and immediately after the total stress removal are assumed to

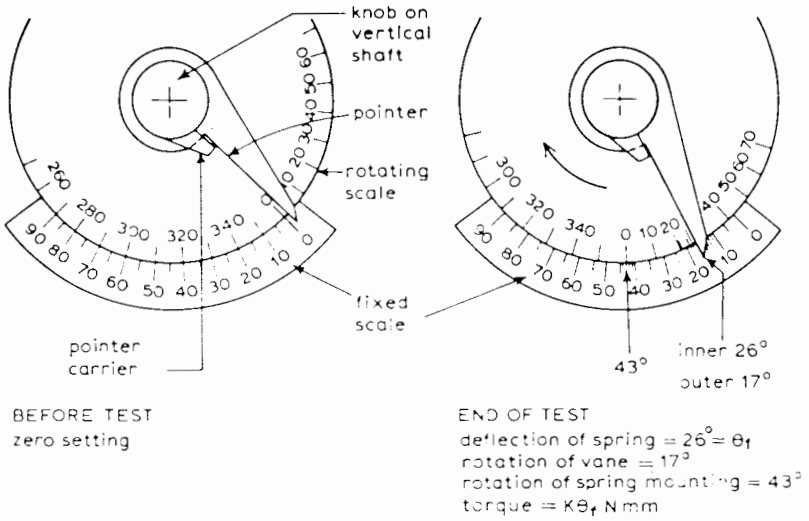

Fig. 6.2 Angular scale on laboratory vane apparatus.

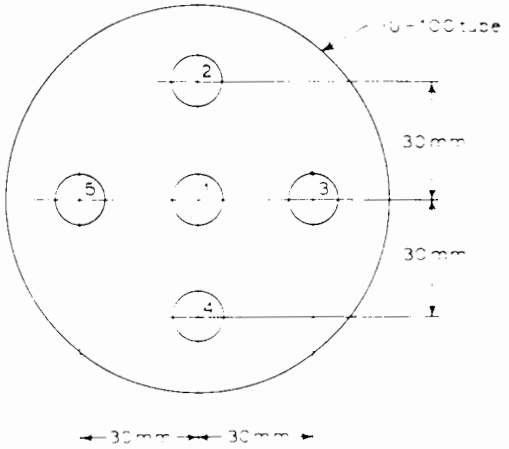

Fig. 6.3 Vane test locations in 100mm diameter sample.

remain the same since the time interval is very small for swelling of the unloaded sample. At the end of the test the moisture content and the degree of saturation of the samples are measured.

6.2.4 OBSERVATIONS:

The measured shear strengths before and immediately after the removal of the total stress were the same in each sample, indicating no excessive swelling in the unloaded sample. The fig(6.4) shows the shear strength measured in the samples with different degrees of saturation (80, 90, 100%) consolidated to a vertical effective stress of 100kN/m^2. The shear strength is plotted against the angle of rotation of the vane. The shear strength readings are obtained continuously until the peak strength is reached, after which the strain softening behaviour is not observed due to the nature of the vane apparatus. However the final remoulded strength is measured at the end of the test after shearing the sample through 360^o. The peak and the remoulded strengths depended on the degree of saturation of the soil. The highest strength is observed in the saturated soil and the strength dropped as the gas content increased. The samples for this strength comparison are consolidated to the same vertical stress of 100kN/m^2.

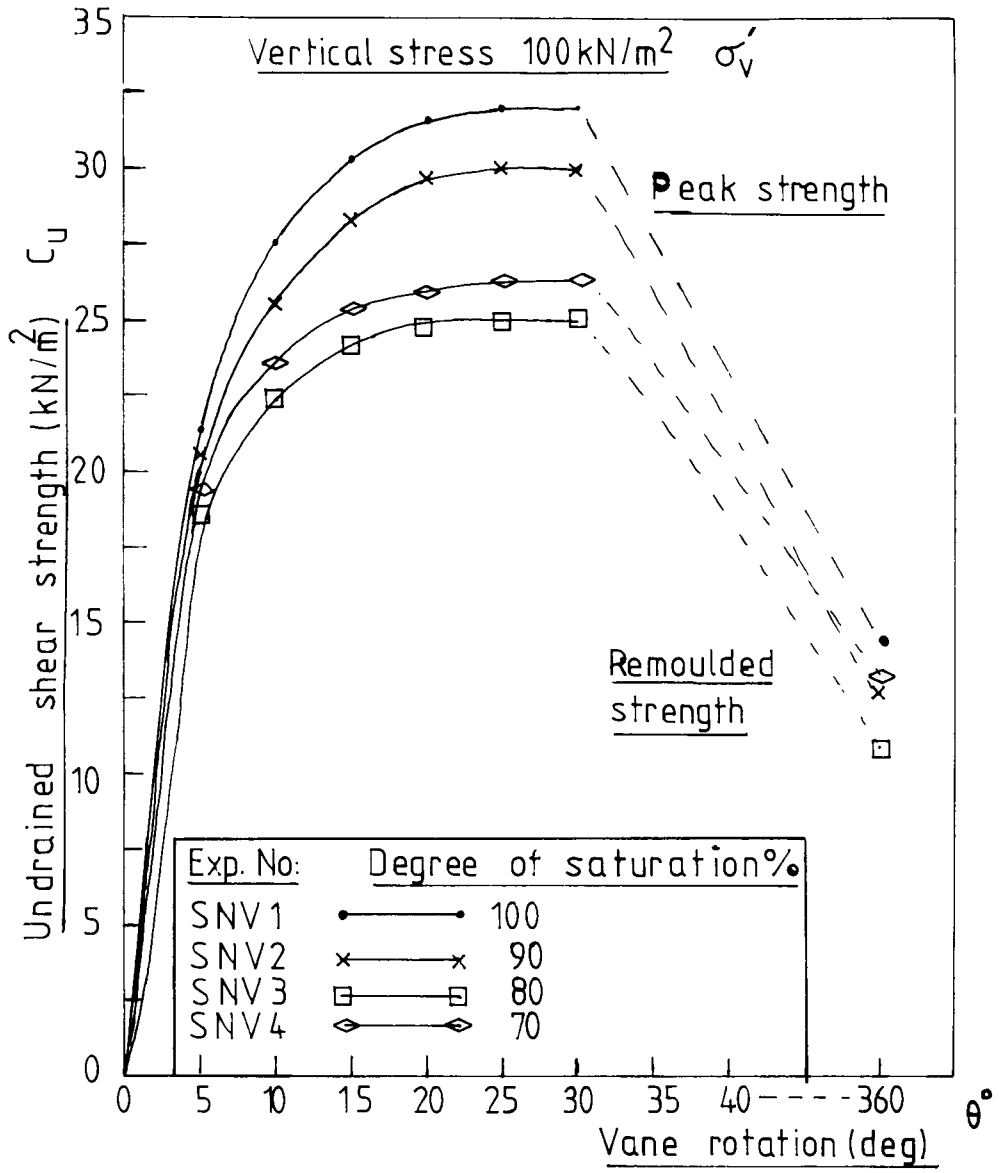

Fig 6.4 Vave shear strength of gassy soils.

Fig(6.5a) shows the shear strength of the samples with different degrees of saturation (80, 90, 100%) after being consolidated to different vertical stress levels (30, 50, 100 kN/m^2). The shear strength corresponding to each point in the figure is the average of four peak vane shear strengths (one before and three after unloading) measured in one sample. The vane shear test suggests the samples with gas bubbles have lower shear strengths than the saturated sample. The shear strength drop in the sample is about 10% for 90% degree of saturation and 20% for 80% degree of saturation. Further reduction in the degree of saturation does not reduce the shear strength of the soil more than that of the soil of 80% degree of saturation. The moisture contents measured in the samples are the same even though the voids ratios are different for each sample depending on the degree of saturation, fig(6.5b). The fig(6.5a) also shows the unconfined compression strength of three samples with different degrees of saturation (100, 90, 80%) which were consolidated to 100 kN/m^2. The test samples of 35mm diameter and 75mm high were cut using standard sampling tubes from the larger samples (100mm diameter) prepared in the same mould used in the vane tests. The unconfined compression strengths also show similar behaviour to that observed in the vane tests. The gassy soil strength is lower than that of the saturated soil. The magnitude of the shear strengths measured in the unconfined test is slightly different from that measured in the vane test (35

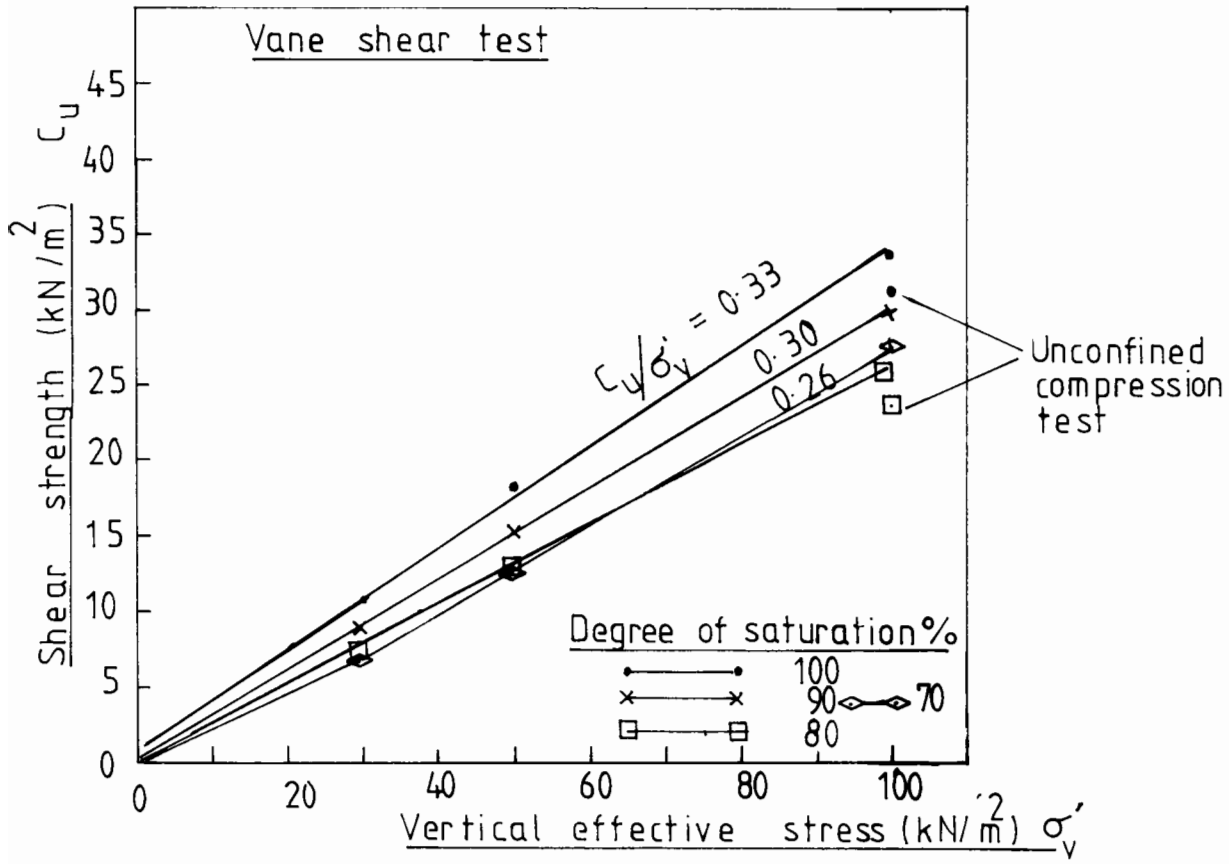

Fig 6.5a Vane shear strength of gassy soils at different vertical stress levels.

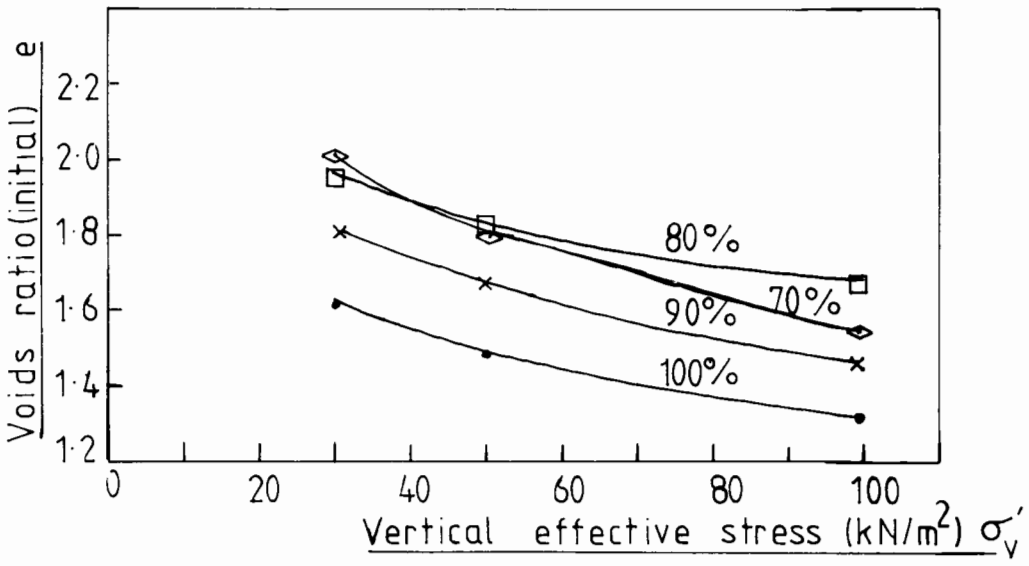

Fig 6.5b Voids ratio of gassy soils

kN/m^2 in the vane test and $32kN/m^2$ in the unconfined test for a saturated soil consolidated to 100 kN/m^2). However the similar behaviour observed in these tests confirms that the presence of gas bubbles in the soil reduces the shear strength. The magnitude of the reduction varies from 0% to a maximum of 20% depending on the degree of saturation of the soil.

6.3 UNDRAINED TRIAXIAL TEST ON GASSY SOILS.

In addition, undrained triaxial tests were carried out on gassy and saturated soils for comparison. The test specimens were initially prepared by one dimensionally consolidating a soil slurry under a vertical stress of $50kN/m^2$ in the large perspex mould (100 mm diameter, 150mm high) used in the vane test. Then two test samples of 35mm diameter were cut from the big sample using standard soil sampling tubes and then isotropically consolidated to 150 kN/m^2 mean effective stress for consolidated undrained triaxial tests. The strain rate used for the undrained test was 3mm/hour. No back pressure was used in these tests. The pore water pressure at the base of the sample, the final degree of saturation and the final moisture

content were measured in addition to the normal axial stress and strain measurements.

The fig(6.6) shows the stress-strain curves for sample tested in an undrained state. The saturated sample failed at a higher deviator stress than the gassy soil. The deviator stress at failure measured in the samples with degrees of saturation 100, 90, 80% are 120, 110, 100 kN/m^2 respectively. The pore water pressures generated and the final failure moisture content in the samples have similar magnitudes, being respectively $30kN/m^2$ at failure and 49%. The shear modulus (the gradient of the shear stress-strain curve) of the soil is also less affected by the presence of gas bubbles in the soil.

6.4 DISCUSSION OF THE RESULTS.

The undrained shear strength measured in the shear vane and triaxial tests shows the reduction in strength due to the presence of gas bubbles. This reduction in undrained strength is linked with the increased voids ratio in the samples. The higher the initial voids ratio (the lower the degree of saturation), the lower the undrained shear strength. The measured final moisture content in the gassy and the saturated samples are the same even though the voids ratios are different. The reduction in undrained shear strength can be qualitatively explained as follows. The presence of gas bubbles in the

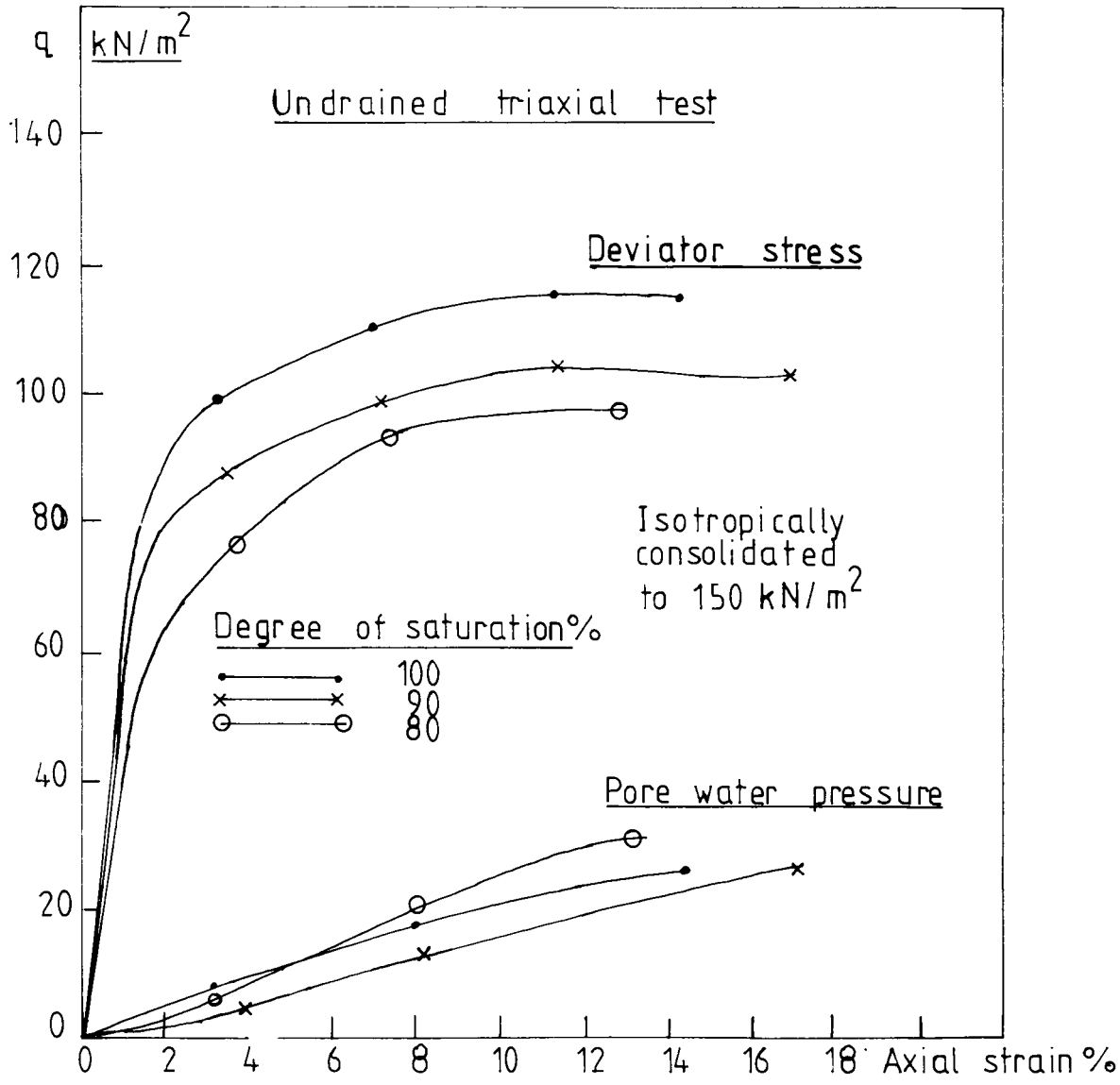

Fig 6.6 Undrained triaxial tests on gassy soils.

soil creates comparatively large hollow voids in the soil. The gassy soil may be considered to be divided into two components, saturated soil and gassy voids as shown in fig(6.7). The above idealisation is the same one used to describe the voids ratio-stress relationship in chapter three. Therefore the undrained shear strength of the gassy soil can be assumed to be derived from the shear strength mobilised in the saturated part of the soil. The shear strength associated with the gassy part of the soil is negligible since it is a large hollow structure. The shear strength mobilised in the saturated part in the gassy soil is assumed to be the same as that of the fully saturated soil since both soils have the same moisture content (from the measurements) and have been consolidated to the same mean effective stress. Therefore the undrained strength of the gassy soil τ_g

$$\tau_g = S\tau_s \qquad 1.00<S<0.80$$

where S the degree of saturation of the soil

and τ_s is the undrained strength of the saturated soil at the same moisture content as the gassy soil.

However the detailed analysis requires the measurement of the degree of saturation and the volume change occurring in the gassy soil during the undrained shearing process which are not measured in the standard tests. Detail investigations are in progress at Oxford University.

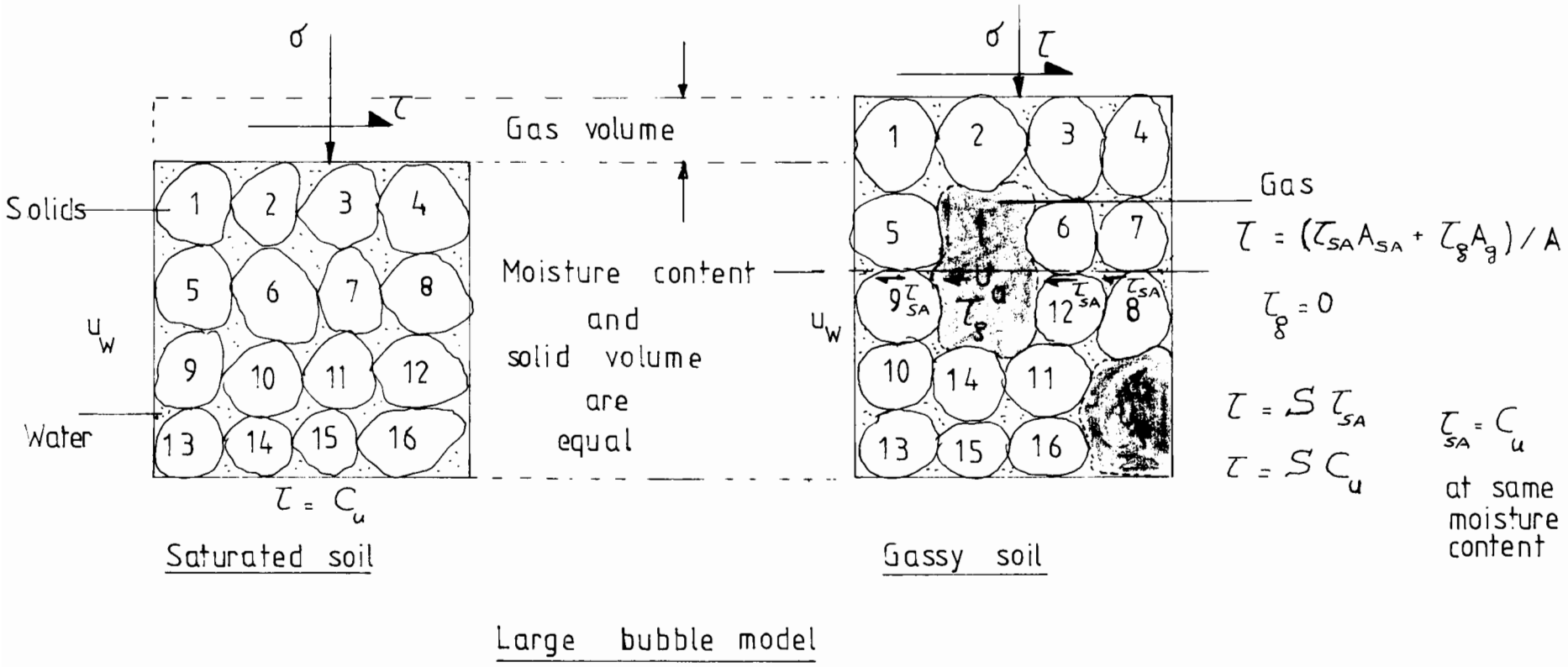

Fig 6.7 Large bubble model used to describe the shear behaviour of gassy soils.

6.5 Conclusion:

The shear strength test using standard laboratory equipment suggests that the undrained shear strength of gassy soil is less than that of the saturated soil. The maximum reduction in undrained shear strength is about 20% which is observed in a soil with 80% degree of saturation. Further reduction in degree of saturation does not reduce the shear strength below that of the 80% saturated soil. The shear modulus [gradient of shear stress-strain curve fig(6.6)] of the soil is also less affected by the presence of gas bubbles in the soil. The significant effect caused by the gas bubbles is in the volume change behaviour of the soil (ie.bulk modulus) rather than on the shear strength behaviour.

CHAPTER 7

IN CONCLUSION

7.1 Conclusions.

7.1.1 Preparation of gassy soil.

7.1.2 Effect of gas bubbles on the geotechnical properties of soil.

(a) Volume change-Stress behaviour.

(b) Settlement-Time behaviour.

(c) The undrained response.

(d) Undrained shear strength.

7.1.3 Practical application.

7.2 Recommendation for future work.

CHAPTER 7

IN CONCLUSION

7.1 CONCLUSIONS

7.1.1 PREPARATION OF GASSY SOIL.

The method of preparation of reconstituted gassy soil with a controllable gas content has proved to be very successful. However there is a limitation on the lowest degree of saturation that can be produced using this method. Soil with degrees of saturation below 80% require a large proportion of zeolite (more than 20% by weight as a proportion of the dry soil) and the basic properties of the soil are changed. Extremely careful preparation is necessary to produce a sufficiently repeatable degree of saturation and uniform gas bubble distribution in the soil.

Although only one specific soil was used throughout, the above technique and the results of the experiments should be applicable to a wide range of clayey soils.

7.1.2 THE EFFECT OF GAS BUBBLES ON THE GEOTECHNICAL PROPERTIES OF THE SOIL

(a) STRESS-VOLUME CHANGE BEHAVIOUR OF THE SOIL

The volume change behaviour of soils containing undissolved gas bubbles when subjected to one dimensional stress increments has been studied in chapter three. The presence of gas bubbles increases the specific volume of the soil when compared to that of the saturated soil consolidated under the same vertical stress. For a given vertical consolidation stress ($\sigma-u_w$), the specific volume increases with the decrease in degree of saturation up to a critical degree of saturation. Beyond this critical value, a further reduction in the degree of saturation does not cause any increase in the specific volume. When the degree of saturation decreases below a critical value the discrete gas bubbles become interconnected and the gas flows as freely as the water. The critical degree of saturation depends on the soil type and is around 85% for the clay used in this experiment. At degrees of saturation below the critical value, the soil behaviour is different to that of the soil containing discrete gas bubbles.

The moisture content of the gassy soil with different degrees of saturation above the critical degree of saturation and that of the saturated soil subjected to the same consolidation stress are the same even though the

specific volume of the samples are different. Using the above experimental evidence the voids ratio (or specific volume) of a gassy soil with a known degree of saturation can be calculated from the voids ratio of the saturated soil. This can be expressed as follows:

$$eS = e_1 + A\ln(\sigma - u_w) \text{ --------- (7.1)}$$

eS/G_s = moisture content in a gassy soil.

where e is the voids ratio of the soil with the degree of saturation S ($0.85 < S < 1.00$).

Constants A and e_1 are determined from the oedometer test on saturated soil.

e_1 corresponds to the voids ratio of the soil at unit effective stress.

The above model does not require the measurement of pore gas pressure, but requires the measurement of pore water pressure and the current degree of saturation of the soil. However the measurement of pore water pressure in gassy soil is difficult and care should be taken. Using a high air entry stone alone is not sufficient to ensure that, in a gassy soil, the measured pore pressure is the pore water pressure. Provision shoud be made to remove the gas bubbles that pass through the stones as they appear in the measuring system.

(b) SETTLEMENT-TIME BEHAVIOUR.

The presence of gas bubbles in the soil affects the confined settlement behaviour of the soil in two ways.

(I) The immediate settlement:

An immediate settlement is observed in a gassy soil as soon as the total stress increment is applied due to the compressibility of the pore fluid. This settlement can be calculated using Boyle's and Henry's laws since it is primarily due to the gas volume change. The amount of settlement depends on the degree of saturation of the soil, the compressibility of the soil and the magnitude of the stress increment. The ratio of the initial settlement to the final settlement at the end of the one dimensional consolidation can be estimated from the following equation:

$$\frac{\Delta_i}{\Delta_f} = (1-B) \qquad B = \frac{1}{1 + \dfrac{(\alpha+H)\, e_o\, p_o}{a_v\, (1+\alpha)\, p^2}} \qquad \text{-----(7.2)}$$

(II) The settlement due to fluid drainage.

The settlement rates due to fluid flow in a gassy soil depend on the permeability and the density of the pore fluid. The permeability of the pore fluid depends on

the degree of saturation and the voids ratio of the soil. The density of the pore fluid depends on the degree of saturation of the soil and the current pore fluid pressure. The theoretical and experimental studies on gassy soil with occluded gas bubbles suggest that the settlement rates due to pore fluid drainage in gassy soils are lower than those of the saturated soil. However the degree of settlement (Δ/Δ_f) at a given time in the gassy soil is greater at the initial stage of the consolidation and becomes equal to that of the saturated soil at the end of the consolidation. The time settlement curves given in fig(4.7) are useful if the consolidation times for a particular degree of settlement of gassy and saturated soils are needed. The time factors used in these plots are in terms of the coefficient of consolidation of the saturated soil. As the degree of saturation decreases below the critical degree of saturation, the curves are no longer useful. The permeability of the soil rapidly increases due to the free gas flow and increases the settlement rates. The time to achieve 90-95% of the final settlement in a gassy soil with degrees of saturation above the critical degree of saturation and in a saturated soil are the same. The design curves in fig(4.7) are sensitive to the compressibility (a_v) of the soil, hence the appropriate design curves should be used.

(c) THE UNDRAINED RESPONSE OF THE GASSY SOIL.

The pore water pressure changes caused by the undrained total stress changes are lower in gassy soil. The pore pressure change is equal to the total vertical stress increment under K_o conditions in saturated soil. Some part of the total stress increment is transferred as effective stress in the gassy soil and the volume of the soil decreases at constant moisture content. The changes in pore water pressure in a gassy soil for a one dimensional total stress increment can be calculated using the equation (7.2).

The undrained response of the gassy soil depends on the degree of saturation of the soil as well as the compressibility of the soil. As the soil becomes stiffer the B value (pore pressure increment/ total stress increment) increases even if the degree of saturation of the soil remains the same. The analysis in chapter four suggests that a low B value measured in a soil does not necessarily mean that the gas content in the soil is high. The B value is a measure of the ratio of the compressibility of the pore fluid and the compressibility of the soil skeleton. The compressibility of the pore fluid depends on the degree of saturation of the soil whereas the volume compressibility of the soil depends on the current mean effective stress in the soil and the over consolidation ratio.

(d) UNDRAINED SHEAR STRENGTH OF GASSY SOIL.

The preliminary shear tests on gassy soil suggest that the undrained shear strength of the soil is reduced by the presence of gas bubbles. The undrained shear strength decreases by 20% of that of the saturated soil when the degree of saturation decreases to 80%. However further reduction in the degree of saturation does not decrease the undrained shear strength of the soil by more than 20%. The undrained shear strength of gassy soils may be expressed approximately as follows:

$$\tau_g = S\ C_u \qquad 1.0 < S < 0.8$$

where S is the degree of saturation of the soil and C_u is the undrained shear strength of the saturated soil at the same moisture content.
Further detailed experiments are necessary to explain the shear behaviour of gassy soil.

7.1.3 PRACTICAL APPLICATION:

The differential piezometer described in chapter five is a useful insitu probe to study the pore water pressure response in the sea bed during tide or wave action. The accuracy of the instrument is higher than the conventional piezometers due its differential nature and suitable for measurements in deep waters. The effect of the presence of gas bubbles in the sea bed on the pore water pressure can be measured using this instrument and the insitu degree of saturation of the soil can also be estimated

with the measurement of stress-strain properties of the soil.

The presence of gas bubbles in a marine sediment may cause vertical movements of the sea bed due to water head changes and this may cause difficulties in defining the depth of the sea bed for dredging and navigation purposes. The simple theoretical model described in chapter4 can be used to estimate the surface movement. The knowledge of incitu gas content is necessary in order to estimate these surface movements. A very rough estimate of this can be obtained from the differential pore water pressure measurement by the piezometer coupled with measurements of the soil skeleton stiffness.

7.2 RECOMMENDATION FOR FUTURE WORK:

The disturbance due to the presence of gas bubbles in the soil during sampling.

When the core samples are taken from the sea bed and brought to the surface a large reduction in total stress occurs. The reduction in the total stress in the saturated soil can cause substantial negative pore water pressures, keeping the effective stresses approximately constant during sampling. If the saturated samples are tested immediately after the recovery, only a small amount of strength is lost due to swelling. The total stress reduction in the gassy sample causes gas bubble expansion in the sample and often gas escapes from the sample.

Growth in the core samples can be observed when samples from the deep sea bed are brought to the surface. The gas dissolved under high pressures reappears and the undissolved gas bubbles expand with the reduction in total stress. Large amounts of structural damage are also evident in gassy soil samples.

A study of shear strength changes due to sampling in gassy soil is useful in order to relate the measured shear strength from core samples to the insitu strength. The sample disturbance caused by the expansion of gas bubbles can be modelled in the laboratory using the reconstituted artificial gassy soil described in chapter two. The following experimental procedure could be used to study the effect of sample disturbance caused by the gas bubble expansion on the strength of soil.

(a) Prepare the gassy soil slurry as described in chapter two.

(b) Consolidate the soil slurry one dimensionally in a sample preparation mould fig(4.17) to prepare a triaxial sample. Use high back pressures and total stress during consolidation.

(c) Unload the sample at the end of the one dimensional consolidation by reducing the total and the back pressures. Trim triaxial specimens from the big sample. This procedure is equivalant to obtaining samples from the sea bed and preparing triaxial

samples for laboratory tests.

(d) Samples are tested after isotropic or K_o consolidation. Most of the offshore samples are tested under unconsolidated undrained conditions. The cell pressure and the back pressure used for testing are estimated from the depth where the sample are taken.

(e) Load the sample axially to failure and calculate the deviator stress at failure. Different combinations of cell pressures, back pressures and one dimensional consolidation pressures can be selected to examine the effect of gas bubble expansion on the shear strength of soil.

This type of test should provide an improved understanding when evaluating the in-situ strength of the gassy samples from the strength measured on the core samples.

Appendix A

Fortran coding for finite difference calculations

(a) One dimensional consolidation

(b) Sinusoidal loading of a gassy sea bed

ONE DIMENSIONAL CONSOLIDATION

```
C*********************************************************
C        LARGE STRAIN CONSOLIDATION
C*********************************************************
         DIMENSION V(52,150)
         DIMENSION U(52,150)
         DIMENSION P(52,150)
         DIMENSION H(52,150),DF(4000)
         DIMENSION MV(52,150),EX(4000)
         REAL T,TO,LA,GW
         REAL VO,HO,PO,D
         INTEGER I,J,K,L,M,N
C************************************************
C PLOT AXIS
C************************************************
         CALL T4010
         CALL PICCLE
         CALL SCALE2(0.025,0.2)
         CALL SHIFT2(600.,-200.)
         CALL MOVTO2(4000.0,730.0)
         CALL MOVTO2(0.0,150.)
         CALL LINTO2(0.0,900.0)
         CALL MOVTO2(20.0,900.0)
         CALL CHAHOL(10HPRESSURE*.)
         DO 21 J=1,8
         CALL MOVTO2(0.,(500.+50.*J))
         CALL LINTO2(100.,(500.+50.*J))
         CALL MOVTO2(-400.,(500.+50.*J))
         CALL CHAFIX((.2*(J-1)),4,2)
21        CONTINUE
         CALL MOVTO2(0.,550.)
         CALL LINTO2(6000.,550.)
         CALL MOVTO2(5000.,580.)
         CALL CHAHOL(13HTIME FACTOR*.)
         CALL MOVTO2(0.,900.)
         CALL LINTO2(6000.,900.)
         CALL MOVTO2(5000.,870.)
         CALL CHAHOL(13HTIME FACTOR*.)
         DO 40 I=1,10
         CALL MOVTO2((600.*I),900.)
         CALL LINTO2((600.*I),890.)
40       CONTINUE
         DO 50 I=1,6
         CALL MOVTO2(0.,((I-1)*50.0+250.))
         CALL LINTO2(100.,((I-1)*50.0+250.))
50       CONTINUE
         DO 60 I=1,11
         CALL MOVTO2(-600.,(950.-50.*I))
         CALL CHAFIX(((I-1)*0.1),6,2)
60       CONTINUE
         CALL MOVTO2(-600.,0.)
         CALL LINTO2(6500.,0.)
         CALL LINTO2(6500.,930.)
         CALL LINTO2(-600.,930.)
         CALL LINTO2(-600.,0.)
         CALL MOVTO2(20.,200.)
```

```
        CALL CHAHOL(13HDEFORMATION*.)
        CALL MOVTO2(0.0,750.0)
C*****************************************************
C     READING INPUT DATA
C UO-INITIAL PORE PRESSURE, T-TOTAL STRESS INCREMENT,
C CF-COEFFICIENT OF CONSOLIDATION, SR-DEGREE OF SATURATION
C VO-INITIAL VOIDS RATIO, D-INITIAL SAMPLE HEIGHT
C HC-COEFFICIENT OF SOLUBILITY,  TI-TIME STEP
C LA-COEFFICIENT OF COMPRESSIBILITY
C*****************************************************
        OPEN(1,FILE='CONINA',STATUS='OLD')
        OPEN(2,FILE='CONINB',STATUS='OLD')
        OPEN(3,FILE='CONINC',STATUS='OLD')
        OPEN(4,FILE='CONIND',STATUS='OLD')
        OPEN(5,FILE='CONINOUT',STATUS='NEW')
        DO 91 I=1,10
        CALL MOVTO2((600.*I),900.)
        CALL LINTO2((600.*I),880.)
        CALL MOVTO2((600.*I),840.)
        CALL CHAFIX((0.2*I),4,2)
91      CONTINUE
        DO 700 M=1,4
        READ(M,*) UO,T,CF
        READ(M,*) VO,D,LA
        READ(M,*) TI,SR,HC
C*****************************************************
C   SETTING THE INITIAL VALUES
C*****************************************************
       GW=10
       AL=(1-SR)/SR
       U(1,1)=UO
       HO=D/50
       DO 100 I=2,52
       A=(HC+AL)*VO*UO/(1+AL)/LA

U(I,1)=T/(1+(0.5*((A/UO/UO)+(A/(100+T)/(100+T)))))+UO
       V(I,1)=VO
       P(I,1)=PO
       H(I,1)=HO
100    CONTINUE
       DO 200 J=2,11
       U(1,J)=UO
200    CONTINUE
C*****************************************************
C   FINITE DIFFERENCE CALCULATION
C*****************************************************
       DO 500 K=1,40000
       DO 400 J=1,10
       TH=0
       DO 300 I=2,51
       U(52,J)=U(50,J)
       R=1+(A/U(I,J)/U(I,J))
       Z=1-HC+((AL+HC)*UO/U(I,J))
       X=Z*TI*CF/((H(I,J))*(H(I,J)))/R
       FD=(U((I+1),J)-(2*(U(I,J)))+U((I-1),J))*X
```

```
        U(I,(J+1))=FD+U(I,J)
C*************************************************
C    UPDATING THE NEW CO-ORDINATES
C*************************************************
       V(I,(J+1))=VO-(LA*((T+UO-U(I,(J+1)))))
       H(I,(J+1))=HO-(((VO-V(I,(J+1)))*HO)/(1+VO))
       TH=HO-H(I,(J+1))+TH
       VF=VO-(LA*(((T))))
       HF=((VO-VF)*D/(1+VO))
300    CONTINUE
400    CONTINUE
       WRITE((5),*) (Z/R), (U(I,J)),(TH*1000),(HF*1000)
C*************************************************************
C    PLOT THE POINTS
C*************************************************************
       DF(K)=-(TH)*250*2/HF
       EX(K)=(U(51,11)-UO)*250/T
       IF(TH.GT.(.99*HF)) GO TO 690
       Y=K-1
       DI1=(SQRT(Y*TI*10*CF/D/D))*3000.
       DI2=(SQRT(K*TI*10*CF/D/D))*3000.
       CALL MOVTO2((DI1),((EX(K-1))+550))
       CALL LINTO2((DI2),((EX(K))+550))
       CALL MOVTO2((DI1),((DF(K-1))+900.))
       CALL LINTO2((DI2),((DF(K))+900.))
       DO 410 I=1,52
       U(I,1)=U(I,11)
       H(I,1)=H(I,11)
       V(I,1)=V(I,11)
410    CONTINUE
500    CONTINUE
690    CALL MOVTO2(100.,(400.-(40*M)))
       CALL CHAHOL(14HTIME FACTOR=*.)
       CALL CHAFIX((TI*((K-1)*10+J)*CF/D/D),10,7)
       CALL CHAHOL(23HDEGREE OF SATURATION=*.)
       CALL CHAFIX((SR*100),10,7)
700    CONTINUE
       CALL MOVTO2(10.,600.)
       CALL CHAMOD
       READ(*,'(A)')TALK
       READ(*,'(A)')TELL
       CALL DEVEND
       CALL OXFHARDCOPY
       STOP
       END
```

SINUSOIDAL LOADING OF A GASSY SEA BED

```
C*************************************************
C  SINUSOIDAL LOADING
C*************************************************
      DIMENSION  D(15)
      DIMENSION F(15), AL(15)
      DIMENSION DF(500)
      DIMENSION DW(500)
      REAL W,AV,KT,DE,CF,H,KO,GW,EO,L,DH
      REAL CM,CM1,CM2
      DIMENSION P(15,150)
      REAL DAO
      DIMENSION EX(500)
      INTEGER M
      OPEN(1,FILE='SEAINA',STATUS='OLD')
      OPEN(2,FILE='SEAINB',STATUS='OLD')
      OPEN(3,FILE='SEAINC',STATUS='OLD')
      OPEN(4,FILE='SEAOUT',STATUS='NEW')
C*************************************************
C  PLOT AXIS
C*************************************************
      CALL T4010
      CALL PICCLE
      CALL SCALE2(0.025,0.15)
      CALL SHIFT2(600.,0.)
      CALL MOVTO2(0.0,750.0)
      CALL LINTO2(4800.0,750.0)
      CALL MOVTO2(4000.0,730.0)
      CALL CHAHOL(11HTIME(HRS)*.)
      CALL MOVTO2(0.0,150.)
      CALL LINTO2(0.0,900.0)
      CALL MOVTO2(20.0,900.0)
      CALL CHAHOL(15HPRESSURE(Kpa)*.)
      CALL MOVTO2(0.,1250.)
      DO 11 I=1,8
      CALL MOVTO2((600.*I),750.)
      CALL LINTO2((600.*I),760.)
      CALL CHAFIX((1.*KO*I/2),6,3)
 11    CONTINUE
      DS=(SR)*100
      DO 21 J=1,6
      CALL MOVTO2(0.,(600.+50.*J))
      CALL LINTO2(100.,(600.+50.*J))
      CALL MOVTO2(-400.,(600.+50.*J))
      CALL CHAINT((50*(J-1)),4)
21    CONTINUE
      CALL MOVTO2(0.,550.0)
      CALL LINTO2(4800.,550.)
      CALL MOVTO2(4000.,520.)
      CALL CHAHOL(11HTIME(HRS)*.)
      DO 31 I=1,8
      CALL MOVTO2((600.*I),550.)
      CALL LINTO2((600.*I),560.)
      CALL CHAFIX((KO*1.*I/2),6,3)
31    CONTINUE
```

```
        CALL MOVTO2(20.,600.)
        CALL CHAHOL(28HEXCESS PORE PRESSURE (Kpa)*.)
        CALL MOVTO2(0.,300.)
        CALL LINTO2(4800.,300.)
        CALL MOVTO2(4000.,280.)
        CALL CHAHOL(11HTIME(HRS)*.)
        DO 40 I=1,8
        CALL MOVTO2((600.*I),300.)
        CALL LINTO2((600.*I),310.)
        CALL CHAFIX((KO*1.*I/2),6,3)
40       CONTINUE
        DO 50 I=1,9
        CALL MOVTO2(0.,(I*50.0+150.))
        CALL LINTO2(100.,(I*50.0+150.))
50       CONTINUE
        DO 60 I=1,5
        CALL MOVTO2(-600.,(650.-50.*I))
        CALL CHAFIX((10-I*5.),6,2)
60       CONTINUE
        TA=W/5.0
        DO 70 I=1,5
        CALL MOVTO2(-600.,(400.-50.*I))
        CALL CHAFIX((12.5-I*6.25),6,2)
70       CONTINUE
        CALL MOVTO2(-600.,0.)
        CALL LINTO2(6500.,0.)
        CALL LINTO2(6500.,930.)
        CALL LINTO2(-600.,930.)
        CALL LINTO2(-600.,0.)
        CALL MOVTO2(20.,350.)
        CALL CHAHOL(17HDEFORMATION(MM)*.)
        CALL MOVTO2(-300.,(180.-50.*M))
        CALL SYMBOL(M+1)
        CALL LINTO2(0.,(180.-50.*M))
        CALL SYMBOL(M+1)
        CALL LINTO2(250.,(180.-50.*M))
        CALL SYMBOL(M+1)
        CALL MOVTO2(250.,(175.-50.*M))
        CALL CHAHOL(21H DEG-SATURATION)=*.)
        CALL CHAFIX(DS,6,2)
        CALL CHAHOL(32H  COEF-COMPRESSIBILITY(1/KPa)=*.)
        CALL CHAFIX(AV,7,5)
        CALL MOVTO2(0.0,750.0)
C*********************************************
C       READ INPUT DATA
C W- SINE WAVE AMPLITUDE, EO-INITIAL VOIDS RATIO
C AV-COEFFICIENT OF COMPRESSIBILITY
C DH-MEAN DEPTH OF WATER, CF-COEFFICIENT OF
COMPRESSIBILITY
C H -HEIGHT OH SEA BED, KO-CYCLE TIME
C GW-DENSITY OF SEA WATER, SR-DEGREEOF SATURATION
C HC-COEFFICIENT OF COMPRESSIBILITY
C*********************************************
        DO 3000 M=1,2
        READ(M,*) W,EO,AV
```

```
      READ(M,*) CF,H
      READ(M,*) KO,GW,DH
      READ(M,*) SR,HC
C**************************************
C SETTING THE INITIAL VARIABLES
C**************************************
      DO90 I=1,12
      AL(I)=(1-SR)/SR
      P(I,1)=100.+(DH*10)+(H*10*(I-1)/10)
90    CONTINUE
C******************************************
C     WRITE INPUT DATA
C******************************************
      WRITE(4,*) AL(5),EO,AV
      WRITE(4,*) CF,GW,H
C******************************************
C     MAIN PROGRAM
C******************************************
      PI=4.0*ATAN(1.0)
      KT=KO/100/100
      X=CF*KT/(H/H/100)
      Y=CF*KT/(H/10)
      DO 1000 K=1,400
      DI=(K-1)*100
      DO 100 J=1,100
      Q=100+(DH*10)
      S=W+(W*(SIN((KT*(DI+J-1)*(PI/KO))+1.5*PI)))
      P(1,J)=Q+S
100   CONTINUE
      DO 200 J=1,100
      DE=0.0
      DO 110 I=2,11
      B=((AL(I)+HC)/(1+AL(I)))*EO*(100.+(DH*10)+
     +(H*(I-1)*GW/10))/AV
      L=(AL(I)+HC)*(100.+(DH*10)+(H*(I-1)*GW/10))
      DCO1=100.+(DH*10)+(H*(I-1)*GW/10)
      DDO2=W+(W*(SIN((KT*(J+DI*10)*(PI/KO))+1.5*PI)))
      DAO=DCO1+DDO2
      DL1=100.+(DH*10)+(H*(I-1)*GW/10)
      DL2=W+(W*(SIN((KT*(J-1+DI)*(PI/KO))+1.5*PI)))
      DL=DL1+DL2
      DK=1+(B/(P(I,J))/(P(I,J)))
      CM1=W*(SIN((KT*(J+DI)*(PI/KO))+1.5*PI))
      CM2=W*(SIN((KT*(J+DI-1)*(PI/KO))+1.5*PI))
      CM=CM1-CM2
      PO=P(I,J)+(1*CM/DK)
      D(I)=1+(B/(PO*PO))
      P(I,(J))=P(I,J)+(1*CM/D(I))
      F(I)=1-HC+(L/P(I,J))
110    CONTINUE
      DO 121 I=2,11
      P(12,(J))=P(10,(J))+(H*2)
      EN=P((I+1),(J))-(2*P(I,(J)))+P((I-1),(J))
      P(I,(J+1))=P(I,(J))+(EN*X*(F(I))/(D(I)))
      DEO1=100.+(DH*10)+(H*(I-1)*GW/10)
```

```
        DFO2=W+(W*(SIN((KT*(J+DI)*(PI/KO))+1.5*PI)))
        DBO=DEO1+DFO2
        DE=((AV*(DBO-(P(I,(J+1))))/(1+EO))*H/10)+DE
C       WRITE(4,*) P(I,(J+1)),DBO
121     CONTINUE
200     CONTINUE
C*********************************************
C PLOT THE RESULTS
C*********************************************
300     DF(K)=-(DE*8000)
        DW(K)=DBO-(50*H/10)
        EX(K)=(P(6,101)-(DBO-(50*H/10)))*10
        DI1=(K-1)*1200/100
        DI2=K*1200/100
        WRITE(4,*) P(6,101),(DBO-(50*H/10)),(KO*K/100),DE
        CALL
MOVTO2((DI1),((DW(K-1))+650.-(100.+DH*10+5*H)))
        CALL LINTO2((DI2),(DW(K)+650.-(100.+DH*10+5*H)))
        DO 308 I=1,10
        AX=40*I
        IF(K.EQ.AX) THEN
        CALL SYMBOL(M+1)
        END IF
308     CONTINUE
        CALL MOVTO2((DI1),((EX(K-1))+550))
        CALL LINTO2((DI2),((EX(K))+550))
        DO 310 I=1,10
        AX=40*I
        IF(K.EQ.AX) THEN
        CALL SYMBOL(M+1)
        END IF
310     CONTINUE
        CALL MOVTO2((DI1),((DF(K-1))+300.))
        CALL LINTO2((DI2),((DF(K))+300.))
        DO 320 I=1,10
        AX=40*I
        IF(K.EQ.AX) THEN
        CALL SYMBOL(M+1)
        END IF
320     CONTINUE
400     DO 500 I=2,11
        P(I,1)=P(I,101)
500      CONTINUE
1000     CONTINUE
3000    CONTINUE
        CALL DEVEND
        CALL OXFHARDCOPY
        STOP
        END
```

REFERENCES

1. Bea, R.G. and Arnold, P. (1973). "Movements and Forces Developed by Wave-Induced Slides in Soft Clays." OTC. Paper No: 1899

2. Bea, R.G. and Audibert, J.M.E. (1980). "Offshore platforms and pipelines in Mississippi River Delta." J. Geotech. Engng Div. Am. Soc. Civ. Engrs 106, GT8, 853-869.

3. Bishop, A.W. and Blight, G.E. (1963). "Some Aspects of Effective stress in saturated and partly saturated soil." Geotechnique 13. NO:3, 177-197

4. Bishop, A.W. and Donald, I.B. (1961). "The experimental study of partly saturated soils in triaxial apparatus." Proc.5th Int.Conf. SM&Fe Paris 1 15-21.

5. Bishop, A.W. and Henkel, D.J. (1962). "The measurement of soil properties in the triaxial test." William Arnold, London (2nd ed). p-227.

6. Bennett, R.H. (1977). "Pore water pressure measurements: Mississippi delta sediments." Marine Geotechnology Vol.2, 177-190.

7. Break, D.W. "Zeolite Molecular Sieves". A Wiley-interscience publication. John Wiley and Sons.

8. Burland, J.B. (1964). "Correspondence: Effective

stresses in partly saturated soils." Geotechnique 14, Vol 1, 64-68.

9. Dunlap, A.W., Bryant, R. and Williams, G.N. (1980). "Storm waves effects on deltatic sediments-Results of SFASWAB I and II" The delta project report Vol 14, U.S.G.S.

10. Esrig, M.I. and Kirby, R.C. (1977). "Implications of gas content for predicting the stability of submarine slopes." Marine geotechnology Vol.2, 81-100.

11. Fannin, N.G.T. (1979). "IGS Pockmark Investigations 1974-1978." IGS Report NO: 98

12. Fredlund, D.G. (1979). "Appropriate concepts and technology for unsaturated soils." Canadian Geotechnical Journal, 16, 121-139.

13. Gibson, R.E. and Hussey, M.J.L. (1967). " The theory of one dimensional consolidation of saturated clays." Geotechnique 17:261-273.

14. Henkel, D.J. (1970). "The role of waves in causing submarine landslides." Geotechnique 20, Vol. 1, 75-80.

15. Henkel, D.J. (1982). "Geology, geomorphology and geotechnics." Geotechnique 32, Vol.3, 175-194.

16. Hottman, E., Josph, Suhayda, N. and Garrison, L.E. (1978). "Shallow experiment to assess storm waves effects on the bottom." OTC 3169.

17. Jennings, J.E.B. and Burland, J.B. ((1962). "Limitations to the use of effective stress in partly saturated soils." Geotechnique 12, No:2, 125-144.

18. Kaplan, I.R. (1974). "Natural Gases in Marine Sediments." Vol.3, Plenum Press pages (2-4), (11-25), (99-139).

19. Lee, K. (1979). "An analytical and experimental study of large strain consolidation." D.Phil Thesis, Oxford.

20. Matyas, E.L. and Radhakrishna, H.S. (1968). "Volume change characteristics of partially saturated soils." Geotechnique 18, 432-448.

21. Prior, D.B. and Coleman, M.J., (1977). "Submarine landslides in the Mississippi River Delta." OTC, Vol. 3170.

22. Skempton, A.W. (1954). "The pore pressure coefficients A and B." Geotechnique 4, Vol 4, 143-147.

23. Whelan, T.III., Coleman, J.M., Suhayda, J.N., and Garrison, L.E. (1975). "The Geochemistry of Recent Mississipi River Delta Sediments: Gas Concentration and Sediment Stability". Offshore Technology Conference, Paper No: 2342.

24. Whelan, T. III., Coleman, J.M., Suhayda, J.N. and Roberts, H. (1976). "Acoustical penetration and shear